

REMARKS

Introduction

Receipt is acknowledged of a final office action dated June 16, 2004. In the action, the examiner rejected claims 1, 4-8, 10-12, 14, 19, 23, 33, and 52 allegedly for non-enablement, claims 33, 30 and 52 as allegedly indefinite, and claims 1, 4-6, 7, 8, 10-12, 14, 19, 23, 33 and 52 for obviousness reasons.

Applicants respectfully request reconsideration of the present application in view of the foregoing amendments and in view of the reasons that follow. The present amendment does not raise new matter.

Status of the Claims

In this response, applicants amended claims 7, 12, 23, 33, 50 and 52, and added new claims 65-66. Support for amended claims can be found throughout the specification, and in particular, in originally filed claims 7, 12, 50 and 52 (amended claims 7, 12, 50 and 52, respectively), and on page 36, lines 11-16 (claims 23 and 52). Claim 33 was amended to more clearly recite the present invention and support for the amendment can be found throughout the specification and in the state of the art as of the priority date. Support for new claims 64-65 can be found in the third example of the specification. Upon entry of this amendment, claims 1, 4-8, 10-12, 14, 19, 23, 33, 50, 52 and 64-65 will be under examination.

35 U.S.C. 112, first paragraph

Enablement

Claims 1, 4-8, 10-12, 14, 19, 23, 33 and 52 were rejected under 35 U.S.C. § 112, first paragraph. The claims were rejected because the specification allegedly “does not provide enablement for any transgenic mouse comprising a cell comprising claimed transgenes” or “a transgenic mouse without any phenotype.” Office action at 3. Regarding phenotype, the examiner maintained that “the phenotype of the transgenic mouse is a critical element for the enablement of the claimed invention because one of skill[] in the art would not know how to use a mouse with the claimed genotype but has no phenotype.” *Id.*

Applicants respectfully assert that a phenotype can be defined as a visible observable or detectable characteristic of an organism resulting from an interaction of its genotype with the environment.

This definition is well-known in the art and can be inferred from, e.g., the following sources:

a) www.ndif.org/Terms/phenotype.html : “The entire physical, biochemical , and physiological makeup of an individual as determined both genetically and environmentally, as opposed to genotype.”

b) www.for.gov.bc.ca/hfd/library/documents/glossary/P.htm : “An organism as observed by its visible characteristics, resulting from the interaction of its genotype with the environment.”

c) http://spaceflight.nasa.gov/history/shuttle-mir/references/glossaries/science/sc-gloss-n_s.htm : “A phenotype is the visible properties of an organism that are produced by the interaction of the genes and the environment.”

The term “visible” is historic as the concept of phenotype has evolved considerably since the first distinction between genotype and phenotype (Johannsen, Elements of Heredity, 1909). A simple illustration would be the widely accepted use of blood group phenotype. Blood group phenotypes are clearly not “visible” in the Johannsen’s sense but are readily observable or detectable by the use of suitable instruments and reagents.

All of the mice of the present invention have a predictable primary phenotype which allows one of skill in the art to detect such mice and to distinguish them from wild-type mice so as to investigate secondary phenotypes that are caused by the primary induced genetic lesion. In fact, the primary phenotype results precisely from the interaction of the genotype of the mice, as defined in the presently claimed invention, and their treatment by synthetic anti-estrogens (environment).

Furthermore, the working examples in the specification describe a method for observing/detecting the primary phenotype resulting from synthetic estrogen treatment. For example, the lack of a defined genomic DNA segment in a specific tissue or cell type is detectable by the use of DNA hybridization techniques or PCR analyses.

Moreover, the specification describes not only adipocyte selective ablation of RXR α using the CRE-ER^{T2} recombinase (Figures 5 and 6), but also keratinocyte selective

ablation of RXR α (Figures 1D, 2K and 2L) and SNF2 β (Figure 4B). Also see Li *et al.*, (2000), Imai *et al.* (2001), Weber *et al.* (2002), Chapellier *et al.* (2002) and Imai *et al.* (2004), which provide additional examples of the claimed system of selective ablation in other tissues (references appended in Appendix B). The attached declaration at paragraph 7 also provides successful ablation of a “floxed” gene in hepatocytes (Appendix A).

Therefore, a skilled artisan would know how to make and use the claimed mice of the present invention.

35 U.S.C. 112, second paragraph

The examiner also rejected claims 33, 50 and 52 under 35 U.S.C. § 112, second paragraph as allegedly indefinite. Accordingly, applicants amended the claims to more clearly recite the present invention. Support for the amendments can be found in the originally filed claims in the present specification, and in the general knowledge in the art at the priority date. See, e.g., in Sedivy, J.M., and Joyner, A.L. Gene Targeting (1992) by W.H. Freeman and Company, USA, especially Chapters 6 and 7 (Appendix C).

35 U.S.C. 103

Claims 1, 4, 5, 7, 8, 10, 11, 19 and 33 were rejected under 35 U.S.C. § 103 as allegedly obvious over Feil *et al.* (*PNAS*, 93:10887 (1996)), In addition, claim 6 was rejected as allegedly obvious over Feil, in view of Schwenk *et al.* (*Nucleic Acids Res.*, 26:1427 (1998)). Lastly, claims 12, 14, 23 and 52 were rejected as allegedly obvious over Feil, in view of Indra *et al.* (*Nucl. Acid Res.* 27:4324-4327 (1999)), Ross *et al.* (*PNAS*, 87:9590 (1990)) and Tontonoz *et al.* (*PNAS*, 94:237 (1997)). Applicants respectfully disagree.

Rejection of the claims over Feil

Claims 1, 4, 5, 7, 8, 10, 11, 19 and 33 were rejected over Feil because “[i]t would have been obvious to one of ordinary skill of art to modif[y] the conditional targeting method taught by Feil *et al.* to have an endogenous gene, such as RXR α or intergenic sequence flanked by loxP sites (instead of a test gene).” Office action at 6.

As previously submitted, and as provided in paragraph 6 of the attached declaration, Feil only describes deletion of floxed DNA segments located within exogenous synthetic reporter transgenes. At best, it would have been obvious to try the method of Feil for inactivating an endogenous floxed gene but there would have been no reasonable

expectation of success in obtaining a system that works with 100% deletion efficiency. See, for example, the teachings of Schwenk, which was published two years after Feil yet only described an 80% deletion efficiency at best, with variable and incomplete excision efficiency, and with high doses of tamoxifen.

Furthermore, if a skilled artisan would have been motivated to modify the teachings of Feil as indicated by the examiner, and if making this modification was “routine experimentation” since allegedly “[t]he level of skill in the art is high” (office action at 6), then it is unclear how applicants were the first to have published a method for efficient life stage and tissue specific modification of an endogenous gene in its natural environment, and this is four years after Feil. Indeed, applicants were the first to publish on the system described in the application (Li et al., *Nature* 407:633-636 (2000)), 4 years after Feil 1996. Clearly, extraordinary skill was required to obtain the present invention based on the teachings of Feil. As such, Feil does not render the present invention obvious.

Rejection of the claims over Feil and Schwenk

Claim 6 was rejected as allegedly obvious over Feil, and further in view of Schwenk because “it would have been obvious to one of ordinary skill of art to use any linker for attachment of ER ligand binding domain to Cre recombinase based on the teaching of Feil et al. and Schwenk et al. because the linker does not affect the conditional induction of Cre recombinase.” Applicants respectfully disagree.

For the reasons discussed above, Feil does not describe the present invention and Schwenk does not cure the deficiencies in the Feil reference. In other words, while Schwenk discloses a Cre-ER fusion protein to delete a floxed DNA segment from an endogenous chromosomal gene, the efficiency by which this occurs is at best 80%. Therefore, it is unexpected that the present invention could achieve a system which exhibits tight temporal control of the generation of cell type/tissue-specific somatic mutations with 100% efficiency. Accordingly, the combination of Feil and Schwenk do not render the presently claimed invention obvious.

Rejection of the claims over Feil, Indra, Ross and Tontonoz

Claims 12, 14, 23 and 52 were rejected over Feil, in view of Indra, Ross and Tontonoz because it would allegedly have been obvious to “make a transgenic mouse with selective RXR α disruption in adipose tissue based on the combined teaching of Indra et al.

and Feil et al., Ross et al. and Tontonoz et al.” Office action at 9. Applicants respectfully disagree.

For the reasons discussed above, Feil does not teach the present invention. The deficiencies of Feil are not described in the other cited references. For example, Indra only describes fusion proteins that could be used to delete floxed DNA segments located within exogenous transgenes.

Ross et al. teach that a transgene can be selectively expressed in adipocytes using the aP2 promoter. It does not teach that a Cre-ER fusion protein (especially Cre-ER^{T2}), when expressed under the control of this promoter, will induce an efficient deletion of floxed DNA segments of endogenous genes after Tamoxifen treatment of transgenic mice.

Tontonoz et al. teach that PPAR γ and RXRs play a regulatory role in adipocyte differentiation, but do not disclose the role of RXRs and PPAR γ in mature adipocytes of the mouse. Indeed, they did not show that RXR α in adipocytes of adult mice controls lipid metabolism and glucose homeostasis, as shown in our application. Moreover, using aP2-Cre-ER^{T2} mice, we recently demonstrated that PPAR γ and RXRs play a crucial role in mature adipocyte survival (Imai *et al.*, *Proc. Natl. Acad. Sci. U. S. A.*, 101, 4543 – 4547 (2004).)

CONCLUSION

Applicants respectfully request reconsideration of the present application in view of the foregoing amendments and arguments.

It is respectfully urged that the present application is now in condition for allowance. Early notice to that effect is earnestly solicited.

The examiner is invited to contact the undersigned by telephone if it is felt that a telephone interview would advance the prosecution of the present application.

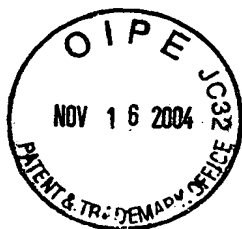
Respectfully submitted,

Date November 16, 2004

FOLEY & LARDNER LLP
Washington Harbour
3000 K Street, N.W., Suite 500
Washington, D.C. 20007-5109
Telephone: (202) 672-5569
Facsimile: (202) 672-5399

By *Kristel Schur* *reg No. 55,600*

for Stephen B. Maebius
Attorney for Applicant
Registration No. 35,264



Pierre CHAMBON
CURRICULUM VITAE

Born : February 7, 1931 - Mulhouse (France)

Marital status : Married - 3 children

Institutional address : Institut Clinique de la Souris (ICS) and
Institut de Génétique et de Biologie Moléculaire et Cellulaire (IGBMC)
BP 10142, 67404 ILLKIRCH CEDEX (France)
Tel. 33+(0)3 88653213/15/10 - Fax 33+(0)3 88653203

University degrees : M.D. - thesis 1958, Strasbourg
Licence ès Sciences 1960, Strasbourg
Agrégation (Medical Biochemistry), 1961.

Professional experience: 1956-1961 - Research Assistant, Institut de Chimie
Biologique, Medical School, Strasbourg

1962-1966 - Associate Professor - same
institution.

1966-1967 - Sabbatical year, sponsored by the
International Union against Cancer, at Stanford
University Medical School (Dept. Biochemistry /
Prof. A. Kornberg).

1968-1991 - Professor of Biochemistry,
Institut de Chimie Biologique, Faculté de
Médecine, Strasbourg.

1992-1993 - Professor at the Institut
Universitaire de France, Faculté de Médecine,
Université Louis Pasteur, Strasbourg

November 1993 to August 2002 - Professor at the Collège de France - Paris

September 2002 - Honorary Professor at the Collège de France, Paris and Professor emeritus at the Faculté de Médecine, Université Louis Pasteur, Strasbourg

Research Responsibilities and Administration :

- Director of the Laboratoire de Génétique Moléculaire des Eucaryotes (LGME) of the CNRS (Centre National de la Recherche Scientifique) from May 1st, 1977 to August 2002
- Director of the Unité 184 de Biologie Moléculaire et de Génie Génétique of the INSERM (Institut National de la Santé et de la Recherche Médicale) from September 1st, 1978 to August 2002
- Director of the Institut de Génétique et de Biologie Moléculaire et Cellulaire (IGBMC), CNRS/ INSERM/ Université Louis Pasteur/ Collège de France, from September 15th, 1994 to August 2002. Director emeritus since September 1st, 2002.
- Chairman of the Conseil Scientifique du Programme National de la Génomique (1999-2002)
- Director of the Génopole Strasbourg Alsace-Lorraine, since 1999
- Director of the Institut Clinique de la Souris (ICS ; Centre de Ressources du CNRG-Génopole de Strasbourg), since June 2002

Other activities :

Editorial Boards :

- Genes and Development
- Cell
- Current Opinion in Endocrinology
- The Breast
- International Journal of Cancer
- Biochimie
- Molecular Medicine
- Journal of Clinical Investigation
- FASEB Journal
- Molecular Cell
- Genome Biology
- IUBMB Life

Scientific Boards

- Founder and Member of the Board of Administrators of the Strasbourg School of Biotechnology (now European School of the Upper Rhine)
- Member of the Council of Scientific Advisers - ICGEB (Trieste)
- Member of the Eurolife Network

Applied Research

- Exonhit Scientific Advisory Board
- CareX : Member of the board
- Cytochroma : Scientific Advisory Board

Academy memberships and Honors :

- Member of the European Molecular Biology Organization, since May 1975.
- Foreign Member of the National Academy of Sciences (USA), since April, 1985.
- Foreign Honorary Member of the American Academy of Arts and Science (USA), since May 1985.
- Member of the Académie des Sciences, Paris (Section : Cell Biology / Molecular Biology), since June 1985 (previously correspondant member since 1977).
- Foreign Member of the Royal Swedish Academy of Sciences, (Sweden) since March, 1987.
- Correspondant member of the Académie Royale des Sciences of Liège (Belgium), since August 1st, 1979.
- Foreign honorary member of the Académie Royale de Médecine of Belgium, since November 1987.
- Member of the Academia Europaea, since 1988.
- Honorary Member of the Chinese Society of Genetics (Taipei) since March 1989.
- Fellow of the American Association for the Advancement of Science , since February 1995.
- Fellow of the American Academy of Microbiology, since August 1992.
- Fellow of the New York Academy of Sciences, since October 1996
- Honorary Member of the German Society for Cell Biology, November 2001.

Honors

- Dr. Honoris Causa, University of Liège, Belgium, June 1985.
- Honorary Doctor of Philosophy, Sapporo Medical University - Japan, October 1999.
- Dr. Honoris Causa ès Sciences, University of Lausanne, Switzerland, October 2001.
- Dr. Honoris Causa, Universidad Autonoma de Nuevo Leon, Monterrey Mexico, December 2002.

Other Honors

- Commandeur in l'Ordre National de la Légion d'Honneur - France
- Commandeur in l'Ordre National du Mérite - France

Scientific Prizes

- "Prix Rosen" in Cancer Research, awarded by the Fondation pour la Recherche Médicale, Paris, 1976.
- Gold Medal of the Centre National de la Recherche Scientifique (CNRS), Paris, 1979.
- Louis and Bert Freeman Foundation Prize for Research in Biochemistry of the New York Academy of Science, 1981.
- Richard Lounsbery Prize of the National Academy of Sciences (USA) and the Académie des Sciences (France), 1982.
- Charles Oberling Prize in Cancer Research, Paris, 1986.
- The Harvey Price of Science and Technology, awarded by TECHNION (Israel Institute of Technology), Haifa, 1987.
- Prix Griffuel of the Association pour la Recherche sur le Cancer, Paris, 1987.
- Prix Henry et Mary-Jane Mitjavile of the Académie Nationale de Médecine, Paris, 1987.
- King Fayçal International Prize in Science, Riyadh, 1988.
- Sir Hans Krebs Medal, Federation of European Biochemical Societies, 1990.
- Prix Roussel, Paris, 1990.
- Prix Louis Jeantet de Médecine 1991, Genève, 1991
- Grand Prix of the French Foundation for Medical Research, Paris, 1996
- Robert A. Welch Award in Chemistry, Houston, 1998
- 1999 Louisa Gross Horwitz Prize (Columbia University)
- 1999 AFRT Prize (Association Française pour la Recherche Thérapeutique), Paris, France.
- 2003 March of Dimes Prize in Developmental Biology, Seattle, 2003
- 2003 Alfred P. Sloan Jr. Prize, General Motors Cancer Research Foundation, Washington, 2003.

Lectureships

- Dunham Lecturer, Harvard University Medical School, April 20-30, 1983.
- Gregory Pincus Memorial Lecture, The Laurentian Hormone Conference, Mont-Tremblant, Canada, August 30 - September 2, 1983.
- Charles B. Smith's Visiting Professorship, Memorial Sloan-Kettering Cancer Center, New York, USA, February 20-25, 1984.
- 1st J.F. Volker Visiting Professorship, University of Alabama, Schools of Medicine and Dentistry, Birmingham, USA, September 15-18, 1985.
- Triton Lecturer at the International Breast Cancer Research Conference of the International Association for Breast Cancer Research, Miami, USA, March 2-4, 1987.
- Steenbock Lecturer in Life Sciences, University of Wisconsin/Madison College of Agricultural and Life Sciences, Madison, USA, May 21-22, 1987.
- 1987 Guest Lecturer of the Japan Foundation for Promotion of Cancer Research, National Cancer Institute, Tokyo and Osaka, Japan, September 12-23, 1987.
- 7th Smith, Kline and French Lecturer, Temple University, Medical School, Philadelphia, USA, December 8-9, 1987.
- Annual Abbott Lecture in Molecular Biology, University of Illinois, College of Medicine, Chicago, USA, May 26-27, 1988
- The Jacques Monod Lecture at the XVth International Congress of Genetics, Toronto, Canada, August 1988.
- First Karlson Lecture, University of Marburg, Germany, October 12, 1988.
- 1988 NOVO Lecture, Danish Biochemical Society, Copenhagen, Denmark, December 14, 1988.
- XIV Lorenzini Annual Lecture, Fondazione G. Lorenzini, Milan, Italy, April 20, 1989.
- Herman Beerman Lecture, Society for Investigative Dermatology, Washington, USA, April 29, 1989.
- Susan Swerling Lecture, Dana Farber Cancer Institute, Boston, USA, May 2, 1989.
- The Samuel Roberts Noble Memorial Address, 2nd Internat. Conf. on "Transglutaminases and Protein Cross-Linking Reactions", Cannes, France, June 26, 1990
- Sir Hans Krebs Lecture "Nuclear Receptors as Inducible Transcriptional Enhancer Factors", 20th FEBS Meeting, Budapest, Hungary, August 19, 1990.
- The Markey Lectures, Harvard University Medical School, Boston, USA, October 31 and November 1, 1990.

- The Merck Frosst Canada lecture series: Frontiers in Molecular Biology "Retinoid receptors and binding proteins in development", Montreal, Canada, June 17, 1992.
- The Merck US Lecture "Cancer Genes: Retinoid Receptors in Development and Acute Promyelocytic Leukemia", Stanford University School of Medicine, Stanford, USA, September 21, 1992.
- Tufts University, School of Medicine "1993 Earl P. Charlton Lecture", Boston, USA, November 8, 1993.
- Karolinska Research Lectures at Nobel Forum, Karolinska Institutet, Stockholm, Sweden, April 20, 1995
- UCSD/American Heart Association - Bugher Foundation - Center for Molecular Biology 1994-1995 Lecture Series, San Diego, USA May 30, 1995
- The 1995 Kligman Lecture - Skin Pharmacology Society Annual Meeting. Vienna, Austria, November 2nd, 1995.
- The 11th Hans L. Falk Memorial Lecture - National Institute of Health, Research Triangle Park, N.C., USA, December 7, 1995.
- Imperial Cancer Research Fund "Special Seminars", London, UK, May 16th, 1996.
- Saitama Medical School, Dept. of Biochemistry, Prof. M. Muramatsu. Honorary Lecture - Saitama, Japan, October 24, 1996.
- Howard Hughes Honorary Lecture, Dept. of Molecular Biophysics & Biochemistry, Yale University, New-Haven, USA, October 13, 1997.
- Zeneca plenary Lecture - EMBL Transcription meeting, Heidelberg, Germany, August 22-26, 1998
- Boehringer Ingelheim Lecture, Institut für Physiologische Chemie & Pathochemie, Johannes Gutenberg Universität, Mainz, Germany, February 12, 1998
- Jean Brachet Memorial Lecture, 10th International Conferences of the International Society of differentiation, Houston, USA, October 3-7, 1998
- The "1998 Welch Award Lecture", Welch Conference on "New Biochemistry, macromolecular machines", Houston, USA, October 26-27, 1998
- Baylor College of Medicine, Distinguished Guest Lecture, Houston, USA, October 28, 1998
- Howard Hughes Medical Institute, Keynote speaker, Chevy Chase, USA, March 21-24, 1999
- EMBO Workshop on Structure and Function of Nuclear Receptors, co-organizer, Villefranche-sur-Mer (Nice), France, May 25-27, 1999. Plenary Lecture
- Forefront Meeting of the International Society of Nephrology, "News in Aldosterone Action", Paris-Chantilly, France, August 15-18 1999. Keynote Speaker

- 6th International congress of Hormones & Cancer - Jerusalem, Israel, September 5-9 1999. Plenary Lecture
- ERRG (European Retinoid Research Group) RETINOIDS'99, organizer, Bischenberg Congress Center (Strasbourg), France, September 26-30, 1999. Plenary Lecture
- 6th IUBMB Conference "Life Science for the next millennium" - Seoul, Korea, October 10-14, 1999. Plenary Lecture
- Journées Dermatologiques de Paris - Paris, France, December 1-4, 1999. Plenary Lecture
- Horwitz Prize Lecture, Columbia University, College of Physicians and Surgeons, New York, USA, October 23, 2000.
- 11th International Congress of Endocrinology, ICE2000. Sydney, Australia, November 1st, 2000. The Harrison Memorial Lecture: Dissection of the retinoid signalling pathway.
- Paul Basset Memorial Meeting "Matrix metalloproteinases in physiological and pathological processes", organizing committee, IGBMC, Illkirch, France, November 24-25, 2000. Plenary lecture
- Meyenburg Stiftung Lecture (Joint International Journal of Cancer), Deutsches Krebsforschungszentrum, Heidelberg, Germany, January 30, 2001.
- EMBO Workshop on Nuclear Receptor Structure and Function, Erice Italy, May 12-15, 2001, Plenary Lecture.
- First Joint French-German Congress on Cell Biology. Strasbourg, November 7-9, 2001. Plenary Lecture and Honorary Membership of the Deutsche Gesellschaft für Zellbiologie,
- Inaugural CNIO Symposium on « Basic and translational cancer research », Madrid, Espagne, February 6-9, 2002. Plenary Lecture.
- First International Nuclear Receptor Meeting, Kyoto, Japan, February 28-March 3, 2002. Keynote speaker
- Opening Symposium Saitama Medical School, Saitama, Japan, April 10-12, 2002. Plenary Lecture
- Keystone Symposium "Nuclear Receptor Superfamily", Snowbird, USA, April 13-19, 2002. Co-organizer and Plenary Lecture
- First International Congress on transthyretin in health & disease, Strasbourg, France, April 22-25, 2002. Plenary lecture
- Congrès Annuel de Recherche Dermatologique, Strasbourg, France, May 23-25, 2002. Plenary Lecture.
- FASEB Summer Conference on Retinoids, Tucson (USA), June 22-27, 2002, James Olson Special Lecture
- 20th World Congress of Dermatology, Paris (France), July 1-5, 2002. Plenary Lecture

- Inaugural Symposium of the Center for Genomic Regulation (CRG) « Genes, Cells and Disease », Barcelone (Espagne), October 25, 2002. Plenary lecture
- -International Centre for Genetic Engineering and Biotechnology, New Delhi, Inde, November 12, 2002. Special lecture
- 13th Symposium on Retinoids, Tokyo (Japon), November 14-15, 2002. Plenary lecture
- XXVII Annual Meeting of the Mexican Human Genetic Society, Veracruz (Mexique), November 23, 2002. Closing Lecture.
- Strasbourg ULP - Weizmann Symposium, January 13-15, 2003. Plenary lecture
- 2003 Miami Nature Biotechnology Winter Symposium. 50 years on: from the double helix to molecular medicine, Miami (USA), Feb. 2-5, 2003. The Feodor Lynen Lecture.
- 2003 March of Dimes Lecture, Seattle (USA), May 5, 2003.
- 50th anniversary symposium "Frontier Research in IMCB: its relation to the world scene", Tokyo (Japan), May 9, 2003. Plenary talk.
- Annual Meeting of the 76th Japan Endocrine Society Meeting, Yokohama (Japan), May 10, 2003. Special lecture.
- EMBO Conference "Biology of Nuclear Receptors" (Organiser) Villefranche-sur-Mer (France), June 4-7, 2003.
- General Motors Cancer Research Foundation Scientific Conference & Awards Ceremony, Washington, D.C. (USA), June 10-11, 2003. Laureate Lecture.
- Special FEBS 2003 Meeting "on Signal Transduction", Brussels (Belgium), July 3-8, 2003. Sir Hans Krebs Lecture.

Publications (almost 700)

Major Publications.

1. P. Walter, S. Green, G. Greene, A. Krust, J.M. Bornert, J.M. Jeltsch, A. Staub, E. Jensen, G. Scarce, M. Waterfield, and P. Chambon: Cloning of the human estrogen receptor cDNA. *Proc. Natl. Acad. Sci. USA* (1985) **82**, 7889-7893.
2. S. Green, P. Walter, V. Kumar, A. Krust, J.M. Bornert, P. Argos and P. Chambon: The human oestrogen cDNA: sequence, expression and homology to v-erbA. *Nature* (1986) **320**, 134-139.
3. S. Kato, H. Endoh, T. Masuhiro, T. Kitamoto, S. Uchiyama, T. Sasaki, S. Masuhige, Y. Gotoh, E. Nishida, H. Kawashima, D. Metzger, and P. Chambon: Activation of the estrogen receptor through phosphorylation by mitogen-activated protein kinase. *Science* (1995) **270**, 1491-1494.
4. S. Green, and P. Chambon: Oestradiol induction of a glucocorticoid-responsive gene by a chimeric receptor. *Nature* (1987) **325**, 75-78.
5. M. Petkovich, N.J. Brand, A. Krust and P. Chambon: A human retinoic acid receptor which belongs to the family of nuclear receptors. *Nature* (1987) **330**, 444-450.
6. P. Chambon: A decade of molecular biology of retinoic acid receptors. *FASEB J.* (1996) **10**, 940-954.
7. M. Leid, P. Kastner, R. Lyons, H. Nakshatri, M. Saunders, T. Zacharewski, J.Y. Chen, A. Staub, J.M. Garnier, S. Mader and P. Chambon: Purification, cloning and RXR identity of the HeLa cell factor with which RAR or TR heterodimerizes to bind target sequences efficiently. *Cell* (1992) **68**, 377-395.
8. P. Kastner, M. Mark and P. Chambon: Nonsteroid nuclear receptors: what are genetic studies telling us about their role in real life? *Cell* (1995) **83**, 859-869.
9. B. Mascres, M. Mark, A. Dierich, N. Ghyselinck, P. Kastner, and P. Chambon : The RXR α ligand-dependent activation function 2 (AF-2) is important for mouse development. *Development* (1998) **125**, 4691-4707.
10. W. Bourguet, M. Ruff, P. Chambon, H. Gronemeyer, and D. Moras: Crystal structure of the ligand binding domain of the human receptor RXR α . *Nature* (1995) **375**, 377-382.
11. J. P. Renaud, N. Rochel, M. Ruff, V. Vivat, P. Chambon, H. Gronemeyer and D. Moras: Crystal structure of the RAR α ligand-binding domain bound to all-trans retinoic acid. *Nature* (1995) **378**, 681-689.
12. J.M. Wurtz, W. Bourguet, J.P. Renaud, V. Vivat, P. Chambon, D. Moras, and H. Gronemeyer : A canonical structure for the ligand-binding domain of nuclear receptors. *Nature Struct. Biology* (1996) **3**, 87-94.
13. R. Taneja, C. Rochette-Egly, J.L. Plassat, L. Penna, M.P. Gaub, and P. Chambon : Phosphorylation of activation functions AF-1 and AF-2 of RAR α and RAR β is indispensable for differentiation of F9 cells upon retinoic acid and cAMP treatment. *EMBO J.*, (1997) **16**, 6452-6565.
14. W. Krezel, N. Ghyselinck, T. Abdel-Samad, V. Dupé, P. Kastner, E. Borrelli, and P. Chambon : Impaired locomotion and dopamine signaling in retinoid receptor mutant mice. *Science* (1998) **279**, 863-867.
15. K. Niederreither, V. Subbarayan, P. Dollé, and P. Chambon : Embryonic retinoic acid synthesis is essential for early mouse post-implantation development. *Nature Genetics* (1999) **21**, 444-448.
16. R. Feil, J. Brocard, B. Mascres, M. LeMeur, D. Metzger, and P. Chambon: Ligand-activated site-specific recombination in mice. *Proc. Natl. Acad. Sci.* (1996) **93**, 10887-10890.
17. M. Li, A.K. Indra, X. Warot, J. Brocard, N. Messaddeq, S. Kato, D. Metzger and P. Chambon. Skin abnormalities generated by temporally-controlled RXR α mutations in adult mouse epidermis. *Nature* (2000) **407**, 633-636.
18. S. Abu-Abed, P. Dollé, D. Metzger, B. Beckett, P. Chambon, and M. Petkovich : The retinoic acid-metabolizing enzyme, CYP26A1, is essential for

- normal hindbrain patterning, vertebral identity and development of posterior structures. *Gene Develop.*, (2001) **15**, 226-240.
19. T. Imai, M. Jiang, P. Chambon and D. Metzger : Impaired adipogenesis and lipolysis in the mouse upon selective ablation of the retinoid X receptor α mediated by a tamoxifen-inducible chimeric Cre recombinase (Cre-ER^{T2}) in adipocytes. *Proc. Natl. Acad. Sci.* (2001) **98**, 224-228.
 - 20 D. Metzger, A. Indra, M. Li, B. Chapellier, C. Calleja, N.B. Ghyselinck and P. Chambon: Targeted conditional somatic mutagenesis in the mouse: temporally-controlled knock out of retinoid receptors in epidermal keratinocytes. *Methods in Enzymology* (2002) in press.

Major Review Articles.

STRUCTURAL AND FUNCTIONAL PROPERTIES OF THREE MAMMALIAN NUCLEAR DNA-DEPENDENT RNA POLYMERASES.

5th Karolinska Symposium, Stockholm, Sweden

Acta Endocrinol. Vol. **168**, 1972, pp. 222-246.

(in collaboration with: F. Gissinger, C. Kédinger, J.L. Mandel, M. Meilhac and P. Nuret)

EUKARYOTIC RNA POLYMERASES.

"The Enzymes", Vol. **X**, 1974, pp. 261-331.

Ed. P.D. Boyer, Academic Press, New York.

ANIMAL NUCLEAR DNA-DEPENDENT RNA POLYMERASES.

"The Cell Nucleus", Vol. **III**, 1974, pp. 269-308.

Ed. H. Busch, Academic Press, New York.

EUKARYOTIC RNA POLYMERASES.

"Annual Review of Biochemistry", Vol. **44**, 1975, pp. 613-633.

Eds. Ann. Rev. Inc., Palo Alto, California, USA.

CHROMATIN 1977 : STRUCTURE AND FUNCTION.

Molecular Biology of eukaryotic genome is coming of age :

Summary of the 42nd Cold Spring Harbor Symp. on Quantitative Biology. CSHSQB, Vol. **42**, 1977, pp. 1209-1234.

Ed. Cold Spring Harbor Laboratory, New York.

THE OVALBUMIN GENE : AN AMAZING GENE IN 8 PIECES.

Trends in Biochemical Sciences, Vol. **3**, 1978, pp. 244-247.

(in collaboration with: P. Kourilsky)

STRUCTURE OF TRANSCRIBING CHROMATIN.

"Progress in Nucleic Acids Res. and Molecular Biology", Vol. **24**, 1980, pp.

1-55. Ed. W. Cohn, Academic Press, New-York.

(in collaboration with D. Mathis and P. Oudet)

ORGANIZATION AND EXPRESSION OF EUKARYOTIC PROTEIN-CODING NUCLEAR SPLIT GENES.

"Annual Review of Biochemistry", Vol. **50**, 1981, pp. 349-383.

Eds. Ann. Rev. Inc., Palo Alto, California, USA.

SPLIT GENES.

"Scientific American", Vol. **244**, 1981, pp 48-59.

PROMOTER ELEMENTS OF GENES CODING FOR PROTEINS AND MODULATION OF TRANSCRIPTION BY OESTROGENS AND PROGESTERONE.

"Recent Progress in Hormone Research - Proceedings of the Laurentian

Hormone Conference", Vol. 40 (Ed. R.O. Greep) 1984, Acad. Press, pp. 1-42

THE SV40 EARLY PROMOTER.

"Molecular Aspects of the Papovavirus", Y. Aloni Ed., Martinus Nijhoff, Pays-Bas, 1987, pp. 53-83.

(in collaboration with M. Zenke et A. Wildeman)

A SUPERFAMILY OF POTENTIALLY ONCOGENIC HORMONE RECEPTORS.

Nature, 1986 324, 615-617.

(in collaboration with S. Green)

STRUCTURE AND FUNCTION OF THE OESTROGEN RECEPTOR AND OTHER MEMBERS OF THE NUCLEAR RECEPTOR FAMILY.

Steroid Receptors and Disorders : Cancer, Bone and Circulatory Disorders, Sheridan, Blum, Trachtenberg, Eds., Marcel Dekker Inc., New York, (1988), pp. 153-189 (in collaboration with H. Gronemeyer, S. Green, V. Kumar and J.M. Jeltsch).

NUCLEAR RECEPTORS ENHANCE OUR UNDERSTANDING OF TRANSCRIPTION REGULATION.

Trends in Genetics (1988) 4, 309-314

(in collaboration with S. Green).

THE OESTROGEN RECEPTOR : FROM PERCEPTION TO MECHANISM

Nuclear Hormone Receptors, Malcom Parker (ed), Academic Press, (1991), 15-33.

(in collaboration with S. Green).

THE p52 GENE, mRNA AND PROTEIN: A POTENTIAL MARKER FOR HUMAN BREAST CANCER.

Cancer Cells (1990) 2, 269-274.

(in collaboration with M-C. Rio).

RETINOIC ACID RECEPTORS IN THE EMBRYO.

Seminars in Developmental Biology. (1991) 2, 153-159.

(in collaboration with E. Ruberte, P. Kastner, P. Dollé, A. Krust, P. Leroy, C. Mendelsohn, and A. Zelent).

LE RECEPTEUR DES OESTROGENES : DE SA STRUCTURE A SA FONCTION.

Annales de L'Institut Pasteur/actualités (1992)

Elsevier, Paris (1992) 1, pp 51-61.

MULTIPLICITY GENERATES DIVERSITY IN THE RETINOIC ACID SIGNALLING PATHWAYS

Trends in Biochemical Sciences, (1992) 17, 427-433.

(in collaboration with M. Leid and P. Kastner).

THE ROLE OF NUCLEAR RETINOIC ACID RECEPTORS IN THE REGULATION OF GENE EXPRESSION.

Vitamin A in Health and Disease, ed. R. Blomhoff, Marcel Dekker Inc. (1994) pp.189-238.

(in collaboration with P. Kastner and M. Leid).

STROMELYSIN-3 IN STROMAL TISSUE AS A CONTROL FACTOR IN BREAST CANCER BEHAVIOUR.

In Cancer Supp. (1994) 74, 1045-1049.

(in collaboration with P. Basset, C. Wolf, N. Rouyer, J.P. Bellocq, and M.C. Rio)

THE RETINOID SIGNALING PATHWAY: MOLECULAR AND GENETIC ANALYSES.

In "Seminars in Cell Biology: Nuclear Hormone Receptors". (1994) 5, 115-125.

ALTERATION OF HOX GENE EXPRESSION IN THE BRANCHIAL REGION OF THE HEAD CAUSES HOMEOTIC TRANSFORMATIONS, HINDBRAIN SEGMENTATION DEFECTS AND ATAVISTIC CHANGES.

Seminars in Developmental Biol. (1995) 6, 275-284.
(in collaboration with M. Mark, and F.M. Rijli)

ROLES OF RETINOIC ACID RECEPTORS AND OF HOX GENES IN THE PATTERNING OF THE TEETH AND OF THE JAW SKELETON.

Int. J. Dev. Biol. (1995) 39, 111-121.
(in collaboration with M. Mark, D. Lohnes, C. Mendelsohn, V. Dupé, J.L. Vonesch, P. Kastner, F. Rijli, and A. Bloch-Zupan)

NONSTEROID NUCLEAR RECEPTORS : WHAT ARE GENETIC STUDIES TELLING US ABOUT THEIR ROLE IN REAL LIFE?

In CELL - reviews (1995) 83, 859-869.
(in collaboration with P. Kastner, and M. Mark)

THE NUCLEAR RECEPTOR SUPERFAMILY: THE SECOND DECADE.

In Cell (1995) 83, 835-839.
(in collaboration with D.J. Mangelsdorf, C. Thummel, M. Beato, P. Herrlich, G. Schütz, K. Umesono, B. Blumberg, P. Kastner, M. Mark, and R.M. Evans).

A DECADE OF MOLECULAR BIOLOGY OF RETINOIC ACID RECEPTORS.

In The FASEB J. "The Retinoid Revolution". W.J. Whelan, ed. (1996) vol. 10, 949-954.

SUR LA GENETIQUE MOLECULAIRE.

(integral text of inaugural conference at the Collège de France in June 1994)
In "Commentaire", Plon ed. (1996), 73, 5-21.

HOMEBOX GENES IN EMBRYOGENESIS AND PATHOGENESIS:

Pediat. Res. (1997) 42, 421-429.
(in collaboration with M. Mark and F. Rijli)

GENETIC INTERACTIONS OF HOX GENES IN LIMB DEVELOPMENT: LEARNING FROM COMPOUND MUTANTS.

In: Curr. Opin. Genet. Develop. (1997) 7, 481-487.
(in collaboration with F. Rijli)

RETINOIDS AND MOUSE PLACENTATION.

In: "The Trophoblast Research". A. Carter, V. Dantzer, T. Jansson eds. (1998) 12, 57-76.
(in collaboration with V. Sapin, R.J. Bègue*, B. Dastugue*, and P. Dollé)

MESECTODERM IS A MAJOR TARGET OF RETINOIC ACID ACTION :

Eur. J. Oral Sci., (1998) 106, 24-31.
(in collaboration with M. Mark, N.B. Ghyselinck, P. Kastner, V. Dupé, O. Wendling, W. Krezel and B. Mascrez)

SEGMENTATION AND SPECIFICATION IN THE BRANCHIAL REGION OF THE HEAD: THE ROLE OF THE HOX SELECTOR GENE.

Int. J. Dev. Biol., (1998) **42**, 398-401.

(in collaboration with F. Rijli and A. Gavalas)

CONTROL OF TRANSCRIPTION AND NEUROLOGICAL DISEASES.

Mol. Psychiatry (News & Views) (1999) **4**, 112-114.

(in collaboration with E. Borrelli)

A GENETIC DISSECTION OF THE RETINOID SIGNALING PATHWAY IN THE MOUSE.

Proc. Nutr. Soc., (1999) **58**, 609-613.

(in collaboration with M. Mark, N. Ghyselinck, O. Wendling, V. Dupé, B. Mascres, P. Kastner)

UN RÔLE ESSENTIEL DES RECEPTEURS DE RETINOÏDES AU COURS DU DÉVELOPPEMENT EMBRYONNAIRE PRÉCOCE ET DE LA PLACENTOGÈNESE.

Médecine/Sciences (1999) **15**, 885-887.

(in collaboration with O. Wendling and M. Mark)

NUCLEAR RECEPTORS COORDINATE THE ACTIVITIES OF CHROMATIN REMODELING COMPLEXES AND COACTIVATORS TO FACILITATE INITIATION OF TRANSCRIPTION

Oncogene (2001) **20**, 3047-3054.

(in collaboration with J. Dilworth)

F9 EMBRYOCARCINOMA CELLS: A CELL AUTONOMOUS MODEL TO STUDY THE FUNCTIONAL SELECTIVITY OF RARS AND RXRS IN RETINOID SIGNALING.

Histology and Histopathology (2001) **16**, 909-922.

(in collaboration with C. Rochette-Egly)

DISSECTION GÉNÉTIQUE DE LA FONCTION DE L'ACIDE RETINOÏQUE DANS LA PHYSIOLOGIE DE L'ÉPIDERME

Ann. Dermatol. Venerol. (2002) **129**, 793-799.

(in collaboration with N. Ghyselinck)

TARGETED CONDITIONAL SOMATIC MUTAGENESIS IN THE MOUSE: TEMPORALLY-CONTROLLED KNOCK OUT OF RETINOID RECEPTORS IN EPIDERMAL KERATINOCYTES

Methods in Enzymology (2002) in press.

(in collaboration with D. Metzger)

DISSECTION GÉNÉTIQUE DE LA FONCTION DE L'ACIDE RETINOÏQUE DANS LA PHYSIOLOGIE DE L'ÉPIDERME

Ann. Dermatol. Venerol. (2003) **129**, 793-799.

(in collaboration with N.B. Ghyselinck, B. Chapellier, C. Calleja, A. Kumar Indra, M. Li, N. Messadeq, M. Mark, D. Metzger)

FUNCTIONS OF RARS and RXRS IN VIVO: GENETIC DISSECTION OF THE RETINOID SIGNALING PATHWAY

Pure & Applied Chemistry (2003) in press

(in collaboration with M. Mark)

Pierre CHAMBON

**Publications directly related to the field
of ligand activated fusion Cre-recombinases**

D. METZGER, J. CLIFFORD, H. CHIBA, and P. CHAMBON :
Conditional site-specific recombination in mammalian cells using a ligand-dependent chimeric Cre recombinase.
Proc. Natl. Acad. Sci. (1995) **92**, 6991-6995.

R. FEIL, J. BROCARD, B. MASCREZ, M. LEMEUR, D. METZGER, and P. CHAMBON:
Ligand-activated site-specific recombination in mice.
Proc. Natl. Acad. Sci. (1996) **93**, 10887-10890.

R. FEIL, J. WAGNER, D. METZGER, and P. CHAMBON :
Regulation of Cre recombinase activity by mutated oestrogen receptor ligand-binding domains.
Biochem. Biophys. Res. Commun. (1997) **237**, 752-757.

J. BROCARD, X. WAROT, O. WENDLING, N. MESSADDEQ, J.L. VONESCH, P. CHAMBON, and D. METZGER :
Spatio-temporally controlled site-specific somatic mutagenesis in the mouse.
Proc. Natl. Acad. Sci. (1997) **94**, 14559-14563.

P. CHAMBON, J. BROCARD, N. MESSADDEQ, D. METZGER, J.L. VONESCH, X. WAROT, and O. WENDLING :
Engineering spatio-temporally-controlled somatic mutations in the mouse skin.
In "Excerpta Medica International Congress Series". Symposium on skin:interface of a living system. Elsevier Science H. Tagami, J.A. Parrish, T. Ozawa, eds. (1998) PP.11-19.

J. BROCARD, R. FEIL, P. CHAMBON, and D. METZGER :
A chimeric Cre recombinase inducible by synthetic, but not by natural ligands of the glucocorticoid receptor.
Nucl. Acids Res., (1998) **26**, 4086-4090.

A.K. INDRA, X. WAROT, J. BROCARD, J.M. BORNERT, J.H. XIAO, P. CHAMBON, and D. METZGER :
Temporally-controlled site-specific mutagenesis in the basal layer of the epidermis: comparison of the recombinase activity of the tamoxifen-inducible Cre-ERT and Cre-ERT² recombinases.
Nucl. Acid. Res. (1999) **27**, 4324-4327.

T. IMAI, P. CHAMBON, and D. METZGER :
Inducible site-specific somatic mutagenesis in mouse hepatocytes.
Genesis (2000) **26**, 147-148.

D. METZGER, and P. CHAMBON :
Site-and time-specific gene targeting in the mouse.
Methods (2001) **24**, 71-80.

M. LI, A.K. INDRA, X. WAROT, J. BROCARD, N. MESSADDEQ, S. KATO, D. METZGER, and P. CHAMBON :
Skin abnormalities generated by temporally-controlled RXR α mutations in adult mouse epidermis.
Nature (2000) **407**, 633-636.

T. IMAI, M. JIANG, P. CHAMBON, and D. METZGER :
Impaired adipogenesis and lipolysis in the mouse upon selective ablation of the retinoid X receptor α mediated by a tamoxifen-inducible chimeric Cre recombinase (Cre-ER^{T2}) in adipocytes.
Proc. Natl. Acad. Sci. (2001) **98**, 224-228.

S. KÜHBANDNER, S. BRUMMER, D. METZGER, P. CHAMBON, F. HOFMANN, and R. FEIL :
Temporally controlled somatic mutagenesis in smooth muscle.
Genesis (2000) **28**, 15-22.

T. IMAI, M. JIANG, P. KASTNER, P. CHAMBON, and D. METZGER :
Selective ablation of retinoid X receptor α in hepatocytes impairs their lifespan and regenerative capacity.
Proc. Natl. Acad. Sci. (2001) **98**, 4581-4586.

P. WEBER, D. METZGER, and P. CHAMBON:
Temporally-controlled targeted somatic mutagenesis in the mouse brain
Europ. J. Neurosci. (2001) **14**, 1777-1783.

B. CHAPPELLIER, M. MARK, J.M. GARNIER, M. LEMEUR, P. CHAMBON, and N. B. GHYSELINCK:
A conditional floxed (loxP-flanked) allele for the Retinoic Acid Receptor alpha (RAR α) gene
Genesis (2002) **32**, 85-89.

B. CHAPPELLIER, M. MARK, J. BASTIEN, A. DIERICH, M. LEMEUR, P. CHAMBON, and N. B. GHYSELINCK:
A conditional floxed (loxP-flanked) allele for the Retinoic Acid Receptor beta (RAR β) gene
Genesis (2002) **32**, 91-94.

B. CHAPPELLIER, M. MARK, J.M. GARNIER, A. DIERICH, P. CHAMBON, and N. B. GHYSELINCK:
A conditional floxed (loxP-flanked) allele for the Retinoic Acid Receptor gamma (RAR γ) gene
Genesis (2002) **32**, 95-98.

P. WEBER, M. SCHULER, C. GERARD, M. MARK, D. METZGER, and P. CHAMBON:
Temporally-controlled site-specific mutagenesis in the germ cell lineage of the mouse testis
Biol. Reprod (2002) **68**, 553-559.

D. METZGER, A. INDRA, M. LI, B. CHAPPELLIER, C. CALLEJA, N.B. GHYSELINCK, and P. CHAMBON:
Targeted conditional somatic mutagenesis in the mouse: temporally-controlled knock out of retinoid receptors in epidermal keratinocytes.
Methods in Enzymology (2002) in press.

D.P. LEONE*, S. GENOUD*, S. ATANASOSKI*, R. GRAUSENBURGER*, P. BERGER*, D. METZGER, W.B. MACKLIN*, P. CH, U. SUTER*: Tamoxifen-inducible glia-specific Cre mice for somatic mutagenesis in oligodendrocytes and Schwann cells. Mol. Cell. Neuroscience (2003) 22, 430-440.

27. Chater, N. Reconciling simplicity and likelihood principles in perceptual organization. *Psychol. Rev.* 103, 566–581 (1996).

Supplementary information is available on Nature's World-Wide Web site and as paper copy from the London editorial office of Nature.

Acknowledgements

Supported in part by a grant from the National Science Foundation. I thank S. J. Hanson, W. A. Richards, J. Tenenbaum and P. Tremoulet for helpful comments, and M. Balaban, E. Barenholtz, D. Berse, N. Folsom-Kovarik, J. Sutton and P. Tremoulet for assistance in data collection.

Correspondence and requests for materials should be addressed to J. F. (e-mail: jacob@rucss.rutgers.edu).

Skin abnormalities generated by temporally controlled RXR α mutations in mouse epidermis

Mel Li^{††}, Arup Kumar Indra^{††}, Xavier Warot^{*}, Jacques Brocard^{*}, Nadia Messaddeq^{*}, Shigeaki Kato^{‡§}, Daniel Metzger^{*} & Pierre Chambon^{*}

^{*} Institut de Génétique et de Biologie Moléculaire et Cellulaire, CNRS/INSERM/ULP, Collège de France, BP 163, 67404 Illkirch Cedex, France

[‡] Institute of Molecular & Cellular Biosciences, University of Tokyo, Yayoi, Bunkyo-ku, Tokyo 113, Japan

[§] CREST, Japan Science and Technology, Kawaguchi, Saitama 332, Japan

[†] These authors contributed equally to this work

Nuclear receptors for retinoids (RARs) and vitamin D (VDR), and for some other ligands (TRs, PPARs and LXRs), may be critical in the development and homeostasis of mammalian epidermis^{1–8}. It is believed that these receptors form heterodimers with retinoid X receptors (RXRs) to act as transcriptional regulators^{9,10}. However, most genetic approaches aimed at establishing their physiological functions in the skin have been inconclusive owing either to pleiotropic effects and redundancies between receptor isotypes in gene knockouts, or to equivocal interpretation of dominant-negative mutant studies in transgenic mice^{11–15}. Moreover, knockout of RXR α , the main skin RXR isotype, is lethal *in utero* before skin formation^{11,12,16,17}. Here we have resolved these problems by developing an efficient technique to create spatio-temporally controlled somatic mutations in the mouse. We used tamoxifen-inducible Cre-ER^T recombinases^{18,19} to ablate RXR α selectively in adult mouse keratinocytes. We show that RXR α has key roles in hair cycling, probably through RXR/VDR heterodimers, and in epidermal keratinocyte proliferation and differentiation.

To ablate RXR α in epidermis, we engineered mice carrying LoxP-site-containing (floxed) RXR α ^{L2} alleles (Fig. 1a) and used the K5-Cre-ER^T transgenic line in which tamoxifen (Tam) efficiently induces Cre-mediated recombination in basal layer keratinocytes¹⁹. K5-Cre-ER^{T(tg/tg)}/RXR α ^{L2/L2} mice mated with RXR α ^{+/-} (Fig. 1a; ref. 16) or RXR α ^{L2/+} mice yielded 'pro-mutant' mice hemizygous (tg/0) for K5-Cre-ER^T and carrying either one RXR α ^{L2} and one RXR α null (–) allele (K5-Cre-ER^{T(tg/0)}/RXR α ^{L2/-} genotype) or two L2 alleles (K5-Cre-ER^{T(tg/0)}/RXR α ^{L2/L2} genotype). At 14 weeks old, the pro-mutant mice were treated with Tam (5 days, 1 mg per day), and then retreated 2, 4 and 6 weeks later. Six weeks after the first Tam treatment (AFT), 80% of RXR α ^{L2} alleles were converted into RXR α ^{L-} alleles in the epidermis of mice carrying one or two floxed alleles (Fig. 1b). By 12 weeks AFT, almost all RXR α ^{L2} alleles had been

converted (Fig. 1b). As expected¹⁹, no RXR α disruption occurred in vehicle (oil)-treated mice (data not shown) and Cre-mediated excision of RXR α exon 4 was restricted to epidermis and some epithelia in which the K5 promoter is also active (for example, tongue, salivary gland, oesophagus; Fig. 1c).

Interestingly, hair loss (alopecia) was observed 6–7 weeks AFT in the ventral region of pro-mutant mice, but not in oil-treated pro-mutant mice or in Tam-treated K5-Cre-ER^{T(tg/0)}/RXR α ^{L2/+} 'control' littermates (data not shown). At 12–16 weeks AFT, large regions of ventral skin and smaller regions of dorsal skin were hairless (Fig. 2a, b; and data not shown). Cysts became visible under the skin surface and these enlarged and spread all over the body with time (Fig. 2c; and data not shown). With increasing age (> 20 weeks AFT), minor focal lesions appeared on hairless dorsal skin, on chins and behind ears (Fig. 2d; and data not shown). These were not caused by fights and were formed of crusts on top of hyperproliferative epidermis and inflammatory dermis (see below).

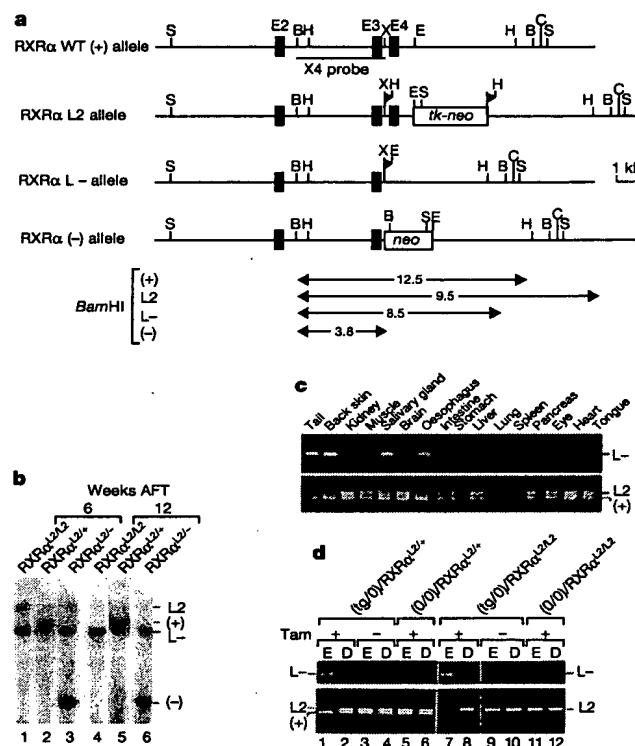


Figure 1 Tamoxifen-induced RXR α null mutation in adult mouse epidermis mediated by Cre-ER^T. **a**, Diagram of the wild-type RXR α genomic locus (+), the floxed RXR α L2 allele, the RXR α L- allele obtained after Cre-mediated excision of exon 4 (encoding the DNA-binding domain), and the RXR α null allele (–)¹⁶. Black boxes indicate exons (E2–E4). Restriction enzyme sites and probe X4 location are indicated. *Bam*HI fragments are in kilobases (kb). B, *Bam*HI; C, *Clal*; E, *Eco*RI; H, *Hind*III; S, *Spe*I; X, *Xba*I. Arrowheads in L2 and L- alleles indicate LoxP sites. **b**, Tamoxifen (Tam)-induced generation of K5-Cre-ER^T-mediated RXR α ^{L-} alleles illustrated by Southern blot analysis of epidermal DNA isolated 6 (lanes 1–3) and 12 (lanes 4–6) weeks after the first Tam (1 mg) injection series (AFT). All mice were K5-Cre-ER^{T(tg/0)} and the RXR α genotypes are indicated. *Bam*HI-digested DNA fragments corresponding to RXR α (+), L2, L- and (–) alleles are displayed. **c**, Tissue-specificity of Cre-ER^T-mediated RXR α disruption. WT (+), L2 and L- alleles were identified by PCR on DNA extracted from various organs of K5-Cre-ER^{T(tg/0)}/RXR α ^{L2/+} mice, 12 weeks AFT. **d**, Tamoxifen-induced generation of RXR α null alleles in adult mouse epidermis using K14-Cre-ER^{T2(tg/0)} or K14-Cre-ER^{T2(0/0)} mice (designated (tg/0) and (0/0), respectively). PCR analysis of genomic DNA from epidermis (E) and dermis (D), isolated two weeks after injection of either Tam (0.1 mg) (+) or vehicle (–). Mouse genotypes are indicated and PCR fragments corresponding to RXR α (+), L2 and L- alleles are displayed.

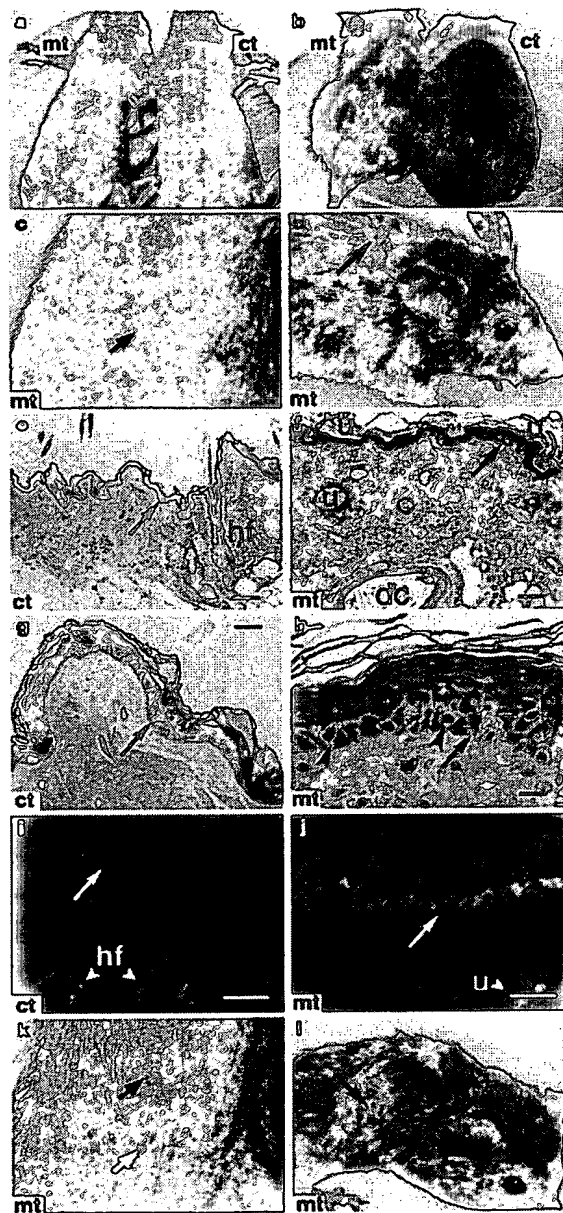


Figure 2 Abnormalities generated by Tam-induced disruption of RXR α in skin of adult mouse mediated by K5-Cre-ER^{T2} and K14-Cre-ER^{T2}. **a, b**, A female K5-Cre-ER^{T2}/RXR α ^{L2/L2} 'mutant' (mt) mouse, and a female K5-Cre-ER^{T2}/RXR α ^{L2/+} 'control' (ct) mouse, 16 weeks AFT (1 mg Tam per injection). **a**, Ventral view. **b**, Dorsal view. **c**, Higher magnification of the ventral region of the K5-Cre-ER^{T2}/RXR α ^{L2/L2} mouse. Arrow, one of the cysts. **d**, Dorsal view of a female K5-Cre-ER^{T2}/RXR α ^{L2/L2} mouse, 28 weeks AFT. Arrow, minor skin lesion. **e–h**, Histological analysis. 2- μ m sections of ventral skin 16 weeks AFT, taken from 'control' (**e, g**) and 'mutant' (**f, h**) mice. hf, hair follicles; u, utriculi; dc, dermal cysts; arrowheads (h), Langerhans cells whose number is increased several-fold in mutant epidermis. **i, j**, Keratin 6 (K6) immunohistochemistry on 'control' (**i**) and 'mutant' (**j**) skin sections (16 weeks AFT). Red, staining of the K6 antibody; cyan, DAPI staining. Arrow (**e–j**), the dermal–epidermal junction. **k, l**, Skin appearance of a female K14-Cre-ER^{T2}/RXR α ^{L2/L2} 'mutant' mouse. **k**, High magnification of the ventral region, 16 weeks after Tam treatment (0.1 mg per injection). White arrow, a cyst; black arrow, a melanosome-containing utriculus. **l**, Dorsal view of the same mutant. Arrow, a skin lesion. Scale bars: **e, f**, 60 μ m; **g, h**, 12 μ m; **i, j**, 25 μ m.

At 16 weeks AFT, histological analysis of ventral and dorsal hairless regions showed hair follicle degeneration, resulting in utriculi and dermal cysts^{20,21} (Fig. 2 compare **e** with **f**; and data not shown). Interfollicular epidermis was hyperplastic with increased incorporation of 5-bromodeoxyuridine (BrdU) and expression of the Ki67 proliferation marker (data not shown). Dermal cellularity was increased and capillaries were dilated (Fig. 2 compare **e, g** with **f, h**; and data not shown) underneath the thickened epidermis, reflecting an inflammatory reaction (data not shown). Keratin 6 (K6), which is usually expressed only in hair follicle outer root sheath (ORS), was also expressed in hyperproliferative interfollicular epidermis (Fig. 2i, j), indicating abnormal keratinocyte terminal differentiation²². All abnormalities were less severe, and/or appeared later in males than in females.

To improve the efficiency of Tam-induced Cre-mediated recombination, we engineered K14-Cre-ER^{T2} transgenic lines. The K14 promoter is selective for the basal layer of stratified squamous epithelia²³, and Cre-ER^{T2} can be induced by a milder Tam treatment (0.1 mg for 5 days)¹⁹. We treated 8–10-week-old K14-Cre-ER^{T2}(tg0)/RXR α ^{L2/L2} mice with Tam, together with 'control' littermates of genotype K14-Cre-ER^{T2}(tg0)/RXR α ^{L2/+}, K14-Cre-ER^{T2}(0/0)/RXR α ^{L2/+} and K14-Cre-ER^{T2}(0/0)/RXR α ^{L2/L2}. In two weeks, RXR α ^{L2} alleles were fully converted into RXR α ^L alleles in epidermis (Fig. 1d, lanes 1 and 7), but not in dermis (Fig. 1d, lanes 2 and 8) of K14-Cre-ER^{T2}-expressing transgenic mice, demonstrating the higher efficiency of Cre-ER^{T2} for mediating the selective somatic mutation of floxed RXR α in epidermis after Tam treatment. No L2 to L⁺ allele conversion occurred in 'controls' lacking the K14-Cre-ER^{T2} transgene (Fig. 1d, lanes 5, 6, 11 and 12) or without Tam treatment (Fig. 1d, lanes 3, 4, 9 and 10). Moreover, 8 weeks after Tam treatment, only the RXR α ^L allele was detected in K14-Cre-ER^{T2}(tg0)/RXR α ^{L2/L2} mouse epidermis (data not shown), indicating that RXR α was disrupted in most, if not all epidermal stem cells. RXR α disruption also occurred in other epithelia in which the K14 promoter is active²⁴ (for example, tongue, oesophagus and stomach, data not shown). Starting 6 weeks after Tam treatment, K14-Cre-ER^{T2}(tg0)/RXR α ^{L2/L2} mice exhibited abnormalities similar to those observed in Tam-treated K5-Cre-ER^{T2}(tg0)/RXR α ^{L2/L2} mice, that is, marked hair loss with visible cysts and focal skin lesions appearing at later stages (Fig. 2k and l; and data not shown). The underlying epidermal and dermal histological abnormalities were also similar to those described above for Tam-treated K5-Cre-ER^{T2}(tg0)/RXR α ^{L2/L2} mice (data not shown).

Thus, disruption of floxed RXR α in adult epidermis is achieved faster and with lower Tam doses in K14-Cre-ER^{T2} than in K5-Cre-ER^{T2} mice, but the resulting skin abnormalities are similar and, in both cases, more severe in females than in males. Interestingly, these abnormalities are also similar to those exhibited by K14-Cre^(tg0)/RXR α ^{L2/L2} or K14-Cre^(tg0)/RXR α ^{L2/+} mice in which floxed RXR α alleles are selectively disrupted in the epidermis during fetal development, leading to RXR α ablation in epidermal keratinocytes and hair follicle ORS (M.L. *et al.*, manuscript in preparation). Indeed, from three weeks of age, these 'constitutive' epidermis-selective RXR α mutants develop progressive alopecia with typical features of degenerated hair follicles, together with utriculi and dermal cysts, which can all be attributed to defects in hair cycles^{20,21}. Furthermore, these mutants also exhibit interfollicular keratinocyte hyperproliferation, as well as abnormal terminal differentiation (with K6 expression) and increased dermal cellularity associated with a skin inflammatory reaction (M.L. *et al.*, manuscript in preparation).

RXR β is expressed at a much lower level than is RXR α in mouse skin, and RXR γ expression is undetectable by polymerase chain reaction after reverse transcription of RNA (RT-PCR; data not shown). Interestingly, we found that the adult skin level of RXR β messenger RNA is several fold higher in males than in females. However, the skin of adult male and female RXR β ^{−/−} mutants

appears normal²⁵ (data not shown) and RXR β mRNA levels did not change upon RXR α ablation (data not shown). Compound mutants were generated to explore a possible functional redundancy between RXRs.

As expected, oil-treated K5-Cre-ER^{T(tg/0)}/RXR α ^{L2/L2}/RXR β ^{-/-} and K5-Cre-ER^{T(tg/0)}/RXR α ^{L2/L2}/RXR β ^{-/-} mice did not exhibit skin abnormalities, but 4 weeks after treatment with Tam they began to lose their hair. Large skin regions were hairless 16–18 weeks AFT, and epidermal flaking on the hairless trunk, chin and ears was much more conspicuous than on single RXR α mutants (compare Fig. 3a; with Fig. 2d; and data not shown). Crusted skin lesions and ulcers lacking epidermis, not seen in RXR α single mutants, were also frequently observed on these RXR α /RXR β double mutants at 14–16 weeks AFT, particularly on the hairless trunk skin, behind the ears and around the mouth (Fig. 3a; and data not shown). But wound repair was not overtly impaired in these mutants when skin biopsies were taken from lesion-free hairless regions (data not shown). Histology of hairless skin showed disappearance of hair follicles and presence of utriculi and dermal cysts (Fig. 3b). The epidermis was highly hyperplastic and hyperkeratinized (compare Fig. 3b, c with Fig. 2e, g; Fig. 2f, h), abnormal K6 expression was observed throughout epidermis (Fig. 3d), and an inflammatory reaction with increased dermal cellularity was also observed (Fig. 3b; and data not shown).

The K5-Cre-ER^{T(tg/0)}/RXR α ^{L2/L2}/RXR β ^{-/-}/RXR γ ^{-/-} triple mutants treated with Tam did not reveal any further role of RXR γ in adult skin (data not shown). Thus, RXR β can partially compensate for a loss of RXR α function. Also, in accordance with the larger amount of RXR β in adult male skin, the functional redundancy was more pronounced in males than in females as RXR α /RXR β double mutant males and females were similarly affected (data not shown) unlike the single mutants (see above).

Collectively, our results demonstrate the effectiveness of Cre-ER^T

recombinases in generating cell-specific temporally controlled targeted somatic mutations in adult mouse tissues. We also show that RXR α , whose knockout is lethal *in utero*^{16,17}, is important postnatally in processes controlling hair cycling and the proliferation and differentiation of epidermal keratinocytes, even though expression of a dominant-negative RXR α mutant in epidermal suprabasal layers has no effect on skin development and maintenance¹⁵.

Our study also reveals a functional redundancy between RXR α and RXR β , although RXR α function is clearly dominant. The molecular events underlying the generation of alopecia and keratinocyte abnormalities in epidermis of mice lacking these receptors are unknown. However, a number of nuclear receptors (for example, RARs, TRs, VDR, PPARs, LXRs) form heterodimers with RXR, and numerous *in vitro* studies using cultured cells and a few *in vivo* targeted-mutagenesis studies^{10–12,26} show that these heterodimers act as signal transducers in different signalling pathways. Interestingly, VDR is also expressed in hair follicle ORS²⁷ and VDR knock-out mice develop progressive secondary alopecia, indicating that VDR is important in hair cycling^{2–4}. Alopecia developed by 14-week-old VDR^{-/-} mice appears similar externally to that developed by K5-Cre-ER^{T(tg/0)}/RXR α ^{L2/L2}/RXR β ^{-/-} mice 18 weeks after Tam treatment, although the skin of VDR^{-/-} mice was free of the lesions seen on RXR-ablated epidermis (compare Fig. 3a with e). At the histological level, similar utriculi and dermal cysts were observed (compare Fig. 3b with f), but no keratinocyte hyperproliferation was observed in the epidermis of VDR^{-/-} mice and keratinocyte differentiation was normal (as revealed by K6 expression (compare Fig. 3c and d with g and h; and data not shown). Thus, alopecia generated by selective RXR ablation in adult mouse keratinocytes may reflect a major role of RXR/VDR heterodimers in hair cycling. Further keratinocyte-specific targeted somatic mutagenesis is necessary to investigate whether other signalling pathways involving nuclear receptors that heterodimerize with RXRs (notably RARs, LXRs² and PPARs²⁸) are implicated in the generation of the other skin abnormalities resulting from keratinocyte-selective RXR ablation.

Methods

Transgenic lines

RXR α ^{L2/L2}, VDR^{-/-} and K5-Cre-ER^T mouse lines have been described^{26,19} and RXR α ^{L2/L2} mice will be described (M.L. *et al.*, manuscript in preparation). The K14-Cre-ER^{T2} transgene was constructed by replacing the K5 promoter region of pK5-Cre-ER^{T2} (ref. 19) by the 2-kilobase (kb) human keratin K14 promoter/enhancer *SalI* DNA fragment²⁹, isolated from pHR2 (a gift from S. Werner), and transgenic mice were generated¹⁹.

Genotyping of RXR α alleles

Genomic DNA was isolated from tissues as described¹⁹. Epidermis was separated from dermis after treating tail skin with dispase (4 mg ml⁻¹ in PBS, Gibco-BRL) for 1–2 h at room temperature. RXR α genotyping was performed by PCR. Primers: ZO243 (5'-TCCTTCACCAAGCACATCTG-3', in exon 3) and ZO244 (5'-TGCAGCCCTCACAACTGTAT-3', in exon 4) for L2 and (+) alleles (700- and 650-base pair (bp) fragment, respectively); ZO243 and UD196 (5'-CAACCTGGACTTGTCACTTAG-3' in the intron between exons 4 and 5) for L- allele (400-bp fragment); ZO243 and RU178 (5'-ATGTTTCATAGTTGGATATC-3', in *neo* cassette) for (-) allele (500-bp fragment). For Southern blot analysis, genomic DNA was digested with *Bam*HI and probed with probe X4 (3-kb *Bam*HI-*Xba*I fragment of RXR α gene)²⁹.

Tamoxifen treatment

Tam (Sigma) solutions have been described¹⁸. Tam (1 mg in 100 μ l sunflower oil) was injected intraperitoneally into K5-Cre-ER^T transgenic mice for five consecutive days, and again for three consecutive days, two, four and six weeks later. K14-Cre-ER^{T2} transgenic mice were injected intraperitoneally with 0.1 mg Tam (in 100 μ l sunflower oil) for five consecutive days.

Histological analysis

Skin biopsies of age- and sex-matched animals were taken from similar body sites. Skin samples were fixed in glutaraldehyde (2.5% in 0.1 M cacodylate buffer pH 7.2) overnight at 4 °C, and post-fixed with 1% osmium tetroxide in cacodylate buffer for 1 h at 4 °C. Tissues were dehydrated with graded concentrations of alcohol and embedded in Epon 812. Semi-thin sections (2 μ m) were stained with toluidine blue.

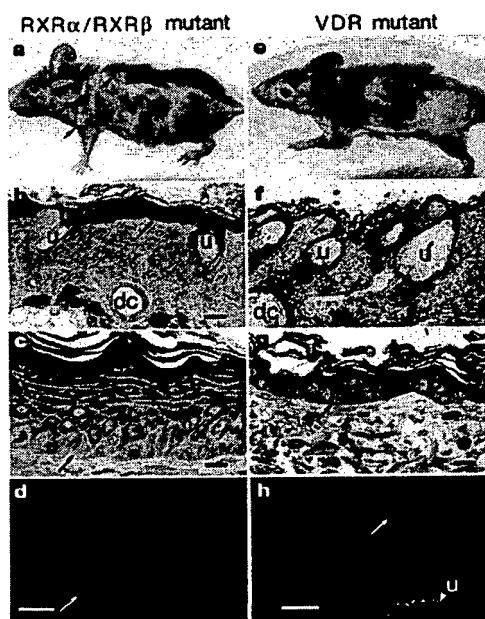


Figure 3 Comparison of skin abnormalities exhibited by a Tam-treated K5-Cre-ER^{T(tg/0)} RXR α ^{L2/L2}/RXR β ^{-/-} mouse and a VDR-null mouse. The figure corresponds to a K5-Cre-ER^{T(tg/0)}/RXR α ^{L2/L2}/RXR β ^{-/-} mouse, 18 weeks AFT (1 mg Tam per injection) (a–d) and to a 14-week-old VDR^{-/-} mouse (e–h). **b, c, f, g**, Histological analysis of 2- μ m dorsal skin sections. **d, h**, Keratin K6 immunohistochemistry on skin sections. u, utriculi; dc, dermal cysts. Arrows: **a**, skin lesions; **b–h**, the dermal–epidermal junction. Scale bar: **b, f**, 60 μ m; **c, g**, 12 μ m; **d, h**, 25 μ m.

Immunohistochemistry

After fixation in 2% paraformaldehyde, 10- μ m frozen sections were blocked in 5% normal goat serum (Vector), incubated with rabbit polyclonal anti-MK6 (Babco). After washing in PBS containing 0.1% Tween 20, sections were incubated with CY3-conjugated donkey anti-rabbit IgG antibody (Jackson ImmunoResearch), and mounted with Vectashield medium (Vector) containing DAPI (4,6-diamidino-2-phenylindole; Boehringer Mannheim)²⁰.

Received 22 May; accepted 28 July 2000.

1. Fisher, G. J. & Voorhees, J. J. Molecular mechanisms of retinoid actions in skin. *FASEB J.* 10, 1002–1013 (1996).
2. Yoshizawa, T. *et al.* Mice lacking the vitamin D receptor exhibit impaired bone formation, uterine hypoplasia and growth retardation after weaning. *Nature Genet.* 16, 391–396 (1997).
3. Li, Y. C. *et al.* Targeted ablation of the vitamin D receptor: an animal model of vitamin D-dependent rickets type II with alopecia. *Proc. Natl Acad. Sci. USA* 94, 9831–9835 (1997).
4. Li, Y. C. *et al.* Normalization of mineral ion homeostasis by dietary means prevents hyperparathyroidism, rickets, and osteomalacia, but not alopecia in vitamin D receptor-ablated mice. *Endocrinology* 139, 4391–4396 (1998).
5. Körmöcs, L. G. *et al.* Ligands and activators of nuclear hormone receptors regulate epidermal differentiation during fetal rat skin development. *J. Invest. Dermatol.* 111, 429–433 (1998).
6. Hanley, K. *et al.* Activators of the nuclear hormone receptors PPAR α and RXR accelerate the development of the fetal epidermal permeability barrier. *J. Clin. Invest.* 100, 705–712 (1997).
7. Hanley, K. *et al.* Oxysterols induce differentiation in human keratinocytes and increase Ap-1-dependent involucrin transcription. *J. Invest. Dermatol.* 114, 545–553 (2000).
8. Hanley, K. *et al.* Farnesol stimulates differentiation in epidermal keratinocytes via PPAR α . *J. Biol. Chem.* 275, 11484–11491 (2000).
9. Mangelsdorf, D. J. *et al.* The nuclear receptor superfamily: the second decade. *Cell* 83, 835–839 (1995).
10. Chambon, P. A decade of molecular biology of retinoic acid receptors. *FASEB J.* 10, 940–954 (1996).
11. Kastner, P., Mark, M. & Chambon, P. Nonsteroid nuclear receptors: what are genetic studies telling us about their role in real life? *Cell* 83, 859–869 (1995).
12. Mascres, B. *et al.* The RXR α ligand-dependent activation function 2 (AF-2) is important for mouse development. *Development* 125, 4691–4707 (1998).
13. Saitou, M. *et al.* Inhibition of skin development by targeted expression of a dominant-negative retinoic acid receptor. *Nature* 374, 159–162 (1995).
14. Imakado, S. *et al.* Targeting expression of a dominant-negative retinoic acid receptor mutant in the epidermis of transgenic mice results in loss of barrier function. *Genes Dev.* 9, 317–329 (1995).
15. Feng, X. *et al.* Suprabasal expression of a dominant-negative RXR α mutant in transgenic mouse epidermis impairs regulation of gene transcription and basal keratinocyte proliferation by RAR-selective retinoids. *Genes Dev.* 11, 59–71 (1997).
16. Kastner, P. *et al.* Genetic analysis of RXR α developmental function: convergence of RXR and RAR signalling pathways in heart and eye morphogenesis. *Cell* 78, 987–1003 (1994).
17. Sucov, H. M. *et al.* RXR α mutant mice establish a genetic basis for vitamin A signaling in heart morphogenesis. *Genes Dev.* 8, 1007–1018 (1994).
18. Metzger, D. & Chambon, P. Site- and time-specific gene targeting in the mouse. *Methods* (in the press).
19. Indra, A. K. *et al.* Temporally-controlled site-specific mutagenesis in the basal layer of the epidermis: comparison of the recombinase activity of the tamoxifen-inducible Cre-ER^T and Cre-ER^{T2} recombinases. *Nucleic Acids Res.* 27, 4324–4327 (1999).
20. Sundberg, J. P. & King, L. E. Mouse models for the study of human hair loss. *Dermatol. Clin.* 14, 619–632 (1996).
21. Panteleyev, A. A., Paus, R., Ahmad, W., Sundberg, J. P. & Christiano, A. M. Molecular and functional aspects of the hairless (hr) gene in laboratory rodents and humans. *Exp. Dermatol.* 7, 249–267 (1998).
22. Porter, R. M., Reichelt, J., Lunney, D. P., Magin, T. M. & Lane, B. The relationship between hyperproliferation and epidermal thickening in a mouse model for BCIE. *J. Invest. Dermatol.* 110, 951–957 (1998).
23. Vassar, R., Rosenberg, M., Ross, S., Tyner, A. & Fuchs, E. Tissue-specific and differentiation-specific expression of a human K14 keratin gene in transgenic mice. *Proc. Natl Acad. Sci. USA* 86, 1563–1567 (1989).
24. Wang, X., Zinkel, S., Polonsky, K. & Fuchs, E. Transgenic studies with a keratin promoter-driven growth hormone transgene prospects for gene therapy. *Proc. Natl Acad. Sci. USA* 94, 219–226 (1997).
25. Kastner, P. *et al.* Abnormal spermatogenesis in RXR β mutant mice. *Genes Dev.* 10, 80–92 (1996).
26. Wendling, O., Chambon, P. & Mark, M. Retinoid X receptors are essential for early mouse development and placentogenesis. *Proc. Natl Acad. Sci. USA* 96, 547–551 (1999).
27. Reichrath, J. *et al.* Hair follicle expression of 1,25-dihydroxyvitamin D3 receptors during the murine hair cycle. *Br. J. Dermatol.* 131, 477–482 (1994).
28. Braissant, O., Foulle, F., Scotto, C., Dauca, M. & Wahli, W. Differential expression of peroxisome proliferator-activated receptors (PPARs): tissue distribution of PPAR- α , - β , and - γ in the adult rat. *Endocrinology* 137, 354–366 (1996).
29. Metzger, D. *et al.* Conditional site-specific recombination in mammalian cells using a ligand-dependent chimeric Cre recombinase. *Proc. Natl Acad. Sci. USA* 92, 6991–6995 (1995).
30. Brocard, J. *et al.* Spatio-temporally controlled site-specific somatic mutagenesis in the mouse. *Proc. Natl Acad. Sci. USA* 94, 14559–14563 (1997).

Acknowledgements

We thank S. Werner for the human K14 promoter; H. Chiba and P. Kastner for RXR α ^{L2/+}, RXR α ^{+/+} and RXR β ^{+/+} mice; J. M. Bornert, S. Bronner, N. Chartoire, M. Duval, C. Gérard, R. Lorentz and J. L. Vonesch for technical help; M. LeMour, R. Matyas and the animal facility staff for animal care; M. Mark for histological analysis; the secretariat for typing the manuscript and the illustration staff for preparing the figures; and all the members of the laboratory for helpful discussions. This work was supported by funds from the Centre National de la Recherche Scientifique, the Institut National de la Santé et de la Recherche Médicale, the Collège de France, the Hôpital Universitaire de Strasbourg, the Association pour la Recherche sur le Cancer, the Fondation pour la Recherche Médicale, the Human Frontier Science Program, the Ministère de l'Éducation Nationale de la Recherche et de la

Technologie and the European Economic Community. M.L. was supported by fellowships from the Association pour la Recherche sur le Cancer and the Fondation pour la Recherche Médicale, A.K.I. by a fellowship from the Université Louis Pasteur (Strasbourg), and J.B. and X.W. by fellowships from the Ministère de l'Éducation Nationale, de la Recherche et de la Technologie and from the Fondation pour la Recherche Médicale.

Correspondence and requests for materials should be addressed to P.C. (e-mail: chambon@igbmc.u-strasbg.fr).

Memory B-cell persistence is independent of persisting immunizing antigen

Mitsuo Maruyama*, Kong-Peng Lam*† & Klaus Rajewsky*

* Institute for Genetics, University of Cologne, Weyertal 121, D-50931 Cologne, Germany

† Institute of Molecular and Cell Biology, The National University of Singapore, 30 Medical Drive, Singapore 117609

Immunological memory in the antibody system is generated in T-cell-dependent responses and carried by long-lived memory B cells that recognize antigen by high-affinity antibodies^{1,2}. But it remains controversial³ whether these B cells represent true 'memory' cells (that is, their maintenance is independent of the immunizing antigen), or whether they are a product of a chronic immune response driven by the immunizing antigen, which can be retained in the organism for extended time periods on the surface of specialized antigen-presenting cells (follicular dendritic cells)³. Cell transfer experiments provided evidence in favour of a role of the immunizing antigen^{4,5}; however, analysis of memory cells in intact animals, which showed that these cells are mostly resting⁶ and can persist in the absence of detectable T-cell help⁷ or follicular dendritic cells⁸, argued against it. Here we show, by using a genetic switch mediated by Cre recombinase, that memory B cells switching their antibody specificity away from the immunizing antigen are indeed maintained in the animal over long periods of time, similar to cells retaining their original antigen-binding specificity.

The main difficulty in the analysis of the antigen-dependence of memory B-cell persistence lies in the elimination of residual antigen from the cellular environment, which is difficult to achieve beyond doubt. We therefore looked for an alternative approach, namely to use induced targeted mutagenesis *in vivo* to equip memory B cells induced by and specific for a particular antigen with an antigen receptor (BCR) that does not bind the inducing antigen; and to study the persistence of the mutant cells in comparison with others that do not switch BCR specificity.

The genetic switch had to be irreversible, in contrast to the system of BCR specificity switching that we previously developed⁹. We therefore generated a mouse strain carrying two distinct, mutant alleles of the immunoglobulin (Ig) heavy (H) chain (IgH) locus. One of these alleles was already available and carried a VDJ segment in its physiological position, flanked by loxP sites in the same orientation¹⁰. This IgH allele, designated VNP here, encodes an H chain that, together with λ 1 light (L) chains, forms an antibody with specificity for the hapten 4-hydroxy-3-nitro-phenylacetyl (NP).

The second IgH allele (Fig. 1) contains a VDJ segment encoding, again in the context of λ 1 L chains, an antibody specific for the fluorescent protein phycoerythrin (PE). This VDJ segment, designated VDJPE, originated from a hybridoma isolated from a PE-immunized mouse, selected for reactivity with PE but not NP (see

Selective ablation of retinoid X receptor α in hepatocytes impairs their lifespan and regenerative capacity

Takeshi Imai, Ming Jiang, Philippe Kastner, Pierre Chambon*, and Daniel Metzger

Institut de Génétique et de Biologie Moléculaire et Cellulaire, Centre National de la Recherche Scientifique/Institut National de la Santé et de la Recherche Médicale/Université Louis Pasteur, Collège de France, BP 163, 67404 Illkirch Cedex, Communauté Urbaine de Strasbourg, France

Contributed by Pierre Chambon, February 5, 2001

Retinoid X receptors (RXRs) are involved in a number of signaling pathways as heterodimeric partners of numerous nuclear receptors. Hepatocytes express high levels of the RXR α isotype, as well as several of its putative heterodimeric partners. Germ-line disruption (knockout) of RXR α has been shown to be lethal *in utero*, thus precluding analysis of its function at later life stages. Hepatocyte-specific disruption of RXR α during liver organogenesis has recently revealed that the presence of hepatocytes is not mandatory for the mouse, at least under normal mouse facility conditions, even though a number of metabolic events are impaired [Wan, Y.-J., et al. (2000) *Mol. Cell. Biol.* 20, 4436–4444]. However, it is unknown whether RXR α plays a role in the control of hepatocyte proliferation and lifespan. Here, we report a detailed analysis of the liver of mice in which RXR α was selectively ablated in adult hepatocytes by using the tamoxifen-inducible chimeric Cre recombinase system. Our results show that the lifespan of adult hepatocytes lacking RXR α is shorter than that of their wild-type counterparts, whereas proliferative hepatocytes of regenerating liver exhibit an even shorter lifespan. These lifespan shortenings are accompanied by increased polyploidy and multinuclearity. We conclude that RXR α plays important cell-autonomous function(s) in the mechanism(s) involved in the lifespan of hepatocytes and liver regeneration.

conditional somatic mutagenesis | Cre-Lox | liver | partial hepatectomy | polyploidy

Nuclear receptors are signal transducers that play crucial roles in vertebrate embryogenesis, organogenesis, cellular proliferation and differentiation, and homeostasis (1, 2). They belong to a superfamily of transcriptional regulators that includes ligand-dependent receptors for steroid and thyroid hormones, retinoic acids (the active forms of vitamin A), vitamin D₃, and a variety of other lipophilic ligands, as well as orphan receptors for which no ligands have yet been found. Within this superfamily, retinoid X receptor (RXR) α , β , and γ play a central role as heterodimeric partners for several nuclear receptors, e.g., retinoic acid receptor α , β , and γ ; thyroid hormone receptor α and β ; peroxisome proliferator-activated receptor α , β , and γ ; liver X receptor α and β ; farnesoid X-activated receptor; and 1,25-dihydroxyvitamin D₃ receptor as well as several orphan nuclear receptors (3, 4). These heterodimers represent the functional units that bind to cognate response elements located in the promoter regions of target genes to regulate their expression (1).

The liver, a key player in mammalian homeostasis, has the unique capacity to restore its mass in response to both toxin and inflammatory injuries, transplantation, and partial hepatectomy (PH) (5, 6). Many members of the nuclear receptor superfamily including RXRs are expressed in the liver, as well as a wealth of genes that contain response elements for RXR–nuclear receptor heterodimers (7, 8). Thus, as RXR α is the most abundant of the three RXR isotypes in the liver, it may play a prominent role in hepatic growth, regeneration, and homeostatic functions. However, the possible postnatal role of RXR α could not be analyzed in knockout mice lacking RXR α (RXR α KO), as RXR α KO fetuses die at

embryonic days 13.5–16.5 from abnormal development of the ventricular myocardium (9, 10). The liver of RXR α KO fetuses appeared morphologically and histologically normal, but its development was delayed by about 24 h, compared with wild-type (wt) fetuses (9, 10). Interestingly, it was recently reported that mice, in which RXR α was selectively ablated in hepatocytes by using the Cre-Lox technology, were viable even though a number of metabolic events regulated by nuclear receptors that heterodimerize with RXR were impaired. No morphological defect could be evidenced in the liver of these conditional mutants (7, 8). This was surprising as there was some indication that RXRs and some of their heterodimeric partners might control hepatocyte proliferation and lifespan (refs. 11–16; see Discussion).

Our present study reports a detailed analysis of the liver of mice in which RXR α was selectively ablated in hepatocytes. It reveals that this ablation reduces the lifespan of adult hepatocytes, induces the formation of spots of focal necrosis in the liver of adult mice, but does not reduce the liver mass. Furthermore, upon partial hepatectomy, the lifespan of RXR α -ablated hepatocytes was further reduced, and additional cellular abnormalities could be detected.

Materials and Methods

Animals. Alb-Cre (17), α AT-Cre-ERT^T (18), and RXR α ^{L2/+} (19) mice and mouse genotyping were as described. Animals were maintained in a 12-h light-dark cycle, with food and water provided *ad libitum*.

Liver resection of the left and median lobes (PH) was performed after midventral laparotomy between 8 a.m. and 12 p.m.

DNA and RNA Analysis. Southern blot analysis of Cre-mediated RXR α ablation was performed on genomic DNA, which was isolated from various tissues, digested with *Bam*HI, and probed as described (20).

Total liver RNA was extracted by the guanidium-thiocyanate-phenol-chloroform method (21). Ten micrograms total RNA was electrophoresed on a 0.8% agarose gel, transferred to a nylon membrane, and hybridized with RXR α , RXR β , RXR γ , ApoCIII, and 36B4-labeled probes, as described (20, 22).

Histology. Liver, rinsed in PBS, was fixed with Bouin's solution and embedded in paraffin. Six-micrometer sections were stained with hematoxylin and eosin.

Abbreviations: ALP, alkaline phosphatase; ALT, alanine aminotransferase; ApoCIII, apolipoprotein CIII; AST, aspartate aminotransferase; Cre-ERT^T, fusion protein between the Cre recombinase and a mutated ligand binding domain of the human estrogen receptor; CT, control; ES, embryonic stem; GOT, glutamate/oxalacetate transaminase; GPI, glucose phosphate isomerase; GPT, glutamate/pyruvate transaminase; PH, partial hepatectomy; PI, proliferative index; RXR, retinoid X receptor; RXR α KO, RXR α knockout; Tam, tamoxifen; wt, wild type.

*To whom reprint requests should be addressed. E-mail: chambon@igbmc.u-strasbg.fr.

The publication costs of this article were defrayed in part by page charge payment. This article must therefore be hereby marked "advertisement" in accordance with 18 U.S.C. §1734 solely to indicate this fact.

RXR α and Ki67 immunohistochemistry was performed on 10- μ m cryosections, by using the biotinylated anti-RXR α 4RX3A2 mAb (1/1,000 dilution in 0.1% BSA/PBS) (19, 23) and the NCL-Ki67p polyclonal antibody (NovoCastra, Newcastle, U.K.), respectively, according to the manufacturer's instructions. The number of Ki67-labeled nuclei was determined by counting the Ki67-positive hepatocyte nuclei in at least three low magnification ($\times 100$) microscope fields for each sample. More than 2,000 hepatocytes were screened per field.

BrdUrd Incorporation. Animals were injected i.p. with 50 mg/kg BrdUrd 2 h before dissection. Liver was rinsed in PBS and embedded in tissue-Tek OCT compound (Sakura, Zoeterwoude, The Netherlands). Ten-micrometer cryosections, fixed with 4% paraformaldehyde, were incubated with an antibody against BrdUrd (Boehringer Mannheim), which was 50-fold diluted in 0.1% BSA/PBS, revealed with CY3-conjugated donkey anti-rabbit IgG antibody, and mounted with Vectorshield medium (Vector Laboratories) containing 4',6-diamino-2-phenylindole dihydrochloride. The number of BrdUrd-labeled hepatocytes was determined by counting the BrdUrd-positive hepatocyte nuclei in at least five low-magnification ($\times 100$) microscope fields for each sample. More than 1,800 hepatocytes were screened per field.

Liver Functions. Alkaline phosphatase (ALP), alanine aminotransferase (ALT; also called glutamate/pyruvate transaminase, GPT), and aspartate aminotransferase (AST; also called glutamate/oxalacetate transaminase, GOT) enzymatic activities were determined on mouse serum with Sigma diagnostic kits, according to the manufacturer's protocols.

Mosaic Mice Study. RXR α ^{-/-} embryonic stem (ES) cells were obtained after electroporation of RXR α ^{+/-} ES cells with a targeting vector similar to pHR(RXR α)0.2 (9), in which the neomycin resistance cassette was replaced by a hygromycin resistance cassette (24), as described (9). RXR α ^{-/-}, RXR α ^{+/-}, and RXR α ^{+/+} 129/SV ES D4 cells were injected into C57BL/6 blastocysts, and proteins were extracted from organs of 10-month-old RXR α ^{-/-}, RXR α ^{+/-}, and RXR α ^{+/+} chimeric mice derived from these blastocysts after implantation into C57BL/6 recipient females. Isoenzymes GPI-1^a (from the 129/SV ES D4 cells) and GPI-1^b (from the C57BL/6 host blastocysts) were resolved on cellulose (Helena Laboratories), and their enzymatic activities were revealed as described (25). The fraction of ES cell-derived cells was evaluated by comparing the intensity of the two isoenzyme activities.

Statistical Analyses. Values are reported as mean \pm SEM. Statistical significance ($P < 0.05$) was determined by unpaired Student's *t* test (STATVIEW, Abacus Concepts, Berkeley, CA).

Results

Ablation of RXR α in Adult Hepatocytes Compromises Their Lifespan and Regenerative Capacity. To investigate the role of RXR α in liver, we first produced chimeric animals by injecting either RXR α ^{-/-} or control (CT; RXR α ^{+/+} or RXR α ^{+/-}) 129/SV ES cells into wt C57BL/6 blastocysts, followed by implantation into recipient females. The contribution of ES cells to various organs of the resulting chimeras was determined by glucose phosphate isomerase (GPI) analysis, as distinct GPI isoenzymes are expressed in cells derived from 129/SV ES cells and C57BL/6 cells. In 10-month-old animals, the CT and RXR α ^{-/-} ES cell contributions were similar in the various organs analyzed, with the exception of the liver, where it was 10-fold lower (Fig. 1A). This finding indicates that RXR α could play an important role in hepatocyte proliferative capacity and/or lifespan, even though it was not found to be essential for liver organogenesis (9, 10).

To investigate the possible role of RXR α on hepatocyte lifespan, RXR α ^{L2/L2} mice, in which the exon encoding the RXR α DNA

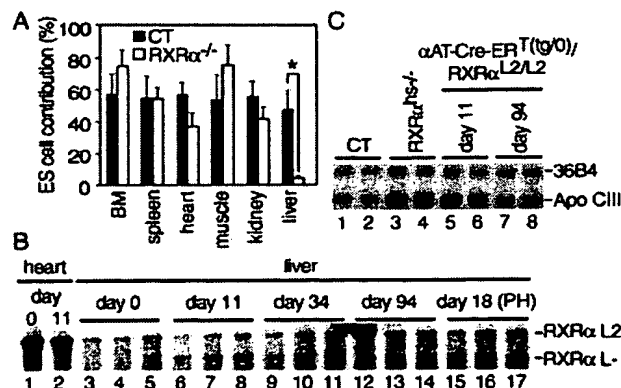


Fig. 1. Impaired lifespan of RXR α null hepatocytes. (A) Low contribution of RXR α ^{-/-} cells in liver of chimeric mice. The fraction of RXR α ^{-/-} cells was evaluated in various organs of 10-month-old chimeric mice by the ratio of the distinct GPI isozymes characteristic of 129/SV or C57BL/6 mice. Six and nine chimeras obtained by injection of CT (RXR α ^{+/+} or RXR α ^{+/-} 129/SV ES cells) and RXR α ^{-/-} 129/SV ES cells into C57BL/6 blastocysts, respectively, were analyzed. BM, bone marrow. Values are expressed as the mean \pm SEM. *, $P < 0.001$. (B) Time-dependent loss of RXR α L- alleles in liver of Tam-treated α AT-Cre-ER^{T(ig0)}/RXR α ^{L2/L2} mice. Cre-ER^T-mediated RXR α ablation was determined by Southern blot analysis, performed on genomic DNA isolated from heart and liver of α AT-Cre-ER^{T(ig0)}/RXR α ^{L2/L2} double-transgenic mice, taken before (day 0; lanes 1 and 3–5), and at the indicated days after the first Tam injection (3-month-old animals) (lanes 2 and 6–17). PH was performed 12 days after the first Tam injection (lanes 15–17). Liver DNA was extracted from three animals for each time point. The position of the fragments corresponding to the RXR α L2 and L- alleles is indicated. (C) Relief of down-regulation of ApoCIII expression in liver of RXR α ^{hs-/-} and Tam-treated α AT-Cre-ER^{T(ig0)}/RXR α ^{L2/L2} mice. ApoCIII RNA levels were analyzed by Northern blot, performed on RNA extracted from livers of CT (Tam-treated α AT-Cre-ER^{T(ig0)}/RXR α ^{L2/L2} double-transgenic mouse or vehicle-treated α AT-Cre-ER^{T(ig0)}/RXR α ^{L2/L2} double-transgenic mouse, lanes 1 and 2, respectively), RXR α ^{hs-/-} (lanes 3 and 4), and Tam-treated α AT-Cre-ER^{T(ig0)}/RXR α ^{L2/L2} double-transgenic mice taken 11 (lanes 5 and 6) and 94 days (lanes 7 and 8) after the first Tam injection. The position of ApoCIII and 36B4 transcripts is indicated.

binding domain is "floxed" on one allele (19), were crossed with α AT-Cre-ER^{T(ig0)} hemizygous transgenic mice, which express selectively the tamoxifen-inducible Cre-ER^T recombinase into more than 50% of the hepatocytes (18). Three-month-old α AT-Cre-ER^{T(ig0)}/RXR α ^{L2/L2} mice generated from these crosses were treated with 1 mg of tamoxifen (Tam) for 5 consecutive days to induce the Cre activity of Cre-ER^T, and the fraction of cells in which RXR α was ablated was estimated by Southern blotting on DNA extracted at various times after Tam treatment. As expected, $\sim 50\%$ of the RXR α L2 alleles were converted into L- alleles by day 11 after the first Tam injection (Fig. 1B, compare lanes 6–8 with lanes 3–5). However, the proportion of L- alleles decreased with time, and almost no RXR α L- alleles could be detected by day 94 (Fig. 1B, lanes 12–14). The progressive disappearance of hepatocytes in which RXR α was ablated was further confirmed by analysis of the expression of the ApoCIII gene, an RXR α target gene whose down-regulation in hepatocytes has been shown to be RXR α mediated (7). By day 11 after the first Tam injection, the amount of ApoCIII transcripts was 2.2-fold higher in livers of α AT-Cre-ER^{T(ig0)}/RXR α ^{L2/L2} mice (Fig. 1C, lanes 5 and 6) than in those of Tam-treated α AT-Cre-ER^{T(ig0)}/RXR α ^{L2/L2} (lane 1) and vehicle-treated α AT-Cre-ER^{T(ig0)}/RXR α ^{L2/L2} (lane 2) CT mice. Note that, as expected, this increase was about 2-fold lower than that observed in RXR α ^{hs-/-} mouse livers in which RXR α was ablated in all hepatocytes (see below; see also Fig. 1C, compare lanes 5 and 6 with lanes 3 and 4). In contrast, by day 94 after the first Tam injection, ApoCIII expression in α AT-Cre-ER^{T(ig0)}/RXR α ^{L2/L2}

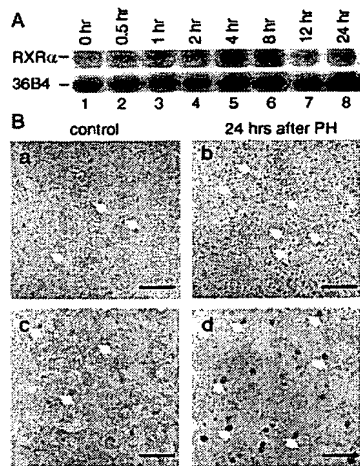


Fig. 2. Analysis of RXR α expression during liver regeneration. (A) Increased RXR α RNA levels. RXR α RNA levels were analyzed by Northern blotting of liver RNA extracted from 129/SV mice before (0 h) or at the indicated times after PH. The positions of RXR α and 36B4 transcripts are indicated. (B) Increased RXR α protein levels. RXR α protein was revealed with the 4RX3A2 mAb on 129/SV mouse liver cryosections, 24 h after sham operation (control a and c) or after PH (b and d). [Scale bar: 160 μ m (a and b) and 40 μ m (c and d).] White arrows point to some of the hepatocyte RXR α -positive nuclei.

mice was similar to that observed in CT mice (Fig. 1C, compare lanes 7 and 8 with lanes 1 and 2), in agreement with the disappearance of hepatocytes in which RXR α was ablated.

PH is well known to trigger liver regeneration (5, 6). Interestingly, 4 and 8 h after PH of 3-month-old wt mice, liver RXR α transcripts increased, whereas those of RXR β and RXR γ were unchanged (Fig. 2A and data not shown). Furthermore, an increase in hepatocyte nuclear RXR α protein was observed 12–24 h after PH (Fig. 2B and data not shown), thus suggesting that RXR α could play a critical role during liver regeneration. PH was therefore performed 12 days after the first Tam treatment of α AT-Cre-ERT^(tg/0)/RXR $\alpha^{L2/L2}$ mice. Most interestingly, almost all hepatocytes in which RXR α had been ablated disappeared within 6 days after PH [Fig. 1B; compare RXR α L⁻ allele at day 11 (lanes 6–8), day 18 (PH) (lanes 15–17), and day 34 (lanes 9–11)]. Thus, RXR α may be required in hepatocytes of adult mice for a vital function(s), notably under proliferative conditions.

Cellular Abnormalities in Liver of Mice Lacking RXR α in Hepatocytes. Taken together, the above observations indicate that the lifespan and regenerative capacity of adult hepatocytes are compromised in the absence of RXR α . In contrast, it was recently reported that mice in which RXR α was efficiently and selectively disrupted in hepatocytes during liver development did not exhibit any apparent morphological abnormality, even though several metabolic pathways that involve RXR α were impaired in the liver of these animals (7, 8). We therefore generated similar mice that do not express RXR α in hepatocytes to further investigate its role at the cellular level.

RXR $\alpha^{L2/+}$ mice were crossed with Alb-Cre^(tg/0) hemizygous transgenic mice that express Cre under the control of the albumin promoter (17) to generate Alb-Cre^(tg/0)/RXR $\alpha^{L2/L2}$ mice. Efficient excision of floxed DNA was previously shown to occur selectively in hepatocytes of these transgenic mice during liver ontogenesis (7, 17). Alb-Cre^(tg/0)/RXR $\alpha^{L2/L2}$ mice (hereafter called RXR $\alpha^{hs-/-}$ for hepatocyte-specific RXR $\alpha^{L-/-}$ genotype) were born at a Mendelian ratio, and no difference in viability and fertility was observed when compared with Alb-Cre^(tg/0)/RXR $\alpha^{+/+}$, Alb-Cre^(tg/0)/RXR $\alpha^{L2/+}$, Alb-Cre^(tg/0)/RXR $\alpha^{L2/L2}$, and Alb-Cre^(tg/0)/

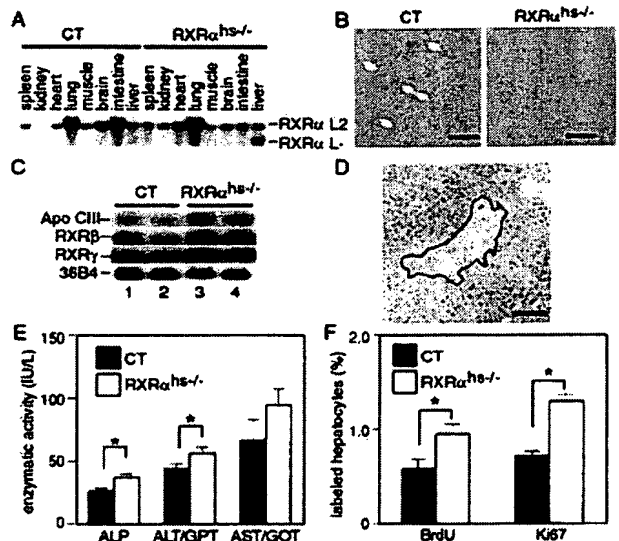


Fig. 3. Hepatocyte-selective RXR α ablation in Alb-Cre^(tg/0)/RXR $\alpha^{L2/L2}$ (RXR $\alpha^{hs-/-}$) mice. (A) Efficiency and selectivity of RXR α gene disruption in liver. Genomic DNA extracted from the indicated organs of 8-week-old Alb-Cre^(tg/0)/RXR $\alpha^{L2/L2}$ CT and Alb-Cre^(tg/0)/RXR $\alpha^{L2/L2}$ (RXR $\alpha^{hs-/-}$) mice was analyzed by Southern blotting. The position of fragments corresponding to the RXR α L2 and L⁻ alleles is indicated. (B) Hepatocytes from Alb-Cre^(tg/0)/RXR $\alpha^{L2/L2}$ (RXR $\alpha^{hs-/-}$) mice do not express the RXR α protein. Liver cryosection of 8-week-old Alb-Cre^(tg/0)/RXR $\alpha^{L2/L2}$ CT and RXR $\alpha^{hs-/-}$ mice were reacted with the 4RX3A2 anti-RXR α mAb. Arrows in CT section point to some of the RXR α -positive nuclei. (Scale bar, 80 μ m.) (C) Expression of ApoCIII, RXR β , and RXR γ in the liver of RXR $\alpha^{hs-/-}$ mice. ApoCIII, RXR β , and RXR γ RNA levels were analyzed by Northern blot on RNA extracted from liver of 2 CT (Alb-Cre^(tg/0)/RXR $\alpha^{L2/L2}$) and 2 RXR $\alpha^{hs-/-}$ 8-week-old mice, as indicated. 36B4 RNA was used as an internal control. (D) Focal necrosis in RXR $\alpha^{hs-/-}$ liver. Histological analysis of a liver section from a 3-month-old RXR $\alpha^{hs-/-}$ mouse, stained with hematoxylin and eosin. The area of focal necrosis is surrounded by a line. (Scale bar, 160 μ m.) (E) Increased ALP, ALT, and AST levels in RXR $\alpha^{hs-/-}$ mice. ALP, ALT/GPT, and AST/GOT levels were determined on serum taken from 3-month-old CT (Alb-Cre^(tg/0)/RXR $\alpha^{L2/L2}$), Alb-Cre^(tg/0)/RXR $\alpha^{L2/L2}$, and RXR $\alpha^{hs-/-}$ animals ($n = 10$ and 11, respectively). Average values (\pm SEM) are presented. *, $P < 0.05$. (F) Higher hepatocyte proliferative index in RXR $\alpha^{hs-/-}$ liver. The percentage of BrdUrd-positive and Ki67-positive hepatocytes was determined on liver sections from CT (Alb-Cre^(tg/0)/RXR $\alpha^{L2/L2}$), Alb-Cre^(tg/0)/RXR $\alpha^{L2/L2}$, and RXR $\alpha^{hs-/-}$ mice at the age of 3 months. Values are expressed as the mean \pm SEM. *, $P < 0.02$. BrdUrd labeling was analyzed in 10 CT and 11 RXR $\alpha^{hs-/-}$ mice. Ki67 labeling was analyzed in three CT and four RXR $\alpha^{hs-/-}$ mice.

RXR $\alpha^{L2/+}$ littermates, which were all used as CT mice. As expected $\approx 80\%$ of the RXR α L2 alleles were converted into RXR α -disrupted L⁻ alleles in the liver of 8-week-old RXR $\alpha^{hs-/-}$ animals, whereas no L⁻ allele could be detected in other tested organs, nor in any organ from control animals (Fig. 3A and data not shown; see also ref. 7). Furthermore, no RXR α protein could be revealed by immunohistochemistry in hepatocyte nuclei of 8-week-old RXR $\alpha^{hs-/-}$ mice, under conditions where it was readily detected in CT animals (Fig. 3B). Finally, in agreement with previous results (7), the expression of ApoCIII, one of the genes whose down-regulation is mediated by RXR α in the liver, was enhanced in RXR $\alpha^{hs-/-}$ mice but not in CT Alb-Cre^(tg/0)/RXR $\alpha^{L2/L2}$ mice (Fig. 3C and data not shown). Thus, RXR α was efficiently and selectively disrupted in hepatocytes of RXR $\alpha^{hs-/-}$ mice. Note that, in agreement with previous data (7), the expression levels of RXR β and RXR γ were not grossly affected in the liver of RXR $\alpha^{hs-/-}$ mice (Fig. 3C and data not shown).

However, in contrast to the previous reports of Wan *et al.* (7,

8), restricted areas of focal necrosis were occasionally observed on liver sections of six of eleven 3-month-old $\text{RXR}\alpha^{\text{hs-/-}}$ mice, whereas no such necrosis was observed on liver sections from control mice (Fig. 3D and data not shown). Note that by using the terminal deoxynucleotidyltransferase-mediated UTP end-labeling assay, we could not detect significant hepatocyte apoptosis in either CT or $\text{RXR}\alpha^{\text{hs-/-}}$ mice (data not shown). The existence of cytolysis and necrosis in 3-month-old $\text{RXR}\alpha^{\text{hs-/-}}$ mice was further supported by assays of ALP, alanine aminotransferase (ALT/GPT), and aspartate aminotransferase (AST/GOT) enzymatic activities (Fig. 3E). ALP and ALT/GPT levels were 1.4- and 1.3-fold higher in $\text{RXR}\alpha^{\text{hs-/-}}$ than in CT mice, respectively ($P < 0.05$). AST/GOT levels were also higher in $\text{RXR}\alpha^{\text{hs-/-}}$ than in CT mice, but the difference may not be statistically significant.

BrdUrd incorporation was used to estimate the proliferative index (PI) of hepatocytes in 3-month-old CT and $\text{RXR}\alpha^{\text{hs-/-}}$ mice. A 1.7-fold increase in the fraction of BrdUrd-positive hepatocytes was observed in $\text{RXR}\alpha^{\text{hs-/-}}$ mice (Fig. 3F), under conditions where the weight and lipid content of $\text{RXR}\alpha^{\text{hs-/-}}$ and control livers were similar (data not shown; see also ref. 7). This hepatocyte PI increase in $\text{RXR}\alpha^{\text{hs-/-}}$ mice was confirmed by immunostaining for Ki-67, a nuclear protein known to be expressed by proliferating cells (26) (Fig. 3F). Thus, hepatocytes in which $\text{RXR}\alpha$ is ablated exhibit both a shorter lifespan and an increased PI.

Liver Regeneration Is Impaired in Mice Lacking $\text{RXR}\alpha$ in Hepatocytes.

We next examined liver regeneration in adult $\text{RXR}\alpha^{\text{hs-/-}}$ mice. Interestingly, although PH postoperative morbidity and mortality were similar in 3-month-old CT and $\text{RXR}\alpha^{\text{hs-/-}}$ mice (less than 2%), ALP, ALT/GPT, and AST/GOT enzymatic activities were markedly increased in sera of $\text{RXR}\alpha^{\text{hs-/-}}$ mice when compared with control mice (Fig. 4A), thus indicating increased liver necrosis in $\text{RXR}\alpha^{\text{hs-/-}}$ mice. In contrast to control mice, histological analysis of liver sections 36–60 h after PH revealed the presence of cytolysis and neutrophil infiltration in $\text{RXR}\alpha^{\text{hs-/-}}$ mice, as well as large areas of focal necrosis (more than 10% of the area of liver sections of $\text{RXR}\alpha^{\text{hs-/-}}$ mice and less than 0.5% in control littermates; Fig. 4B, compare *a* and *e* and *b* and *f*; Fig. 4C; data not shown). Interestingly, 48–72 h after PH, highly polyploid ($\geq 8C$) hepatocytes were 5-fold more numerous in $\text{RXR}\alpha^{\text{hs-/-}}$ mice than in CT mice (Fig. 4B, *c* and *g* and *D*; data not shown). In addition, periodic acid-Schiff positive giant multinucleated hepatocytes were also observed 7 days after PH on sections of $\text{RXR}\alpha^{\text{hs-/-}}$ livers but not on sections of control livers (Fig. 4B, compare *d* and *h*; data not shown). BrdUrd incorporation indices were similar in control and $\text{RXR}\alpha$ -ablated hepatocytes 36 h post-PH, which corresponds to maximal BrdUrd incorporation in hepatocytes of control mice (Fig. 4E; data not shown). However, 48 and 60 h after PH, the fraction of hepatocytes that incorporated BrdUrd was 1.3- and 1.5-fold higher in $\text{RXR}\alpha^{\text{hs-/-}}$ mice than in control mice (Fig. 4E). One week after PH, $\text{RXR}\alpha^{\text{hs-/-}}$ and control mice had a similar liver weight (liver/body weight ratio: $3.9 \pm 0.1\%$ and $4.1 \pm 0.1\%$, respectively).

Discussion

$\text{RXR}\alpha$ null ($\text{RXR}\alpha\text{KO}$) mutant fetuses die *in utero* at embryonic days 13.5–16.5, most probably from heart failure caused by abnormalities of ventricular myocardium (9, 10). However, the liver of $\text{RXR}\alpha\text{KO}$ mutant fetuses appeared essentially normal both morphologically and histologically, although its development may be delayed by about 24 h when compared with wt littermates (9, 10). Thus, $\text{RXR}\alpha$ did not appear to be critically required for the formation of hepatocytes during liver organogenesis, but it remained to be determined whether $\text{RXR}\alpha$ could be required for further fetal and postnatal liver development. It was also unknown

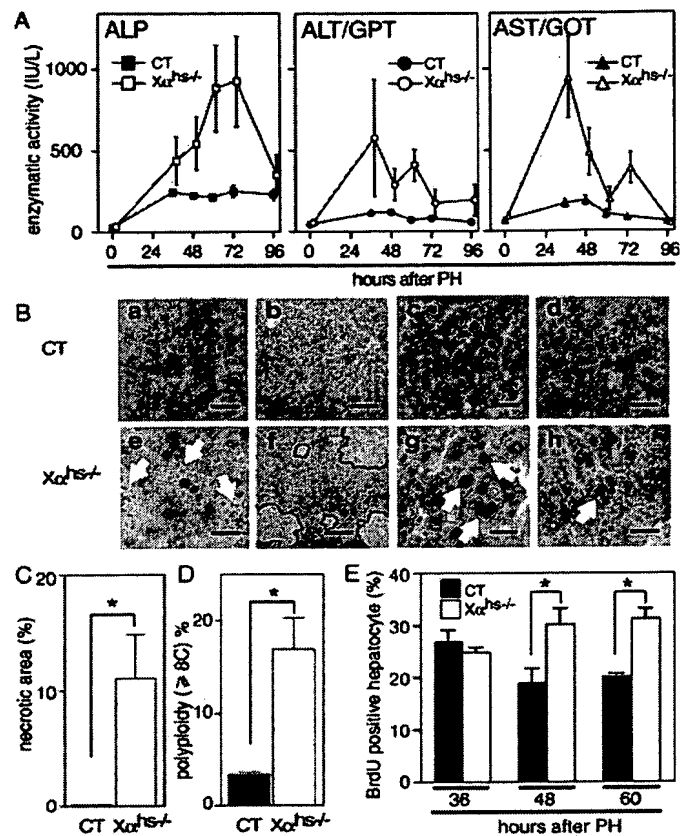


Fig. 4. Cell defects in $\text{RXR}\alpha^{\text{hs-/-}}$ mice during liver regeneration. (A) Increased ALP, ALT, and AST activities in $\text{RXR}\alpha^{\text{hs-/-}}$ mice after PH. ALP, ALT/GPT, and AST/GOT enzymatic activities were determined on sera from 3-month-old CT (Alb-Cre^(tg/tg)/ $\text{RXR}\alpha^{+/+}$, Alb-Cre^(tg/tg)/ $\text{RXR}\alpha^{+/+$, Alb-Cre^(tg/tg)/ $\text{RXR}\alpha^{\text{L2/L2}}$, and $\text{RXR}\alpha^{\text{hs-/-}}$ ($\text{X}\alpha^{\text{hs-/-}}$) mice, at various times after PH. Values are expressed as the mean \pm SEM ($n = 3-5$). (B) Highly polyploid hepatocytes, giant multinucleated cells, neutrophil infiltration, and focal necrosis in $\text{RXR}\alpha^{\text{hs-/-}}$ mice after PH. Histological analysis of hematoxylin and eosin-stained sections of liver taken 36 h (a and e), 48 h (b and f), 72 h (c and g), and 1 week (d and h) after PH of CT (a–d) and $\text{RXR}\alpha^{\text{hs-/-}}$ (e–h) mice. Arrows indicate neutrophil infiltration in a, polyploid ($\geq 8C$) hepatocyte in g, and giant multinucleated cell in h. Lines surround areas of focal necrosis in f. [Scale bar, 20 μm (a, c–e, g, and h) and 80 μm (b and f).] (C) Quantification of necrotic areas of focal necrosis in $\text{RXR}\alpha^{\text{hs-/-}}$ mice. Necrotic areas were determined on liver sections from five CT (Alb-Cre^(tg/tg)/ $\text{RXR}\alpha^{+/+}$, Alb-Cre^(tg/tg)/ $\text{RXR}\alpha^{+/+}$, Alb-Cre^(tg/tg)/ $\text{RXR}\alpha^{\text{L2/L2}}$) and five $\text{RXR}\alpha^{\text{hs-/-}}$ ($\text{X}\alpha^{\text{hs-/-}}$) animals. Samples were taken 36 and 48 h after PH, from three and two animals from each group, respectively, and three fields containing more than 1,800 hepatocytes each were analyzed for each animal. (D) Quantification of polyploid hepatocytes in $\text{RXR}\alpha^{\text{hs-/-}}$ mice. Polyploid hepatocytes ($\geq 8C$) were determined on liver sections from five CT (Alb-Cre^(tg/tg)/ $\text{RXR}\alpha^{+/+}$, Alb-Cre^(tg/tg)/ $\text{RXR}\alpha^{+/+}$, Alb-Cre^(tg/tg)/ $\text{RXR}\alpha^{\text{L2/L2}}$) and five $\text{RXR}\alpha^{\text{hs-/-}}$ ($\text{X}\alpha^{\text{hs-/-}}$) animals. Samples were taken 60 and 72 h after PH, from two and three animals from each group, respectively, and three fields containing more than 1,800 hepatocytes each were analyzed for each animal. Note that the number of polyploid hepatocytes is undervalued as 6- μm sections were analyzed. *, $P < 0.001$. (E) Increased hepatocyte proliferative index in $\text{RXR}\alpha^{\text{hs-/-}}$ mice after PH. Hepatocyte proliferation was analyzed by BrdUrd incorporation 36, 48, and 60 h after PH. The percentage of BrdUrd-positive hepatocytes was determined on liver sections from five 3-month-old CT (Alb-Cre^(tg/tg)/ $\text{RXR}\alpha^{+/+}$, Alb-Cre^(tg/tg)/ $\text{RXR}\alpha^{+/+}$, Alb-Cre^(tg/tg)/ $\text{RXR}\alpha^{\text{L2/L2}}$) and five $\text{RXR}\alpha^{\text{hs-/-}}$ ($\text{X}\alpha^{\text{hs-/-}}$) animals. Values are expressed as mean \pm SEM. *, $P < 0.05$.

whether $\text{RXR}\alpha$ could be required for the maintenance of adult hepatocytes that have a low rate of cell turnover, with a lifespan of at least 300–400 days (27–29), and/or for their remarkable pro-

liferative capacity during the liver regeneration that can be induced by PH or a variety of injuries (5, 6, 30).

Our present analysis of adult mouse chimeras, obtained through injection of $\text{RXR}\alpha^{-/-}$ ES cells into wt blastocytes, clearly demonstrates that $\text{RXR}\alpha^{-/-}$ cells are selectively under-represented in livers of these chimeras when compared with other tissues. This may originate from impaired proliferation of $\text{RXR}\alpha^{-/-}$ hepatocytes during liver postnatal growth and/or their premature death. This latter possibility was supported by studies in which the Tam-inducible Cre-ER^T recombinase system was used to selectively ablate $\text{RXR}\alpha$ in $\approx 50\%$ of the hepatocytes of adult mice. Indeed, these $\text{RXR}\alpha$ -ablated hepatocytes disappear in less than 90 days, which is much shorter than the lifespan of wt hepatocytes. Moreover, we also show that $\text{RXR}\alpha$ levels are increased in hepatocytes shortly after PH and, interestingly, that the selective disappearance of $\text{RXR}\alpha$ -ablated hepatocytes is even faster during liver regeneration, thus suggesting that proliferating hepatocytes lacking $\text{RXR}\alpha$ could be particularly prone to premature death.

The conclusion that $\text{RXR}\alpha$ plays an important cell-autonomous function(s) in the mechanism(s) involved in the lifespan of hepatocytes was unexpected, as it was recently reported that selective ablation of $\text{RXR}\alpha$ in all hepatocytes during liver development has no effect on adult liver morphological characteristics (7, 8). However, a detailed histological analysis of similar adult mutants generated in our laboratory ($\text{RXR}\alpha^{\text{hs-/-}}$ mice) reveals the existence of occasional focal necrotic areas, whose presence is correlated with increased serum levels of enzymes known to be released during liver necrosis. Concomitantly, the PI of $\text{RXR}\alpha^{\text{hs-/-}}$ hepatocytes is significantly increased. Moreover, PH-induced liver regeneration in adult $\text{RXR}\alpha^{\text{hs-/-}}$ generates much more pronounced enzymatic and histological stigmas of liver necrosis accompanied by neutrophil infiltration. Twenty-four hours post-PH, the PI of hepatocytes is similarly increased in CT and $\text{RXR}\alpha^{\text{hs-/-}}$ livers, indicating that their replicative capacity is identical at an early stage of liver regeneration. However, this PI becomes higher in mutant hepatocytes at later stages of regeneration, most probably reflecting a compensatory growth subsequent to necrosis of hepatocytes lacking $\text{RXR}\alpha$, to restore the optimal liver mass.

Polyploidization is a characteristic feature of the growth of liver in rats, as well as in other mammals, including humans (see refs. 12 and 30–34). In newborn rats, actively dividing diploid hepatocytes dominate. Binucleate hepatocytes, resulting from acytokinetic mitosis, markedly increase over the next few weeks. Mononucleate tetraploid cells resulting from disturbance in karyokinesis then appear (60–70% in adults), followed by binucleated cells with two tetraploid nuclei ($\approx 20\%$ in adults) and finally by mononucleated octoploid cells (1–3% in adults), whereas a small fraction of diploid cells ($\approx 10\%$) is still present. In contrast to developmental growth, PH-induced regeneration growth is characterized by a marked decrease of binuclearity as a consequence of a reduced rate of

binucleation (31, 34). The biological significance of hepatic polyploidy is unclear, but it is generally considered that advanced polyploidy in mammalian cells is an indication of terminal differentiation and senescence of cells (33, 34). In this respect, it is remarkable that the PH-induced proliferative hepatocytes that lack $\text{RXR}\alpha$ exhibit much higher degrees of polyploidy than their wt counterparts and that this increased polyploidy is correlated with an increase in their death rate. In any event, our present data show that the lifespan of hepatocytes depends on cell-autonomous events mediated by $\text{RXR}\alpha$. The lifespan of adult hepatocytes lacking $\text{RXR}\alpha$ is shorter than that of their wt counterparts, whereas PH-induced proliferative hepatocytes lacking $\text{RXR}\alpha$ have an even shorter lifespan. Whether two distinct $\text{RXR}\alpha$ -mediated mechanisms are involved in the death of “quiescent” and “replicative” $\text{RXR}\alpha$ -ablated hepatocytes, or whether the same $\text{RXR}\alpha$ -mediated mechanism would operate in the two cases and be magnified just under replicative conditions, remains to be determined.

Which $\text{RXR}\alpha$ heterodimer(s) could mediate the events that prevent early death of quiescent and proliferative hepatocytes is unknown. The liver contains a wealth of members of the nuclear receptor superfamily that can heterodimerize with $\text{RXR}\alpha$ (2, 7–10). Among these RXR partners, retinoic acid receptors and thyroid hormone receptors are potential candidates. First, it has been shown that PH of vitamin A-deficient rats leads to focal necrosis of the liver in the course of its regeneration (15) and that this necrosis could be prevented by vitamin A administration just before PH (14). Second, Torres *et al.* (12) have shown that, in the rat, normal hepatocyte polyploidization is regulated by the T3 thyroid hormone. Whether retinoic acid receptors (α , β , or γ) and/or thyroid hormone receptors (α or β) are RXR partners in the regulation of hepatocyte lifespan and replication will require further studies in which hepatocyte-specific somatic ablation of these receptor genes will be performed, remembering that double mutants might be required to circumvent problems linked to functional redundancy between receptor isotypes.

We thank M. A. Magnuson for Albumin-Cre mice, J. Auwerx for ApoCIII probe, and R. Lorentz, C. Gérard, and S. Bronner for technical assistance; we also thank M. LeMeur and the animal facility staff for animal care and the secretarial staff for preparation of the manuscript. This work was supported by funds from Centre National de la Recherche Scientifique, the Institut National de la Santé et de la Recherche Médicale, the Collège de France, the Hôpital Universitaire de Strasbourg, the Association pour la Recherche sur le Cancer, the Fondation pour la Recherche Médicale, the Human Frontier Science Program, the European Economic Community, and the Ministère de l'Éducation Nationale de la Recherche et de la Technologie. T.I. was supported by postdoctoral fellowships from the Centre National de la Recherche Scientifique, the Fondation de la Recherche Médicale, and the Toyobo Science Foundation. M.J. was supported by fellowships from the Association pour la Recherche sur le Cancer and the Institut National de la Santé et de la Recherche Médicale.

- Mangelsdorf, D. J., Thummel, C., Beato, M., Herrlich, P., Schütz, G., Umesono, K., Blumberg, B., Kastner, P., Mark, M., Chambon, P. & Evans, R. M. (1995) *Cell* 83, 835–839.
- Kastner, P., Mark, M. & Chambon, P. (1995) *Cell* 83, 859–869.
- Chambon, P. (1996) *FASEB J.* 10, 940–954.
- Giguère, V. (1999) *Endocr. Rev.* 20, 689–725.
- Steer, C. J. (1995) *FASEB J.* 9, 1396–1400.
- Michalopoulos, G. K. & DeFrances, M. C. (1997) *Science* 276, 60–66.
- Wan, Y.-J. Y., An, D., Cai, Y., Repa, J. J., Chen, T. H. P., Flores, M., Postic, C., Magnuson, M. A., Chen, J., Chien, K. R., *et al.*, (2000) *Mol. Cell. Biol.* 20, 4436–4444.
- Wan, Y.-J., Cai, Y., Lungu, W., Fu, P., Locker, J., French, S. & Sucov, H. M. (2000) *J. Biol. Chem.* 275, 28285–28290.
- Kastner, P., Grondana, J., Mark, M., Gansmuller, A., LeMeur, M., Décimo, D., Vonesch, J. L., Dollé, P. & Chambon, P. (1994) *Cell* 78, 987–1003.
- Sucov, H. M., Dyson, E., Gumeringer, C. L., Price, J., Chien, K. R. & Evans, R. M. (1994) *Genes Dev.* 8, 1007–1018.
- Ohmura, T., Columbano, G. L., Columbano, A., Katyal, S. L., Locker, J. & Shinozuka, H. (1996) *Pharmacol. Lett. Life Sci.* 58, 211–216.
- Torres, S., Diaz, B. P., Cabrera, J. J., Diaz-Chico, J. C., Diaz-Chico, B. N. & Lopez-Guerra, A. (1999) *Am. J. Physiol.* 276, G155–G163.
- Francavilla, A., Carr, B. I., Azzarone, A., Polimeno, L., Wang, Z., Van Thiel, D. H., Subbotin, V., Prelich, J. G. & Starzl, T. E. (1994) *Hepatology* 20, 1237–1241.
- Evarts, R. P., Hu, Z., Omori, N., Omori, M., Marsden, E. R. & Thorgeirsson, S. S. (1995) *Am. J. Pathol.* 147, 699–706.
- Hu, Z., Fujio, K., Marsden, E. R., Thorgeirsson, S. S. & Evarts, R. P. (1994) *Cell Growth Differ.* 5, 503–508.
- Desvergnès, B. & Wahli, W. (1999) *Endocr. Rev.* 20, 649–688.
- Postic, C. & Magnuson, M. A. (2000) *Genesis* 26, 149–150.
- Imai, T., Chambon, P. & Metzger, D. (2000) *Genesis* 26, 147–148.
- Li, M., Chiba, H., Warot, X., Messaddeq, N., Gérard, C., Chambon, P. & Metzger, D. (2001) *Development (Cambridge, U.K.)*, 128, 675–688.
- Imai, T., Jiang, M., Chambon, P. & Metzger, D. (2001) *Proc. Natl. Acad. Sci. USA* 98, 224–228. (First Published December 26, 2000; 10.1073/pnas.011528898)
- Chomczynski, P. & Sacchi, N. (1987) *Anal. Biochem.* 162, 156–159.

22. Peters, J. M., Hennuyer, N., Staels, B., Fruchart, J. C., Fievet, C., Gonzalez, F. J. & Auwerx, J. (1997) *J. Biol. Chem.* **272**, 27307–27312.
23. Rochette-Egly, C., Lutz, Y., Pfister, V., Heyberger, S., Scheuer, I., Chambon, P. & Gaub, M. P. (1994) *Biochem. Biophys. Res. Commun.* **204**, 525–536.
24. te Riele, H., Maandag, E. R., Clarke, A., Hooper, M. & Berns, A. (1990) *Nature (London)* **348**, 649–651.
25. Nagy, A., Rossant, J., Nagy, R., Abramow-Newerly, W. & Roder, J. C. (1993) *Proc. Natl. Acad. Sci. USA* **90**, 8424–8428.
26. Schlüter, C., Duchrow, M., Wohlenberg, C., Becker, M. H. G., Key, G., Flad, H.-D. & Gerdes, F. (1993) *J. Cell Biol.* **123**, 513–522.
27. Bralet, M.-P., Branchereau, S., Brechot, C. & Ferry, N. (1994) *Am. J. Pathol.* **144**, 896–905.
28. MacDonald, R. A. (1961) *Arch. Intern. Med.* **107**, 335–343.
29. Ponder, K. P. (1996) *FASEB J.* **10**, 673–684.
30. Columbano, A. & Shinozuka, H. (1996) *FASEB J.* **10**, 1118–1128.
31. Saeter, G., Schwarze, P. E. & Seglen, P. O. (1998) *J. Natl. Cancer Inst.* **80**, 950–957.
32. Saeter, G., Schwarze, P. E., Nesland, J. M., Juul, N., Pettersen, E. O. & Seglen, P. O. (1988) *Carcinogenesis* **9**, 939–945.
33. Gupta, S. (2000) *Semin. Cancer Biol.* **10**, 161–171.
34. Gerlyng, P., Grotmol, A. T., Erikstein, B., Huitfeldt, H. S., Stokke, T. & Seglen, P. O. (1993) *Cell Prolif.* **26**, 557–565.

Impaired adipogenesis and lipolysis in the mouse upon selective ablation of the retinoid X receptor α mediated by a tamoxifen-inducible chimeric Cre recombinase (Cre-ER^{T2}) in adipocytes

Takeshi Imai, Ming Jiang, Pierre Chambon*, and Daniel Metzger

Institut de Génétique et de Biologie Moléculaire et Cellulaire, Centre National de la Recherche Scientifique/Institut National de la Santé et de la Recherche Médicale/Université Louis Pasteur, Collège de France, BP 163, 67404 Illkirch Cedex, Communauté Urbaine de Strasbourg, France

Contributed by Pierre Chambon, November 6, 2000

Retinoid X receptor α (RXR α) is involved in multiple signaling pathways, as a heterodimeric partner of several nuclear receptors. To investigate its function in energy homeostasis, we have selectively ablated the RXR α gene in adipocytes of 4-week-old transgenic mice by using the tamoxifen-inducible Cre-ER^{T2} recombination system. Mice lacking RXR α in adipocytes were resistant to dietary and chemically induced obesity and impaired in fasting-induced lipolysis. Our results also indicate that RXR α is involved in adipocyte differentiation. Thus, our data demonstrate the feasibility of adipocyte-selective temporally controlled gene engineering and reveal a central role of RXR α in adipogenesis, probably as a heterodimeric partner for peroxisome proliferator-activated receptor γ .

peroxisome proliferator-activated receptor γ | conditional mutagenesis | obesity | fasting | adipocyte fatty acid binding protein

In vertebrates, the adipose tissue is critical for energy homeostasis (1, 2). Whereas the brown adipose tissue can dissipate energy through thermogenesis, the white adipose tissue (WAT) stores excess energy in the form of triglycerides, when caloric intake exceeds expenditure, and releases free fatty acids (FFAs) when expenditure exceeds intake. The size of the adipose tissue can be modulated by the formation of new adipocytes from precursor cells (adipocyte differentiation) and/or increase in adipocyte size (adipocyte hypertrophy). Adipocyte differentiation has been studied mainly with preadipocyte culture systems (1). Three classes of transcription factors have been identified that influence fat cell development. These include CCAAT/enhancer-binding proteins (C/EBPs), adipocyte differentiation determinant-dependent factor 1 (ADD1)/sterol response element-binding protein (SREBP1), and the peroxisome proliferator-activated receptor (PPAR) family proteins (3–7). PPAR γ , one of the three PPAR isotypes, is abundantly expressed in adipose tissue and has been recently shown to play a critical role in both adipocyte differentiation and hypertrophy *in vivo* (8–10). As other members of the nuclear hormone receptor superfamily, such as the retinoic acid, vitamin D₃, and thyroid hormone receptors, it forms heterodimers with the three retinoid X receptor (RXR) isotypes (α , β , or γ) (6, 11, 12).

That RXR–PPAR heterodimers could mediate adipocyte differentiation has been demonstrated *in vitro* by using cultured cells and RXR- and PPAR γ -specific ligands (13). RXR α is expressed in a number of mouse tissues, including the adipose tissue, in which high levels of transcripts were detected (14). However, its role in adipocyte differentiation and hypertrophy could not be investigated *in vivo* in RXR α knockout (KO) mice, because RXR α ^{−/−} fetuses die *in utero* (15, 16).

We have used the Cre–lox system to generate mice in which RXR α could be specifically ablated in adipocytes in a temporally controlled manner. To this end, we have generated a transgenic mouse line that specifically expresses the tamoxifen (Tam)-

inducible fusion protein between the Cre recombinase and a mutated ligand-binding domain of the human estrogen receptor (Cre-ER^{T2}) (17, 18) in adipocytes, under the control of the promoter of the adipocyte fatty acid binding protein (aP2) (19). After treatment with Tam, transgenic mice harboring the aP2-Cre-ER^{T2} transgene and a LoxP site containing (floxed) RXR α gene, yielded animals in which RXR α was specifically ablated in adipocytes. We show that such mice have impaired adipogenesis and lipolysis.

Materials and Methods

Generation of Transgenic Mice. The aP2-Cre-ER^{T2} transgene was constructed as follows: a 5.4-kb blunt-ended *NotI* fragment containing the aP2 promoter, amplified from mouse genomic DNA by PCR with the LA-PCR kit (Perkin–Elmer) using the oligonucleotides 5′-ATACGCGGCCGCGAATTCCAGCAG-GAATCAGGTAGCT-3′ and 5′-ATAGCGCCGGCGCTG-CAGCACAGGAGGGTGCTATGAG-3′. The product was cloned into the blunt-ended *SaII* site of pGS-Cre-ER^{T2} (17), resulting in paP2-Cre-ER^{T2}. The aP2-L-EGFP-L transgene was constructed as follows: the 5.4-kb blunt-ended *NotI* fragment containing the aP2 promoter was cloned into the blunt-ended *SaII* site of pL-EGFP-L, resulting in paP2-L-EGFP-L. pL-EGFP-L was obtained by cloning the 0.7-kb blunt-ended *EcoRI* fragment isolated from pCX-EGFP (20) into the blunt-ended *BamHI* site of pLox2 (21). The 8.3-kb and 7-kb *NotI* DNA fragments were purified from paP2-Cre-ER^{T2} and paP2-L-EGFP-L, respectively, and injected into (C57BL/6 × SJL) F₁ zygotes at a concentration of 4 ng/ml, as described (22, 23). Four aP2-Cre-ER^{T2}(^u) transgenic lines were obtained from 54 founder animals. RXR α ^{+/−}, RXR α ^{+/aP2(1)}, and RXR α ^{L2/+} mice were as described (15, 18, 24).

Animal Treatments. Under normal conditions, mice were fed a standard laboratory chow (regular diet, RD; 2,800 kcal/kg; 1 cal = 4.18 J; Usine d’Alimentation Rationnelle, Villemoisson-sur-Orge, France). The high-fat and high-sucrose diet (HFD) study was carried out with a chow containing 4,056 kcal/kg (fat = 1,600 kcal/kg and sucrose = 1,600 kcal/kg; Research

Abbreviations: aP2, adipocyte fatty acid binding protein; Cre-ER^{T2}, fusion protein between the Cre recombinase and a mutated ligand-binding domain of the human estrogen receptor; EGFP, enhanced green fluorescent protein; FFA, free fatty acid; HFD, high-fat and high-sucrose diet; KO, knockout; LPL, lipoprotein lipase; MSG, monosodium glutamate; PPAR, peroxisome proliferator-activated receptor; RD, regular diet; RXR, retinoid X receptor; Tam, tamoxifen; WAT, white adipose tissue; RT-PCR, reverse transcription–PCR; WT, wild type; CT, control.

*To whom reprint requests should be addressed. E-mail: chambon@igbmc.u-strasbg.fr.

The publication costs of this article were defrayed in part by page charge payment. This article must therefore be hereby marked “advertisement” in accordance with 18 U.S.C. §1734 solely to indicate this fact.

Article published online before print: *Proc. Natl. Acad. Sci. USA*, 10.1073/pnas.011528898. Article and publication date are at www.pnas.org/cgi/doi/10.1073/pnas.011528898

Diets, New Brunswick, NJ). HFD was given to animals at weaning.

Monosodium glutamate (MSG) dissolved in saline solution was injected at 0.1 g/ml s.c. [2 mg per g (body weight) per day] from postnatal days 1 to 7 (19, 25, 26).

Tam (1 mg in 100 μ l of sunflower oil) was injected i.p. into mice for 5 consecutive days, as described (18, 27).

Reverse Transcription-PCR (RT-PCR) and Northern and Southern Blot Analyses. RNA was prepared from mouse organs by guanidine thiocyanate extraction (28). Cre-ER^{T2} expression was analyzed by RT-PCR. cDNA was synthesized for 20 min at 50°C from 1 μ g of RNA, 50 units of Moloney murine leukemia virus reverse transcriptase and the 3'-primer 5'-GGCGATCCCTGAACATGTCC-3' and was amplified by 30 cycles of PCR using the same 3'-primer and the 5'-primer 5'-TTGACCTCCATAGAAGACA-3'. The 254-bp Cre-ER^{T2} cDNA fragment was identified by Southern blotting using the ³²P-radiolabeled oligonucleotide 5'-ATCCGAAAAGAAAACGTTGA-3'. The primers used to amplify the 310-bp Pref-1 cDNA fragment were 5'-CAACAAGGAGCTGGTGATG-3' and 5'-CGAGATGAAATCTTAT-TAT-3'. The probe corresponds to the ³²P-radiolabeled oligonucleotide 5'-GAGTTTGCTCTATTGTGAGG-3'. Hypoxanthine phosphoribosyltransferase (HPRT) was used as an internal control, as described (23). For Northern blotting, 10 μ g of total RNA was electrophoresed on a 0.8% agarose gel, transferred to a nylon membrane, hybridized with radiolabeled RXR β (29); RXR γ (30); PPAR γ , aP2, and lipoprotein lipase (LPL) (31); and 36B4 (32) probes, as described (33).

aP2-Cre-ER^{T2}-mediated DNA excision was determined by Southern blot analysis, performed on *Bam*HI-digested genomic DNA isolated from organs of aP2-Cre-ER^{T2}(tg⁰)/RXR α ^{+/af2(I)} or aP2-Cre-ER^{T2}(tg⁰)/RXR α ^{L2/-} double-transgenic mice, or from RXR α ^{+/af2(II)} mouse tail (18, 23). Purification of adipocytes by collagenase II treatment of adipose tissue and centrifugation was as described (34, 35).

Histological Analysis. Organs were taken from mice perfused with paraformaldehyde (4% in PBS), fixed in formaldehyde (20% in PBS), and frozen in tissue-Tek OCT compound (SAKURA, Zoeterwoude, The Netherlands). Ten-micrometer cryosections were stained with hematoxylin and eosin or Oil red O and examined by light microscopy. 4',6-Diamidino-2-phenylindole dihydrochloride and green fluorescence was analyzed on cryosections by confocal microscopy as described (36).

Plasma-Free Fatty Acids Analysis. Plasma-free fatty acids were determined by an enzymatic assay, adapted to microtiter plates, and commercially available reagents (Boehringer Mannheim) (37).

Statistical Analysis. Values are reported as mean \pm SEM. Statistical significance ($P < 0.05$) was determined by unpaired Student's *t* test (STATVIEW, Abacus Concepts, Berkeley, CA).

Results and Discussion

Cre-ER^{T2}-Mediated Targeted Mutagenesis in Mouse Adipocytes. Transgenic mice expressing the conditional Cre-ER^{T2} recombinase selectively in adipocytes were obtained by using the aP2 promoter (19). Cre-ER^{T2} transcripts were found to be expressed specifically in WATs and brown adipose tissues in three of four transgenic lines (Fig. 1A and data not shown). The line expressing the highest level of Cre-ER^{T2} (referred to as the aP2-Cre-ER^{T2}(tg⁰) line in the hemizygous state) was then crossed with an aP2-L-EGFP-L(tg⁰) reporter line that expresses a floxed enhanced green fluorescent protein (EGFP) gene under the control of the aP2 promoter. A green fluorescence was detected in \approx 30% of WAT adipocytes of aP2-Cre-ER^{T2}(tg⁰)/aP2-L-EGFP-L(tg⁰) bigenic mice, but not in other cell types of adipose tissue

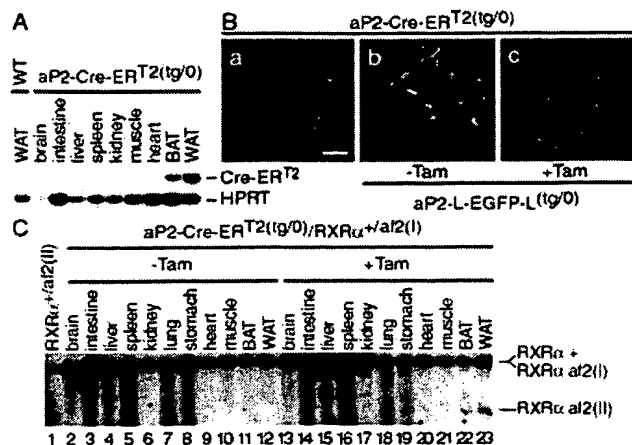


Fig. 1. Characterization of aP2-Cre-ER^{T2} transgenic mice. (A) Cre-ER^{T2} mRNA is selectively expressed in adipose tissue of aP2-Cre-ER^{T2} transgenic mice. Cre-ER^{T2} expression was analyzed by RT-PCR on RNA extracted from WAT of a 3-month-old WT mouse and from the indicated tissues of a 3-month-old aP2-Cre-ER^{T2}(tg⁰) transgenic mouse. The PCR products corresponding to Cre-ER^{T2} and HPRT mRNA are indicated. (B) After Tam treatment, aP2-Cre-ER^{T2} transgenic mice efficiently excise a floxed EGFP cassette in adipocytes. Cryosections of WAT isolated from a 3-month-old Tam-treated aP2-Cre-ER^{T2}(tg⁰) mouse (a), vehicle-treated aP2-Cre-ER^{T2}(tg⁰)/aP2-L-EGFP-L(tg⁰) bigenic mouse (b), and Tam-treated aP2-Cre-ER^{T2}(tg⁰)/aP2-L-EGFP-L(tg⁰) bigenic mouse (c), 30 days after the injection, were analyzed by confocal microscopy. The blue color corresponds to 4',6-diamidino-2-phenylindole dihydrochloride-stained nuclei, and the green color corresponds to GFP fluorescence. (Scale bar, 20 μ m.) (C) Cre-ER^{T2} mice selectively excise floxed DNA in adipocytes after Tam treatment. Cre-ER^{T2}-mediated DNA excision was determined by Southern blot analysis, performed on genomic DNA isolated from organs of 6-month-old aP2-Cre-ER^{T2}(tg⁰)/RXR α ^{+/af2(I)} bigenic mice, 7 days after the last injection of vehicle (lanes 2–12) or Tam (lanes 13–23) or from RXR α ^{+/af2(II)} mouse tail (lane 1). The position of the WT (+), floxed [af2(I)], and recombined [af2(II)] RXR α alleles are indicated. BAT, brown adipose tissue.

nor in cells of other organs (Fig. 1Bb and data not shown). Interestingly, the floxed EGFP cassette was efficiently excised upon Tam treatment, as judged from the total disappearance of the green fluorescence (Fig. 1Bc). In contrast, no aP2-Cre-ER^{T2}-mediated excision occurred in other cell types (e.g., pancreas, skeletal muscle, and myocardium cells), as no 5-bromo-4-chloro-3-indolyl β -D-galactoside staining was observed upon Tam treatment of aP2-Cre-ER^{T2}(tg⁰)/ACZL bigenic mice, under conditions where Cre-mediated recombination in the ACZL reporter transgenic mouse is known to result in β -galactosidase expression in these cells (refs. 38 and 39 and unpublished results).

Tissue-specific Cre-ER^{T2}-mediated excision upon Tam treatment also was observed in aP2-Cre-ER^{T2}(tg⁰)/RXR α ^{+/af2(I)} mice in which a floxed neomycin-resistance cassette is present within the RXR α locus (24). Excision of the cassette was restricted to brown adipose tissue and WAT, as shown by the presence of the “recombined” RXR α af2(II) allele 7 days after Tam treatment (Fig. 1C, compare lanes 22 and 23 with lanes 11 and 12; similar blots were obtained 30 and 90 days after Tam treatment, data not shown).

Temporally Controlled RXR α Ablation in Adipocytes. To selectively disrupt the RXR α gene in adipocytes, we generated aP2-Cre-ER^{T2}(tg⁰)/RXR α ^{L2/L2} mice, in which the exon encoding the RXR α DNA binding domain is floxed on both alleles (18). These mice then were crossed with RXR α ^{+/+} mice (15) to generate aP2-Cre-ER^{T2}(tg⁰)/RXR α ^{L2/-} mice which, after Tam-induced Cre-mediated excision, should yield mice in which adipocytes have a disrupted RXR α ^{L-/-} genotype (hereafter called

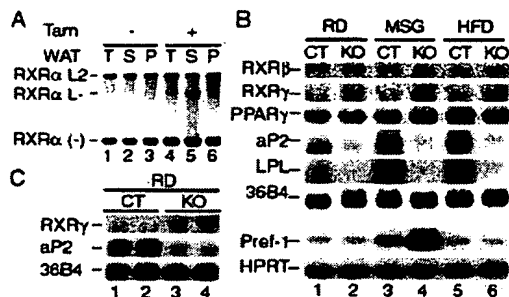


Fig. 2. Adipocyte-selective $RXR\alpha$ ablation in mice. (A) Efficiency of $RXR\alpha$ inactivation in adipocytes. Cre- ER^{T2} -mediated $RXR\alpha$ disruption was analyzed by Southern blotting DNA extracted from WAT (T) isolated from 4-month-old $aP2$ -Cre- $ER^{T2(tg/0)}$ / $RXR\alpha^{L2/-}$ mice, 3 months after vehicle (–) and Tam (+) treatments, and from the supernatant (S) and pellet (P) fractions after centrifugation of collagenase-treated WAT. Positions of $RXR\alpha$ L2, L–, and (–) alleles are indicated. (B) Expression of nuclear receptors, $PPAR\gamma$ target genes, and $Pref-1$ in $RXR\alpha$ -deficient adipose tissue. $RXR\beta$, $RXR\gamma$, $PPAR\gamma$, $aP2$, and LPL mRNA levels were analyzed by Northern blotting RNA isolated from WAT of 6-month-old CT (lanes 1, 3, and 5) and $RXR\alpha^{adL-/-}$ (KO, lanes 2, 4, and 6) mice, under RD (lanes 1 and 2), after MSG treatment (lanes 3 and 4) and under HFD (lanes 5 and 6). $36B4$ was used as an internal control. $Pref-1$ expression was analyzed by RT-PCR performed on the same RNA samples, and $HPRT$ was used as an internal control. (C) Altered $RXR\gamma$ and $aP2$ expression in the adipose tissue of $RXR\alpha^{adL-/-}$ mice 2 weeks after Tam injection. $RXR\gamma$ and $aP2$ mRNA levels were analyzed by Northern blotting RNA isolated from adipose tissue of two 6-week-old CT (lanes 1 and 2) and $RXR\alpha^{adL-/-}$ (KO, lanes 3 and 4) mice, 2 weeks after Tam treatment. $36B4$ was used as an internal control.

$RXR\alpha^{adL-/-}$ mice), whereas other cell types have a $RXR\alpha^{L2/-}$ genotype. Their littermates, particularly, $aP2$ -Cre- $ER^{T2(tg/0)}$ / $RXR\alpha^{+/-}$ mice, were indistinguishable from wild-type (WT) mice and used as control (CT) animals. Four-week-old $aP2$ -Cre- $ER^{T2(tg/0)}$ / $RXR\alpha^{L2/-}$ mice were treated with Tam. Three months later, the selective presence of the L– allele in the adipose tissue was found to depend on Tam treatment (Fig. 2A, compare lanes 1 and 4, and data not shown). Importantly, WAT fractionation into purified adipocytes [supernatant (S) fraction] and stromal-vascular cells [pellet (P) fraction] indicated that at least 80% of the purified adipocytes had a $RXR\alpha^{L2/-}$ genotype, whereas no Cre-mediated recombination had occurred in stromal-vascular cells (Fig. 2A, compare lanes 5 and 6).

The above results demonstrate that $RXR\alpha$ was selectively and efficiently disrupted in adipocytes upon Tam treatment of $aP2$ -Cre- $ER^{T2(tg/0)}$ / $RXR\alpha^{L2/-}$ mice. Although this disruption did not affect $RXR\beta$ levels in the adipose tissue of $RXR\alpha^{adL-/-}$ mice, $RXR\gamma$ levels were increased (Fig. 2B, compare lanes 1 and 2), indicating a possible compensatory up-regulation of $RXR\gamma$ expression. Interestingly, the transcripts of the $aP2$ and LPL genes, whose expression is known to be under $PPAR\gamma$ control (14, 31), were drastically reduced in WAT of $RXR\alpha^{adL-/-}$ mice, even though $PPAR\gamma$ levels were not modified (Fig. 2B). These observations suggest that $aP2$ and LPL expressions are controlled by $RXR\alpha$ - $PPAR\gamma$ heterodimers. Note that $RXR\gamma$ and $aP2$ expressions were already up- and down-regulated, respectively, 2 weeks after Tam treatment (Fig. 2C), which indicates that $RXR\alpha$ must be functionally ablated in $RXR\alpha^{adL-/-}$ mice shortly after Tam-induced Cre-mediated disruption of the $RXR\alpha$ gene.

$RXR\alpha$ Ablation in Adipocytes Results in Alteration of Preadipocyte Differentiation and Resistance to Obesity. The body weight of $RXR\alpha^{adL-/-}$ mice generated by Tam treatment at the age of 4 weeks and fed with a RD (named RD-KO mice) was followed for 28 weeks and compared with that of CT mice, named RD-CT (Fig. 3Aa). The weight of RD-KO mice was significantly lower

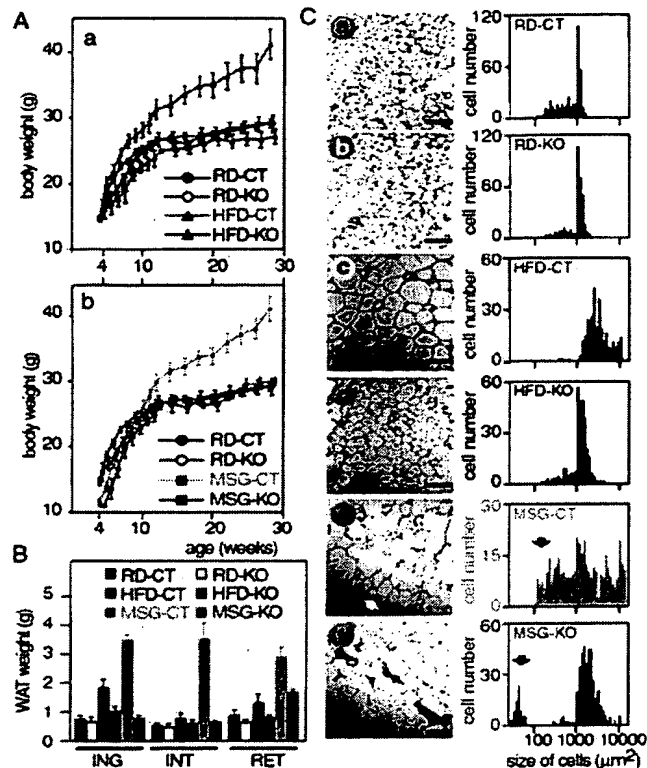


Fig. 3. $RXR\alpha^{adL-/-}$ mice are resistant to obesity and are impaired in preadipocyte differentiation. (A) $RXR\alpha^{adL-/-}$ mice are resistant to HFD- and MSG-induced obesity. Total body weight of CT and $RXR\alpha^{adL-/-}$ (KO) mice under RD (a and b), under HFD (a) and after MSG treatment (b) was measured weekly. The number of animals monitored in each group was 10–15 males. Values are expressed as the mean \pm SEM. (B) Reduced adipose tissue weight in $RXR\alpha^{adL-/-}$ mice under HFD or after MSG treatment compared with CT mice. Inguinal (ING), interscapular (INT), and retroperitoneal (RET) WAT weight was determined in 6-month-old CT and $RXR\alpha^{adL-/-}$ (KO) mice, fed with RD or HFD and after MSG treatment. Each group was composed of 5–7 males. Values are expressed as the mean \pm SEM. (C) Impaired adipogenesis in $RXR\alpha^{adL-/-}$ mice. Cryosections of s.c. inguinal WAT from 6-month-old CT (a, c, and e) and $RXR\alpha^{adL-/-}$ (b, d, and f) mice, under RD (a and b), HFD (c and d), and after MSG treatment (e and f) were stained with hematoxylin and eosin. (Scale bar, 160 μ m.) The areas of at least 400 cells per sample were determined with the *nsurx* software (J. L. Vonesch, Institut de Génétique et de Biologie Moléculaire et Cellulaire Illkirch). The distribution of the cell size is shown in the corresponding size graphs to the right. Arrows point to small adipocytes and preadipocytes or poorly differentiated adipocytes in e and f, respectively.

by approximately 10% during the first 4 weeks after Tam treatment and progressively reached that of adult RD-CT mice. From the age of 10 weeks, the weight of RD-KO mice was indistinguishable to that of RD-CT animals, suggesting that $RXR\alpha$ ablation may delay the formation of fat deposits. No differences in s.c. (inguinal and interscapular) and retroperitoneal WAT was observed between 6-month-old RD-KO and RD-CT mice (Fig. 3B), and their adipocytes exhibited a similar size distribution (Fig. 3C a and b).

We next investigated whether $RXR\alpha$ ablation in adipocytes may affect obesity induced in mice fed with a HFD. As expected, CT animals became obese under HFD (HFD-CT in Fig. 3Aa and B). In contrast, no obesity was induced by HFD in HFD-KO mice (Fig. 3Aa), and their WAT weight remained similar to that of RD-CT and RD-KO animals (Fig. 3B). As would be predicted, the adipocytes of HFD-CT mice were much larger than those of RD-CT mice, whereas those of HFD-KO mice exhibited a size

distribution similar to those of RD-CT and RD-KO animals. Clearly, RXR γ , which is increased upon RXR α ablation in adipose tissue (Fig. 2*B*), cannot replace RXR α to mediate the HFD-induced (and chemically induced, see below) hypertrophy of adipocytes, which leads to obesity. Interestingly, it has been reported that heterozygous PPAR $\gamma^{+/-}$ mice are partially resistant to HFD-induced obesity and maintain a smaller size of their adipocytes relative to WT adipocytes under HFD conditions (10). Thus, these observations suggest that HFD-induced adipocyte hypertrophy is mediated by RXR α -PPAR γ heterodimers. However, we note that, in contrast to PPAR $\gamma^{+/-}$ heterozygous mice, heterozygous RXR $\alpha^{+/-}$ mice developed HFD-induced obesity and adipocyte hypertrophy that were similar to those of WT animals (data not shown).

MSG administration to newborn mice induces hypothalamic lesions that result in a marked obesity in the adult (refs. 19, 25, and 26 and see Fig. 3*A**b*). To investigate whether ablation of RXR α in adipocytes also will prevent against the development of MSG-induced obesity, MSG was administered to aP2-Cre-ER^{T2}(tg0)/RXR $\alpha^{L2/-}$ newborn mice that were treated with Tam at the age of 4 weeks. As expected, MSG-treated CT animals (MSG-CT) developed obesity from the age of 10 weeks onward, compared with CT mice fed with a RD (RD-CT) (Fig. 3*A**b* and *B*). Interestingly, the adipocyte population in WAT of obese MSG-CT animals included not only hypertrophic adipocytes but also a markedly increased population of small adipocytes that was not found in HFD-induced obesity [Fig. 3*C*, compare *e* (MSG-CT, arrows) with *a* (RD-CT) and *c* (HFD-CT)]. These smaller adipocytes most probably represent maturing adipocytes derived from an increased population of preadipocytes in MSG-treated animals. There is indeed in MSG-CT animals an increase in RNA transcripts encoding Pref-1, a protein abundant in preadipocytes but not expressed in mature adipocytes (refs. 40 and 41; see Fig. 2*B*, lanes 1 and 3). Note that, in contrast, Pref-1 expression was not increased by a high-fat diet (Fig. 2*B*, lane 5) that results in adipocyte hypertrophy only (Fig. 3*C**e*). Thus, MSG treatment appears to cause both generation of preadipocytes and adipocyte hypertrophy in adult mice.

In contrast, the weights of the body and WAT deposits of adult MSG-treated RXR $\alpha^{adL-/-}$ (MSG-KO) mice were similar to those of adult RD-CT animals (Fig. 3*A**b* and *B*). Most of the adipocytes present in MSG-KO WAT were reduced in size compared with MSG-CT adipocytes and were only slightly larger than adipocytes present in mice fed a RD (RD-CT; in Fig. 3*C*, compare *f* with *e* and *a*). Interestingly, much smaller cells, which were not or only poorly stained with Oil red O, were seen in MSG-KO WAT deposits (Fig. 3*C**f*, arrows, and data not shown). It is likely that these cells correspond to preadipocytes or poorly differentiated adipocytes, because their presence was accompanied by a further increase in Pref-1 transcripts compared with MSG-CT mice (Fig. 2*B*, compare lanes 3 and 4). Thus, in MSG-treated mice, RXR α appears to be required for adipogenesis during both the differentiation of preadipocytes to adipocytes and the formation of hypertrophic adipocytes.

RXR α Ablation in Adipocytes Impairs Lipolysis During Fasting. The liberation of fatty acids from the adipose tissue (i.e., lipolysis) is a critical event in the fasting response aimed at maintaining whole-body energy homeostasis in the absence of an external energy supply. That RXR $\alpha^{adL-/-}$ mice, in which RXR α is specifically ablated in adipocytes, could suffer from decreased lipolysis and, therefore, from a fuel shortage of FFAs was first suggested by the observations that three of nine RXR $\alpha^{adL-/-}$ mice, but none of the 10 littermate controls, died after 2 days of fasting. Furthermore, a more pronounced hypothermia was observed upon fasting in RXR $\alpha^{adL-/-}$ mice than in CT littermates (Fig. 4*A*). After 2 days of fasting, WAT deposits completely disappeared in CT mice but not in RXR $\alpha^{adL-/-}$ (KO)

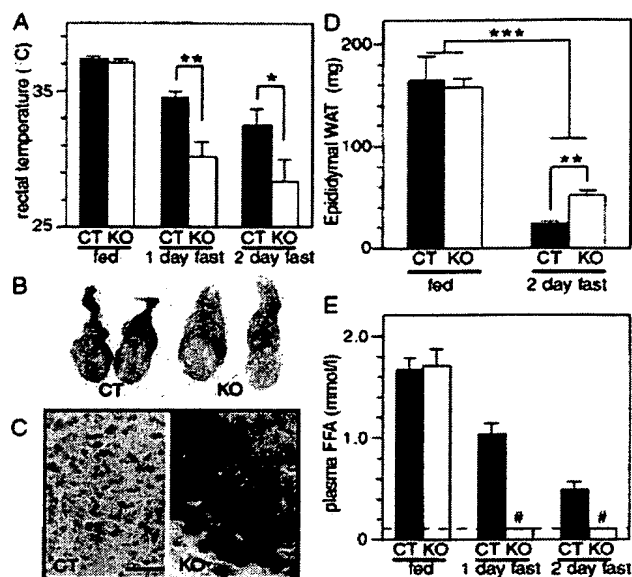


Fig. 4. Impaired lipolysis in RXR $\alpha^{adL-/-}$ mice during fasting. (A) Fasted RXR $\alpha^{adL-/-}$ mice suffer from hypothermia. Rectal temperature was determined on 10-week-old CT and RXR $\alpha^{adL-/-}$ (KO) mice at the beginning of the light cycle (fed state) and after a 1- or 2-day fast that was started at the beginning of the light cycle. (Error bars, SEM.) *, $P < 0.05$; **, $P < 0.001$. (B) Gross appearance of epididymal fat pad after fasting. Testes and epididymal fat pads from 3-month-old CT and RXR $\alpha^{adL-/-}$ (KO) mice after a 2-day fast are presented. (C) Histological analysis of epididymal fat pad. Sections of the epididymal fat pads shown in *B* were stained with Oil red O. (Scale bar, 20 μ m.) (D) Weight of epididymal fat pad. Epididymal fat pad weight of fed and fasted (2 days) 10-week-old CT and KO mice was measured. Values are expressed as the mean \pm SEM ($n = 9-10$). **, $P < 0.001$; ***, $P < 0.0001$. (E) Plasma FFA concentrations. FFA was determined in 10-week-old fed and fasted (1 and 2 days) CT and KO mice. Values are expressed as the mean \pm SEM ($n = 9-10$). # indicates values below background levels (dashed line, 0.1 mmol/liter).

mice, as illustrated by the epididymal fat pads in Fig. 4*B* and *D*. There was an almost total lack of Oil red O neutral lipid staining in a section of the epididymal fat pad of a CT mouse, whereas a corresponding section from a RXR $\alpha^{adL-/-}$ mutant mouse was intensely stained (Fig. 4*C*). Defective lipolysis in mutant mice was confirmed by the analysis of the FFA levels in the blood of fasting animals (Fig. 4*E*). No FFA could be detected above background level in plasma of RXR $\alpha^{adL-/-}$ mice after 1 day of fasting. Under similar conditions FFA levels were readily detectable in CT animals. Thus, the above data indicate that the presence of RXR α in adipocytes is required for the efficient release of FFA from white adipose fat.

Conclusion

We show herein the effectiveness of the Tam-inducible Cre-ER^{T2} chimeric recombinase expressed under the control of the aP2 promoter to generate adipocyte-selective temporally controlled targeted mutations in transgenic mice. These mice will be useful to analyze the function of many genes that are involved in energy homeostasis obesity and diabetes and often are expressed in several tissues where they exert pleiotropic effects (refs. 4, 6, 7, and 42 and references therein). In the present study, we have used the aP2-Cre-ER^{T2} transgenic line to investigate the functions of the RXR α gene in adipocytes.

We found that mice lacking RXR α in their adipocytes are resistant to obesity induced by a HFD or a treatment with MSG. It has been reported (10) that, under a HFD, the size of

adipocytes from PPAR γ ^{+/-} mice is significantly smaller than that of adipocytes from WT mice. Thus, the formation of hypertrophic adipocytes appears to be mediated by RXR α -PPAR γ heterodimers. Furthermore, our results indicate that RXR α not only is involved in adipocyte hypertrophy, as seen after HFD or MSG treatment, but also is probably involved in *de novo* differentiation of preadipocytes. Because PPAR γ has been shown to be required for adipocyte differentiation *in vitro* and probably *in vivo* (refs. 8–10 and references therein), RXR α -PPAR γ heterodimers may mediate fat accretion during both adipocyte differentiation and hypertrophy.

Finally, our results also reveal that RXR α is required during fasting for efficient lipolysis, demonstrating that RXR α plays an important role in both fat storage and mobilization. The molecular mechanisms involved in FFA release from the adipocytes and controlled by RXR α are at present unknown. Whether PPAR γ also is involved in the control of lipolysis as an het-

erodimeric partner for RXR α will require its temporally controlled adipocyte-specific ablation.

We thank J. Auwerx, B. Desvergne, W. Wahli, and G. Richards for probes, helpful discussions, and critical reading of the manuscript; S. Bronner, M. F. Champy, C. Gérard, R. Lorentz, and J. L. Vonesch for excellent technical help; M. LeMeur and the animal facility staff for animal care; and the secretarial staff for preparation of the manuscript. This work was supported by funds from the Centre National de la Recherche Scientifique, the Institut National de la Santé et de la Recherche Médicale, the Collège de France, the Hôpital Universitaire de Strasbourg, the Association pour la Recherche sur le Cancer, the Fondation pour la Recherche Médicale, the Human Frontier Science Program, European Economic Community Contract FAIR-CT97-3220, and the Ministère de l'Éducation Nationale de la Recherche et de la Technologie Déc.97.C.0115. T.I. was supported by postdoctoral fellowships from the Centre National de la Recherche Scientifique, the Fondation de la Recherche Médicale, and the Toyobo Science Foundation.

1. Spiegelman, B. M. & Flier, J. S. (1996) *Cell* **87**, 377–389.
2. Mandrup, S. & Lane, M. D. (1997) *J. Biol. Chem.* **272**, 5367–5370.
3. Fajas, L., Fruchart, J. C. & Auwerx, J. (1998) *Curr. Opin. Cell Biol.* **10**, 165–173.
4. Loftus, T. M. & Lane, M. D. (1997) *Curr. Opin. Genet. Dev.* **7**, 603–608.
5. Lowell, B. B. (1999) *Cell* **99**, 239–242.
6. Desvergne, B. & Wahli, W. (1999) *Endocr. Rev.* **20**, 649–688.
7. Rosen, E. D., Walkey, C. J., Puigserver, P. & Spiegelman, B. M. (2000) *Genes Dev.* **14**, 1293–1307.
8. Barak, Y., Nelson, M. C., Ong, E. S., Jones, Y. Z., Ruiz-Lozano, P., Chien, K. R., Koder, A. & Evans, R. (1999) *Mol. Cell.* **4**, 585–595.
9. Rosen, E. D., Sarraf, P., Troy, A. E., Bradwin, G., Moore, K., Milstone, D. S., Spiegelman, B. M. & Mortensen, R. M. (1999) *Mol. Cell.* **4**, 611–617.
10. Kubota, N., Terauchi, Y., Miki, H., Tamemoto, H., Yamauchi, T., Komeda, K., Satoh, S., Nakano, R., Ishii, C., Sugiyama, T., *et al.* (1999) *Mol. Cell.* **4**, 597–609.
11. Mangelsdorf, D. J., Thummel, C., Beato, M., Herrlich, P., Schutz, G., Um, K., Blumberg, B., Kastner, P., Mark, M., Chambon, P., *et al.* (1995) *Cell* **83**, 835–839.
12. Chambon, P. (1996) *FASEB J.* **10**, 940–954.
13. Tontonoz, P., Singer, S., Forman, B. M., Sarraf, P., Fletcher, J. A., Fletcher, C. D. M., Brun, R. P., Mueller, E., Altiock, S., Oppenheimer, H., *et al.* (1997) *Proc. Natl. Acad. Sci. USA* **94**, 237–241.
14. Tontonoz, P., Hu, E. & Spiegelman, B. M. (1994) *Cell* **79**, 1147–1156.
15. Kastner, P., Grondona, J. M., Mark, M., Gansmuller, A., LeMeur, M., Decimo, D., Vonesch, J.-L., Dollé, P. & Chambon, P. (1994) *Cell* **78**, 987–1003.
16. Sucov, H. M., Dyson, E., Gumeringer, C. L., Price, J., Chien, K. R., Evans, R. M., *et al.* (1994) *Gene Dev.* **8**, 1007–1018.
17. Indra, A. K., Warot, X., Brocard, J., Bornert, J.-M., Xiao, J.-H., Chambon, P. & Metzger, D. (1999) *Nucleic Acid Res.* **27**, 4324–4327.
18. Li, M., Indra, A. K., Warot, X., Brocard, J., Messaddeq, N., Kato, S., Metzger, D. & Chambon, P. (2000) *Nature (London)* **407**, 633–636.
19. Ross, S. R., Graves, R. A. & Spiegelman, B. M. (1993) *Genes Dev.* **7**, 1318–1324.
20. Okabe, M., Ikawa, M., Kominami, K., Nakanishi, T. & Nishimune, Y. (1997) *FEBS Lett.* **407**, 311–319.
21. Sumi-Ichinose, C., Ichinose, H., Metzger, D. & Chambon, P. (1997) *Mol. Cell. Biol.* **17**, 5976–5986.
22. Feil, R., Brocard, J., Mascréz, B., LeMeur, M., Metzger, D. & Chambon, P. (1996) *Proc. Natl. Acad. Sci. USA* **93**, 10887–10890.
23. Imai, T., Chambon, P. & Metzger, D. (2000) *Genesis (Dev. Genet.)* **26**, 147–148.
24. Mascréz, B., Mark, M., Dierich, A., Ghyselinck, N. B., Kastner, P. & Chambon, P. (1998) *Development (Cambridge, U.K.)* **125**, 4691–4707.
25. Olney, J. W. (1969) *Science* **164**, 719–721.
26. Pizzi, W. J. & Barnhart, J. E. (1976) *Pharmacol. Biochem. Behav.* **5**, 551–557.
27. Metzger, D. & Chambon, P. (2001) *Methods*, in press.
28. Chomczynski, P. & Sacchi, N. (1987) *Anal. Biochem.* **162**, 159–159.
29. Kastner, P., Mark, M., Leid, M., Gansmuller, A., Grondona, J. M., Decimo, D., Krezel, W., Dierich, A. & Chambon, P. (1996) *Genes Dev.* **10**, 80–92.
30. Krezel, W., Dupé, V., Mark, M., Dierich, A., Kastner, P. & Chambon, P. (1996) *Proc. Natl. Acad. Sci. USA* **93**, 9010–9014.
31. Schoonjans, K., Peinado-Onsurbe, A. M., Heyman, R. A., Briggs, M., Deeb, S., Staels, B. & Auwerx, J. (1996) *EMBO J.* **15**, 5336–5348.
32. Bouillet, P., Oulad-Abdelghini, M., Vicaire, S., Garnier, J. M., Schuhbaur, B., Dollé, P. & Chambon, P. (1995) *Dev. Biol.* **170**, 420–433.
33. Sambrook, J., Fritsch, E. F. & Maniatis, T. (1989) *Molecular Cloning: A Laboratory Manual* (Cold Spring Harbor Lab. Press, Plainview, NY), 2nd Ed.
34. Rodbell, M. (1964) *J. Biol. Chem.* **239**, 375–380.
35. Hotamisligil, G. S., Shargill, N. S. & Spiegelman, B. M. (1993) *Science* **259**, 87–91.
36. Brocard, J., Warot, X., Wendling, O., Messaddeq, N., Vonesch, J.-L., Chambon, P. & Metzger, D. (1997) *Proc. Natl. Acad. Sci. USA* **94**, 14559–14563.
37. Peters, J. M., Hennuyer, N., Staels, B., Fruchart, J. C., Fievet, C., Gonzalez, F. J. & Auwerx, J. (1997) *J. Biol. Chem.* **272**, 27307–27312.
38. Akagi, K., Sandig, V., Vooijs, M., Van der Valk, M., Giovannini, M., Strauss, M. & Berns, A. (1997) *Nucleic Acids Res.* **25**, 1766–1773.
39. Postic, C., Shiota, M., Niswender, K. D., Jetton, T. L., Chen, Y., Moates, J. M., Shelton, K. D., Lindner, J., Cherrington, A. D. & Magnuson, M. A. (1999) *J. Biol. Chem.* **274**, 305–315.
40. Smas, C. M. & Sul, H. S. (1993) *Cell* **73**, 725–734.
41. Smas, C. M., Chen, L. & Sul, H. S. (1997) *Mol. Cell. Biol.* **17**, 977–988.
42. Kadowaki, T. (2000) *J. Clin. Invest.* **106**, 459–465.

Germ cell expression of the transcriptional co-repressor TIF1 β is required for the maintenance of spermatogenesis in the mouse

Philipp Weber^{*,†}, Florence Cammas[†], Christelle Gerard, Daniel Metzger, Pierre Chambon, Régine Losson[‡] and Manuel Mark[‡]

Institut de Génétique et de Biologie Moléculaire et Cellulaire, CNRS/INSERM/ULP/Collège de France, BP163, 67404 Illkirch-cedex, France

^{*}Present address: Brain Research Institute, University and ETH Zurich, Winterthurerstrasse 190, CH 8057 Zurich, Switzerland

[†]These authors contributed equally to this work

[‡]Authors for correspondence (e-mail: losson@titus.u-strasbg.fr and marek@titus.u-strasbg.fr)

Accepted 22 February 2002

SUMMARY

The gene for transcriptional intermediary factor 1 β (TIF1 β) encodes a transcriptional co-repressor known to play essential roles in chromatin remodeling as well as in early embryonic development. During spermatogenesis, TIF1 β is preferentially associated with heterochromatin structures of Sertoli cells and round spermatids, as well as with meiotic chromosomes. Its expression is tightly regulated within spermatocyte and spermatid populations, and it is undetectable in spermatogonia. Spatiotemporally controlled ablation of TIF1 β by using a germ cell lineage-specific CreER^T/loxP system leads to testicular degeneration. This degeneration is not due to impairment of chromatin remodeling processes during meiosis and

spermiogenesis, as TIF1 β -deficient spermatocytes are able to complete their differentiation into spermatozoa. It rather occurs as a consequence of shedding of immature germ cells (spermatocytes and spermatids), and disappearance of stem spermatogonia. These results indicate that TIF1 β has important functions in the homeostasis of the seminiferous epithelium, and probably plays a crucial role in the network of paracrine interactions between germ cell subpopulations and/or Sertoli cells.

Key words: Heterochromatin protein 1, Transcriptional silencing, KRAB zinc-finger proteins, Testis-specific conditional knockout, Cellular interactions, Mouse

INTRODUCTION

Transcriptional regulation of gene expression in eukaryotes in response to developmental and other environmental signals is a multi-step process that requires the concerted action of many cellular factors. Central players in this elaborate process are sequence-specific transcription factors that activate and/or repress transcription through interactions with co-activators and co-repressors, whose ultimate function is to remodel chromatin structure (reviewed by Hassan et al., 2001; Muller and Leutz, 2001), to stimulate or inhibit (pre)initiation complex formation (reviewed by Hampsey and Reinberg, 1999; Rachez and Freedman, 2001) or to associate target genes with specialized nuclear compartments (Cockell and Gasser, 1999; Francastel et al., 2000).

Mammalian transcriptional intermediary factor 1 β (TIF1 β ; Trim28 – Mouse Genome Informatics) (also called KAP-1 or KRIP-1), which was originally identified as a co-repressor for the large family of KRAB domain-containing zinc-finger proteins (Friedman et al., 1996; Kim et al., 1996; Moosmann et al., 1996), has also been defined as a member of an emerging family of transcriptional regulators that includes TIF1 α and TIF1 γ in mammals (Le Douarin et al., 1995; Le Douarin et al., 1996; Venturini et al., 1999), and Bonus in *Drosophila*

(Beckstead et al., 2001). The domain structure that characterizes these proteins consists of an N-terminal RBCC (RING finger, B boxes, coiled coil) motif and a C-terminal bromodomain preceded by a PHD finger (Le Douarin et al., 1996). All TIF1 family members have been reported to repress basal and activated transcription when tethered to DNA through fusion to an heterologous DNA-binding domain. In the case of TIF1 β , an epigenetic mechanism of control has been suggested by the finding of an association with members of the heterochromatin protein 1 (HP1) family (Nielsen et al., 1999; Ryan et al., 1999), a class of non-histone chromosomal proteins with a well-established function in heterochromatin-mediated silencing (reviewed by Eissenberg and Elgin, 2000). TIF1 β has been shown to colocalize with members of the HP1 family in interphase nuclei of several mammalian cell lines (Nielsen et al., 1999; Ryan et al., 1999). In vitro, TIF1 β interacts with and phosphorylates the HP1 proteins (Nielsen et al., 1999). This interaction is required for the TIF1 β -mediated repression of transcription (Nielsen et al., 1999; Ryan et al., 1999) and for its association with pericentromeric heterochromatin in cultured cells (Matsuda et al., 2001) (F. C., M. Oulad-Abdelghani, J. L. Vonesch, P. C. and R. L., unpublished). A mechanistic link between TIF1 β repression and histone modification has also been established, with the

demonstration that deacetylase inhibitors such as Trichostatin A can interfere with TIF1 β -mediated repression in transient transfection assays (Nielsen et al., 1999; Schultz et al., 2001). In agreement with this result, TIF1 β has recently been reported to be an intrinsic component of a novel histone deacetylase complex, called N-CoR-1 (Underhill et al., 2000), and to interact both physically and functionally with the subunit Mi-2 α of the nucleosome remodeling and deacetylation (NuRD) complex (Schultz et al., 2001). Thus, TIF1 β may exert its co-repressor function via the assembly and/or maintenance of transcriptionally inactive, higher order chromatin structures through histone deacetylation and heterochromatinization.

We have recently shown that mice devoid of *Tif1 β* expression die at the egg cylinder stage, prior to the onset of gastrulation (Cammas et al., 2000). Analysis of the *Tif1 β* -null embryos has revealed a reduced cell number in the ectoderm, morphological alterations of the visceral endoderm and absence of mesoderm formation (Cammas et al., 2000). This phenotype indicates that TIF1 β exerts essential functions in early embryogenesis. However, the lethal outcome of this null mutation precludes the analysis of the roles of TIF1 β in later developmental and cell differentiation processes. Spermatogenesis is a cyclic cell differentiation process that includes spermatogonia self-renewal and their differentiation towards spermatozoa. We now show that during spermatogenesis, TIF1 β is expressed in a finely regulated pattern and is preferentially associated with heterochromatin. To investigate whether TIF1 β has a role in spermatogenesis, we have generated a conditional germline-specific *Tif1 β* mutation in mice by using the tamoxifen-inducible Cre-ER^T/loxP recombination system (Metzger and Chambon, 2001). Mice homozygous for a conditional allele of *Tif1 β* (TIF1 $\beta^{L2/L2}$), an allele in which essential coding exons are flanked by loxP sites (Cammas et al., 2000), were crossed with a transgenic PrP-Cre-ER^T(tg⁰) hemizygous line, in which tamoxifen selectively induces DNA excision in spermatogonia and spermatocytes (P. W., C. G., M. M., D. M. and P. C., unpublished). Analysis of the testes of tamoxifen-treated TIF1 $\beta^{L2/L2}$:PrP-Cre-ER^T(tg⁰) mice reveals that TIF1 β plays a key role in the maintenance of spermatogenesis.

MATERIALS AND METHODS

Mice

Mice allowing conditional inactivation of *Tif1 β* were obtained by crossing *Tif1 $\beta^{L2/L2}$* mice (Cammas et al., 2000) with CMV-Cre transgenic mice (Dupé et al., 1997). Offspring harboring the partially excised L2 allele of the *Tif1 β* gene without the antibiotic resistance cassette were identified by a PCR screen performed on DNA of tail biopsies using primers YD208, VR211 and TV210 as described (Cammas et al., 2000). Positive *Tif1 $\beta^{L2/+}$* mice were bred with wild-type mice and offspring which had lost the CMV-Cre transgene, but not the *Tif1 β* L2-allele, were intercrossed to generate homozygous *Tif1 $\beta^{L2/L2}$* mice. *Tif1 $\beta^{L2/L2}$* mice were viable, and did not show any phenotypic abnormalities.

Transgenic mice harboring a testis-restricted expression of the ligand-inducible Cre-ER^T (Feil et al., 1996) under control of the murine Prion (PrP)-promoter (PrP-Cre-ER^T line 28.8) are described elsewhere (P. W., C. G., M. M., D. M. and P. C., unpublished). *Tif1 $\beta^{L2/L2}$* males with (PrP-Cre-ER^T(tg⁰)) or without (PrP-Cre-ER^T(0/0)) the testis-specific transgene were generated and injected intra-peritoneally (IP) at 4 weeks of age for 5 consecutive days with

tamoxifen (1 mg/day) (Metzger and Chambon, 2001). Experimental (TIF1 $\beta^{L2/L2}$:PrP-Cre-ER^T(tg⁰)) and control (TIF1 $\beta^{L2/L2}$:PrP-Cre-ER^T(0/0)) males were sacrificed 1 day, and 2, 4, 6, 7 and 8 weeks after tamoxifen treatment (i.e. after the last tamoxifen injection).

Immunohistochemical detection of TIF1 β in mouse testes

Rabbit antisera were raised against two peptides (PF64 and PF65) corresponding to the N-terminal sequence (amino acids 140-154 and 66-80, respectively) of the TIF1 β protein and purified on a sulfonik coupling gel (Oulad-Abdelghani et al., 1996). Cellular localization of TIF1 β in testis of TIF1 $\beta^{L2/L2}$:PrP-Cre-ER^T(0/0) mice was performed on 10 μ m thick cryosections hydrated in phosphate-buffered saline (PBS) and fixed in 4% paraformaldehyde (PFA) in PBS (for 10 minutes at 4°C). Sections were rinsed in PBS containing 0.1% Triton X-100 (PBST; 3 \times 5 minutes at room temperature), then saturated with 5% normal goat serum (NGS) in PBST (30 minutes at room temperature), and incubated with the antibody against the PF64 and PF65 peptides (4 μ g/ml; 2 hours at room temperature). Sections were washed in PBST (3 \times 5 minutes), then PBS (5 minutes), incubated with the secondary antibody (Cy3-coupled donkey anti-rabbit diluted at 1/400 in PBS, Jackson Laboratories) (1 hour at room temperature), washed in PBST and mounted in Vectashield (Vector) containing DAPI at 10 μ g/ μ l. In another set of immunohistochemical experiments, testis of TIF1 $\beta^{L2/L2}$:PrP-Cre-ER^T(tg⁰) (experimental) and TIF1 $\beta^{L2/L2}$:PrP-Cre-ER^T(0/0) (control) mice were fixed in 4% PFA in PBS (16 hours at 4°C) and embedded in paraplast. Sections (7 μ m) were dewaxed, hydrated, rinsed in PBS, then placed into 5 mM sodium citrate buffer pH 6.0 and exposed to a microwave treatment (power output 800 W; 2 \times 2.5 minutes) (Balaton et al., 1993). After cooling down to room temperature, sections were rinsed in PBST, treated with 5% NGS in PBST (30 minutes) to block nonspecific antibody binding to the tissue sections and incubated for 16 hours at 4°C with the anti-PF64 and PF65 antibodies. Sections were then washed, incubated with the secondary antibody (1 hour at room temperature) and mounted as described for cryosections.

Preliminary experiments indicated that the antibodies against PF64 and PF65 labeled the same cells in the seminiferous epithelium. However, the signal was more intense with the later antibody, which was therefore used in subsequent immunostaining experiments. In immunohistochemical experiments, some differences were observed in the nuclear localization of TIF1 β and intensities of the signals in germ cell and Sertoli cell between frozen and microwave-treated paraffin wax-embedded sections. These differences were reproduced with both anti-PF64 and anti-PF65 antibodies. They could not be accounted by prolonged fixation in paraformaldehyde before paraffin wax embedding (i.e. 16 hours versus 10 minutes after cryosectioning) nor by the microwave treatment. Indeed, prolonged post-fixation of cryosections for 16 hours resulted in a global decrease of the anti-TIF1 β immunoreactivity in all cell types within the seminiferous epithelium. Likewise, microwave treatment globally restored the immunostaining that was decreased in all cell types upon a 16 hours stay of the tissue in paraformaldehyde. These differences in immunostaining may result from diffusion of the TIF1 β protein within the chromatin during the paraffin wax embedding process. As negative controls of the immunostaining procedure, histological sections were incubated either with non-immune rabbit IgGs (5 μ g/ml) or with a mixture of the primary antibody and 12-fold excess of the immunizing peptide (10 μ g/ml).

Histological analysis and detection of proliferating and apoptotic cells

For histological analysis, testes of tamoxifen-treated TIF1 $\beta^{L2/L2}$:PrP-Cre-ER^T(tg⁰) and TIF1 $\beta^{L2/L2}$:PrP-Cre-ER^T(0/0) mice were fixed in Bouin's fluid. Paraffin wax embedded sections (7 μ m) were stained with Hematoxylin and Mallory's trichrome (Mark et al., 1993). Detection of apoptotic cells on sections from PFA-fixed and paraffin wax-embedded testes was performed by TdT-mediated dUTP nick

end labeling (TUNEL), according to the manufacturers instructions (In Situ Cell Death Detection Kit, Fluorescein, Roche); sections were counterstained with DAPI. To identify proliferating cells, adult TIF1 $\beta^{L2/L2};PrP-Cre-ER^{T(0/0)}$ mice were injected intra-peritoneally four times at intervals of 2 hours with 50 mg/kg of BrdU. Testes were collected 2 hours after the last BrdU injection, fixed in 4% PFA in PBS (16 hours; 4°C). Paraffin wax-embedded sections were incubated with an antibody against BrdU (Boehringer Mannheim) diluted 1/100 in 0.1% NGS/PBS (16 hours; 4°C), revealed with Cy3-conjugated donkey anti-rabbit IgG, and mounted in Vectashield medium containing DAPI.

Statistical analysis

The number of seminiferous tubules showing abnormal expression of TIF1 β (i.e. partial staining along the circumference of spermatocyte and/or spermatid layers in a given tubular cross section, instead of staining along the whole circumference of these layers) was scored on testes from TIF1 $\beta^{L2/L2};PrP-Cre-ER^{T(0/0)}$ and TIF1 $\beta^{L2/L2};PrP-Cre-ER^{T(0/0)}$ animals 2 weeks after tamoxifen treatment. The number of degenerating tubules (i.e. tubules showing signs of vacuolation) was scored on histological sections from testes of TIF1 $\beta^{L2/L2};PrP-Cre-ER^{T(0/0)}$ and TIF1 $\beta^{L2/L2};PrP-Cre-ER^{T(0/0)}$ 8 weeks after tamoxifen treatment. Testicular sections of three individuals were analyzed for each genotype and experimental group. Statistical analysis of data was performed using ANOVA and the Fischer's protected least significant difference test (Fischer's PLSD).

RESULTS

TIF1 β is associated with heterochromatin and expressed in a finely regulated pattern during spermatogenesis

The expression pattern of TIF1 β was analyzed by immunohistochemistry on sections from frozen and paraffin wax-embedded TIF1 $\beta^{L2/L2};PrP-Cre-ER^{T(0/0)}$ testes (referred hereafter as control testes). On frozen sections, fluorescent nuclear signal for TIF1 β was present in all Sertoli cells (S; Fig. 1A-C), round spermatids (RS; Fig. 1A-C) and spermatids at early stages of elongation (ES-9; Fig. 1D-F). In all these cells, the intensity of the immunostaining paralleled that of the DNA-specific DAPI counterstain (arrowheads in Fig. 1A-F) (Barcellona and Gratton, 1990). A stippled signal was detected in the nuclei from large pachytene spermatocytes (P and arrows in Fig. 1D-F), whereas other meiotic cells as well as spermatogonia and elongated spermatids appeared negative (e.g. ES-13 in Fig. 1A-C and data not shown).

Confocal microscopy was used to assess the subnuclear localization of TIF1 β further. Single optical sections counterstained with DAPI showed that the TIF1 β staining was consistently more intense in heterochromatin than in euchromatin in both Sertoli cells and round and early elongating (step 9) spermatids. In Sertoli cells, TIF1 β was predominantly localized in nucleolar satellites (Sa in Fig. 1G-I) (Russell et al., 1990); in round spermatids, it was concentrated within the chromocenter, a structure formed from the association of the centromeric heterochromatin of all chromosomes (confocal data not shown, see arrowheads in Fig. 1D-F) (Pardue and Gall, 1970; Hoyer-

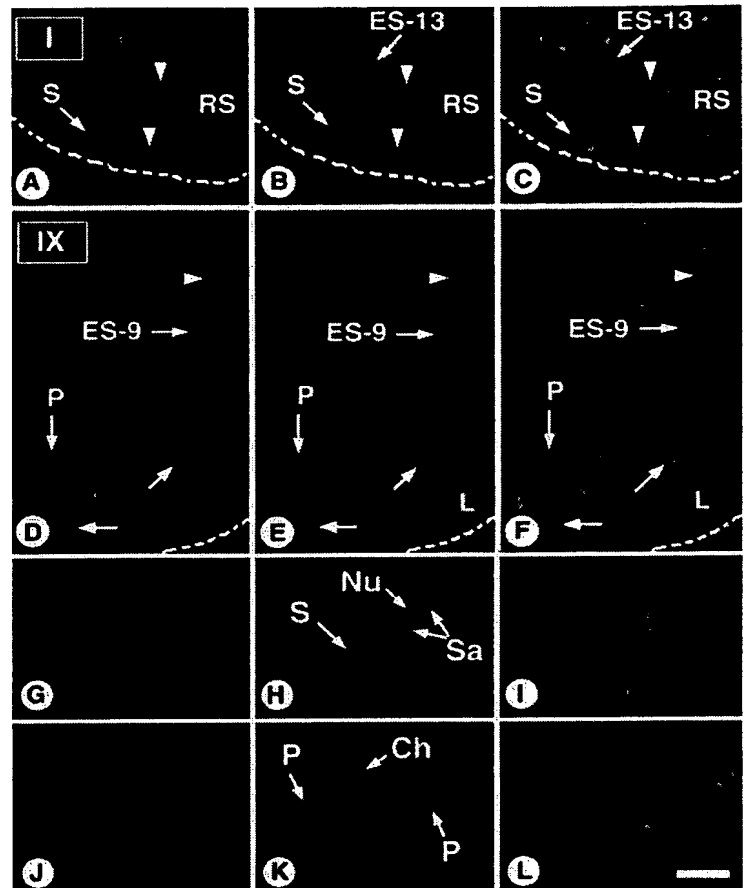


Fig. 1. Immunolocalization of TIF1 β in post-pubertal wild-type testis. Frozen histological sections were incubated with the anti-TIF1 β antibody whose binding to cell structures was then revealed with a Cy3-conjugated secondary antibody (red signal) and nuclei were counterstained with DAPI (blue signal). (A,D,G,J) Cy3 and (B,E,H,K) DAPI labeling. (C,F,I,L) Superimposition of the two fluorochromes. (G-L) Single optical sections of confocal microscopic analysis. Roman numerals refer to stages of the seminiferous epithelium cycle (Russell et al., 1990). Each stage is defined by a specific association of germ cell types. The cycle corresponds to the series of changes occurring at a given level of the seminiferous tubule between two successive appearances of the same cell association. In normal mice, there are 12 stages, designated I to XII, each corresponding to one of the first 12 steps of spermatid maturation. ES-9 and ES-13 correspond to steps in spermatid maturation. Ch, meiotic chromosomes; L, leptotene spermatocytes; P, pachytene spermatocytes; Nu, nucleolus of Sertoli cell; RS, round spermatids; S, Sertoli cells; Sa, satellite nucleolar heterochromatin of the Sertoli cell. The arrowheads and arrows in A-F indicate heterochromatin- and chromosome-associated TIF1 β , respectively. The broken lines indicate the contours of seminiferous tubules. Scale bar: 30 μ m in A-C; 15 μ m in D-F; 3 μ m in G-L.

Fender et al., 2000). Confocal microscopic analysis also showed a specific association of TIF1 β with chromosomes in pachytene spermatocytes (Ch in Fig. 1J-L).

Immunostaining with the anti-TIF1 β antibody of microwave-treated paraffin wax-embedded sections from control testes revealed an intense fluorescent signal in many spermatocytes (P in Fig. 2A-C) and round spermatids (RS).

The signal detected in Sertoli cells (S) was in general weaker than that observed on frozen sections. Moreover, in both germ cells and Sertoli cells, this immunostaining was exclusively nuclear, but was evenly distributed in the nucleus, instead of being associated with heterochromatin, as in the case of frozen sections (see Materials and Methods). Detection of TIF1 β in germ cells was dependent on their state of maturation and, therefore, on the stage of the seminiferous epithelium cycle (Russell et al., 1990) (see legend of Fig. 1). Immunostaining was undetectable in spermatogonia (SG) and young (preleptotene, leptotene, zygotene and early pachytene) spermatocytes (PR and L) (Fig. 2A-C and data not shown). It was intense in growing pachytene and in diplotene spermatocytes populating stage VI-XI tubules (P, Fig. 2A-C), at all steps of round spermatid maturation (e.g. RS in Fig. 2A,C) and in early elongating spermatids (i.e. step 9 spermatids, data not shown). Step 10 spermatids were only faintly immunostained (ES-10, Fig. 2B and data not shown), and spermatids at later stages of elongation (i.e. steps 11-16) were negative (ES-16 in Fig. 2A,C and data not shown). Unmasking of the epitope after microwave-induced disruption of heterochromatin structures in germ cells is likely to account for the discrepancies in patterns and intensities of immunostaining between sections from frozen and paraffin wax-embedded testes. These discrepancies were reproduced with antibodies raised against two distinct peptides derived from TIF1 β , indicating that they were not caused by auto-antibodies that might contaminate rabbit antisera. Note also that no immunostaining could be found when the primary antibody was replaced by non-immune IgG or a mixture of the primary antibody and immunizing peptide (data not shown).

To further investigate the possibility that some spermatogonia might express TIF1 β , control mice were injected with BrdU, which incorporates into the nuclei of spermatogonia and preleptotene spermatocytes. In double immunostaining experiments, colocalization of TIF1 β and BrdU was never observed (Fig. 2C and data not shown). Altogether, these data indicate that within the seminiferous epithelium, TIF1 β is present in all Sertoli cells, as well as in specific subpopulations of meiotic cells (i.e. mid-pachytene spermatocytes) and post-meiotic cells (i.e. step 1-10 spermatids). By contrast, this protein is undetectable in proliferating germ cells (i.e. spermatogonia), in preleptotene and early pachytene spermatocytes, as well as in condensing (step 12-14) and condensed (step 15-16) spermatids (Baarends et al., 1999).

PrP-Cre-ERT^T mediates inactivation of the floxed TIF1 β gene in spermatogonia and spermatocytes

PrP-Cre-ERT^T transgenic mice (line 28.8), which enable a tamoxifen-induced time-controlled and tissue-specific DNA excision in germ cells are described elsewhere (P. W., C. G., M. M., D. M. and P. C., unpublished). Before tamoxifen treatment, TIF1 β ^{L2/L2}:PrP-Cre-ERT^{T(g/0)} mice harboring both *Tif1 β* floxed alleles and the PrP-Cre-ERT^T transgene (referred hereafter as experimental animals) were normal with respect to fertility and testicular morphology (data not shown). The feasibility of spatiotemporal inactivation of TIF1 β in the

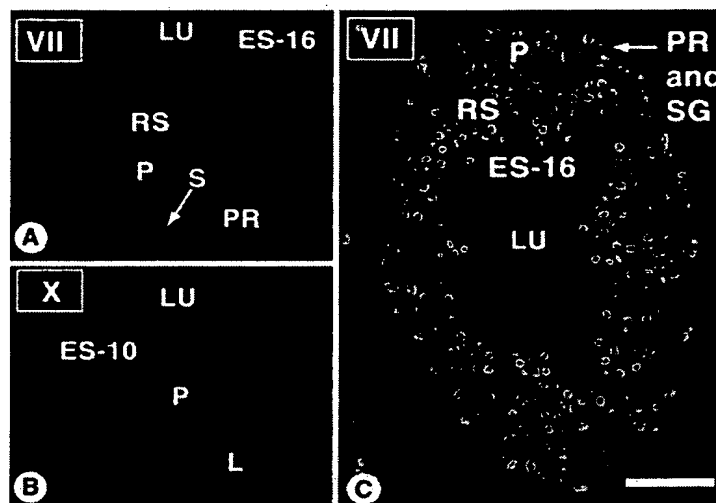


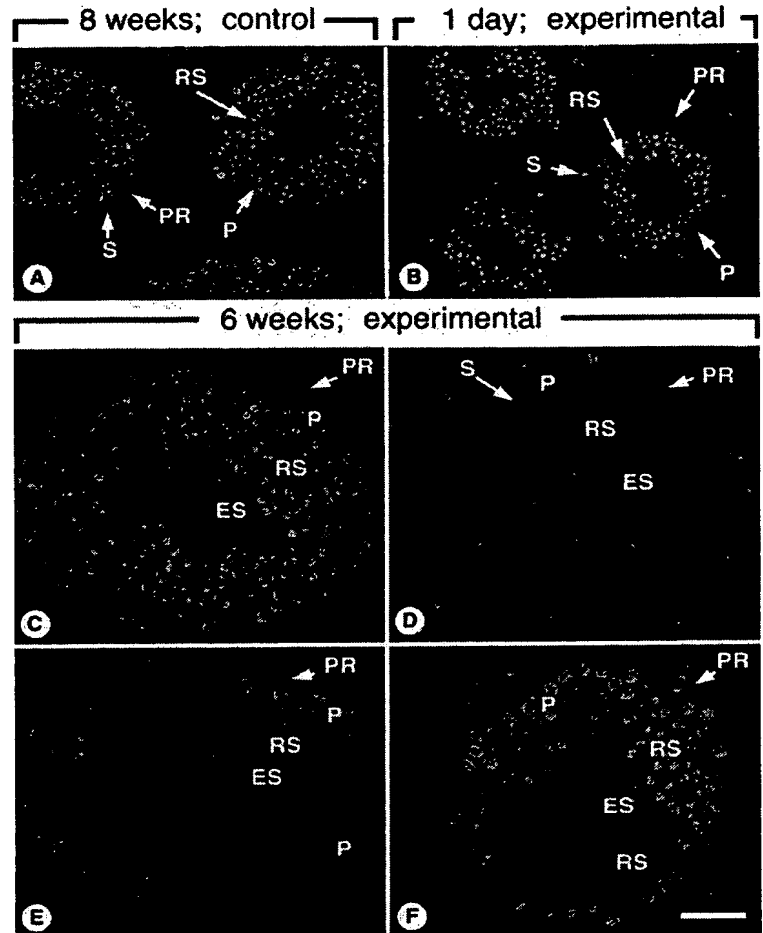
Fig. 2. Immunolocalization of TIF1 β in post-pubertal wild-type testis. Histological sections from paraffin wax-embedded testes were incubated with the anti-TIF1 β antibody, whose binding to cell structures was then revealed with a Cy3-conjugated secondary antibody (red signal) and nuclei were counterstained with DAPI (blue signal). BrdU incorporation in the tubular cross section shown in C was detected using a green fluorochrome. Roman numerals refer to stages of the seminiferous epithelium cycle. ES-10 and ES-16 correspond to steps in spermatid maturation. L, leptotene spermatocytes; LU, lumen of the seminiferous tubules; P, pachytene spermatocytes; PR, preleptotene spermatocytes; RS, round spermatids; S, Sertoli cells; SG, spermatogonia. Scale bar: 25 μ m in A,B; 55 μ m in C.

testis was assessed by following up the disappearance of the TIF1 β protein on histological sections of experimental animals at different time points after tamoxifen treatment. For the sake of simplicity, only observations of tubular cross-sections in stage VII (and beginning of stage VIII) will be reported, unless otherwise mentioned. Stage VII (and the beginning of stage VIII) are characterized by the alignment of elongated spermatid nuclei at the luminal side of the seminiferous epithelium, immediately before their release, as spermatozoa, into the lumen of the seminiferous tubules. Histological sections of TIF1 β control (TIF1 β ^{L2/L2}:PrP-Cre-ERT^{T(0/0)}) testes displayed a normal TIF1 β signal in all seminiferous tubules one day and 2, 4, 6 and 8 weeks after tamoxifen treatment (Fig. 3A and data not shown). By contrast, experimental (TIF1 β ^{L2/L2}:PrP-Cre-ERT^{T(g/0)}) testes displayed an abnormal pattern of TIF1 β distribution as early as 1 day after the end of the tamoxifen treatment: all pachytene spermatocytes were negative for TIF1 β (Fig. 3B). This finding indicates that the 'induced' Cre can rapidly and efficiently mediate disruption of the floxed *Tif1 β* gene in most (possibly all) spermatocytes. Experimental testes analyzed 2, 4 and 6 weeks after tamoxifen treatment contained only histologically normal seminiferous tubules, which were classified into three categories based on TIF1 β expression patterns: (1) tubules expressing TIF1 β specifically in pachytene spermatocytes and round spermatids, which were undistinguishable from their counterparts in controls (Fig. 3C); (2) tubules devoid of TIF1 β positive germ cells (Fig. 3D); (3) tubules showing an abnormal, mosaic, expression of

Fig. 3. Distribution of the TIF1 β protein in control (TIF1 $\beta^{L2/L2};PrP-Cre-ER^{T(0/0)}$) and experimental (TIF1 $\beta^{L2/L2};PrP-Cre-ER^{T(tg/0)}$) testes, 1 day (B), 6 weeks (C-F) and 8 weeks (A) after tamoxifen treatment. All the seminiferous tubules displayed here correspond to histologically normal stage VII tubules. C-F are from the same experimental testis. ES, elongated spermatids; P, pachytene spermatocytes; PR, preleptotene spermatocytes; RS, round spermatids; S, Sertoli cells. Immunostaining for TIF1 β (pink and red signals) with DAPI counterstain (blue signal). Scale bar: 100 μ m in A,B; 50 μ m in C-F.

TIF1 β in pachytene spermatocytes and/or round spermatids (Fig. 3E,F).

In the mouse, proceeding from spermatogonia to spermatozoa takes about 35 days (Oakberg, 1956a; Oakberg, 1956b). Therefore, the presence of TIF1 β -negative tubules in testes analyzed more than 40 days after tamoxifen treatment demonstrates that Cre-mediated DNA excision can occur in stem spermatogonia, in accordance with our previous observations (P. W., C. G., M. M., D. M. and P. C., unpublished). It is clear, however, that not all stem spermatogonia underwent excision, as indicated by the reappearance of TIF1 β -positive spermatocytes 2 weeks after tamoxifen treatment (Fig. 3C,E,F and data not shown). Moreover, in experimental testes analyzed 2 weeks after tamoxifen treatment about half of the tubules (53.17 \pm 11.82%) showed an abnormal TIF1 β expression in the spermatocyte layers (e.g. Fig. 3E,F and data not shown), instead of expression in tubules (0.76 \pm 0.16%) of similarly treated control mice ($P<0.0001$) (Fig. 4). Eight weeks after tamoxifen treatment, about half of the seminiferous tubules in experimental testes (52.92 \pm 3.19%) exhibited histological signs of degeneration (i.e. vacuolation of the seminiferous epithelium (V in Fig. 5E,F) instead of only 2.70 \pm 0.68% in similarly treated control mice ($P<0.0001$) (Fig. 4). The similarity in the percentages of tubules exhibiting immunohistochemical and histo-pathological abnormalities strongly suggests that Cre-mediated DNA excision in spermatogonia actually had occurred only in approximately half of the seminiferous tubules. Importantly, upon excision in germ cells, immunostaining of Sertoli cell nuclei remained very strong on frozen sections and was also unaltered on paraffin wax-embedded sections (Fig. 3B,D, Fig. 5G,H and data not shown). Moreover, tamoxifen treatment did not affect

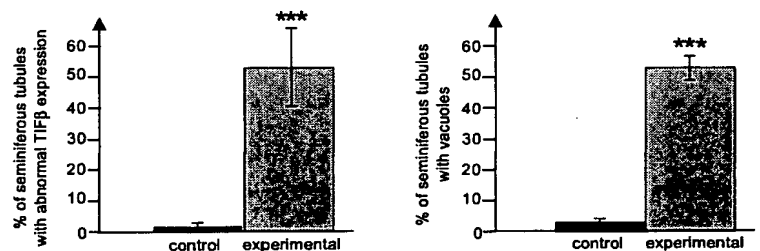


the expression of TIF1 β in other organs of TIF1 $\beta^{L2/L2};PrP-Cre-ER^{T(tg/0)}$ mice (data not shown).

Cre-mediated disruption of *Tif1 β* in spermatogonia causes testicular degeneration

Histological analysis of experimental and control testes was performed 1 day, and 2, 4, 6, 7 and 8 weeks after tamoxifen treatment. Experimental testes were histologically normal up to 6 weeks after treatment (data not shown). Histological sections through testes of experimental mice 7 and 8 weeks after treatment showed a mosaic of seminiferous tubules

Fig. 4. Percentages of seminiferous tubules exhibiting an abnormal expression pattern of TIF1 β or displaying vacuoles in TIF1 $\beta^{L2/L2};PrP-Cre-ER^{T(0/0)}$ (control) and TIF1 $\beta^{L2/L2};PrP-Cre-ER^{T(tg/0)}$ (experimental) mice. The percentage of seminiferous tubules cross sections showing abnormal expression of TIF1 β (i.e. partial staining of spermatocyte and/or spermatid layers along the circumference of a given tubule, instead of staining along its whole circumference) was determined by immunohistochemistry 2 weeks after tamoxifen treatment (left). The percentage of degenerating (vacuolated) versus normal tubules was determined 8 weeks after tamoxifen treatment (right). Results are mean \pm s.e.m. from at least three animals of each genotype and age (***) $P<0.0001$ according to Fischer's PLSD).



Results are mean \pm s.e.m. from at least three animals of each genotype and age (***) $P<0.0001$ according to Fischer's PLSD).

displaying normal germ cell associations (NT in Fig. 5B and data not shown) and of morphologically abnormal tubules exhibiting different patterns and extents of germ cell loss (e.g. ST in Fig. 5B). Interestingly, all abnormal tubular cross-sections were devoid of TIF1 β expression in germ cells (Fig. 5G,H). Some of the abnormal tubules contained apparently normal populations of spermatogonia and spermatocytes but lacked spermatids, probably reflecting their premature detachment from the seminiferous epithelium. By contrast, other tubules contained healthy round spermatids and Sertoli cells without mitotic and meiotic germ cells (compare Fig. 5C with 5D, and 5E with 5G). In the third category of abnormal tubules, germ cell depletion yielded Sertoli cell-only seminiferous tubules (Fig. 5B,F,H) whose epithelium was reduced to a row of Sertoli cells (showing extensive intercellular vacuolation; V in Fig. 5F) and to a few elongated spermatids (ES, Fig. 5F,H), but was devoid of spermatogonia. TUNEL analysis did not reveal any increase in apoptotic cell death in the epithelium of the degenerating tubules (Fig. 6A-D). The abnormal DNA fragmentation detected in nuclei from mature elongated spermatids (Fig. 6B,D), probably reflects their phagocytosis and degradation by Sertoli cells (Kastner et al., 1996). Germ cell depletion resulted in part from sloughing off of apparently healthy immature germ cells (mainly round spermatids) into the lumen of the tubules (arrowhead in Fig. 5E), probably yielding large and irregular vacuoles in the epithelium (V, in Fig. 5E,F). In accordance with this observation, the number of round spermatids was markedly increased in the lumen of the epididymis from experimental males examined 7 and 8 weeks after tamoxifen treatment (arrowheads in Fig. 6E,F). No sign of testicular degeneration was observed in age-matched tamoxifen-treated control mice (Fig. 5A,C).

DISCUSSION

Spermatogenesis includes spermatogonial stem cell self-renewal and the differentiation of spermatogonia. Proliferative spermatogonia generate differentiating spermatogonia that are irreversibly committed towards the production of spermatozoa. The most mature spermatogonia divide to form preleptotene spermatocytes that replicate their DNA, then initiate the meiotic process leading to round spermatids. Round spermatids undergo spermiogenesis, which involves nuclear shaping and chromatin compaction as well as major cytoplasmic transformations, to yield mature spermatozoa (Brinster and Avarbock, 1994; Brinster and Zimmermann, 1994; Kistler et al., 1996). In mice, the entire developmental process takes 35 days and is regulated by a complex signaling network involving endocrine, paracrine and autocrine factors (Grootegeed et al., 2000), as well as multiple transcriptional regulators (Sassone-Corsi, 1997).

We have shown here that the TIF1 β protein is expressed in germ cells during a restricted window of time corresponding

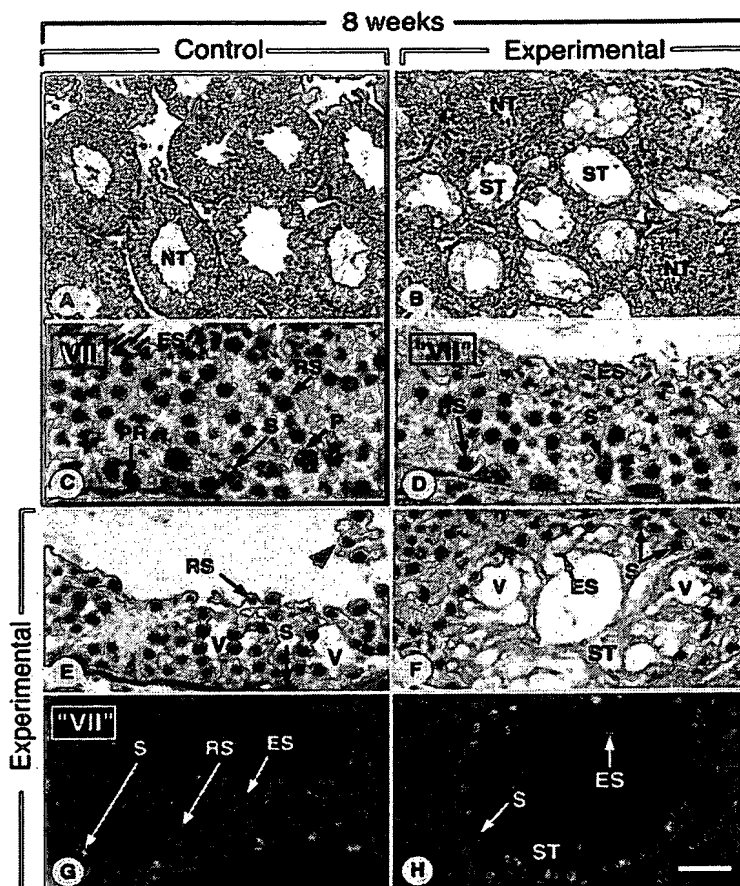


Fig. 5. Histological aspect of TIF1 β ^{(L2/L2):PrP-Cre-ER^{T(0/0)}} control testis (A,C) and TIF1 β ^{L2/L2:PrP-Cre-ER^{T(0/0)}} experimental testis (B,D-H), 8 weeks after tamoxifen treatment. The seminiferous tubule in C is at stage VII. The abnormal seminiferous tubules in D,G are difficult to stage because of the complete absence of spermatocyte populations; however, they have features in common with a stage VII tubule ('VII'), namely the aspect of acrosomes in round spermatids (not visible at this magnification) and/or alignment of elongated spermatids. Groat Hematoxylin and Malloy's trichrome (A-F) or immunolabeling for TIF1 β and DAPI counterstaining (G,H). L, Leydig cells; NT, tubules showing normal germ cell associations; P, pachytene spermatocytes; PR, preleptotene spermatocytes; RS, round spermatids; S, Sertoli cells; ST, Sertoli cell-only seminiferous tubules. The arrowhead in E indicates exfoliated round spermatids. Scale bar: 100 μ m (A,B), 15 μ m (C,D,F) and 20 μ m (E,G,H).

to the maturation of mid-pachytene spermatocytes into elongating (i.e. step 10) spermatids, and is associated with heterochromatin structures in these cells. TIF1 β is localized preferentially with the chromocenter of round (i.e. step 1 to step 9) spermatids indicating that it might repress expression of specific genes by sequestering them in this subnuclear compartment (Francastel et al., 2000). However, as TIF1 β expression is turned off prior to the onset of spermatid condensation, it is unlikely to be necessary for the protamine-dependent DNA compaction process which is characteristic of spermiogenesis (Kistler et al., 1996; Sassone-Corsi, 1997; Baarends et al., 1999). Moreover, although it is expressed in

pachytene spermatocytes, TIF1 β may also be dispensable for chromatin remodeling processes during meiosis, as TIF1 β -deficient spermatocytes can generate morphologically normal TIF1 β -deficient round spermatids, which in turn yield terminally differentiated condensed spermatids. Whether this reflects a possible functional redundancy with other members of the TIF1 family remains to be determined. Indeed, based on biochemical data, both TIF1 α and TIF1 β have previously been shown to interact directly with HP1 proteins (Le Douarin et al., 1996). However, in the case of TIF1 α , the biological significance of the HP1 interaction is unclear, as TIF1 α does not require HP1 binding for repression in a transfection assay (Nielsen et al., 1999), and no significant subnuclear colocalization of TIF1 α and HP1 α has been observed in cultured cells (Remboutsika et al., 1999). Moreover, TIF1 β , but neither TIF1 α nor TIF1 γ , has been reported to interact with and act as a co-repressor for KRAB domains (Abrink et al., 2001), supporting the view that members of the TIF1 family may be functionally distinct.

TIF1 β has nevertheless important physiological functions in the maintenance of the structural integrity of the seminiferous epithelium, as its loss in spermatocytes and round spermatids results in testicular degeneration with complete disappearance of germ cells. Spermatogenesis is crucially dependent on intimate contacts and paracrine interactions between Sertoli cells and germ cells. Sertoli cells support and nurture the germ cells (Russell et al., 1990; Sharpe, 1993; Griswold, 1998). Spermatocytes and spermatids can, in turn, influence Sertoli cell functions and gene expression, as demonstrated in models of germ cell depletion in vivo and in co-cultures of Sertoli and germ cells (Jegou, 1993; Boujrad et al., 1995; Syed and Hecht, 1997; Wright et al., 1995; Griswold, 1995; Yomogida et al., 1994). The disappearance of TIF1 β in TIF1 β ^{L2/L2}:PrP-Cre-ERT^(tg/0) spermatocytes after tamoxifen treatment and the subsequent generation, within the next 10 days (Oakberg, 1956a), of TIF1 β -deficient round spermatids from these TIF1 β -less spermatocytes, indicates that TIF1 β is not cell-autonomously required for their survival and differentiation. Thus, the timing of degeneration of the TIF1 β -less seminiferous epithelium rather suggests that *Tif1 β* expression is required for short-range cellular interactions in this epithelium. For example, TIF1 β present in round spermatids could, indirectly, regulate the expression of a Sertoli cell-derived factor(s) that mediate cell adhesion; the generation of TIF1 β -deficient round spermatids, as a consequence of *Tif1 β* disruption, may progressively result in depletion of this Sertoli cell factor, leading to immature germ cells detachment. However, neither shedding of immature germ cells, nor germ cell apoptosis can account for the observed selective depletion in spermatogonia and spermatocytes in TIF1 β -deficient degenerating seminiferous tubules still containing spermatids. Rather, this 'window of missing germ cells' may reflect an absence of spermatogonial proliferation or a failure of self-renewing stem spermatogonia to maintain their

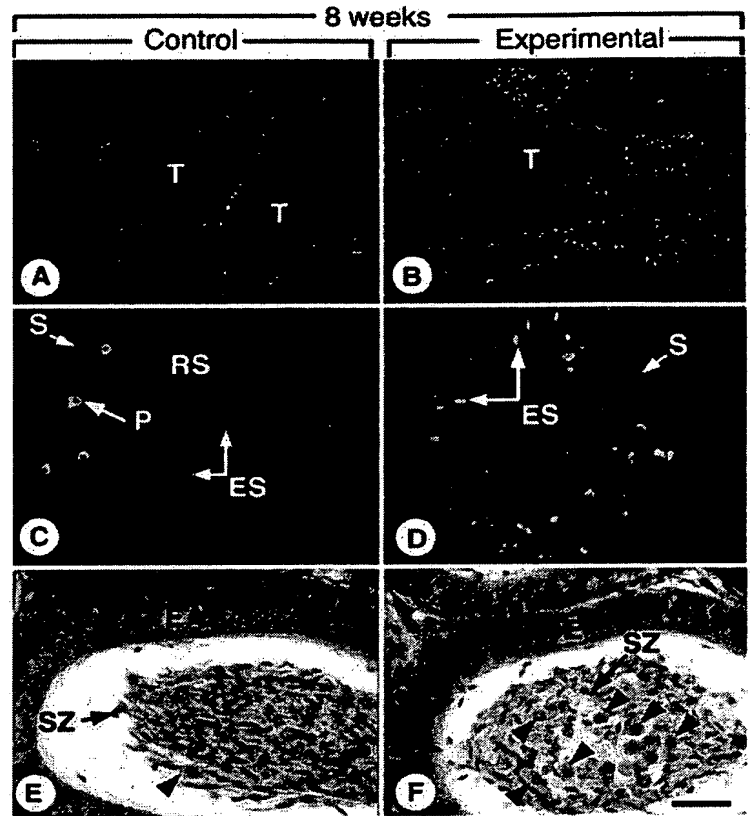


Fig. 6. Tunnel labeling (A-D) of the testis and histological detection (E,F) of immature germ cells in the epididymis of TIF1 β ^{L2/L2}:PrP-Cre-ERT(0/0) control and TIF1 β ^{L2/L2}:PrP-Cre-ERT(tg/0) experimental males 8 weeks after tamoxifen treatment. The green fluorescent signal corresponds to nuclei containing DNA fragments. Arrowheads indicate exfoliated round spermatids. E, epithelium of the cranial portion of the epididymis; ES, elongated spermatids; P, pachytene spermatocytes; RS, round spermatids; S, Sertoli cells; SZ, spermatozoa; T, seminiferous tubules. Scale bar: 100 μ m in A,B; 20 μ m in C-F.

normal, undifferentiated, state. In any event, as TIF1 β is not detectable in wild-type spermatogonia at any stage of the cycle of the seminiferous epithelium, the deleterious effects of its ablation on this cell type must be mediated through paracrine mechanisms possibly involving Sertoli cells. Accordingly, it is interesting to note that BMP8B secreted by spermatocytes and round spermatids is thought to play an important role in the paracrine regulation of spermatogonial self-renewal and/or differentiation (Zhao et al., 1996). Similar functions in the regulation of spermatogonial cell fate decision have been ascribed to Sertoli cell-derived GDNF (Meng et al., 2000), but it is not known whether secretion of GDNF is under germ cell control.

In conclusion, we have demonstrated that TIF1 β is localized preferentially in heterochromatin of round spermatids, indicating that it might repress expression of specific genes in these cells. Moreover, the observation that seminiferous tubules in which *Tif1 β* is specifically disrupted in spermatogonia are initially normal, while they subsequently

degenerate, indicates that TIF1 β has important functions in the homeostasis of the seminiferous epithelium, and probably plays a crucial role in the network of paracrine interactions between germ cell subpopulations and/or Sertoli cells.

We gratefully acknowledge N. B. Ghyselinck for stimulating discussions, and R. Lorenz, X. Belin, C. Dennefeld and the animal facility staff for excellent technical assistance. This work was supported by funds from the Centre National de la Recherche Scientifique, the Institut National de la Santé et de la Recherche Médicale, the Collège de France, the Institut Universitaire de France, the Hôpital Universitaire de Strasbourg, the Association pour la Recherche sur le Cancer, the Fondation pour la Recherche Médicale, the Human Frontier Science Program, the Ministère de l'Éducation Nationale de la Recherche et de la Technologie and the European Community. P. W. was supported by a fellowship (823A-056725) from the Swiss National Science Foundation.

REFERENCES

- Abrink, M., Ortiz, J. A., Mark, C., Sanchez, C., Looman, C., Hellman, L., Chambon, P. and Losson, R. (2001). Conserved interaction between distinct Krüppel-associated box domains and the transcriptional intermediary factor 1 β . *Proc. Natl. Acad. Sci. USA* **98**, 1422-1426.
- Baarends, W. M., Hoogerbrugge, J. W., Roest, H. P., Ooms, M., Vreeburg, J., Hoeijmakers, J. H. and Grootegoed, J. A. (1999). Histone ubiquitination and chromatin remodeling in mouse spermatogenesis. *Dev. Biol.* **207**, 322-333.
- Balaton, A. J., Ochando, F. and Painchaud, M. H. (1993). Use of microwaves for enhancing or restoring antigens before immunohistochemical staining. *Ann. Pathol.* **13**, 188-189.
- Barcellona, M. L. and Gratton, E. (1990). The fluorescence properties of a DNA probe. 4'-6-Diamidino-2-phenylindole (DAPI). *Eur. Biophys. J.* **17**, 315-323.
- Beckstead, R., Ortiz, J. A., Sanchez, C., Prokopenko, S. N., Chambon, P., Losson, R. and Belten, H. (2001). Bonus, a Drosophila homolog of TIF1 proteins, interacts with nuclear receptors and can inhibit β FTZ-F1-dependent transcription. *Mol. Cell* **7**, 753-765.
- Boujrad, N., Hochereau-de Reviers, M. T. and Carreau, S. (1995). Evidence for germ cell control of Sertoli cell function in three models of germ cell depletion in adult rat. *Biol. Reprod.* **53**, 1345-1352.
- Brinster, R. L. and Avarbock, M. R. (1994). Germline transmission of donor haplotype following spermatogonial transplantation. *Proc. Natl. Acad. Sci. USA* **91**, 11303-11307.
- Brinster, R. L. and Zimmermann, J. W. (1994). Spermatogenesis following male germ-cell transplantation. *Proc. Natl. Acad. Sci. USA* **91**, 11293-11302.
- Cammas, F., Mark, M., Dollé, P., Dierich, A., Chambon, P. and Losson, R. (2000). Mice lacking the transcriptional corepressor TIF1 β are defective in early postimplantation development. *Development* **127**, 2955-2963.
- Cockell, M. and Gasser, S. (1999). Nuclear compartments and gene regulation. *Curr. Opin. Genet. Dev.* **9**, 199-205.
- Dupé, V., Davenne, M., Brocard, J., Dollé, P., Mark, M., Dierich, A., Chambon, P. and Rijl, F. M. (1997). In vivo functional analysis of the Hoxa-1 3' retinoic acid response element (3'RARE). *Development* **124**, 399-410.
- Elissenberg, J. C. and Elgin, S. C. R. (2000). The HP1 protein family: getting a grip on chromatin. *Curr. Opin. Genet. Dev.* **10**, 204-210.
- Feil, R., Brocard, J., Mascres, B., LeMeur, M., Metzger, D. and Chambon, P. (1996). Ligand-activated site-specific recombination in mice. *Proc. Natl. Acad. Sci. USA* **93**, 10887-10890.
- Francastel, C., Schubeler, D., Martin, D. I. and Groudine, M. (2000). Nuclear compartmentalization and gene activity. *Nat. Rev. Mol. Cell Biol.* **1**, 137-143.
- Friedman, J. R., Fredericks, W. J., Jensen, D. E., Speicher, D. W., Huang, X.-P., Neilson, E. G. and Rauscher, F. J., III (1996). KAP-1, a novel corepressor for the highly conserved KRAB repression domain. *Genes Dev.* **10**, 2067-2078.
- Griswold, M. D. (1995). Interactions between germ cells and Sertoli cells in the testis. *Biol. Reprod.* **52**, 211-216.
- Griswold, M. D. (1998). The central role of Sertoli cells in spermatogenesis. *Semin. Cell Dev. Biol.* **9**, 411-416.
- Grootegoed, J. A., Slep, M. and Baarends, W. M. (2000). Molecular and cellular mechanisms in spermatogenesis. *Bailliere's Clin. Endocrinol. Metab.* **14**, 331-343.
- Hampsey, M. and Reinberg, D. (1999). RNA polymerase II as a control panel for multiple coactivator complexes. *Curr. Opin. Genet. Dev.* **2**, 132-139.
- Hassan, A. H., Neely, K. E., Vignali, M., Reese, J. C. and Workman, J. L. (2001). Promoter targeting of chromatin-modifying complexes. *Front. Biosci.* **6**, 1054-1064.
- Hoyer-Fender, S., Singh, P. B. and Motzkus, D. (2000). The murine heterochromatin protein M31 is associated with the chromocenter in round spermatids and is a component of mature spermatozoa. *Exp. Cell Res.* **254**, 72-79.
- Jégou, B. (1993). The Sertoli-germ cell communication network in mammals. *Int. Rev. Cytol.* **147**, 25-96.
- Kastner, P., Mark, M., Leid, M., Gansmuller, A., Chin, W., Grondona, J. M., Declimo, D., Krezel, W., Dierich, A. and Chambon, P. (1996). Abnormal spermatogenesis in RXR beta mutant mice. *Genes Dev.* **10**, 80-92.
- Kim, S.-S., Chen, Y.-M., O'Leary, E., Witzgall, R., Vidal, M. and Bonventre, J. V. (1996). A novel member of the RING finger family, KRIP-1, associates with the KRAB-A transcriptional repressor domain of zinc finger proteins. *Proc. Natl. Acad. Sci. USA* **93**, 15299-15304.
- Kistler, W. S., Henriksen, K., Mali, P. and Parvinen, M. (1996). Sequential expression of nucleoproteins during rat spermiogenesis. *Exp. Cell Res.* **225**, 374-381.
- Le Douarin, B., Zechel, C., Garnier, J.-M., Lutz, Y., Tora, L., Pierrat, B., Heery, D., Gronemeyer, H., Chambon, P. and Losson, R. (1995). The N-terminal part of TIF1, a putative mediator of the ligand-dependent activation function (AF-2) of nuclear receptors, is fused to B-raf in the oncogenic protein T18. *EMBO J.* **14**, 2020-2033.
- Le Douarin, B., Nielsen, A. L., Garnier, J.-M., Ichinose, H., Jeanmougin, F., Losson, R. and Chambon, P. (1996). A possible involvement of TIF1 α and TIF1 β in the epigenetic control of transcription by nuclear receptors. *EMBO J.* **15**, 6701-6715.
- Mark, M., Lufkin, T., Vonesch, J. L., Ruberte, E., Olivo, J. C., Dollé, P., Gorry, P., Lumsden, A. and Chambon, P. (1993). Two rhombomeres are altered in Hoxa-1 mutant mice. *Development* **119**, 319-338.
- Matsuda, E., Agata, Y., Sugai, M., Katakai, T., Gonda, H. and Shimizu, A. (2001). Targeting of Krüppel-associated box-containing zinc finger proteins to centromeric heterochromatin. Implication for the gene silencing mechanisms. *J. Biol. Chem.* **276**, 14222-14229.
- Meng, X., Lindahl, M., Hyvönen, M. E., Parvinen, M., de Rooij, D. G., Hess, M. W., Raatikainen-Ahokas, A., Sainio, K., Rauvala, H., Lakso, M. et al. (2000). Regulation of cell fate decision of undifferentiated spermatogonia by GDNF. *Science* **287**, 1489-1493.
- Metzger, D. and Chambon, P. (2001). Site- and time-specific gene targeting in the mouse. *Methods* **24**, 71-80.
- Moosmann, P., Georgiev, O., Le Douarin, B., Bourquin, J.-P. and Schaffner, W. (1996). Transcriptional repression by RING finger protein TIF1 β that interacts with the KRAB repression domain of KRX1. *Nucleic Acids Res.* **24**, 4859-4867.
- Muller, C. and Leutz, A. (2001). Chromatin remodeling in development and differentiation. *Curr. Opin. Genet. Dev.* **11**, 167-174.
- Nielsen, A. L., Ortiz, J. A., You, J., Oula-Abdelghani, M., Khechumian, R., Gansmuller, A., Chambon, P. and Losson, R. (1999). Interaction with members of the heterochromatin protein 1 (HP1) family and histone deacetylation are differentially involved in transcriptional silencing by members of the TIF1 family. *EMBO J.* **18**, 6385-6395.
- Oakberg, E. F. (1956a). Duration of spermatogenesis in the mouse and timing of stages of the cycle of the seminiferous epithelium. *Am. J. Anat.* **99**, 507-516.
- Oakberg, E. F. (1956b). A description of spermiogenesis in the mouse and its use in analysis of the cycle of the seminiferous epithelium and germ cell renewal. *Am. J. Anat.* **99**, 391-414.
- Oulad-Abdelghani, M., Bouillet, P., Chazaud, C., Dollé, P. and Chambon, P. (1996). AP-2.2: a novel AP-2-related transcription factor induced by retinoic acid during differentiation of P19 embryonal carcinoma cells. *Exp. Cell Res.* **225**, 338-347.
- Pardue, M. L. and Gall, J. G. (1970). Chromosomal localization of mouse satellite DNA. *Science* **168**, 1356-1358.
- Rachez, C. and Freedman, L. P. (2001). Mediator complexes and transcription. *Curr. Opin. Cell Biol.* **13**, 274-280.

- Remboutsika, E., Lutz, Y., Gansmuller, A., Vonesch, J. L., Losson, R. and Chambon, P. (1999). The putative nuclear receptor mediator TIF1 α is tightly associated with euchromatin. *J. Cell Sci.* **112**, 1671-1683.
- Russell, L. D., Hikim, A. P. S., Ettlin, R. A. and Clegg, E. D. (1990). *Histological and Histopathological Evaluation of the Testis*. Clearwater: Cache River Press.
- Ryan, R. F., Schultz, D. C., Ayyanathan, K., Singh, P. B., Friedman, J. R., Fredericks, W. J. and Rauscher III, F. J. (1999). KAP-1 corepressor protein interacts and colocalizes with heterochromatic and euchromatic HP1 proteins: a potential role for Krüppel-associated box-zinc finger proteins in heterochromatin-mediated gene silencing. *Mol. Cell. Biol.* **19**, 4366-4378.
- Sassone-Corsi, P. (1997). Transcriptional checkpoints determining the fate of male germ cells. *Cell* **88**, 163-166.
- Schultz, D. C., Friedman, J. R. and Rauscher, F. J., III (2001). Targeting histone deacetylase complexes via KRAB-zinc finger proteins: the PHD and bromodomains of KAP-1 form a cooperative unit that recruits a novel isoform of the Mi-2 α subunit of NuRD. *Genes Dev.* **15**, 428-443.
- Sharpe R. (1993). Experimental evidence for Sertoli-germ cell and Sertoli-Leydig cell interactions. In *The Sertoli Cell* (ed. Russell and Griswold), pp. 391-418. Clearwater: Cache River Press.
- Syed, V. and Hecht, N. B. (1997). Up-regulation and down-regulation of genes expressed in cocultures of rat Sertoli cells and germ cells. *Mol. Reprod. Dev.* **47**, 380-389.
- Underhill, C., Qutob, M. S., Yee, S.-P. and Torchia, J. (2000). A novel nuclear receptor corepressor complex, N-CoR, contains components of the mammalian SWI/SNF complex and the corepressor KAP-1. *J. Biol. Chem.* **275**, 40463-40470.
- Venturini, L., You, J., Stadler, M., Gallen, R., Lallemand, V., Koken, M. H. M., Mattel, M. G., Ganser, A., Chambon, P., Losson, R. and de Thé, H. (1999). TIF1 γ , a novel member of the transcriptional intermediary factor 1 family. *Oncogene* **18**, 1209-1217.
- Wright, W. W., Zabludoff, S. D., Penttilä, T. L. and Parvinen, M. (1995). Germ cell-Sertoli cell interactions: regulation by germ cells of the stage-specific expression of CP-2/cathepsin L mRNA by Sertoli cells. *Dev. Genet.* **16**, 104-113.
- Yomogida, K., Ohtani, H., Harigae, H., Ito, E., Nishimune, Y., Engel, J. D. and Yamamoto, M. (1994). Developmental stage- and spermatogenic cycle-specific expression of transcription factor GATA-1 in mouse Sertoli cells. *Development* **120**, 1759-1766.
- Zhao, G. Q., Deng, K., Labosky, P. A., Liaw, L. and Hogan, B. L. M. (1996). The gene encoding bone morphogenetic protein 8B is required for the initiation and maintenance of spermatogenesis in the mouse. *Genes Dev.* **10**, 1657-1669.

Physiological and retinoid-induced proliferations of epidermis basal keratinocytes are differently controlled

Benoit Chapellier, Manuel Mark, Nadia Messaddeq, Cécile Calléja, Xavier Warot, Jacques Brocard, Christelle Gérard, Mei Li, Daniel Metzger, Norbert B.Ghyselinck and Pierre Chambon¹

Institut de Génétique et de Biologie Moléculaire et Cellulaire, CNRS/INSERM/ULP, Collège de France, BP 10142, 67404 Illkirch Cedex, CU de Strasbourg, France

¹Corresponding author
e-mail: chambon@igbmc.u-strasbg.fr

N.B.Ghyselinck and P.Chambon contributed equally to this work

To investigate the roles of retinoic acid (RA) receptors (RARs) in the physiology of epidermis that does not express RAR β , conditional spatio-temporally controlled somatic mutagenesis was used to selectively ablate RAR α in keratinocytes of RAR γ -null mice. Keratinocyte proliferation was maintained in adult mouse epidermis lacking both RAR α and RAR γ , as well as in RAR β -null mice. All RAR-mediated signalling pathways are therefore dispensable in epidermis for homeostatic keratinocyte renewal. However, topical treatment of mouse skin with selective retinoids indicated that RXR/RAR γ heterodimers, in which RXR transcriptional activity was subordinated to that of its RAR γ partner, were required for retinoid-induced epidermal hyperplasia, whereas RXR homodimers and RXR/RAR α heterodimers were not involved. RA-induced keratinocyte proliferation was studied in mutant mice in which RXR α , RXR β and RAR α , RAR γ , or RXR α and RAR γ genes were specifically disrupted in either basal or suprabasal keratinocytes. We demonstrate that the topical retinoid signal is transduced by RXR/RAR γ heterodimers in suprabasal keratinocytes, which, in turn, stimulate proliferation of basal keratinocytes via a paracrine signal that may be heparin-binding EGF-like growth factor.

Keywords: conditional somatic mutagenesis/heparin-binding EGF-like growth factor/nuclear receptor/paracrine control/synthetic retinoids

Introduction

The initial observations of abnormal keratinization of various epithelia in vitamin A-deficient rats (Wolbach and Howe, 1925) and humans (Frazier and Hu, 1931) were followed by numerous pharmacological studies with vitamin A derivatives (retinoids), which led to the development of retinoid therapy for several skin diseases (Livrea, 2000). When applied topically on adult skin, retinoic acid (RA, the biologically active metabolite of vitamin A) generates an epidermal hyperplasia that results

from an hyperproliferation of basal keratinocytes leading, upon their vectorial migration towards the skin surface, to thickening of the differentiated suprabasal (spinous and granular) layers (Fisher and Voorhees, 1996). RA treatment also decreases the cohesiveness of the stratum corneum, impairing the adult skin barrier and increasing trans-epidermal water loss (Elias *et al.*, 1981). Similar effects were induced by synthetic retinoids (Chen *et al.*, 1995; Thacher *et al.*, 1997). Although retinoid pharmacological effects have been more studied in skin than in any other tissue, the skin cell-type(s) in which RA regulates gene expression and the network of RA-responsive target genes remain largely unknown.

Retinoids exert their highly pleiotropic effects through two groups of nuclear receptors (NRs), the retinoic acid receptors (RAR α , β and γ) and the retinoid X receptors (RXR α , β and γ), which belong to the NR superfamily of ligand-dependent transcriptional regulators. RARs bind *all trans*- and *9cis*-RA stereo-isomers, whereas RXRs interact exclusively with *9cis*-RA. RARs and RXRs act through binding to *cis*-acting response elements located in the regulatory regions of retinoid-responsive genes, and RARs, like NRs for thyroid hormone (TRs), vitamin D3 (VDR), peroxisome proliferators (PPARs) and several orphan receptors, require heterodimerization with RXRs to function *in vitro* and *in vivo* (Kastner *et al.*, 1995; Chambon, 1996; Morriss-Kay and Ward, 1999).

RXR α , RXR β , RAR α and RAR γ are expressed in epidermis, and RXR α and RAR γ are the predominant receptors (Fisher and Voorhees, 1996). However, their precise function in mediating retinoid effects on epidermis are unknown. Mouse transgenic expression of a dominant-negative (dn) RAR α that subverts wild-type RAR functions has suggested that RARs could be involved in keratinocyte differentiation and RA-induced hyperproliferation (Imakado *et al.*, 1995; Saitou *et al.*, 1995; Xiao *et al.*, 1999). Furthermore, expression of a dnRXR α in epidermal suprabasal layers indicated that RXR α could also be involved in retinoid-induced cell proliferation in adult mouse skin (Feng *et al.*, 1997). However, as dn receptors could artefactually repress the expression of genes that are not 'normal' targets of co-repressor-associated unliganded RXR/RAR heterodimers (Chen and Evans, 1995), and/or interfere through sequestration with a variety of signalling pathways mediated by NRs that heterodimerize with RXRs (Mangelsdorf *et al.*, 1995), the abnormalities exhibited by these transgenic models may not reflect the possible physiological roles of RA in epidermis homeostasis.

Targeted gene disruption through homologous recombination has been used extensively to investigate the physiological functions of retinoid receptors in the mouse. These genetic studies have indicated that RAR α is apparently dispensable for epidermal homeostasis,

whereas RAR γ is involved in minor aspects of granular keratinocyte differentiation (our unpublished data). However, due to functional redundancy amongst retinoid receptors, some functions of RAR α and/or RAR γ in epidermis could have been overlooked (Kastner *et al.*, 1995, 1997; Mascres *et al.*, 1998 and references therein). Unfortunately, compound germ-line disruptions of RAR α and RAR γ lead to lethality before embryonic day (E)11.5 (Wendling *et al.*, 2001), thus precluding any epidermis analysis. Similarly, the possible effect of RXR α knockout on mouse epidermis could not be assessed, as this mutation is lethal at E14.5, i.e. at the onset of epidermal morphogenesis. We have recently circumvented these limitations by using the Cre/loxP technology and a tamoxifen-inducible Cre-ER^T recombinase (Metzger and Chambon, 2001) in order to selectively abrogate RXR α expression in adult mouse keratinocytes. This approach allowed us to demonstrate that RXR α is dispensable for epidermal morphogenesis, but is involved in the control of hair cycling, most probably through RXR α /VDR heterodimers (Li *et al.*, 2000, 2001). We also found that RXR α , heterodimerized with other NRs, could be implicated in the control of interfollicular keratinocyte proliferation and differentiation (Li *et al.*, 2000, 2001). To further investigate the skin function of RAR α , RAR γ and RXR α , we produced mice selectively lacking them in epidermal keratinocytes.

Results

RAR-mediated signalling is dispensable for homeostatic epidermal proliferation

As RAR β was not detected in epidermis (Fisher *et al.*, 1994; see below) and epidermis of RAR β -null mice is apparently normal (Ghyselinck *et al.*, 1997), the cell-autonomous requirement of the RAR-mediated signalling pathway in epidermis homeostasis can be studied in mutant mice selectively lacking RAR α and RAR γ in keratinocytes. To generate such mutants, RAR α ^{L2/L2} mice (Figure 1A; Chapellier *et al.*, 2002a) were first crossed with RAR γ ^{+/-} heterozygotes (Lohnes *et al.*, 1993), and subsequently with K5-Cre-ER^{T(igf0)} transgenic mice that express the tamoxifen-inducible Cre recombinase specifically in basal keratinocytes (Indra *et al.*, 1999). These crosses generated RAR α ^{L2/L2}, RAR α ^{L2/L2}/RAR γ ^{+/-} and K5-Cre-ER^{T(igf0)}/RAR α ^{L2/L2}/RAR γ ^{+/-} animals. These mice were subjected to the tamoxifen (TAM) treatment known to permanently ablate RXR α in epidermis and hair follicle (i.e. RXR α ^{ep/-} mice; Li *et al.*, 2000). Excision at the RAR α ^{L2/L2} locus in TAM-treated mice harbouring the K5-Cre-ER^T transgene was efficient, permanent and selective, as RAR α L2 alleles were converted into L-alleles in tail epidermis, no RAR α L2 allele could be recovered in tail epidermis, even 12 months after TAM treatment, and no excision could be detected in dermis (thus yielding RAR α ^{ep/-} mice; Figure 1B; data not shown). To check whether RAR β could be aberrantly expressed in epidermis upon RAR α and/or RAR γ ablation, RAR β RNA levels were determined in skin samples. RAR β 1/3 isoforms were not detected, whereas similar levels of RAR β 2 isoform were present in control and RAR α ^{ep/-}/RAR γ ^{+/-} mice (Figure 1C). As RAR β is selectively expressed in dermis (Redfern and Todd,

1992; our unpublished data), these data show that it is neither upregulated in dermis nor ectopically expressed in epidermis of RAR α ^{ep/-}/RAR γ ^{+/-} mice, which therefore exhibit a 'panRAR-null' epidermis (panRAR^{ep/-} mice).

Topical RA alters epidermal cell differentiation (Fisher and Voorhees, 1996). However, histology of skin biopsies did not reveal any alteration in panRAR^{ep/-} mice (compare Figure 1D with F; and see below), and there was no alteration of keratin 5, 6, 10 and 13 expression (immunohistochemical data not shown). Moreover, electron microscopy of epidermis from panRAR^{ep/-} mice did not reveal abnormalities other than those exhibited by RAR γ ^{+/-} mice (data not shown), indicating that RAR α does not compensate for the loss of RAR γ during keratinocyte differentiation in adult mice.

About 1% of basal keratinocytes were BrdU positive in epidermis of 12-month-old RAR α ^{L2/L2} mice (Figure 1G). This low labelling index relative to that observed in younger adults (5 ± 2%, see below and Table I) is a normal feature of epidermal ageing (Engelke *et al.*, 1997). Similarly, in 12-month-old RAR γ ^{+/-} and panRAR^{ep/-} animals, 1% of basal keratinocytes were BrdU positive (Figure 1H and I). Thus, homeostatic keratinocyte proliferation is maintained for >1 year in absence of RAR α , β and γ in epidermis.

Pharmacological evidence that RXR/RAR γ heterodimers are involved in RA-induced epidermal hyperplasia

Dorsal epidermis of 2- to 3-month-old mice consists of (i) an irregular layer of basal keratinocytes, (ii) suprabasal layers formed by scattered spinous and granular keratinocytes (arrowheads) and (iii) several rows of cornified keratinocytes (Figure 2A). Topical RA treatment causes epidermal thickening due to basal cell hyperproliferation (Fisher and Voorhees, 1996). Accordingly, suprabasal layers were thickened in RA-treated wild-type mice, due to marked increases in numbers of spinous and granular keratinocytes; mitotic figures were frequent in basal keratinocytes (Figure 2B), and the number of basal keratinocytes expressing the proliferation marker Ki67 or incorporating BrdU was ~10-fold higher in RA- than in vehicle-treated epidermis (56 ± 5% versus 6 ± 2%; Figure 2C and D; Table I; data not shown). Simultaneous administration of the panRAR antagonist BMS493 prevented RA-induced epidermal hyperplasia, demonstrating that keratinocyte proliferation resulted from RAR activation (Figure 2E; Table I). Interestingly, a panRAR antagonist application on its own had no apparent effect on keratinocyte proliferation (data not shown).

To determine the potency of RAR isotypes in mediating retinoid-induced epidermal hyperplasia, wild-type mice were treated topically with selective ligands for RARs or RXRs. On their own or in association (Figure 2H), the panRXR agonist BMS649 (Figure 2F) and the RAR α -selective agonist BMS753 (Figure 2G) did not alter the percentage of proliferating, Ki67-positive, basal keratinocytes (Table I). In contrast, the number of proliferating keratinocytes was strongly increased by the RAR γ -selective agonist BMS961 (Figure 2I). However, the potency of this latter retinoid was below that of RA, while co-administration of BMS961 and BMS649 fully reproduced the effects of RA (compare Figure 2D, I and J; Table I).

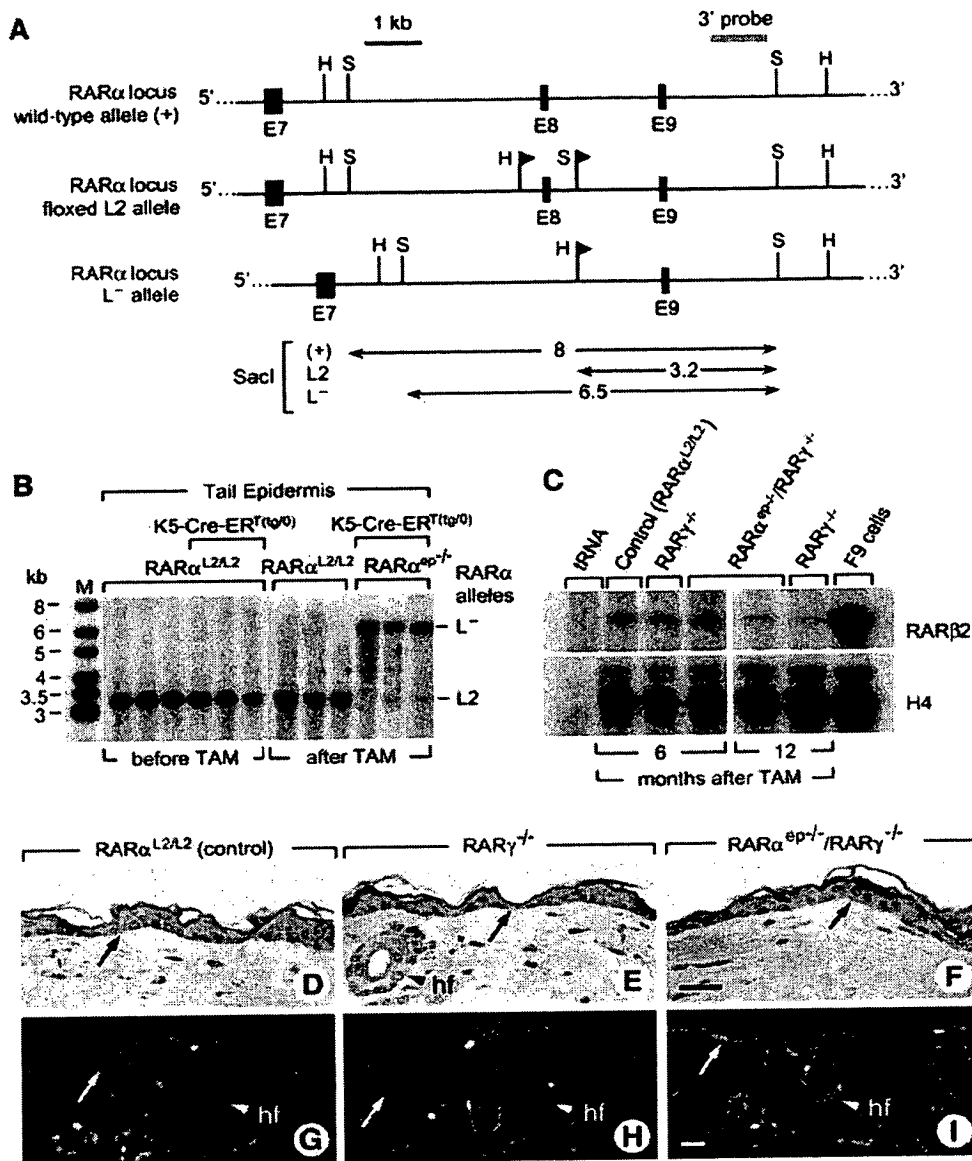


Fig. 1. Conditional mutagenesis of *RARα* in epidermis and homeostatic keratinocyte proliferation. (A) Schematic drawing of wild-type *RARα* locus (+), floxed L2 and excised (L⁻) alleles. Black boxes stand for exons 7–9 (E7–E9). Restriction sites and location of the 3' probe are indicated. Sizes of restriction fragments are in kilobases (kb). H, *HpaI*; S, *SacI*. Arrowhead flags represent loxP sites. (B) Efficiency of Cre-ER^T-mediated *RARα* gene disruption. Fourteen-week-old mice (genotypes as indicated) received TAM (5 days, 1 mg/day), and were treated again 2, 4 and 6 weeks later. *RARα* L2 and L⁻ alleles were identified on tail epidermis genomic DNA, before and 6 months after TAM injection. M: DNA ladder. (C) *RARβ2* expression in skin samples. RNase protection assay was performed on total RNA (20 μg) from control (*RARα*^{L2/L2}) and mutant mice (*RARγ*^{+/+} and *RARα*^{ep-/-}/*RARγ*^{+/+}). 6 and 12 months after TAM administration. A tRNA sample and total RNAs from RA-treated F9 teratocarcinoma cells were used as controls. Histone H4 protection was included for quantitation of the RNA samples. (D–F) Representative skin semi-thin sections, 12 months after TAM administration (genotypes as indicated). (G–I) Representative skin sections labelled with BrdU (white colour), showing proliferation of basal keratinocytes 12 months after TAM administration (genotypes as indicated). Sections were counterstained with DAPI (blue colour). Arrows point to the dermal-epidermal junction. hf, hair follicles. Scale bar (in F and I): 50 μm.

Altogether, these observations indicate that RA-induced skin hyperplasia most probably involves RXR/RAR γ heterodimers, in which RXR transcriptional activity is subordinated to that of RAR γ , i.e. liganded RXR is inactive unless its RAR partner is itself liganded

(Chambon, 1996). However, these pharmacological experiments do not reveal which cells are retinoid primary targets in epidermis and/or even in dermis, which is known to secrete various growth factors involved in epidermal cell proliferation (Werner and Smola, 2001). We therefore

Table I. Overview of retinoid effects on proliferation and gene expression in the epidermis

Genotype	Treatment	Epidermal status	% BrdU-positive nuclei	% Ki67-positive nuclei	CRABP II mRNA abundance	HB-EGF mRNA abundance
Wild type	none	Resting (control)	5 ± 2	6 ± 2	+	+
Wild type or wild-type-like*	RA	RA-stimulated	54 ± 6	56 ± 5	++++	++++
Wild type	RA + BMS493	Antagonism of RA stimulation	ND	6 ± 3	+	+
Wild type	BMS649 (SR11237)	Activation of RXR signalling	ND	10 ± 4	+	+
Wild type	BMS753	Activation of RARα signalling	ND	7 ± 2	ND	ND
Wild type	BMS753 + BMS649	Activation of RARα and RXR signalling	ND	9 ± 3	ND	ND
Wild type	BMS961	Activation of RARγ signalling	ND	35 ± 6	+++	+++
Wild type	BMS961 + BMS649	Activation of RARγ and RXR signalling	ND	51 ± 8	++++	++++
RARα ^{-/-}	RA	RARα-null	50 ± 4	ND	++++	++++
K5-Cre-ER ^{T(tg0)} /RXRα ^{L2/L2}	RA	RXRα-null in all layers (RXRα ^{ep-/-})	12 ± 4	ND	++	++
K5-Cre-ER ^{T(tg0)} /RXRα ^{L2/L2} /RARα ^{-/-}	RA	RXRα-null in all layers and RARα-null (RXRα ^{ep-/-} /RARα ^{-/-})	13 ± 4	ND	ND	ND
RARγ ^{-/-}	RA	RARγ-null	12 ± 3	14 ± 3	+	+
K5-Cre-ER ^{T(tg0)} /RXRα ^{L2/L2} /RARγ ^{-/-}	RA	RXRα-null in all layers and RARγ-null (RXRα ^{ep-/-} /RARγ ^{-/-})	7 ± 2	ND	+	+
CMV-Cre-ER ^{T(tg0)} /RARγ ^{L3/L3}	RA	RARγ-null in granular layer only (RARγ ^{sb-/-})	ND	13 ± 4	+	+

*Wild-type-like include RXRα^{L2/L2}; CMV-Cre-ER^{T(tg0)}/RARγ^{L3/L3} and CMV-Cre-ER^{T(tg0)}/RXRα^{L2/L2}; +, basal level of expression; ++ to +++, increasing level of expression; ND, not determined.

analysed RA-induced epidermal hyperplasia in mice carrying RAR- and RXR-null mutations selectively in their epidermis.

Genetic evidence that RXRα/RARγ heterodimers are the functional units responsible for RA-induced epidermal hyperplasia

RXRα^{L2/L2} mice were crossed with either RARα^{+/-} or RARγ^{+/-} mice. These animals were further mated with K5-Cre-ER^{T(tg0)} transgenic mice (see above) to generate RXRα^{L2/L2}, RARα^{-/-}, RARγ^{-/-}, K5-Cre-ER^{T(tg0)}/RXRα^{L2/L2}, K5-Cre-ER^{T(tg0)}/RXRα^{L2/L2}/RARα^{-/-} and K5-Cre-ER^{T(tg0)}/RXRα^{L2/L2}/RARγ^{-/-} animals, which were treated with TAM at 14 weeks of age (Figure 3A). The efficacy of RXRα gene excision in keratinocytes was quantified after separation of epidermis from dermis. Whereas no RXRα^{L-} excised allele was found in epidermis before TAM administration (Figure 3B, left panel), this treatment resulted in almost 100% L⁻ alleles in mice carrying the K5-Cre-ER^T transgene (yielding RXRα^{ep-/-} mice), but had no effect in those lacking the transgene (Figure 3B, right panel). The RXRα^{L-} allele was never detected in the dermis (data not shown). No RXRα protein was detected by immunohistochemistry in the interfollicular epidermis and hair follicles of RXRα^{ep-/-} mice at D11 (compare Figure 3C with D). Thus, TAM administration efficiently and selectively abolishes RXRα expression in epidermis of mice bearing the K5-Cre-ER^T transgene and the RXRα^{L2} alleles. Note

that the RXRα-ablated epidermis did not exhibit any interfollicular hyperplasia shortly after the TAM treatment (Figure 3D), in agreement with our previous report showing that hyperproliferation is a late event occurring 10–12 weeks after RXRα ablation (Li *et al.*, 2000).

Cell proliferation was quantified by counting BrdU-labelled basal keratinocytes (see Table I). In 'control' mice (RXRα^{L2/L2}), about half (54 ± 6%) of the basal keratinocytes were BrdU positive after RA treatment (Figure 3E; note that 5 ± 2% of the basal keratinocytes were BrdU positive in vehicle-treated mice). RA-induced epidermal thickening and cell hyperproliferation in RARα^{-/-} mice was similar to that of controls (Figure 3F, 50 ± 4%), while it was much reduced in RARγ^{-/-} mice (Figure 3G, 12 ± 3%) and in RXRα^{ep-/-} mice (Figure 3H, 12 ± 4%). Ablation of RXRα in epidermis of RARα^{-/-} mice (i.e. RXRα^{ep-/-}/RARα^{-/-} mice) did not further decrease RA-induced proliferation (Figure 3I, 13 ± 4%). In contrast, RA treatment had almost no effect in RXRα^{ep-/-}/RARγ^{-/-} mice (Figure 3J, 7 ± 2%). Thus, RXRα/RARγ, but not RXRα/RARα, heterodimers appear to be required within the epidermis to mediate RA-induced hyperplasia. Note that the percentage of proliferating keratinocytes in vehicle-treated mice (~6%) is below that observed in RA-treated RARγ^{-/-} or RXRα^{ep-/-} epidermis (~13%), but is similar to that of RA-treated RXRα^{ep-/-}/RARγ^{-/-} mice (~7%). As RARα and RXRβ are also expressed in epidermis (Fisher *et al.*, 1994; Li *et al.*, 2000), these observations suggest some functional redundancy (see

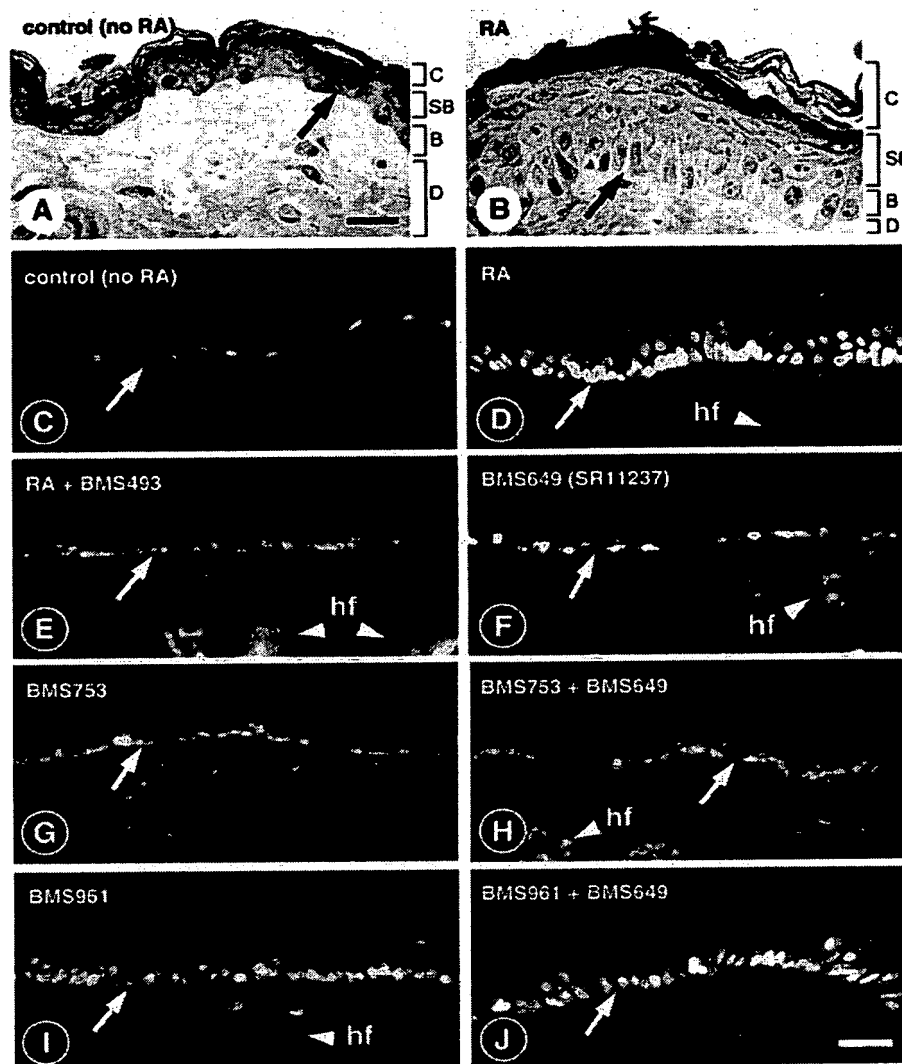


Fig. 2. Histology and proliferative response of wild-type skin upon topical retinoid treatment. Dorsal skin was treated for four consecutive days with 40 nmol (in 400 μ l acetone) of RA (B and D) or synthetic retinoids (E–J), as indicated. Controls (A and C) were treated with acetone vehicle. (A and B) Histology of control and RA-treated epidermis. Semi-thin sections (2- μ m thick) were stained with toluidine blue. Arrowheads point to the spinous and granular keratinocytes in control epidermis. (C–J) Skin sections showing the proliferation marker Ki67 (white colour) and counterstained with DAPI (blue colour). Arrows point to the dermal-epidermal junction. RA, retinoic acid; BMS493, panRAR-selective antagonist; BMS649 (SR11237), panRXR-selective agonist; BMS753, RAR α -selective agonist; BMS961, RAR γ -selective agonist. B, basal layer; C, cornified layer; D, dermis; hf, hair follicle; SB, suprabasal layers (spinous and granular keratinocytes). Scale bar: 15 μ m in (A) and (B); 25 μ m in (C)–(I).

Introduction) between RAR γ and RAR α , and between RXR α and RXR β , even though, on their own, disruption of either the RAR α gene (see above) or the RXR β gene (Kastner *et al.*, 1996) did not affect the RA-induced proliferation (data not shown). Disruption of the RAR β gene (Ghyselinck *et al.*, 1997), which is expressed in dermal fibroblasts but not in epidermis (see above), did not perturb RA-induced epidermal hyperproliferation (data not shown).

To determine in which epidermal cell layer RA exerts its primary effect (i.e. basal or suprabasal), we next ablated RAR γ and RXR α in suprabasal layers.

Genetic evidence that RAR γ is required in suprabasal cell layers for RA-induced epidermal hyperplasia

RAR $\gamma^{L3/L3}$ mice (Figure 4A; Chapellier *et al.*, 2002b) were crossed with CMV-Cre-ER^{T(tg0)} transgenic mice, in which TAM administration can induce Cre-mediated recombination in suprabasal layers but not in the basal layer (Brocard *et al.*, 1997), to produce 'control' (CMV-Cre-ER^{T(tg0)}/RAR $\gamma^{+/L3}$) and experimental (CMV-Cre-ER^{T(tg0)}/RAR $\gamma^{L3/L3}$) animals. At 14 weeks of age, all mice were treated with TAM (Figure 4B) and RAR γ gene disruption was quantified. No RAR γ^L excised allele was

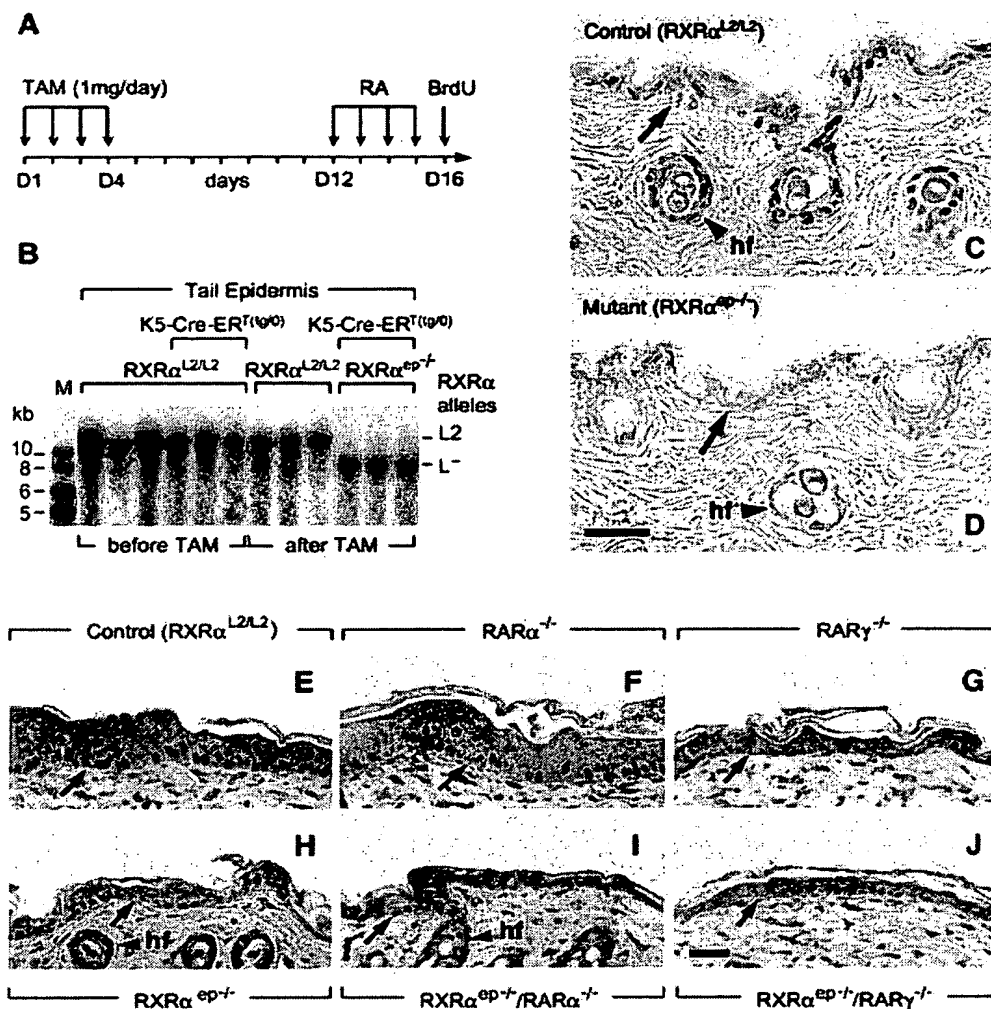
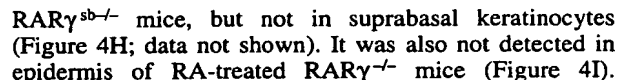


Fig. 3. Conditional mutagenesis of RXR α in epidermis, and RA-induced proliferative response. (A) Scheme of the experimental protocol. Intraperitoneal injection of TAM (1 mg) was performed from day 1 (D1) to day 4 (D4). A tail biopsy was made on day 11 to check for RXR α gene disruption. RA (40 nmol) was topically applied on skin for 4 days (D12–D15). On day 16 (D16), an injection of BrdU (50 mg/kg) was given 2 h before skin sampling. (B) Efficiency of RXR α gene disruption in mice bearing the K5-Cre-ER^T(tg0) transgene (as indicated). RXR α L2 and L⁻ alleles were identified on tail epidermis genomic DNA before and after TAM administration. M: DNA ladder. (C and D) Immunohistochemical detection of RXR α on skin sections from control (RXR α ^{L2/L2}) and mutant (RXR α ^{ep-/-}) mice. (E–J) Representative skin sections labelled with BrdU (brown colour), showing epidermis thickness and basal keratinocyte proliferation in mutants (genotypes as indicated). Arrows point to the dermal–epidermal junction. hf, hair follicles. Scale bar: 25 μ m in (C) and (D); 50 μ m in (E)–(J).

found before TAM treatment (Figure 4C, left panel). As expected from the selective expression of the CMV-Cre-ER^T transgene in suprabasal (sb), but not in basal keratinocytes (Brocard *et al.*, 1997), this treatment resulted only in a partial conversion of RAR γ L3 alleles into L2Neo (in which the neo gene was not removed; see Figure 4A) and L⁻ alleles (Figure 4C, middle panel). Importantly, no RAR γ L⁻ and L2Neo alleles could be detected a few weeks after the end of TAM treatment (data not shown), proving that no disruption of the RAR γ gene had occurred in basal keratinocytes (see also below; Figure 4H). Thus, TAM administration to CMV-Cre-ER^T(tg0)/RAR γ L3/L3 mice

effectively resulted in selective disruption of the RAR γ gene in epidermal suprabasal layers, yielding RAR γ ^{sb-/-} mice.

In RA-treated ‘control’ mice, the epidermis was markedly thickened and about half ($56 \pm 5\%$) of basal keratinocytes expressed Ki67 (Figure 4D), instead of $6 \pm 2\%$ in vehicle-treated mice (Figure 2C; Table I). In contrast, epidermal proliferation was lower in RA-treated RAR γ ^{sb-/-} mice (Figure 4E, $13 \pm 4\%$; Table I), a situation similar to that observed in RAR γ ^{-/-} mice (Figure 4F, $14 \pm 3\%$; Table I). Following RA treatment, the RAR γ protein was easily detected by immunohistochemistry



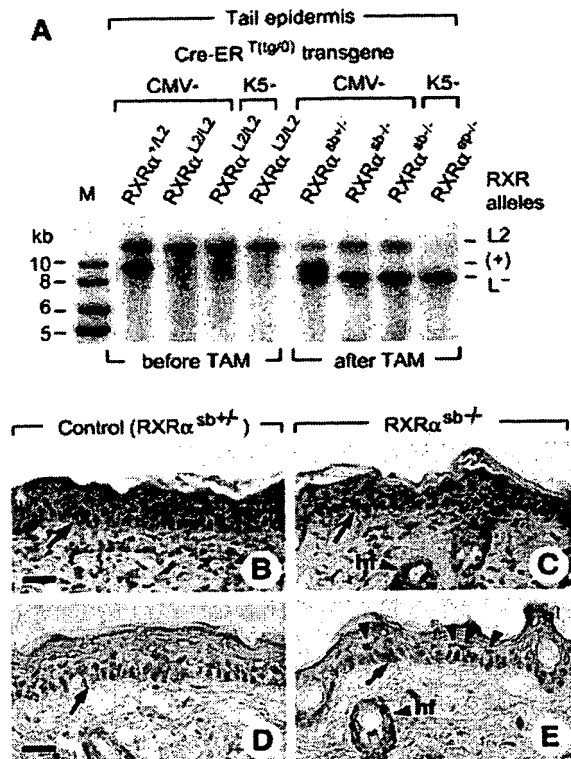


Fig. 5. Conditional mutagenesis of RXR α in epidermis suprabasal layers, and RA-induced proliferative response in RXR $\alpha^{sb/+}$ mice. (A) Efficiency of RXR α gene disruption in mice bearing the CMV-Cre-ER^T transgene as compared with the K5-Cre-ER^T transgene (as indicated). The experimental protocol is the same as in Figure 4B. RXR α wild-type (+), L2 and L⁻ alleles were detected on tail epidermis genomic DNA before and after TAM administration. M: DNA ladder. (B and C) Representative back skin sections labelled with BrdU (brown colour), showing RA-induced epidermal thickening and increased basal keratinocytes proliferation. (D and E) Immunohistochemical detection of RXR α on skin sections from control [(D), RXR $\alpha^{sb/+}$] and experimental [(E), RXR $\alpha^{sb/+}$] mice, after RA treatment. Arrowheads indicate nuclei of suprabasal keratinocytes expressing RXR α . Arrows point to the dermal-epidermal junction. hf, hair follicles. Scale bar (in D): 50 μ m.

Importantly, RA-induced epidermal hyperproliferation in RAR $\gamma^{sb/+}$ mice was restored to 'control' levels a few weeks after the end of TAM treatment (data not shown), clearly demonstrating that RAR γ disruption was restricted to suprabasal cells. Altogether, these results indicate that RAR γ expressed in suprabasal cells is required to transduce the retinoid signal that triggers proliferation of basal keratinocytes.

Persistence of the RXR α protein in epidermal suprabasal cells in which the RXR α gene is disrupted

To determine whether RXR α could be the heterodimeric partner of RAR γ in suprabasal cells, RXR $\alpha^{L2/L2}$ mice were crossed with CMV-Cre-ER^T transgenic mice, to produce 'control' (CMV-Cre-ER^T/RXR $\alpha^{+/L2}$) and 'experimental' (CMV-Cre-ER^T/RXR $\alpha^{L2/L2}$) mice. Before TAM administration, no RXR α L⁻ allele

was found in epidermis (Figure 5A, left panel), whereas this treatment induced conversion of RXR α L2 alleles into L⁻ alleles in 'experimental' mice (Figure 5A, right panel). The remaining L2 alleles originated from the basal keratinocytes, as this species was absent in DNA from an RXR $\alpha^{ep/+}$ mouse skin sample. Importantly, as in the case for the RAR $\gamma^{L3/L3}$ gene (see above), no disrupted RXR $\alpha^{L2/L2}$ gene could be detected a few weeks after the end of TAM treatment (data not shown), indicating that the RXR α gene was not disrupted in the basal cell layer.

Thus, TAM administration successfully induced disruption of the floxed RXR α gene in suprabasal, but not basal, keratinocytes of mice bearing the CMV-CreER^T transgene, yielding RXR $\alpha^{sb/+}$ mice. However, RA-induced proliferation was similar in TAM-treated 'control' and 'experimental' (RXR $\alpha^{sb/+}$) mice (Figure 5B and C, $54 \pm 6\%$ and $47 \pm 8\%$, respectively), and unexpectedly RXR α was readily detected by immunohistochemistry throughout epidermis, including in suprabasal keratinocytes (arrowheads in Figure 5E) of both RA-treated 'control' and RXR $\alpha^{sb/+}$ mice (compare Figure 5D with E). Thus, the RXR α protein was still present in epidermis suprabasal cells of experimental mice, even though TAM administration efficiently induced Cre-mediated disruption of the RXR α L2 alleles in these cells. This indicates that there is little turnover of the RXR α protein upon differentiation of basal into suprabasal cells.

RA-induced epidermal hyperplasia is associated with induction of HB-EGF expression

Altogether, the above observations suggest that disruption of RAR γ in suprabasal keratinocytes impairs a paracrine signalling system mediating the effects of RA on basal keratinocyte proliferation. Epidermal growth is modulated by several factors, including epidermal growth factor (EGF), TGF α , heparin-binding EGF-like growth factor (HB-EGF), amphiregulin, epiregulin, heregulin and β -cellulin (Jost *et al.*, 2000). Expression of HB-EGF was previously shown to be selectively induced by RA in epidermis suprabasal layers (Stoll and Elder, 1998; Xiao *et al.*, 1999). To investigate whether the epidermal response to synthetic retinoids (see Figure 2) could be correlated with activation of the HB-EGF signalling pathway, HB-EGF mRNA levels were determined (Figure 6A). The panRAR antagonist BMS493 abolished the RA-induced increase of HB-EGF mRNA, while the increase observed upon treatment with the RAR γ agonist, BMS961, was potentiated by co-administration of the panRXR agonist BMS649, which, on its own, did not induce HB-EGF mRNA expression. Thus, retinoid-induced epidermis hyperplasia is correlated with an increased expression of HB-EGF mRNA in the epidermis. Furthermore, the ability of RA to induce HB-EGF mRNA was severely impaired whenever RAR γ expression was abrogated either in epidermis or selectively in suprabasal keratinocytes (i.e. in RAR $\gamma^{-/-}$, RXR $\alpha^{ep/+}$ /RAR $\gamma^{-/-}$ and RAR $\gamma^{sb/+}$ mice), but was unaffected in mice lacking RAR α (Figure 6B). Expression of HB-EGF mRNA was also significantly reduced, but not abolished, in mice lacking RXR α in epidermis (RXR $\alpha^{ep/+}$ animals), most probably due to some functional redundancy between RXR α and RXR β , even though no decrease of HB-EGF transcripts was observed in the skin of RXR $\beta^{-/-}$ mice (data

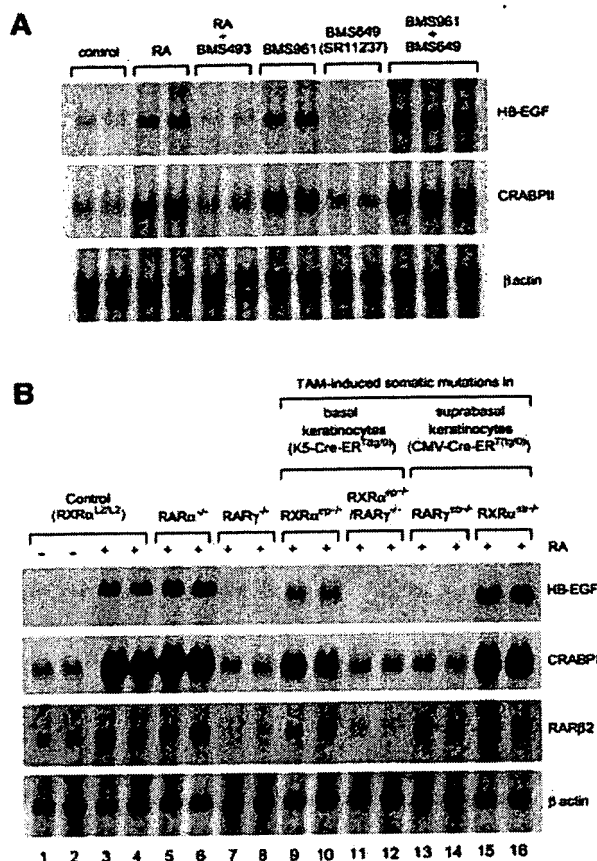


Fig. 6. Expression of HB-EGF, CRABP II, RAR β 2 and β -actin mRNA in whole back skin following topical application of retinoids. (A) Northern blot analysis of total RNA (25 μ g) before (control) and after retinoid administration, as indicated. RA, retinoic acid; BMS493, panRAR antagonist; BMS961, RAR γ agonist; BMS649 (SR11237), panRXR agonist. (B) Northern blot analysis of total RNA (25 μ g) from control (RXR $\alpha^{L2/L2}$) and mutant mice (genotypes as indicated) before (-) and after (+) RA administration.

not shown). In contrast, selective disruption of the RXR α gene in suprabasal keratinocytes (RXR $\alpha^{sb/-}$ mice) had no effect on HB-EGF mRNA levels, in keeping with persistence of the RXR α protein (see above).

The cellular retinoic acid-binding protein II (CRABP II), which is expressed in suprabasal keratinocytes, is considered as an indicator of RA activity in the epidermis (Fisher and Voorhees, 1996). Variations in levels of CRABP II mRNA in response to retinoid treatments and in RAR γ and RXR α mutants strictly paralleled those of HB-EGF mRNA (Figure 6). It is therefore likely that, within the RAR/RXR heterodimers controlling RA target gene expression in suprabasal cells (e.g. HB-EGF and CRABP II), RAR γ plays a crucial role, whereas RXR α can, to some extent, be functionally replaced by RXR β .

Interestingly, RAR β 2 mRNA, which is not or barely detectable in skin under normal conditions (Fisher *et al.*, 1994; see Figure 6B, lanes 1 and 2), but is known to be RA-inducible in dermal fibroblasts (Redfern and Todd, 1992; Tsou *et al.*, 1994), was present in all RA-treated

samples (Figure 6B), except in those from mice harbouring a germ-line RAR γ -null mutation (RAR $\gamma^{-/-}$ and RXR $\alpha^{P-/-}$ /RAR $\gamma^{-/-}$ mice). This observation suggests that (i) topical RA treatment was efficient down to the dermis and (ii) induction of RAR β 2 expression by RA in the dermis is mediated through heterodimers involving RAR γ .

Discussion

Based on their expression patterns (Fisher and Voorhees, 1996) and on results from overexpression of dn retinoid receptors in epidermis of transgenic mice (see Introduction), it has been proposed that RARs and RXRs (notably RAR γ and RXR α) play important physiological functions in epidermis. To gain insight into the role of retinoid receptors, and more generally of RA signalling in epidermis, we have investigated here the phenotype of mutant mice in which RAR α , RAR γ and/or RXR α have been selectively disrupted in this tissue.

RARs are dispensable for homeostatic self-renewal of epidermal keratinocytes

The skin of RAR α -null and RAR β -null mutants appears normal, while skin of RAR γ -null mutants exhibit only minor defects of granular keratinocyte differentiation (Lohnes *et al.*, 1993; Lufkin *et al.*, 1993; Ghyselinck *et al.*, 1997; our unpublished results). Functional redundancy between RAR α and RAR γ (see Introduction), which, in contrast to RAR β , are both expressed in epidermis (Fisher *et al.*, 1994), could have accounted for the paucity of alterations in epidermis of RAR α - and RAR γ -null mice. Such a functional redundancy could not be assessed from examination of RAR α /RAR γ -null mice, as they die before the onset of epidermis formation (Wendling *et al.*, 2001). The inducible conditional somatic mutagenesis strategy used here has allowed us to generate mice selectively lacking both RAR α and RAR γ in adult epidermis. As RAR β is not ectopically expressed in the epidermis of these mice, they actually display a 'panRAR-null' epidermis fully devoid of RAR α , β and γ . As this panRAR-null epidermis is similar to that of a RAR γ -null mice (our unpublished results), we conclude that there is little (and possibly no) redundancy between RAR α and RAR γ for adult keratinocyte proliferation and differentiation. Moreover, as the complete absence of RARs in basal keratinocytes does not alter their homeostatic proliferation, our study demonstrates for the first time that self-renewal of epidermal keratinocytes does not require an epidermal RAR-dependent signalling pathway.

We have previously shown that RXR α ablation in basal keratinocytes results notably in hair follicle degeneration and hyperproliferation of interfollicular keratinocytes (Li *et al.*, 2000, 2001). These features most probably reflect a role of RXR α /VDR heterodimers in hair follicle cycling, and the involvement of other heterodimeric partners of RXR α in the control of interfollicular keratinocytes proliferation (Li *et al.*, 2000, 2001). Such possible partners known to be expressed in epidermis include RARs (Fisher *et al.*, 1994), TRs (Billoni *et al.*, 2000) and PPARs (Peters *et al.*, 2000; Michalik *et al.*, 2001). As RAR γ -null and RAR α /RAR γ -null keratinocytes cultured *in vitro* have been shown to be refractory to RA-induced growth arrest (Goyette *et al.*, 2000), RARs could have been the partners

of RXR α that mediate an anti-proliferative effect in resting (i.e. unstimulated) epidermis. However, our present data demonstrate that ablation of the RARs in keratinocytes does not result in epidermal hyperplasia, ruling out the possibility that RAR/RXR α heterodimers could be critically involved in controlling the keratinocyte proliferation under physiological conditions *in vivo*. Interestingly, mutant mice expressing an RXR α lacking its AF-2 ligand-dependent activation function do not exhibit an epidermal interfollicular hyperplasia (B.Mascrez, N.B.Ghyselinck, M.Mark, D.Metzger, M.Li and P.Chambon, unpublished observations). Therefore, basal keratinocyte homeostatic proliferation might be controlled through heterodimers comprising a transcriptionally inactive (unliganded) RXR α and a nuclear receptor other than a RAR.

As essential components of the vitamin A metabolic machinery are expressed in keratinocytes (Niederreither *et al.*, 2002), RA could be synthesized in the epidermis. However, the observations that (i) a RXR-specific agonist has no effect on its own on keratinocyte proliferation (Thacher *et al.*, 1997; our present data), and (ii) the panRAR antagonist BMS493 does not reduce the homeostatic rate of basal keratinocyte proliferation (data not shown), indicate that endogenous RA available for activation of RARs is either lacking, or present at very low levels in resting epidermis. Along the same lines, it is noteworthy that RA is undetectable in human epidermis (Vahlquist, 1982).

The RA signal inducing epidermal hyperproliferation is transduced through RAR γ /RXR α heterodimers in suprabasal keratinocytes

Although RARs are apparently not involved in the control of homeostatic epidermal proliferation under resting conditions, our pharmacological and genetic data demonstrate that topical treatment of skin with retinoids results in a marked increase in keratinocyte proliferation that is mediated in suprabasal keratinocytes through RAR γ /RXR heterodimers. In human and mouse epidermis, RAR γ represents 90% of the RARs, the remaining 10% being RAR α (Fisher *et al.*, 1994; our unpublished results). The fact that RAR γ -null epidermis exhibits some RA-induced increased proliferation raised the possibility that RAR α could be involved in a RA-triggered cell proliferation pathway distinct from that involving RAR γ . However, RA-induced hyperproliferation of RAR α -null epidermis is identical to that of wild-type epidermis, and hyperproliferation is not induced by a RAR α -selective agonist. Thus, the residual hyperproliferation observed in RAR γ -null epidermis probably results from a functional redundancy with RAR α , which is artefactually generated by the knockout of RAR γ and similar to that previously seen in RAR γ -null cells *in vitro* (Taneja *et al.*, 1996; see Introduction for further references). Similarly, the slight increase in proliferation still observed upon RA-stimulation of epidermis lacking RAR γ selectively in the suprabasal layers (RAR γ ^{sb-/-} mice; Table I) could also reflect a redundancy with RAR α . Therefore, RAR γ is the main, if not the only, RAR-mediating RA-induced keratinocyte hyperproliferation in wild-type mice.

Likewise, the residual RA-induced proliferation increase in RXR α -null epidermis most probably reflects a functional redundancy with RXR β (Li *et al.*, 2000).

In any event, the striking synergism between RAR γ - and RXR α -null mutations strongly supports the conclusion that RXR α /RAR γ heterodimers are the functional units mediating RA-induced epidermal hyperplasia. The alternative possibility that two different converging pathways could be involved in the generation of keratinocyte hyperproliferation, the first one requiring RAR γ and the other one RXR α , is unlikely: (i) the RXR-specific agonist BMS649 has no effect on its own, indicating that RA acts neither through RXR homodimers nor through heterodimers in which RXR activity is not subordinated to that of its partner (e.g. RXR/PPAR heterodimers); and (ii) the effect of the RAR γ -selective agonist is potentiated by the RXR-selective agonist. It is noteworthy that our present study also demonstrates that the subordination of the ligand-dependent RXR activity to its liganded-RAR partner that was previously evidenced *in vitro* (Roy *et al.*, 1995; Taneja *et al.*, 1996), also occurs in the animal.

Paradoxically, RA induces opposite responses in keratinocytes depending on whether they are studied *in vivo* or cultured *in vitro*. For example, RA treatment induces keratinocyte growth-arrest *in vitro* (Goyette *et al.*, 2000) and has no effect on CRABP II expression (Fisher and Voorhees, 1996). In contrast, RA stimulates keratinocyte proliferation and increases transcription of the CRABP II gene *in vivo*. We have shown here that these RA effects are transduced by RAR γ present in epidermis suprabasal cell layers. Thus, the failure of RA to increase proliferation and CRABP II expression in cultured keratinocytes may just reflect their similarity with basal keratinocytes. This raises the interesting possibility that the RAR γ -dependent pathway involved in inhibition of keratinocyte proliferation *in vitro* (Goyette *et al.*, 2000) may also operate in basal keratinocytes *in vivo*, in order to finely tune pathophysiological epidermal responses to RA signalling, for example during skin wound healing (see below).

The RA signal transduced by RAR γ /RXR α heterodimers in suprabasal keratinocytes generates a paracrine signal inducing hyperproliferation of basal keratinocytes

As cell proliferation only takes place in the basal layer, our finding that RAR γ /RXR α heterodimers present in suprabasal keratinocytes are required for RA-induced epidermal hyperplasia demonstrates that retinoids induce, through these heterodimers, the synthesis of a paracrine signal in suprabasal keratinocytes, which in turn causes hyperproliferation of basal keratinocytes. This is in keeping with previous data showing that expression of a dnRAR α in suprabasal layers abrogate RA-induced hyperplasia (Xiao *et al.*, 1999). However, as an excess of dnRAR may, through binding to RXRs, interfere with the function of both RARs and a number of other heterodimeric partners of RXRs (e.g. PPARs), this previous study could not reveal which RXR/NR heterodimer generates the RA-induced hyperproliferation signal in suprabasal cells.

Several growth factors released from both the epidermis and the dermis affect proliferation of basal keratinocytes through binding to epidermal growth factor receptors that

are located in basal keratinocyte membranes and belong to the ErbB family (Piepkorn *et al.*, 1998; Jost *et al.*, 2000; Werner and Smola, 2001). Amongst the ligands for the ErbB isoforms that are expressed in epidermis, HB-EGF appears to be the only one regulated by RA (Stoll and Elder, 1998; Xiao *et al.*, 1999). Furthermore, its mRNA is exclusively expressed in suprabasal keratinocytes (Xiao *et al.*, 1999), whereas mature HB-EGF proteins are localized only in epidermal basal cells (Downing *et al.*, 1997). Our present data demonstrate that RXR α /RAR γ heterodimers play a key role in RA-induced HB-EGF expression in suprabasal cells, although they do not reveal whether these heterodimers act directly, or rather through a RA-responsive factor, on this expression. Our study also underlines a positive correlation between expression of HB-EGF and RA-induced proliferation (Table I), further supporting the possibility that HB-EGF could be 'the' paracrine factor that is synthesized in the suprabasal layers and mediates RA-induced hyperplasia (Xiao *et al.*, 1999). We note, however, that RA does not increase HB-EGF expression in RAR $\gamma^{-/-}$ and RAR $\gamma^{sb/-}$ mice, whereas it still exerts some proliferative effect on their epidermis (Table I). Thus, HB-EGF may not be the only signalling molecule involved in RA-induced proliferation. Interestingly, a recent study has shown that expression of keratinocyte growth factor is stimulated by RA in cultured gingival fibroblasts (Mackenzie and Gao, 2001).

In conclusion, our data indicate that a retinoid-inducible RAR γ /RXR α heterodimer-mediated pathway, which functions in epidermal suprabasal cells to synthesize a paracrine signal triggering hyperproliferation of basal keratinocytes, is dispensable for their homeostatic proliferation in resting skin. It is tempting to speculate that this pathway could be required under stress conditions, such as wound healing. In this respect, it is noteworthy that: (i) vitamin A deficiency causes delayed wound healing, whereas pre-treatment with vitamin A or RA improves epidermal regeneration (Hunt, 1986); (ii) HB-EGF secretion is increased in response to epidermal injury (Marikovsky *et al.*, 1993; McCarthy *et al.*, 1996); (iii) RA-induced HB-EGF expression occurs prior to the onset of basal cell layer proliferation (Xiao *et al.*, 1999). Thus, the possibility exists that the beneficial actions of retinoids during wound healing could be mediated through activation of RAR γ /RXR α heterodimers, which at the very least may control HB-EGF signalling in suprabasal keratinocytes.

Materials and methods

Mice and treatments

RAR α - and RAR γ -null, floxed RXR α , RAR α and RAR γ , and CMV-Cre-ER^T and K5-Cre-ER^T transgenic lines have been described previously (Lohnes *et al.*, 1993; Lufkin *et al.*, 1993; Brocard *et al.*, 1997; Indra *et al.*, 1999; Li *et al.*, 2000; Chapellier *et al.*, 2002a,b). Tail epidermis was separated from dermis as described previously (Li *et al.*, 2000). Each experiment (two to three females of each genotype) was repeated three times. Neither acetone nor TAM treatments affected epidermal proliferation.

Histochemistry and proliferation analysis

For histology, skin samples were fixed with 2.5% glutaraldehyde (0.1 M cacodylate pH 7.2). RXR α and RAR γ immunolocalization were as described previously (Ghyselinck *et al.*, 1997; Li *et al.*, 2001). Proliferating cells were detected using an anti-BrdU antibody, revealed

by peroxidase activity and counterstained with Harris haematoxylin. The proliferation marker Ki67 was detected by immunohistochemistry (Novocastra's protocol) on frozen sections post-fixed in 2% paraformaldehyde, and counterstained with 0.01% DAPI. The number of either BrdU- or Ki67-positive and total basal keratinocytes were counted on five areas from three animals of each genotype. The mean \pm SD percentage of proliferating over total basal cells (>200) was then estimated.

Supplementary data

More details of Materials and methods are available as supplementary data at *The EMBO Journal* Online, or on request.

Acknowledgements

We are grateful to C.Suzi (Bristol-Myers Squibb) for synthetic retinoids. We thank B.Féret, B.Bondeau, I.Tilly, B.Weber, O.Wendling and C.Dennefeld for excellent technical assistance, as well as the staff of the animal facility. We are indebted to A.Dierich and E.Blondelle for embryonic stem cell culture. This work was supported by funds from the Centre National de la Recherche Scientifique, the Institut National de la Santé et de la Recherche Médicale, the Collège de France, the Association pour la Recherche sur le Cancer, the Fondation pour la Recherche Médicale, the Human Frontier Science Program, the Ministère de l'Éducation Nationale de la Recherche et de la Technologie and the EEC (CT 97-3220).

References

- Billoni, N., Buan, B., Gautier, B., Gaillard, O., Mahé, Y.F. and Bernard, B.A. (2000) Thyroid hormone receptor β 1 is expressed in the human hair follicle. *Br. J. Dermatol.*, **142**, 645–652.
- Brocard, J., Warot, X., Wendling, O., Messaddeq, N., Vonesch, J.L., Chambon, P. and Metzger, D. (1997) Spatio-temporally controlled site-specific somatic mutagenesis in the mouse. *Proc. Natl Acad. Sci. USA*, **94**, 14559–14563.
- Chambon, P. (1996) A decade of molecular biology of retinoic acid receptors. *FASEB J.*, **10**, 940–954.
- Chapellier, B., Mark, M., Garnier, J.M., LeMour, M., Chambon, P. and Ghyselinck, N.B. (2002a) A conditional floxed (loxP-flanked) allele for the Retinoic Acid Receptor alpha (RAR α) gene. *Genesis*, **32**, 87–89.
- Chapellier, B., Mark, M., Garnier, J.M., Dierich, A., Chambon, P. and Ghyselinck, N.B. (2002b) A conditional floxed (loxP-flanked) allele for the Retinoic Acid Receptor gamma (RAR γ) gene. *Genesis*, **32**, 95–98.
- Chen, J.D. and Evans, R.M. (1995) A transcriptional co-repressor that interacts with nuclear hormone receptors. *Nature*, **377**, 454–457.
- Chen, S. *et al.* (1995) Retinoic acid receptor γ mediates topical retinoid efficacy and irritation in animal models. *J. Invest. Dermatol.*, **104**, 779–783.
- Downing, M.T., Brigstock, D.R., Luquette, M.H., Crissman-Combs, M. and Besner, G.E. (1997) Immunohistochemical localization of heparin-binding epidermal growth factor-like growth factor in normal skin and skin cancers. *Histochem. J.*, **29**, 735–744.
- Elias, P.M., Fritsch, P.O., Lampe, M., Williams, M.L., Brown, B.E., Nemanic, M. and Grayson, S. (1981) Retinoid effects on epidermal structure, differentiation and permeability. *Lab. Invest.*, **44**, 531–540.
- Engelke, M., Jensen, J.M., Ekanayake-Mudiyanse, S. and Proksch, E. (1997) Effects of xerosis and ageing on epidermal proliferation and differentiation. *Br. J. Dermatol.*, **137**, 219–225.
- Feng, X., Peng, Z.H., Di, W., Li, X.Y., Rochette-Egly, C., Chambon, P., Voorhees, J.J. and Xiao, J.H. (1997) Suprabasal expression of a dominant-negative RXR α mutant in transgenic mouse epidermis impairs regulation of gene transcription and basal keratinocyte proliferation by RAR-selective retinoids. *Genes Dev.*, **11**, 59–71.
- Fisher, G.J. and Voorhees, J.J. (1996) Molecular mechanisms of retinoid actions in skin. *FASEB J.*, **10**, 1002–1013.
- Fisher, G.J., Talwar, H.S., Xiao, J.H., Datta, S.C., Reddy, A.P., Gaub, M.P., Rochette-Egly, C., Chambon, P. and Voorhees, J.J. (1994) Immunological identification and functional quantitation of retinoic acid and retinoid X receptor proteins in human skin. *J. Biol. Chem.*, **269**, 20629–20635.
- Frazier, C.N. and Hu, C.K. (1931) Cutaneous lesions associated with a deficiency in vitamin A in man. *Arch. Intern. Med.*, **48**, 507–514.
- Ghyselinck, N.B., Dupé, V., Dierich, A., Messaddeq, N., Garnier, J.M., Rochette-Egly, C., Chambon, P. and Mark, M. (1997) Role of the

- retinoic acid receptor beta (RAR β) during mouse development. *Int. J. Dev. Biol.*, **41**, 425–447.
- Goyette, P., Feng-Chen, C., Wang, W., Seguin, F. and Lohnes, D. (2000) Characterization of retinoic acid receptor-deficient keratinocytes. *J. Biol. Chem.*, **275**, 16497–16505.
- Hunt, T.K. (1986) Vitamin A and wound healing. *J. Am. Acad. Dermatol.*, **15**, 817–821.
- Imakado, S. et al. (1995) Targeting expression of a dominant-negative retinoic acid receptor mutant in the epidermis of transgenic mice results in loss of barrier function. *Genes Dev.*, **9**, 317–329.
- Indra, A.K., Warot, X., Brocard, J., Bornert, J.M., Xiao, J.H., Chambon, P. and Metzger, D. (1999) Temporally-controlled site-specific mutagenesis in the basal layer of the epidermis: comparison of the recombinase activity of the tamoxifen-inducible Cre-ER^T and Cre-ER^{T2} recombinases. *Nucleic Acids Res.*, **27**, 4324–4327.
- Jost, M., Kari, C. and Rodeck, U. (2000) The EGF-receptor—an essential regulator of multiple epidermal functions. *Eur. J. Dermatol.*, **10**, 505–510.
- Kastner, P., Mark, M. and Chambon, P. (1995) Nonsteroid nuclear receptors: what are genetic studies telling us about their role in real life? *Cell*, **83**, 859–869.
- Kastner, P. et al. (1996) Abnormal spermatogenesis in RXR β mutant mice. *Genes Dev.*, **10**, 80–92.
- Kastner, P., Mark, M., Ghyselinck, N., Krezel, W., Dupé, V., Grondona, J.M. and Chambon, P. (1997) Genetic evidence that the retinoid signal is transduced by heterodimeric RXR/RAR functional units during mouse development. *Development*, **124**, 313–326.
- Li, M., Indra, A.K., Warot, X., Brocard, J., Messaddeq, N., Kato, S., Metzger, D. and Chambon, P. (2000) Skin abnormalities generated by temporally controlled RXR α mutations in mouse epidermis. *Nature*, **407**, 633–636.
- Li, M., Chiba, H., Warot, X., Messaddeq, N., Gérard, C., Chambon, P. and Metzger, D. (2001) RXR α ablation in skin keratinocytes results in alopecia and epidermal alterations. *Development*, **128**, 675–688.
- Livrea, M.A. (2000) *Vitamin A and Retinoids: An Update of Biological Aspects and Clinical Applications*. Birkhauser Verlag, Basel, Switzerland.
- Lohnes, D., Kastner, P., Dierich, A., Mark, M., LeMeur, M. and Chambon, P. (1993) Function of retinoic acid receptor γ in the mouse. *Cell*, **73**, 643–658.
- Lufkin, T., Lohnes, D., Mark, M., Dierich, A., Gorry, P., Gaub, M.P., LeMeur, M. and Chambon, P. (1993) High postnatal lethality and testis degeneration in retinoic acid receptor α mutant mice. *Proc. Natl Acad. Sci. USA*, **90**, 7225–7229.
- Mackenzie, I.C. and Gao, Z. (2001) Keratinocyte growth factor expression in human gingival fibroblasts and stimulation of *in vitro* gene expression by retinoic acid. *J. Periodontol.*, **72**, 445–453.
- Mangelsdorf, D.J. et al. (1995) The nuclear receptor superfamily: the second decade. *Cell*, **83**, 835–839.
- Marikovsky, M., Breuing, K., Liu, P.Y., Eriksson, E., Higashiyama, S., Farber, P., Abraham, J. and Klagsbrun, M. (1993) Appearance of heparin-binding EGF-like growth factor in wound fluid as a response to injury. *Proc. Natl Acad. Sci. USA*, **90**, 3889–3893.
- Mascres, B., Mark, M., Dierich, A., Ghyselinck, N.B., Kastner, P. and Chambon, P. (1998) The RXR α ligand-dependent activation function 2 (AF-2) is important for mouse development. *Development*, **125**, 4691–4707.
- McCarthy, D.W., Downing, M.T., Brigstock, D.R., Luquette, M.H., Brown, K.D., Abad, M.S. and Besner, G.E. (1996) Production of heparin-binding epidermal growth factor-like growth factor (HB-EGF) at sites of thermal injury in pediatric patients. *J. Invest. Dermatol.*, **106**, 49–56.
- Metzger, D. and Chambon, P. (2001) Site- and time-specific gene targeting in the mouse. *Methods*, **24**, 71–80.
- Michalik, L. et al. (2001) Impaired skin wound healing in peroxisome proliferator-activated receptor (PPAR) α and PPAR β mutant mice. *J. Cell Biol.*, **154**, 799–814.
- Morris-Kay, G.M. and Ward, S.J. (1999) Retinoids and mammalian development. *Int. Rev. Cytol.*, **188**, 73–131.
- Niederreither, K., Fraulob, V., Garnier, J.M., Chambon, P. and Dollé, P. (2002) Differential expression of retinoic-acid-synthesizing (RALDH) enzymes during fetal development and organ differentiation in the mouse. *Mech. Dev.*, **110**, 165–171.
- Peters, J.M., Lee, S.S., Li, W., Ward, J.M., Gavrilova, O., Everett, C., Reitman, M.L., Hudson, L.D. and Gonzalez, F.J. (2000) Growth, adipose, brain and skin alterations resulting from targeted disruption of the mouse peroxisome proliferator-activated receptor β (δ). *Mol. Cell Biol.*, **20**, 5119–5128.
- Piepkorn, M., Pittelkow, M.R. and Cook, P.W. (1998) Autocrine regulation of keratinocytes: the emerging role of heparin-binding, epidermal growth factor-related growth factors. *J. Invest. Dermatol.*, **111**, 715–721.
- Redfern, C.P.F. and Todd, C. (1992) Retinoic acid receptor expression in human skin keratinocytes and dermal fibroblast *in vitro*. *J. Cell Sci.*, **102**, 113–121.
- Roy, B., Taneja, R. and Chambon, P. (1995) Synergistic activation of retinoic acid (RA)-responsive genes and induction of embryonal carcinoma cell differentiation by an RA receptor alpha (RAR α), RAR β , or RAR γ -selective ligand in combination with a retinoid X receptor-specific ligand. *Mol. Cell Biol.*, **15**, 6481–6487.
- Saitou, M., Sugai, S., Tanaka, T., Shimouchi, K., Fuchs, E., Narumiya, S. and Kakizuka, A. (1995) Inhibition of skin development by targeted expression of a dominant negative retinoic acid receptor. *Nature*, **374**, 159–162.
- Stoll, S.W. and Elder, J.T. (1998) Retinoid regulation of heparin-binding EGF-like growth factor gene expression in human keratinocytes and skin. *Exp. Dermatol.*, **7**, 391–397.
- Taneja, R., Roy, B., Plassat, J.L., Zusi, C.F., Ostrowski, J., Reczek, P.R. and Chambon, P. (1996) Cell-type and promoter-context dependent retinoic acid receptor (RAR) redundancies for RAR β 2 and Hoxa-1 activation in F9 and P19 cells can be artefactually generated by gene knockouts. *Proc. Natl Acad. Sci. USA*, **93**, 6197–6202.
- Thacher, S.M., Standeven, A.M., Athanikar, J., Kopper, S., Castilleja, O., Escobar, M., Beard, R.L. and Chandraratna, R.A. (1997) Receptor specificity of retinoid-induced epidermal hyperplasia: effect of RXR-selective agonists and correlation with topical irritation. *J. Pharmacol. Exp. Ther.*, **282**, 528–534.
- Tsou, H.C., Lee, X., Si, S.P. and Peacocke, M. (1994) Regulation of retinoic acid receptor expression in dermal fibroblasts. *Exp. Cell Res.*, **211**, 74–81.
- Vahlquist, A. (1982) Vitamin A in human skin: I. detection and identification of retinoids in normal epidermis. *J. Invest. Dermatol.*, **79**, 89–93.
- Wendling, O., Ghyselinck, N.B., Chambon, P. and Mark, M. (2001) Roles of retinoic acid receptors in early embryonic morphogenesis and hindbrain patterning. *Development*, **128**, 2031–2038.
- Werner, S. and Smola, H. (2001) Paracrine regulation of keratinocyte proliferation and differentiation. *Trends Cell Biol.*, **11**, 143–146.
- Wolbach, S.B. and Howe, P.R. (1925) Tissue changes following deprivation of fat-soluble A vitamin. *J. Exp. Med.*, **42**, 753–777.
- Xiao, J.H., Feng, X., Di, W., Peng, Z.H., Li, L.A., Chambon, P. and Voorhees, J.J. (1999) Identification of heparin-binding EGF-like growth factor as a target in intercellular regulation of epidermal basal cell growth by suprabasal retinoic acid receptors. *EMBO J.*, **18**, 1539–1548.

Received March 18, 2002; revised April 29, 2002;
accepted May 6, 2002

Peroxisome proliferator-activated receptor γ is required in mature white and brown adipocytes for their survival in the mouse

Takeshi Imai*, Reiko Takakuwa*, Sandra Marchand†, Emilie Dentz*, Jean-Marc Bornert*, Nadia Messaddeq*, Olivia Wendling**, Manuel Mark**, Béatrice Desvergne†, Walter Wahli†, Pierre Chambon**, and Daniel Metzger**§

*Institut de Génétique et de Biologie Moléculaire et Cellulaire, Centre National de la Recherche Scientifique, Institut National de la Santé et de la Recherche Médicale, Université Louis Pasteur, BP10142, 1 Rue Laurent Fries, 67404 Illkirch Cedex, France; †Institut Clinique de la Souris, BP 10142, 1 Rue Laurent Fries, 67404 Illkirch Cedex, France; and **Center for Integrative Genomics, National Center of Competence in Research Frontiers in Genomics, University of Lausanne, CH-1015 Lausanne, Switzerland

Contributed by Pierre Chambon, February 6, 2004

The peroxisome proliferator-activated receptor γ (PPAR γ) mediates the activity of the insulin-sensitizing thiazolidinediones and plays an important role in adipocyte differentiation and fat accretion. The analysis of PPAR γ functions in mature adipocytes is precluded by lethality of PPAR $\gamma^{-/-}$ fetuses and tetraploid-rescued pups. Therefore we have selectively ablated PPAR γ in adipocytes of adult mice by using the tamoxifen-dependent Cre-ER^{T2} recombination system. We show that mature PPAR γ -null white and brown adipocytes die within a few days and are replaced by newly formed PPAR γ -positive adipocytes, demonstrating that PPAR γ is essential for the *in vivo* survival of mature adipocytes, in addition to its well established requirement for their differentiation. Our data suggest that potent PPAR γ antagonists could be used to acutely reduce obesity.

conditional somatic mutagenesis | tamoxifen-dependent | adipocyte maintenance | obesity | nuclear receptor

The nuclear receptor PPAR γ is a ligand-dependent transcriptional regulator that heterodimerizes with retinoid X receptors (RXRs) and is activated by natural ligands, such as arachidonic acid metabolites and fatty acid-derived components, and by the insulin-sensitizing drugs thiazolidinediones. Activation of PPAR γ by thiazolidinediones in white and brown preadipocyte cell lines results in robust differentiation into adipocytes, and administration of thiazolidinediones to rodents increases accumulation of white (WAT) and brown (BAT) adipose tissue deposits. Moreover, overexpression of PPAR γ in fibroblasts induces adipogenesis, and PPAR γ -null embryonic stem cells and fibroblastic cells from PPAR γ -deficient embryos cannot differentiate into adipocytes *in vitro*. PPAR γ is also known to be indispensable for adipose tissue formation *in vivo*, because mice chimeric for WT and PPAR γ -null cells show little or no contribution of null cells to adipose tissue, and PPAR γ -deficient pups, derived by tetraploid rescue that bypasses placental defects, lack BAT and WAT (for reviews, see refs. 1–4). To study PPAR γ functions in mature adipocytes, we ablated PPAR γ in adipocytes of adult mice through Tamoxifen (Tam) treatment of transgenic mice bearing a LoxP site-containing (floxed) PPAR γ gene and expressing the ligand-dependent fusion protein between the Cre recombinase and a mutated ligand-binding domain of the human estrogen receptor α (Cre-ER^{T2}) recombinase selectively in brown and white adipocytes. We show here that PPAR γ -deficient adipocytes die within a few days, which triggers an inflammatory reaction in BAT and WAT, and are replaced by newly differentiated PPAR γ -expressing adipocytes, which most probably derive from fibroblast-like preadipocyte cells.

Materials and Methods

Transgenic Mice. The aP2-Cre-ER^{T2} transgenic mice were described (5).

Genotyping. Genomic DNA was isolated from various tissues and cell types as described (5). Macrophages were collected from the i.p. cavity. The aP2-Cre-ER^{T2} transgene was genotyped on tail DNA (5). To identify the various PPAR γ alleles on DNA extracted from tissues and cell types, genomic PCR was performed with the following primers (see Fig. 1A): P1 (5'-CAGAAACATCTCTAGTGAAG-3') and P2 (5'-ATGGGAGCATAGAAGCTTTGA-3'), 241 bp PPAR γ + allele; P1 and P3 (5'-AAGTTATGCTAGCAAGCTTTGA-3'), 239 bp PPAR γ L2 allele; P4 (5'-AAGAGAAGAGAAGGATATGGAG-3') and P5 (5'-ATATTAATATGCTTAATATTACAGC-3'), 234 bp PPAR γ L⁻ allele; and P1 and P6 (5'-TGACATAGTAATTTTGTAGTTCCC-3'), 226 bp control (CT) allele. The ³²P-end-labeled oligonucleotide O7 (5'-TATACTATACACTGTG-CAGCC-3') was used as a probe to reveal the PCR products by Southern blotting. Purification of adipocytes by collagenase II treatment of adipose tissue and centrifugation was described (5).

Animal Treatments and Analyses. Mice were housed on a 12 h light/12 h dark cycle and fed a standard laboratory chow [2,800 kcal/kg (1 cal = 4.184 J); Usine d'Alimentation Rationnelle, Villemoisson-sur-Orge, France]. Tam (1 mg in 100 μ l of sunflower oil) was i.p. injected as described (6). Body fat content was evaluated by dual energy x-ray absorptiometry (PIXIMUS, GE Medical Systems, Buc, France) (7).

Histological and Electron Microscopic Analysis. For 5- μ m sections, samples were fixed in Bouin's fixative, embedded in paraffin, and stained with hematoxylin and eosin or trichrome. Electron microscopy (EM) was performed as described (8).

RNA Analysis. RNA was isolated and Pref-1 expression analyzed by RT-PCR (5). Other transcripts levels were determined by real-time PCR with a Roche light cycler (Roche Diagnostics) and the Cyber Green kit (Qiagen, Valencia, CA), according to the manufacturer's instructions. Hypoxanthine phosphoribosyltransferase was used as an invariant control. The following oligonucleotides were used: PGC1 α , 5'-GGCTCTTGGTGACAGTGTGT-3' and 5'-TGTGTCTTCATGGAAATGCTG-3'; ANC, 5'-CGTTCTCAGAGGCATGGGT-3' and 5'-GATGAATATTATTGCTTCCCAC-3'; α ATPase, 5'-ACGACTTCATGTTGAGTTCCA-3' and 5'-CCGAATTCATAGTG-

Abbreviations: BAT, brown adipose tissue; Cre-ER^{T2}, fusion protein between the Cre recombinase and a mutated ligand-binding domain of the human estrogen receptor α ; CT, control; EM, electron microscopy; iBAT, interscapular BAT; MT, mutant; PPAR, peroxisome proliferator-activated receptor; PPAR $\gamma^{ad/-}$, adipocyte-selective PPAR γ -deficient; RXR, retinoid X receptor; RXR $\alpha^{ad/-}$, adipocyte-selective RXR α -deficient; Tam, tamoxifen; WAT, white adipose tissue; Dn, day n.

§To whom correspondence should be addressed. E-mail: metzger@igbmc.u-strasbg.fr.

© 2004 by The National Academy of Sciences of the USA

GACAG-3'; β ATPase, 5'-CTTCCATGCAGGCCACACA-3' and 5'-CCACCACTGTGAGCTCAATT-3'; δ ATPase, 5'-CAGCAGTGCTCCAGTTGCT-3' and 5'-CCTGGTGTTAATGGAGACAG-3'; cytochrome c, 5'-GTTGATCTGCAATTAAAAATGCT-3' and 5'-CAGGATCTGTGGTTGTTTAAAT-3'; COX II, 5'-CCCCTCCCTAGGACTTAAA-3' and 5'-TGGGCATAAAGCTATGGTTAG-3'; and COX IV, 5'-ACTTTCGATCGTGACTGGGT-3' and 5'-AACTGGTCTTTTATTAGCATGG-3'.

Statistical Analysis. Values are reported as mean \pm SEM. Statistical significance ($P < 0.05$) was determined by unpaired Student's *t* test (STATVIEW, Abacus Concepts, Berkeley, CA).

Results

To determine the function of PPAR γ in mature adipocytes, PPAR γ was selectively ablated in adipocytes of adult mice by using mice bearing LoxP-flanked PPAR γ L2 alleles (Fig. 1*A* and *Supporting Text*, which is published as supporting information on the PNAS web site) and aP2-Cre-ER^{T2} transgenic mice that express, under the control of the adipocyte-selective aP2 promoter, the conditional Cre-ER^{T2} Cre recombinase whose activity depends on Tam administration (5). Eight-week-old aP2-Cre-ER^{T2}(tg0)/PPAR γ ^{L2/L2} mice (hemizygous for the aP2-Cre-ER^{T2} transgene and homozygous for the PPAR γ L2 allele, hereafter named PPAR γ ^{ad-/-} premutant mice) and control littermates (aP2-Cre-ER^{T2}(tg0)/PPAR γ ^{L2/+}, aP2-Cre-ER^{T2}(tg0)/PPAR γ ^{L2/L2}, aP2-Cre-ER^{T2}(tg0)/PPAR γ ^{+/+}, and aP2-Cre-ER^{T2}(tg0)/PPAR γ ^{L2/L2} mice), were i.p. injected with 1 mg of Tam [day 0 (D0), Fig. 1*B*] to produce PPAR γ ^{ad-/-} mutant (MT) mice, selectively bearing a PPAR γ -null mutation (see *Supporting Text*) in adipocytes, and CT mice that were indistinguishable from WT mice. At day 4 (D4), 30–40% and 20–30% of the PPAR γ L2 alleles from epididymal WAT and interscapular brown adipose tissue (iBAT) of PPAR γ ^{ad-/-} premutant mice, respectively, were converted into PPAR γ ^{L-} alleles, whereas no Cre-mediated recombination was observed in other cell types or tissues, such as peritoneal macrophages, muscle, kidney, and liver (Fig. 1*C*, lanes 6–11, and data not shown). Similar levels of PPAR γ ablation were observed after Tam treatment for 5 consecutive days (data not shown). Purification of adipocytes from epididymal WAT of MT mice revealed that PPAR γ was ablated in >90% of D4 adipocytes, whereas no DNA excision was observed at D0 (Fig. 1*C*, lanes 12 and 13, and data not shown). Thus, temporally controlled PPAR γ ablation in mature white and brown adipocytes was efficiently induced by Tam treatment of premutant mice. Epididymal fat pad and iBAT weights were \sim 30% lower in MT than in CT mice at D7 (Fig. 1*D*). Moreover, dual-energy x-ray adsorptiometry (DEXA) scanning revealed 17–25% reductions of the relative body fat content in MT animals from D7 to D21, whereas at D42 and D49 the relative body fat content was similar in MT and CT mice (Fig. 1*E*).

To estimate the fraction of PPAR γ -deficient adipocytes over time, PPAR γ alleles were characterized in purified epididymal adipocytes and iBAT from Tam-treated PPAR γ ^{ad-/-} premutant (MT) and aP2-Cre-ER^{T2}(tg0)/PPAR γ ^{L2/+} CT mice at various times after Tam administration. In WAT adipocytes from CT mice, most if not all PPAR γ L2 alleles were converted into L⁻ alleles at D4, and similar amounts of L⁻ alleles were found for at least 6 weeks (Fig. 1*C*, lanes 16–18). In marked contrast, whereas PPAR γ L2 alleles were efficiently converted into PPAR γ ^{L-} alleles at D4 in WAT adipocytes from MT mice, only half of these PPAR γ ^{L-} alleles were left by D14, and none were present at D42 (Fig. 1*C*, lanes 12–15). A similar disappearance of PPAR γ ^{L-} alleles between D4 and D42 also occurred in BAT of MT, but not of CT mice (Fig. 1*C*, compare lanes 19–22 and 23–25). Because the aP2 promoter is known to be active only at

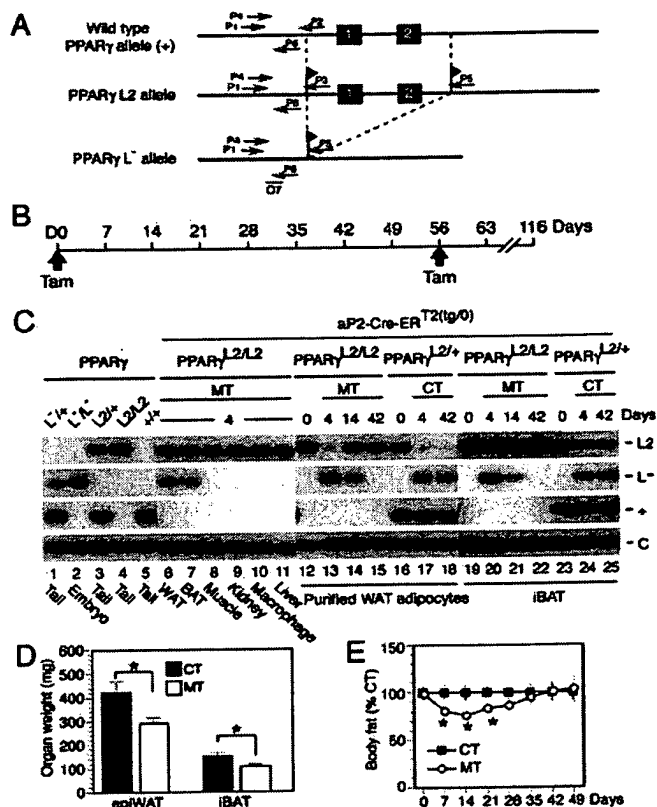


Fig. 1. Selective Tam-induced PPAR γ gene disruption in adipocytes of WAT and BAT of adult mice. (A) Diagram of the WT PPAR γ genomic locus (+), the floxed PPAR γ L2 allele, and the PPAR γ L⁻ null allele obtained after Cre-mediated excision of exons 1 and 2. Black boxes and arrows indicate exons and PCR primers, respectively. The probe O7 location is shown. (B) Timing of Tam administration and phenotypic analysis. (C) Adipocyte-selective Tam-induced generation of PPAR γ L⁻ alleles. PCR analysis of DNA from the indicated cell types and tissues of 8-week-old aP2-Cre-ER^{T2}(tg0)/PPAR γ ^{L2/L2} mice at D4 (lanes 6–11), from purified epididymal adipocytes and iBAT isolated from (i) aP2-Cre-ER^{T2}(tg0)/PPAR γ ^{L2/L2} mice at D0, D4, D14, and D42 (lanes 12–15 and lanes 19–22, respectively) and (ii) control aP2-Cre-ER^{T2}(tg0)/PPAR γ ^{L2/+} mice at D0, D4, and D42 (lanes 16–18 and lanes 23–25, respectively). Control PCR on genomic DNA from of PPAR γ ^{L-/-}, PPAR γ ^{L2/+}, PPAR γ ^{L2/L2}, and PPAR γ ^{+/+} mice and from 9.5 days postconception PPAR γ ^{L-/-} embryos are presented in lanes 1–5; PCR fragments corresponding to the PPAR γ L2, L⁻, and + alleles are displayed. Macrophage: i.p. cells containing \sim 30% macrophages. (D) Epididymal fat pad (epiWAT) and iBAT weight of CT and of MT mice at D7. Values are expressed as the mean \pm SEM ($n = 5$). *, $P < 0.05$. (E) Body fat content evaluated by DEXA scanning. CT and PPAR γ ^{ad-/-} premutant mice (MT) were analyzed before and for 7 weeks after Tam treatment. The percentage of fat content in mutant mice relative to CT mice for each time point is shown. Values (black squares for CT and open circles for MT) are expressed as the mean \pm SEM ($n = 7$). The body fat content of CT mice for each time point was set to 100. *, $P < 0.05$.

late stages of adipocyte differentiation (2), we concluded from these data that mature white and brown adipocytes most probably died within 2–3 weeks after PPAR γ ablation, to be progressively replaced by new adipocytes generated from PPAR γ ^{L2/L2} preadipocytes. This possibility was first investigated at the histological level.

Before Tam treatment of PPAR γ ^{ad-/-} premutant and CT mice and after Tam treatment of CT mice, epididymal fat pad contained large cells with a single, central large fat droplet and a peripheral nucleus surrounded by a thin rim of cytoplasm (Fig.

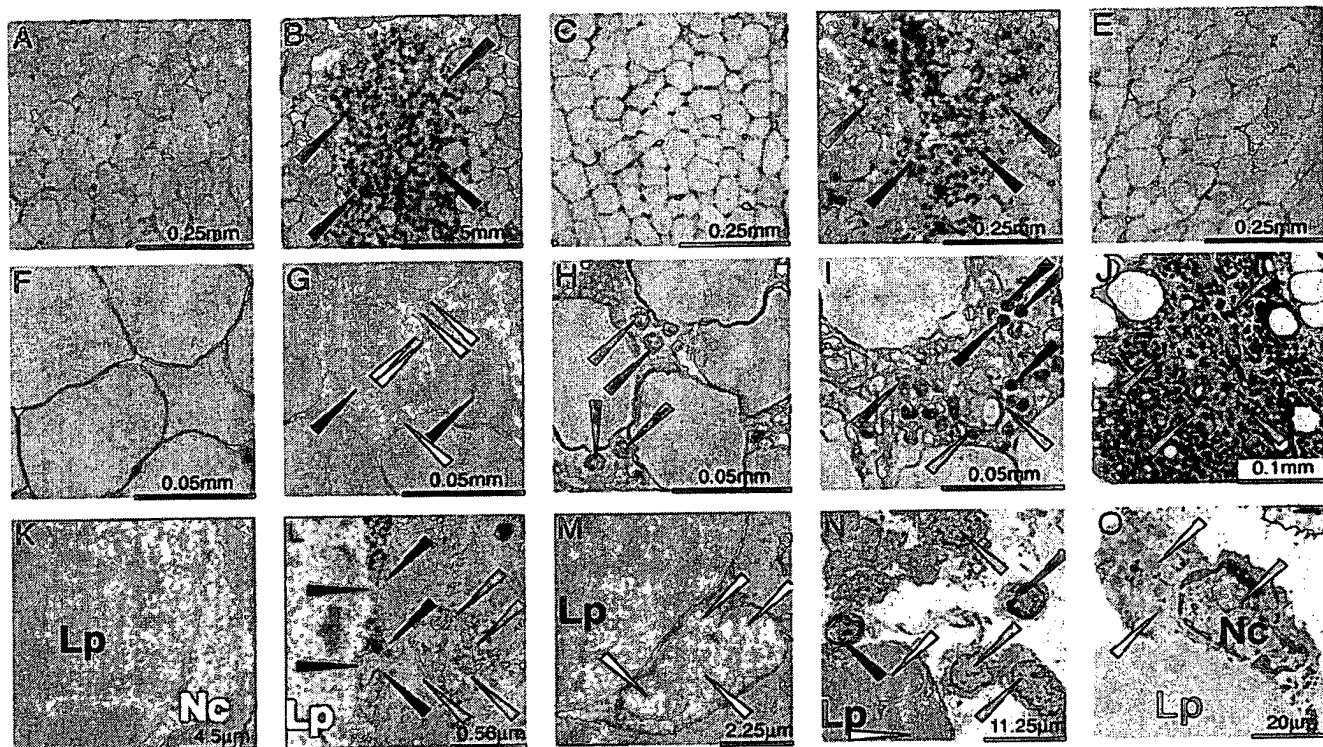


Fig. 2. Histological analysis of WAT of Tam-treated $PPAR^{\gamma ad/-}$ premutant mice. Histological sections from paraffin-embedded epididymal WAT from CT (aP2-Cre- $ERT^{2(0/0)}/PPAR^{\gamma 2L/2}$) mice at D4 (A) and D2 (F) and MT mice at D2 (G), D4 (H and I), D7 (B), D14 (J), and D42 (C) (Tam injection at D0), and D67 (D) and D116 (E), after a second Tam injection at D56. (A–F) Hematoxylin/eosin staining. (J) Trichrome staining. Ultrastructure of adipose tissue of CT (aP2-Cre- $ERT^{2(0/0)}/PPAR^{\gamma 2L/2}$) at D4 (K) and MT mice at D4 (L) and D7 (M–O). Blue arrows point to clusters of infiltrating cells (B and D); black arrows point to adipocytes with abnormal profiles (G); white arrows point to small lipid droplets in adipocytes (G, M, and N) and to phagocytosed lipid droplets (O); green arrows point to neutrophils (H and I); red arrows point to lymphocytes (J and N); yellow arrows point to macrophages (I, N, and O); orange arrows point to fibroblast-like cells (J and N); and black and gray arrows point to disrupted adipocyte cell membrane and cell debris (L). Lp, lipid droplet; Nc, nucleus. (Scales are indicated in each image.)

2 A and F, and data not shown). At D1 and D2, few (<5%) epididymal adipocytes of MT mice displayed irregular outlines, and about half of them contained supernumerary small lipid droplets (Fig. 2, compare G and F, and data not shown). Neutrophil infiltration was occasionally seen in the vicinity of adipocytes with irregular outlines (data not shown). With time, the number of abnormal adipocytes increased, and by D4 to D7 ~30% of the adipocytes were affected and fat droplets were laying free in the connective tissue. Lymphocytes (B and T cells) and macrophages were infiltrating the adipose tissue, forming inflammatory foci in some regions (Fig. 2, compare A and B, see H and I, and data not shown). EM performed at D4 and D7 revealed the presence of adipocytes with a disrupted cell membrane (e.g., Fig. 2L). Because only some of these necrotic adipocytes contained groups of small lipid droplets adjacent to the large lipid droplet (Fig. 2M and N and data not shown), it is unlikely that adipocyte death was caused by defects in lipid droplet formation or holding. Lymphocytes, macrophages, and fibroblasts were present in the vicinity of necrotic adipocytes and lipid droplets (Fig. 2N and O; see below). Trichrome staining of histological sections at D7, D14, and D21 revealed abundant collagen deposits in inflammatory regions (Fig. 2J and data not shown). Similar defects were observed in s.c. fat (data not shown). In marked contrast, at D42–D56 epididymal and s.c. fat pads of mutant mice were similar to those of CT mice (Fig. 2C and data not shown), thus suggesting that WAT had regenerated through differentiation of preadipocytes into mature adipocytes. This possibility was further supported by the expression of the

Pref-1 gene which is known to occur in preadipocytes but not in mature adipocytes (9). Pref-1 transcripts were strongly increased at D7 and D14 in epididymal fat pad of MT mice, whereas their levels remained unchanged in CT mice (Fig. 3A). In agreement with the histological data, Pref-1 RNA levels were similar in D42 MT and CT mice (see Fig. 3A and data not shown). However, when Tam was readministered to MT mice at D56, abnormalities similar to those described above were observed over a 4-week period, but had totally disappeared by D116 (Fig. 2D and E, respectively, and data not shown).

Histological examination of BAT sections at D1 and D2 did not reveal any obvious difference between CT and MT animals (data not shown). However, at D4 ~30% of brown adipocytes from MT mice contained much larger lipid droplets than those from CT mice (Fig. 4, compare B and G with A and F, respectively). This increase was not caused by hypertriglyceridemia, as seen in *ob/ob* or *fatless* mice for example, because a 30% reduction of triglyceride plasma levels occurred in MT mice 1–4 weeks after Tam treatment (data not shown). EM analysis revealed the presence of numerous brown adipocytes with clumping of nuclear chromatin in MT mice (Fig. 4 compare K and L). Moreover, hypertrophic mitochondria, with normal or increased cristae density and swollen mitochondria, characterized by rare or peripherally displaced cristae, were seen in 5–10% and 60–70% of adipocytes, respectively (Fig. 4M and N and data not shown). Impaired mitochondrial function was supported by a 25–50% reduction in transcripts of nuclear genes involved in respiratory chain function, such as the ATP synthase F1 α , β , and

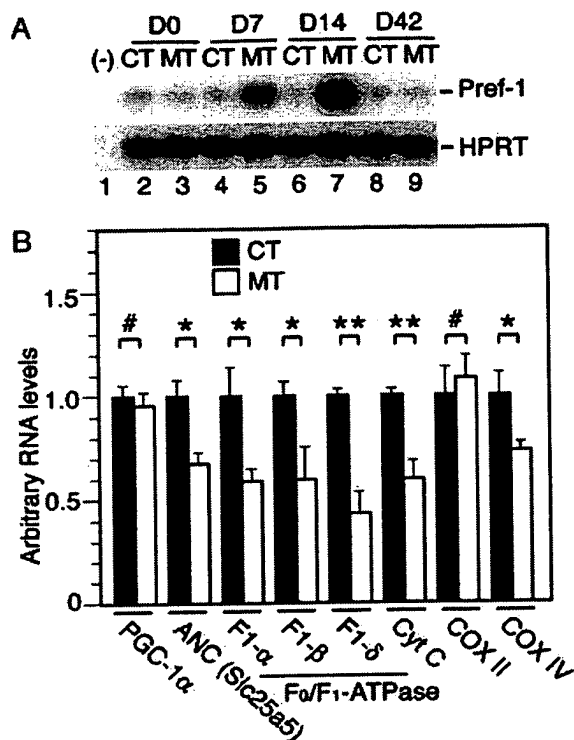


Fig. 3. Expression of Pref-1 and genes involved in respiratory chain function in Tam-treated PPAR $\gamma^{ad/-}$ pre-mutant mice. (A) Pref-1 expression was analyzed by RT-PCR performed on RNA extracted from epididymal WAT of CT (lanes 2, 4, 6, and 8) and MT (lanes 3, 5, 7, and 9) mice at D0, D7, D14, and D42. Hypoxanthine phosphoribosyltransferase was used as an internal control. (B) Transcript levels of the indicated genes analyzed by quantitative RT-PCR on RNA isolated from BAT of CT (filled bars) and MT (open bars) mice at D4. Values are expressed as mean \pm SEM (relative to CT). $n = 5$. *, $P < 0.05$; **, $P < 0.005$; #, no statistically significant difference.

δ subunits, the adenine nucleotide translocator, the cytochrome *c* and the cytochrome *c*-oxidase subunit COX IV at D4, whereas those of the cold-inducible coactivator of nuclear receptors PGC-1 α , and of the mitochondrially encoded COX II were not altered (Fig. 3B). At D7 and D14, 30–40% of the BAT section areas contained necrotic adipocytes (Fig. 4 C and H), markedly infiltrated by lymphocytes (Fig. 4 D and I). Moreover, foci of fibrosis were much larger than at D4 (Fig. 4J and data not shown). EM analysis at D14 confirmed the presence of numerous necrotic brown adipocytes with swollen and hypertrophic mitochondria and fibroblasts and collagen fibers (data not shown). However, \sim 30% of cells with a high number of mitochondria contained numerous small lipid droplets (diameter, $<0.3 \mu\text{m}$), abundant ribosomes and polysomes, and small clusters of glycogen (Fig. 4O and data not shown), features reported in newborn adipoblasts (see ref. 10). Taken together with the progressive loss of PPAR γ L $^{-}$ alleles and the concomitant increase of PPAR γ L2 alleles (Fig. 1C), it appears that PPAR γ -null brown adipocytes were progressively replaced by newly differentiated brown adipocytes. At D42, all BAT abnormalities had disappeared (Fig. 4E and data not shown).

Discussion

The present study, in which PPAR γ is selectively ablated in white and brown adipocytes of adult mice, shows that PPAR γ -null adipocytes die within a few days, thus demonstrating that this nuclear receptor is essential for the survival of mature adipo-

cytes. Surprisingly, since the completion of our study, it was reported that mice in which PPAR γ was ablated in adipocytes by the Cre recombinase expressed under the control of the aP2 promoter became lipodystrophic only after several months (11). Because PPAR γ is most probably ablated in these mice during adipocyte differentiation rather than in mature adipocytes, compensatory mechanisms might substitute for PPAR γ functions during adipocyte differentiation. Alternatively or concomitantly, in young mutant animals, PPAR γ null adipocytes might die and be efficiently replaced by newly differentiated adipocytes, but with age, progenitor cells might be exhausted, thus leading to lipodystrophy. The high number of small adipocyte-like cells in aged mutant mice (11) might correspond to PPAR γ -null preadipocytes that cannot further differentiate, whereas the hypertrophic adipocytes might represent, at least in part, PPAR γ -expressing adipocytes, because PPAR γ was only ablated in 90–95% of adipocytes.

Even though no adipocyte death was noticed in either RXR β - or RXR γ -null mice (refs. 12 and 13 and unpublished results) or in mice selectively lacking RXR α in adipocytes [RXR $\alpha^{ad/-}$ mice (5)], PPAR γ most probably exerts its adipocyte vital functions as a heterodimer with RXR. Indeed, ablation of RXR α in adipocytes of RXR γ -null mice (but not of RXR β -null mice) also results in similar mature adipocyte death, thus revealing a functional redundancy between RXR α and RXR γ , which could result from a compensatory enhanced expression of RXR γ in adipocytes of RXR $\alpha^{ad/-}$ mice (5). No such redundancy occurs between RXR α and RXR γ for the function(s) exerted by PPAR γ /RXR heterodimers when hypertrophic adipocytes are formed during a high-fat diet treatment, because mice selectively lacking RXR α in their adipocytes are resistant to high-fat diet-induced obesity (5). It appears, therefore, that the vital and lipogenic functions exerted by PPAR γ in mature adipocytes have different requirements for RXR heterodimeric partners: the vital function can be mediated by either PPAR γ /RXR α or PPAR γ /RXR γ heterodimers, whereas the lipogenic function requires PPAR γ /RXR α heterodimers. Because much more RXR α than RXR γ occurs in adipocytes, the threshold level of PPAR γ /RXR heterodimers required to ensure the survival of adipocytes is therefore much lower than that required to trigger lipogenesis. These differential requirements offer an explanation as to why heterozygous PPAR γ -deficient mice (14, 15) and mice treated with low-affinity PPAR γ or RXR antagonists (15, 16) are resistant to high-fat diet-induced obesity, whereas administration for several weeks of such low-affinity RXR or PPAR γ antagonists to heterozygous PPAR γ -deficient mice is necessary to reach a lipodystrophic state with disappearance of visible WAT (16). It has been proposed (15, 16) that partial antagonists of PPAR γ /RXR activity could be used to prevent obesity and related diseases such as type 2 diabetes. Our present data further suggest that high-affinity full antagonists of PPAR γ /RXR α activity could possibly be used in treatment strategies aimed at acutely reducing obesity.

Finally, our study shows that, after the death of PPAR γ -ablated white and brown adipocytes, newly differentiated adipocytes expressing PPAR γ appear within a few weeks. They most probably derive from fibroblast-like cells, whose number was strongly increased after ablation of PPAR γ . This adipocyte regeneration is in agreement with previous findings showing that adipose progenitor cells, the origin of which remains controversial, are widely distributed in connective tissues and can proliferate and differentiate into adipocytes in adult tissues (17). The present possibility to massively stimulate this process in adult mice might allow further characterization of the origin and nature of these precursor cells *in vivo*.

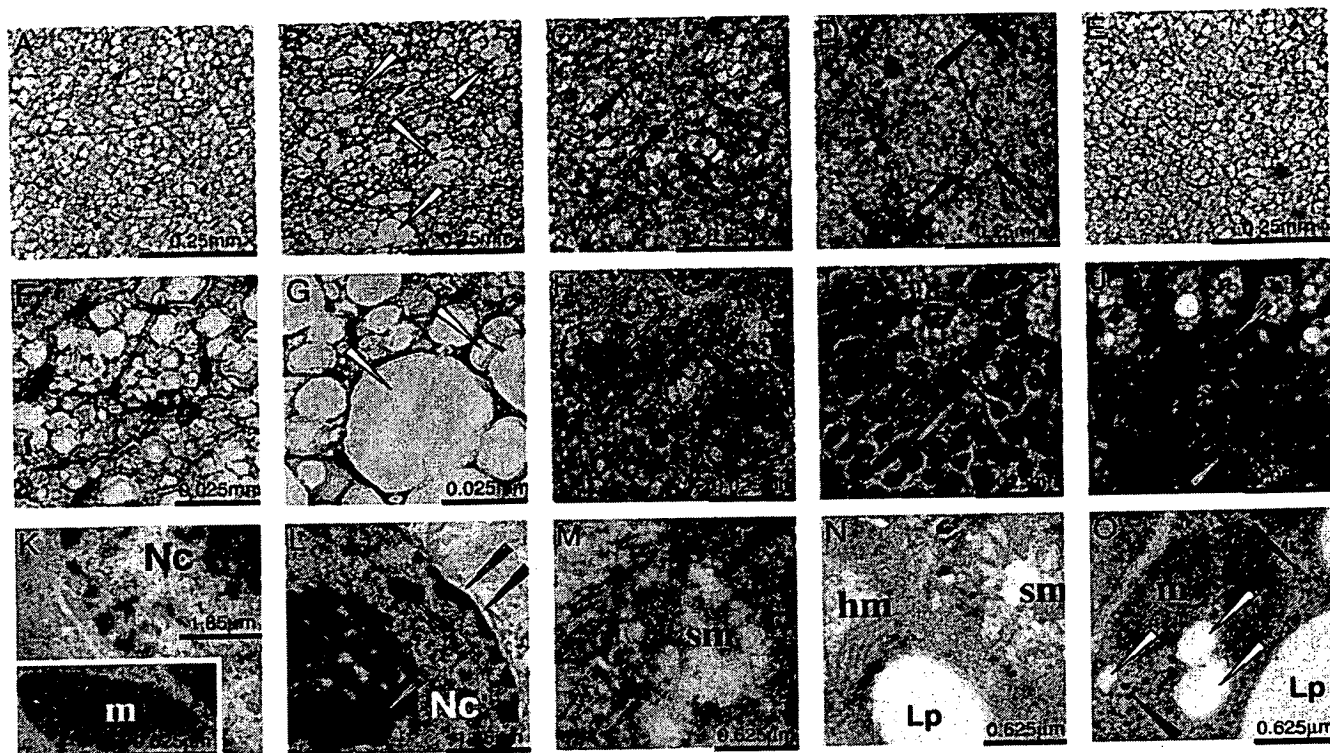


Fig. 4. Histological analysis of BAT of Tam-treated PPAR- $\gamma^{2/-}$ premutant mice. Histological sections from paraffin-embedded interscapular BAT from CT (aP2-Cre-ER^{T2(OO)}/PPAR- $\gamma^{2/+}$) mice at D4 (A and F) and MT mice (B-E and G-J) at D4 (B and G), D7 (C and H), D14 (D, I, and J), and D42 (E). (A-F) Hematoxylin and eosin staining. (J) Trichrome staining. (K-O) EM. (K) CT (aP2-Cre-ER^{T2(OO)}/PPAR- $\gamma^{2/+}$) at D4. (Inset) Typical mitochondria. (L-M) MT at D4. (O) mutant at D14. White arrows point to fused lipid droplets (B and G) and small lipid droplets (O); blue arrows point to necrotic area (C and H) and clumped chromatin (L); green arrows point to detached nuclear membrane (L); red arrows point to lymphocytes (D and I); orange arrows point to fibroblast-like cells (J); purple arrows point to glycogen (O). Lp, lipid droplet; Nc, nucleus; m, mitochondria; hm and sm, hypertrophic and swollen mitochondria, respectively. (Scales are indicated in each image.)

We thank R. Lorenz, N. Chartoire, M. F. Champy (Institut Clinique de la Souris), A. Dierich, and the animal facility staff for excellent technical assistance, and the secretariat for typing the manuscript. R.T. was supported by a fellowship from the Fondation de la Recherche Médicale, and E.D. was supported by a fellowship from the Ministère de la Jeunesse, de l'Éducation Nationale et de la Recherche. This work was supported by funds from the Centre National de la

Recherche Scientifique, the Institut National de la Santé et de la Recherche Médicale, the Collège de France, the Hôpital Universitaire de Strasbourg, the Association pour la Recherche sur le Cancer, the Fondation pour la Recherche Médicale, the Human Frontier Science Program, the Ministère de l'Éducation Nationale de la Recherche et de la Technologie, the Swiss National Science Foundation, the Etat de Vaud, and the European Community.

- Desvergne, B. & Wahli, W. (1999) *Endocr. Rev.* **20**, 649–688.
- Rosen, E. D., Walkey, C. J., Puigserver, P. & Spiegelman, B. M. (2000) *Genes Dev.* **14**, 1293–1307.
- Kadowaki, T. (2000) *J. Clin. Invest.* **106**, 459–465.
- Lee, C. H., Olson, P. & Evans, R. M. (2003) *Endocrinology* **144**, 2201–2207.
- Imai, T., Jiang, M., Chambon, P. & Metzger, D. (2001) *Proc. Natl. Acad. Sci. USA* **98**, 224–228.
- Metzger, D. & Chambon, P. (2001) *Methods* **24**, 71–80.
- Picard, F., Gehin, M., Annicotte, J., Rocchi, S., Champy, M. F., O'Malley, B. W., Chambon, P. & Auwerx, J. (2002) *Cell* **111**, 931–941.
- Li, M., Chiba, H., Warot, X., Messaddeq, N., Gérard, C., Chambon, P. & Metzger, D. (2001) *Development (Cambridge, U.K.)* **128**, 675–688.
- Gregoire, F. M., Smas, C. M. & Sul, H. S. (1998) *Physiol. Rev.* **78**, 783–809.
- Cinti, S. (1999) *The Adipose Organ* (Editrice Kurtis, Milano, Italy).
- He, W., Barak, Y., Hevener, A., Olson, P., Liao, D., Le, J., Nelson, M., Ong, E., Olefsky, J. M. & Evans, R. M. (2003) *Proc. Natl. Acad. Sci. USA* **100**, 15712–15717.
- Kastner, P., Mark, M., Leid, M., Gansmuller, A., Chin, W., Grondona, J. M., Decimo, D., Krezel, W., Dierich, A. & Chambon, P. (1996) *Genes Dev.* **10**, 80–92.
- Krezel, W., Dupe, V., Mark, M., Dierich, A., Kastner, P. & Chambon, P. (1996) *Proc. Natl. Acad. Sci. USA* **93**, 9010–9014.
- Kubota, N., Terauchi, Y., Miki, H., Tamemoto, H., Yamauchi, T., Komeda, K., Satoh, S., Nakano, R., Ishii, C., Sugiyama, T., et al. (1999) *Mol. Cell* **4**, 597–609.
- Rieusset, J., Touri, F., Michalik, L., Escher, P., Desvergne, B., Niesor, E. & Wahli, W. (2002) *Mol. Endocrinol.* **16**, 2628–2644.
- Yamauchi, T., Waki, H., Kamon, J., Murakami, K., Motojima, K., Komeda, K., Miki, H., Kubota, N., Terauchi, Y., Tsuchida, A., et al. (2001) *J. Clin. Invest.* **108**, 1001–1013.
- Kawaguchi, N., Toriyama, K., Nicodemou-Lena, E., Inou, K., Torii, S. & Kitagawa, Y. (1998) *Proc. Natl. Acad. Sci. USA* **95**, 1062–1066.

TRANSGENIC MICE— TWO APPROACHES

A **transgenic** organism is one that has an extra or exogenous fragment of DNA in its genome. Various methods have been developed for making transgenic plants as well as some species of animals, with the most common research animals being the nematode worm, the fruit fly, and the mouse. In order to achieve stable inheritance of the exogenous DNA fragment, the integration event must occur in a cell type that can give rise to functional germ cells, either sperm or oocytes. Two mouse cell types that can form germ cells and into which DNA can be readily introduced are fertilized egg cells and embryonic stem cells.

At present, mouse embryonic stem cells, commonly referred to as **ES cells**, are preferred for gene targeting experiments since (1) they can be screened in culture for rare homologous recombination events, (2) homologous recombination with some vectors occurs in these cells at a high frequency, and (3) the cells can be returned from in vitro culture to a "host" embryo where they become incorporated into the developing mouse. Of greatest importance, the mouse embryonic stem cells can give rise to cells of all tissues, including germ cells. To create a targeted mutation in mice, the homologous recombination event is performed in embryonic stem cells in culture and then the mutation is transmitted into the germline by injecting the cells into an embryo. The mice carrying mutated germ cells are then bred to produce transgenic offspring that are heterozygous for the mutation.

Zygote Injection

A number of techniques are available for making transgenic mice, the most efficient of which is zygote injection. This method involves injecting DNA into a fertilized egg, or **zygote**, and then allowing the egg to develop in a pseudopregnant (see below) mother (Figs. 6.1 and 6.2). The transgenic animal that is born is called a **founder**, and it is bred to produce more animals with the same DNA insertion. In this method of making transgenic animals, the new DNA typically randomly integrates into the genome by a nonhomologous recombination event (Fig. 6.3). One to many thousands of copies of the DNA may integrate at one site in the genome. Homologous recombination has been found to occur in somatic cells in culture after delivering the DNA to the nucleus by injection. It therefore should be feasible for germline gene targeting to be achieved by zygote injection. This, of course, requires that zygotes undergo homologous recombination at a high frequency. The results to date have

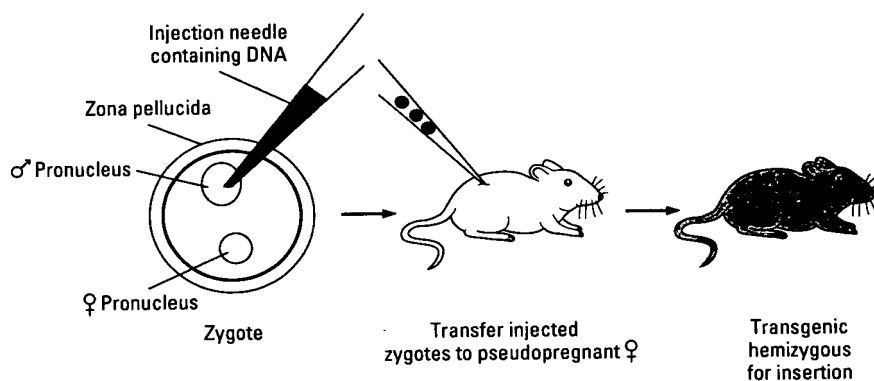


FIGURE 6.1 Procedure for making transgenic mice using zygote injection. Zygotes are removed from the oviducts of a female mouse that has mated the night before. The zygotes must be released from the cumulus cells that surround them. The zygotes are placed under a microscope with two micromanipulator setups. The zygote is held in place with a blunt holding pipette and the tip of the injection needle is filled with a solution containing DNA ($\sim 5 \mu\text{g}/\text{ml}$). The DNA is then injected into one of the pronuclei, usually the larger male pronucleus. The zygotes are then either transferred the same day, or cultured overnight to form 2-cell embryos and then transferred, into the oviducts of 0.5-day pseudopregnant females. Approximately 50 percent of the eggs survive to the 2-cell stage and approximately 20 percent to term. Twenty to thirty embryos are therefore transferred to the uterus of each female. Of the animals born, 10 to 30 percent should be transgenic (hemizygous) and contain one site of DNA integration.

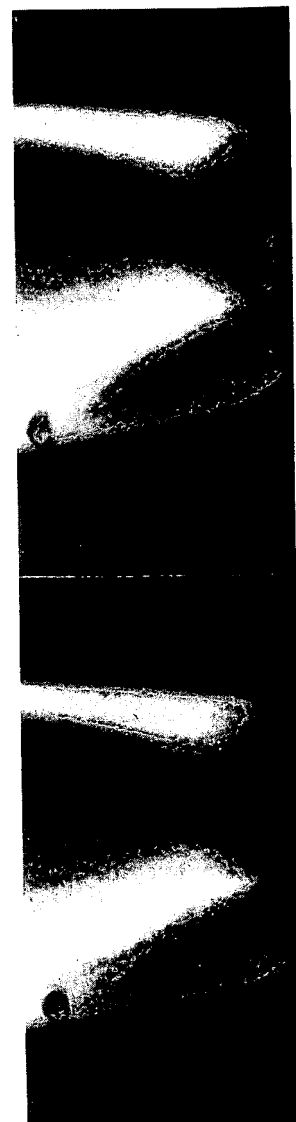


FIGURE 6.2 Microinjector keeping the zygote (middle) in place towards the egg. The nucleus is inside the nucleus of the zygote. (Photographs courtesy of An)

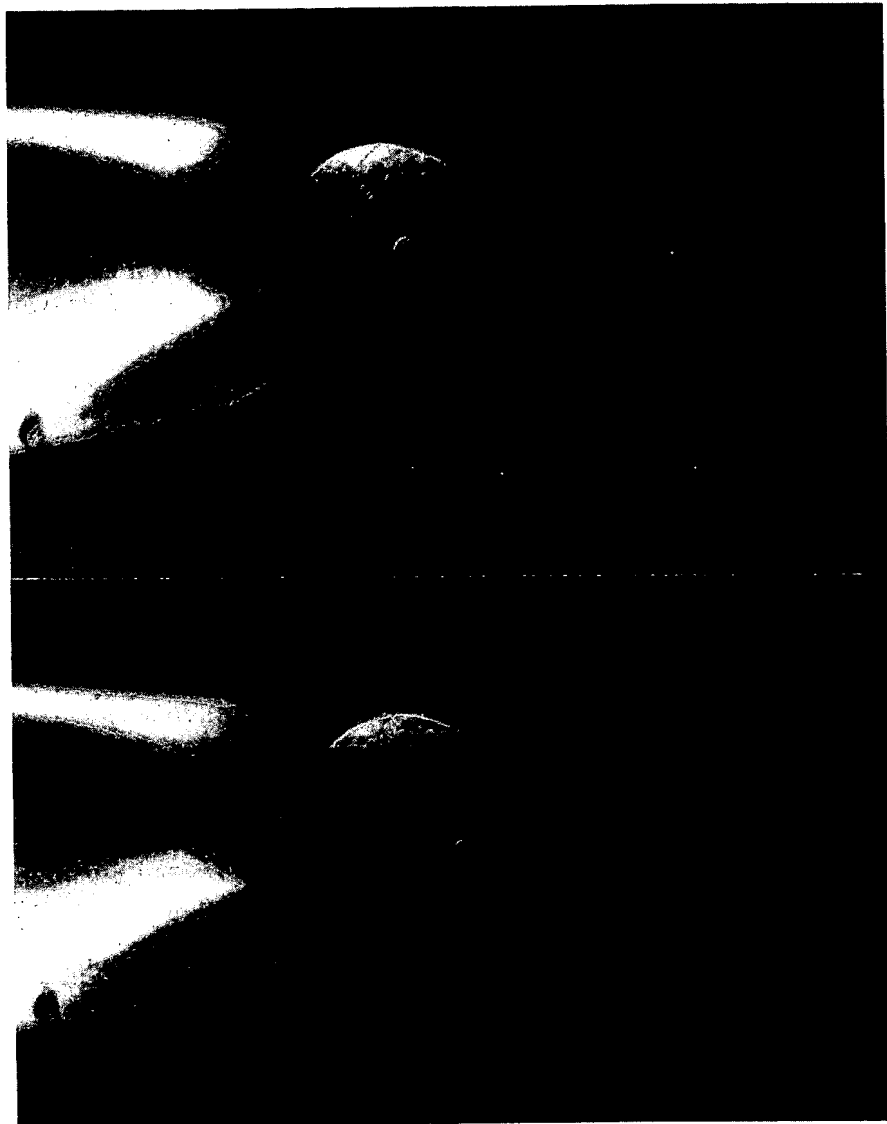


FIGURE 6.2 Microinjection of DNA into a mouse zygote. *Top:* The holding pipette (left) is keeping the zygote (middle) in place while the injection pipette containing DNA (right) is brought towards the egg. The nucleus can be seen in the middle of the egg. *Bottom:* The injection needle is inside the nucleus of the zygote. The nucleus has expanded in size due to the injection of DNA. (Photographs courtesy of Anna Auerbach.)

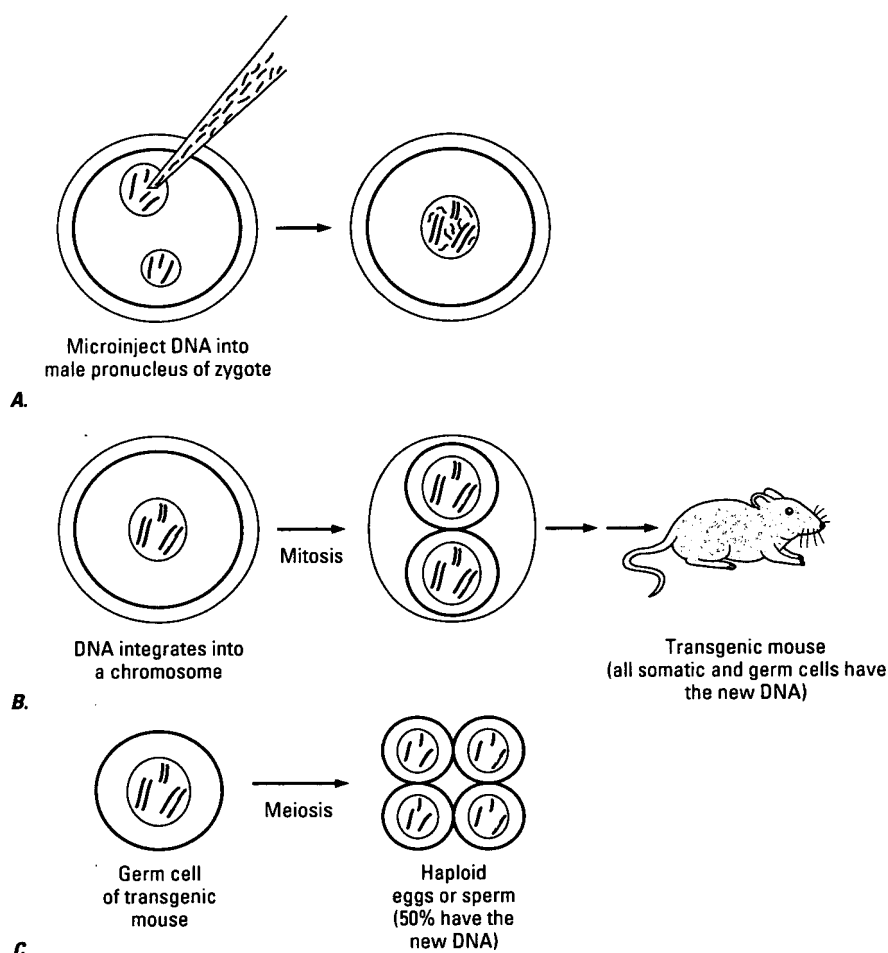


FIGURE 6.3 Random integration of DNA at one site in a transgenic. Three pairs of chromosomes are shown as pairs of lines of different lengths. The integrated DNA is shown as a green line. (A) DNA is injected into a pronucleus of a zygote and the two pronuclei fuse. (B) The DNA inserts randomly at one site in the genome of the zygote. The egg develops and all somatic cells of the transgenic contain one copy of the inserted DNA. (C) A germ cell from the transgenic is shown schematically. Following meiosis, only two of the four haploid germ cells contain the transgene insertion.

not been encouraging the same targeting

Regardless of success in injection for germline ES cell clones (see transgenic animals), it can vary many orders of magnitude and is likely to be limited to give a high frequency of homologous integration.

An understanding of the first nine days of mouse embryogenesis is to produce a body plan that is embryogenesis involves all cells. The fertilized adult mouse and is, however, some loss of restricted capacity gone this process of Development involves and in parallel. An

Embryonic development subsequent joining of father to form a cell. mucopolysaccharide approximately 10% occur in the oviduct the wall of the uterus the embryo occurs implantation, however, makes direct contact development of a the embryonic coat surround the embryo

not been encouraging, although further investigation is required in which the same targeting vector is compared in ES cells and zygotes.

Regardless of such results, the big advantage of ES cells over zygote injection for germline targeting is that it is relatively easy to screen 1000 ES cell clones (see Fig. 7.9) compared to making and screening 1000 transgenic animals. Since the frequency of homologous recombination can vary many orders of magnitude from locus to locus, zygote injection is likely to be limited to genes that have been tested in ES cells and shown to give a high frequency of homologous recombination relative to non-homologous integration.

Early Embryonic Development

An understanding of the basic developmental events that occur during the first nine days of mouse embryogenesis is necessary for a full comprehension of mouse embryonic stem cells. The function of embryonic development is to produce from a single egg a three-dimensional organism with a body plan that is predetermined by the genetic code. The process of embryogenesis involves a progressive loss of the developmental potential of cells. The fertilized egg has the capacity to give rise to all cell types in the adult mouse and is thus said to be **totipotent**. As the embryo cells divide, however, some lose their ability to form all cell types and retain only a restricted capacity to develop into certain tissues. A cell that has undergone this process of becoming restricted is said to have **differentiated**. Development involves many differentiation events that occur in series and in parallel. An example of this is shown in Figure 6.4.

Embryonic development begins with fertilization of the egg and the subsequent joining of the two haploid nuclei from the mother and the father to form a diploid zygote. The egg is surrounded by a layer of mucopolysaccharides called the **zona pellucida** and has a diameter of approximately 100 μm . The first four days of development (Fig. 6.5) occur in the oviducts and uterus before the egg becomes implanted in the wall of the uterus. During this preimplantation stage no growth of the embryo occurs, since there is no external source of nutrition. After implantation, however, rapid growth is possible since the embryo makes direct contact with the mother's blood supply through the development of a set of specialized extraembryonic tissues that form the embryonic component of the placenta and the membranes that surround the embryo.

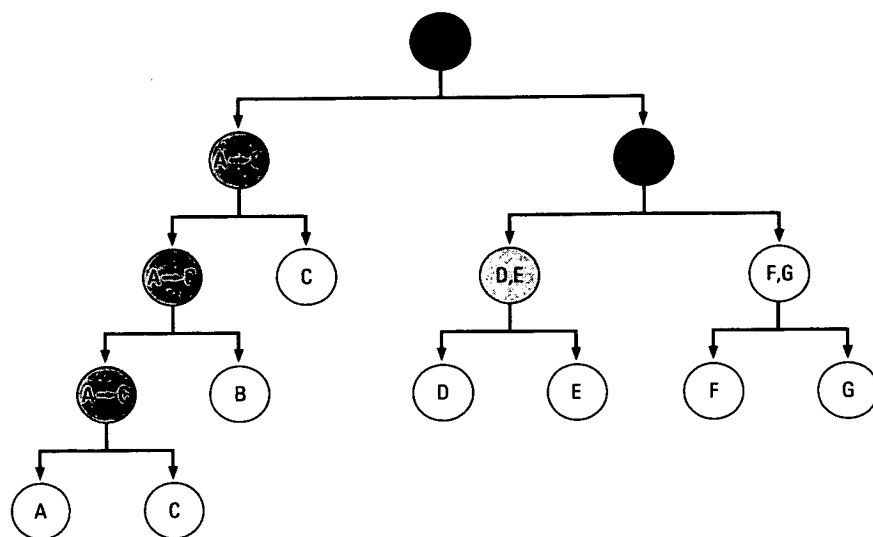


FIGURE 6.4 Lineage of a multipotent cell (A→G). Cell A→G divides and gives rise to two daughter cells (A→C; D→G) that have more restricted and different developmental potentials. Cell A→C divides three times and gives rise to three differentiated cell types (A; B; C). Cell D→G divides only once to give rise to two cells (D, E; F, G) with more restricted developmental potential. These two cells divide once each to give rise to four different differentiated cell types (D; E; F; G).

The first two days of development are referred to as the early cleavage stage. The embryo undergoes three cell divisions during this period (Fig. 6.5B, C, D) to form an 8-cell embryo, called a **morula**, in which all the cells appear to be totipotent and thus have an equivalent developmental potential. During the next 24 hours, however, the embryo undergoes two more rounds of cell division, the cells compact, and the ones on the outside of the morula differentiate to form a layer of cells called **trophoblast**. The undifferentiated totipotent cells on the inside are called the **inner cell mass (ICM) cells** (Fig. 6.5E). A fluid-filled cavity, or **blastocoel**, forms in the interior, leaving the ICM as a clump of cells attached to one end of the outer layer of trophoblast (see Fig. 6.5F). This approximately 32-cell embryo is referred to as a **blastocyst**. It is the ICM cells that, when transferred into culture, give rise to embryonic stem cell lines.

The trophoblast goes on to form extraembryonic tissues, whereas the ICM gives rise to additional extraembryonic tissues as well as to all the

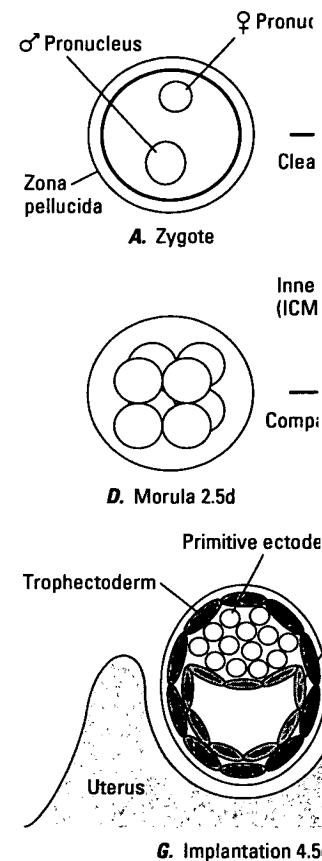


FIGURE 6.5 Preimplantation development indicated are pos what the middle of an embryo half. Trophoblast cells and the ICM are in black, the cells that will give rise to the embryo (ICM) in white, and the trophoblast in black.

cells of the embryo. During "hatching" from the zona, the embryo is released. The uterus of the female is about five days after mating with a vasectomized male.

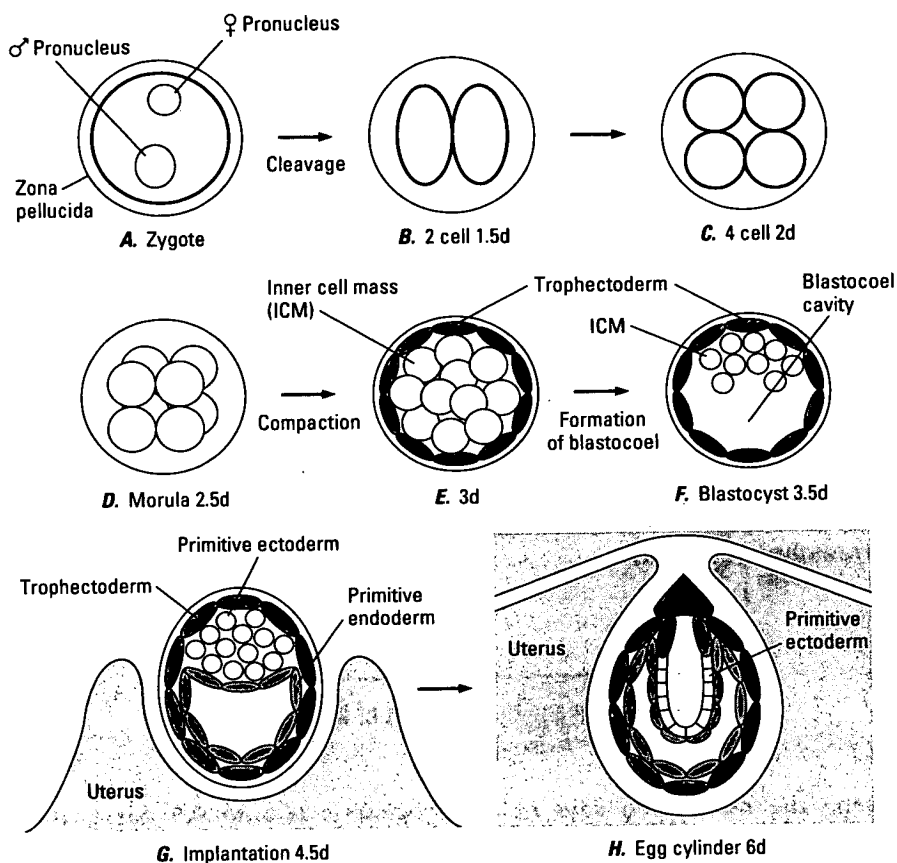


FIGURE 6.5 Preimplantation and early postimplantation development. The days of development indicated are postfertilization. Diagrams E—H depict a representative view of what the middle of an embryo (sagittal section) would look like if the embryo were cut in half. Trophoblast cells and their derivatives are shown in dark green, primitive endoderm in black, the cells that will give rise to the embryo (zygote up to morula, inner cell mass, and primitive ectoderm) in white, and the uterus in light green.

cells of the embryo. During the next day the blastocyst fully expands, "hatches" from the zona pellucida, and becomes implanted in the uterus. The uterus of the female is competent to receive the embryo for only about five days after mating with a male. A female in estrous and mated with a vasectomized male is referred to as a **pseudopregnant** mother

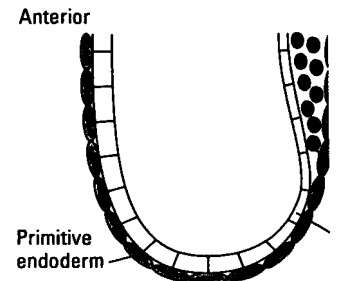
since she is competent to receive embryos but does not contain any fertilized eggs. Pseudopregnant mothers are important for making transgenic mice since they serve as the surrogate mothers for embryos that have been injected with DNA or embryonic stem cells.

During implantation, the cells of the ICM facing the blastocoel differentiate into a layer of **primitive endoderm** cells that migrate and cover the inner wall of the trophoctoderm. These cells also give rise to extraembryonic tissues. The inner cells that will give rise to the embryo are referred to as the **primitive ectoderm** (Fig. 6.5G). The trophoctoderm cells adjacent to the primitive ectoderm proliferate and push a fingerlike projection including the primitive ectoderm down into the blastocoel. A cavity then forms in the projection and the primitive ectoderm takes on the form of a cylinder that is a single cell layer thick (Fig. 6.5H). Up until this **egg cylinder** stage of development (six days), the cells that will give rise to the embryo remain undifferentiated and are set aside first as the ICM and then as the primitive ectoderm. The only development of defined or differentiated cell types involves the extraembryonic tissues.

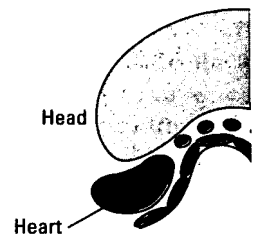
Gastrulation and Development of the Embryo

During the next three days of embryogenesis (6.5 to 9.5 days), the primitive ectoderm undergoes a complicated set of events involving regional differences in cell proliferation, precise cell movements, and differentiation of the three cell layers to form an embryo that has the basic features of a mouse. This stage of embryogenesis, called **gastrulation**, is perhaps the most complicated and critical period of development. At 6.5 days, a group of cells in the primitive ectoderm adjacent to the trophoctoderm begin to separate from the surrounding cells and move under and spread out across the ectoderm. The cells invaginating through the ectoderm form a sort of trough that is called the **primitive streak** (Fig. 6.6A). It is not known what stimulates a group of cells to begin gastrulation, nor is it possible to predict which cells in the egg cylinder will form the primitive streak. The position where the cells begin this process marks the future posterior end of the embryo and defines where the midline of the animal will be. During the next day the primitive streak extends to the anterior end of the embryo (Fig. 6.6B). These cells lay down a layer of mesoderm and under it a layer of endoderm. One of the functions of gastrulation is therefore to differentiate the three germ layers of the

Trans



A. Early primitive streak 7



Somites

FIGURE 6.6 Gastrula-stage embryo are shown, as in Figure 6.5. The endoderm, are not shown. The ectoderm is shown in white, and the primitive endoderm is replaced by ectoderm cells that move through the primitive streak (precursor of the central nervous system) is shown in grey.

embryo: ectoderm, mesoderm, and endoderm. The process is to establish the three germ layers (back/front) and the process of **pattern formation**. The three germ layers then begin to differentiate. For example, the ectoderm gives rise to the **neuroectoderm** that later

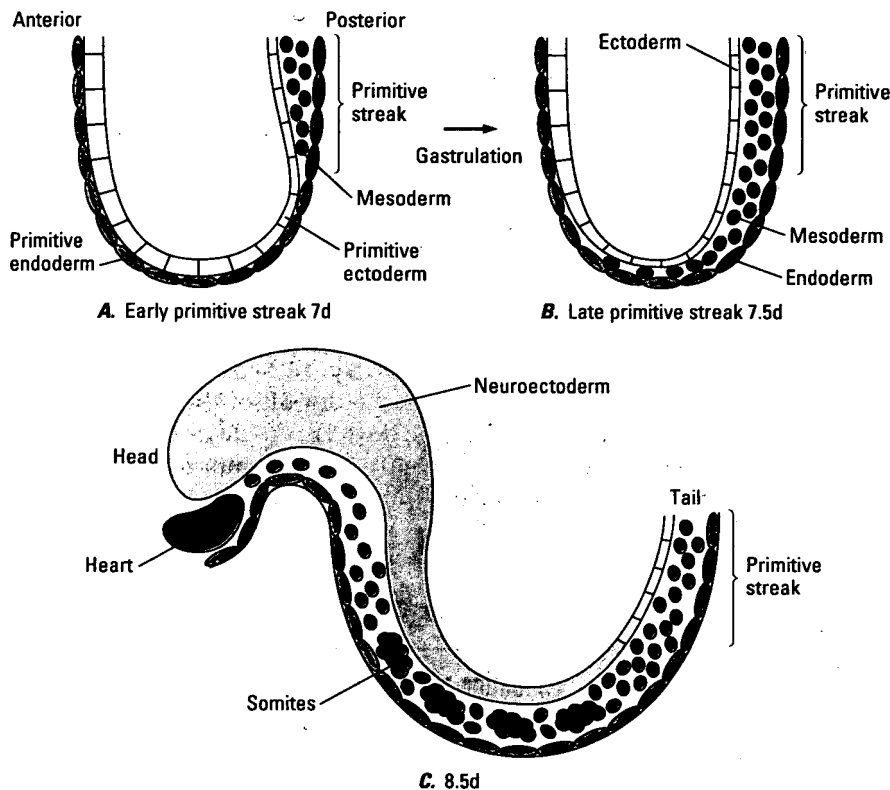


FIGURE 6.6 Gastrula-stage embryos. Representative sagittal sections through an embryo are shown, as in Figure 6.5E–H. The extraembryonic tissues, except primitive endoderm, are not shown. The days of development are postfertilization. The primitive ectoderm is shown in white, embryonic mesoderm in green, and endoderm as black. The primitive endoderm is replaced during gastrulation by embryonic endoderm from ectoderm cells that move through the primitive streak and differentiate. The neuroectoderm (precursor of the central nervous system) that is derived from midline ectoderm is shown in grey.

embryo: ectoderm, mesoderm, and endoderm. Another important function is to establish the three basic body axes: anterior/posterior (head/tail), dorsal/ventral (back/front), and right/left sides. This is the beginning of the process of **pattern formation**, or laying down the body plan. The three germ layers then begin to subdivide to give rise to particular tissues. For example, the ectoderm in the middle of the embryo develops into **neuroectoderm** that later gives rise to the entire central nervous system.

(Fig. 6.6C). A series of groups of mesodermal cells lying on either side of the midline form epithelial balls called **somites** that later give rise to the vertebrae, the muscles of the trunk and limbs, and the dermal (inner) layer of the skin. Endoderm cells form the inner layer of the digestive tract, lungs, and liver.

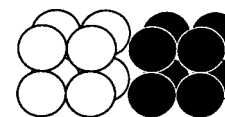
The next stage of pattern formation involves regional development, or specialization within tissues. This process requires that cells at different positions along seemingly homogeneous tissues like the neuroectoderm or along the series of repeated somites later develop into the cell types appropriate for their positions along the body. For example, the anterior end of the neuroectoderm must form the brain, whereas posterior regions form the spinal cord. By 12.5 days of embryonic development, the precursors, or primordia, for all of the organs of the adult mouse have been formed. The last seven days of embryonic development involves extensive growth of the embryo and further development and differentiation of the organs in a process called **organogenesis**.

Formation of Chimeras

From the description of embryonic development in the previous sections, it can be seen that embryogenesis involves a number of events. During the preimplantation and early postimplantation period, differentiation of the extraembryonic tissues occurs, whereas the cells that will give rise to the whole embryo are temporarily set aside and proliferate without differentiation. The next event, gastrulation, involves rapid cell proliferation and cell movement and the establishment of the basic body plan. Finally, with all the body structures in place, the organs grow in size and the cells further differentiate to their final cell types. Before gastrulation, there is extensive cell mixing within the ICM and primitive ectoderm. Thus, if one ICM cell is marked at the blastocyst stage such that all of its progeny can be identified after gastrulation, the cells of this clone would likely be found in all tissues and be highly intermixed with nonmarked cells.

This extensive cell mixing works to advantage when it comes to making chimeric animals. A **chimera** is an animal that is made up of cells from two different embryos. Such animals are made by mixing together two morula-stage embryos or by injecting ICM cells from one embryo into another "host" blastocyst (see Fig. 6.7). The embryos are then transferred

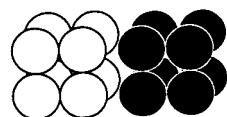
A. Morula aggregation



Aggregate
white and
black morulae

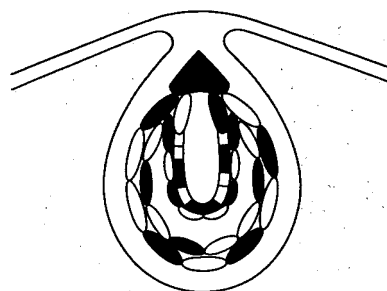
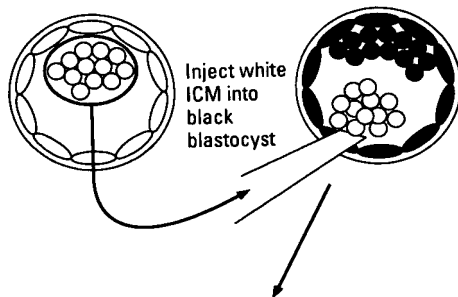
FIGURE 6.7 Two procedure black and the other in white to sagittal section through a 6-da and white) are randomly mix morulae, the oviducts are re medium to wash out the embr morulae, each from a different small depression on a dish. Gra develop into a blastocyst durin then transferred to the uterus embryos/uterus). Approximate later) and approximately 70 per Blastocysts are flushed from th inner cell masses (ICM) are munosurgery that selectively l tocyts are placed under a micromanipulator is used to hol micromanipulator is used to hc blastocyst. The injected blastoc dopregnant mother. Approxima approximately 90 percent of the:

A. Morula aggregation



Aggregate
white and
black morulae

B. Blastocyst injection



Allow chimera to develop
in pseudopregnant ♀

FIGURE 6.7 Two procedures for making chimeric embryos. One embryo is shown in black and the other in white to indicate two different genotypes. At the bottom is shown a sagittal section through a 6-day chimeric embryo in which cells from each embryo (black and white) are randomly mixed in all cell layers. (A) Morula aggregation: To obtain morulae, the oviducts are removed from 2.5-day pregnant females and flushed with medium to wash out the embryos. The zona pellucida is removed from the morulae. Two morulae, each from a different genetically marked mother, are then placed together in a small depression on a dish. Gravity forces the embryos together and the cells intermix and develop into a blastocyst during the following 24 hours of incubation. The blastocysts are then transferred to the uterus of a 2.5-day pseudopregnant female (approximately 12 embryos/uterus). Approximately 60 percent of the embryos could be born at term (17 days later) and approximately 70 percent of these should be chimeras. (B) Blastocyst injection: Blastocysts are flushed from the uteri of 3.5-day pregnant females of two genotypes. The inner cell masses (ICM) are isolated from the blastocysts of one genotype by immunosurgery that selectively kills the outer trophectoderm cells. The ICMs and blastocysts are placed under a microscope with two micromanipulator setups. One micromanipulator is used to hold the blastocyst in place with the holding pipette. The other micromanipulator is used to hold the ICM and inject it through a tiny hole made in the blastocyst. The injected blastocysts are then transferred to the uterus of a 2.5-day pseudopregnant mother. Approximately 80 percent of the embryos should reach term and approximately 90 percent of these be chimeric.

into the uterus of a pseudopregnant mother where they implant and continue embryonic development. The resulting chimeric animals that are born are composed of a mixture of cells from both embryos in most, and in many cases all, tissues.

To test whether the germ cells are derived from either or both embryos, each embryo is marked with a genetic trait that can be recognized in the chimera and in its offspring. The most common genetic marker used is coat color. For example, if ICM cells from a white mouse homozygous for a recessive mutation at the albino locus (c/c) are injected into a blastocyst from a black mouse homozygous for the normal, or wild type, albino gene (C/C), then any resulting chimeras can be identified by the presence of patches of white and black fur. To test whether the germ lines of the chimeras are made up of cells from either or both genotypes, the chimeras are bred with a white mouse (c/c). Since black is dominant over white coat color, any white offspring must be homozygous c/c and thus be derived from the injected ICM cells, whereas any black mice must be heterozygous C/c and be derived from the host blastocyst (see Fig. 6.8).

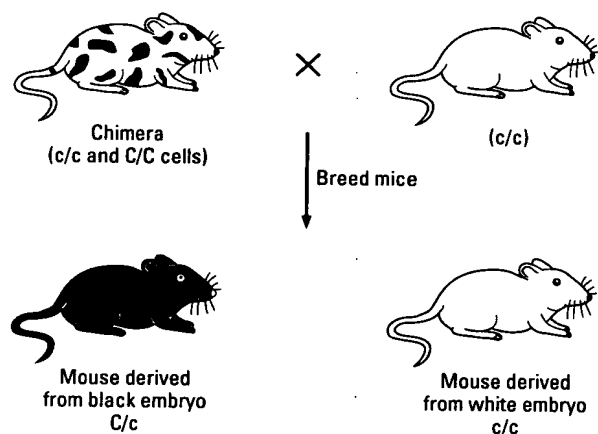


FIGURE 6.8 Breeding scheme for determining the genotypes of the cells that have populated the germline. The chimera is black and white, indicating that the genotypes of the two embryos used to form the chimera were homozygous wild type for albino (C/C), giving a black coat color phenotype, and homozygous mutant for albino (c/c), giving a white coat color. The wild type allele is dominant, and thus offspring of a chimera bred with a white (c/c) mouse can be either black and heterozygous for albino (C/c) or white and homozygous mutant for albino (c/c). The C/c mice are derived from the C/C morula and the c/c mice from the c/c morula.

In 1981, two independent mouse blastocyst can be type of cell line is the E that they remain diploid. This is in contrast to o remain diploid but spontaneous rate. A second unique totipotent and maintain. These two properties, n contribution in chimerational germ cells in chin by introducing a DNA v chimera (see Fig. 6.10)

In order to maintain E must be grown in condit mote proliferation and r. Many different factors prepotent. The first critical proliferation of ES cells w cells. The fibroblast cells drugs to inhibit further ce referred to as **feeder** cell: which are essential for E layer, ES cells divide onl typical of an early embryo further divide. A recently tiation Inhibiting Activity found to allow ES cells to an interesting factor since cells, the cellular respon differentiate. Some labora absence of feeders. This is there is some evidence th satisfy all the growth requ

The second factor that i the length of time they are is an inverse correlation passaged and the percenta cell contribution to the ge

Embryonic Stem Cells

In 1981, two independent groups demonstrated that ICM cells from a mouse blastocyst can be propagated in culture¹ (see Fig. 6.9). This new type of cell line is the ES cell line. One distinct property of ES cells is that they remain diploid even after being cultured for many weeks. This is in contrast to other tissue culture cell lines that often do not remain diploid but spontaneously gain and lose chromosomes at a high rate. A second unique property of ES cells is that they remain totipotent and maintain the ability, like ICM cells, to form chimeras. These two properties, maintaining a normal karyotype and extensive contribution in chimeras, are both necessary for ES cells to form functional germ cells in chimeras. ES cells can be used to make transgenics by introducing a DNA vector into them and then forming and breeding chimeras (see Fig. 6.10)

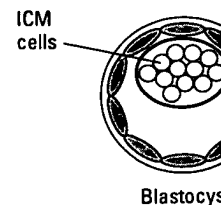
In order to maintain ES cells that can contribute to the germ cells, they must be grown in conditions that inhibit differentiation and instead promote proliferation and retention of a diploid number of chromosomes. Many different factors probably determine whether ES cells remain pluripotent. The first critical factor that was identified as a requirement for proliferation of ES cells was a layer of fibroblast cells seeded under the ES cells. The fibroblast cells are treated before seeding with irradiation or drugs to inhibit further cell division but not metabolism. These cell layers, referred to as **feeder** cells, produce and excrete proteins, one or some of which are essential for ES cell proliferation. In the absence of this cell layer, ES cells divide only a few times and differentiate into cell types typical of an early embryo, usually primitive endoderm, that are unable to further divide. A recently identified protein factor, called either Differentiation Inhibiting Activity (DIA) or Leukemia Inhibiting Factor (LIF), was found to allow ES cells to proliferate in the absence of feeders. DIA/LIF is an interesting factor since depending on the cell type, ES or leukemia cells, the cellular response to the factor is either to proliferate or to differentiate. Some laboratories are now growing ES cells in LIF in the absence of feeders. This is much simpler than preparing feeder cells, but there is some evidence that LIF, unlike feeder cells, does not completely satisfy all the growth requirements of ES cells.

The second factor that influences the pluripotential status of ES cells is the length of time they are grown in culture. With most ES cell lines there is an inverse correlation between the number of times the cells are passaged and the percentage of chimera made with them that have an ES cell contribution to the germline. This is because abnormal variants ac-

cumulate in the cell population. To minimize the number of cell passages for each cell line, newly established ES cell lines are expanded immediately to produce a large number of cells and the cells are then frozen in small portions for future use. This produces a large stock of cells, all frozen after a minimum of passages, that can be used for years to come. Typically, an aliquot is thawed, grown, and used for experiments for four to six weeks and then discarded. A new frozen sample can then be thawed. Because of the presence of variants in the cell line population, when cells are subcloned, or isolated as single ES cells and grown up as clones, many of the clones will be derived from the variants that cannot populate the germline. A stringent test of the state of an ES cell line and the growth conditions used, therefore, is to subclone several lines and test how many of them can contribute to the germline. Ideally, at least 50 percent should remain totipotent.

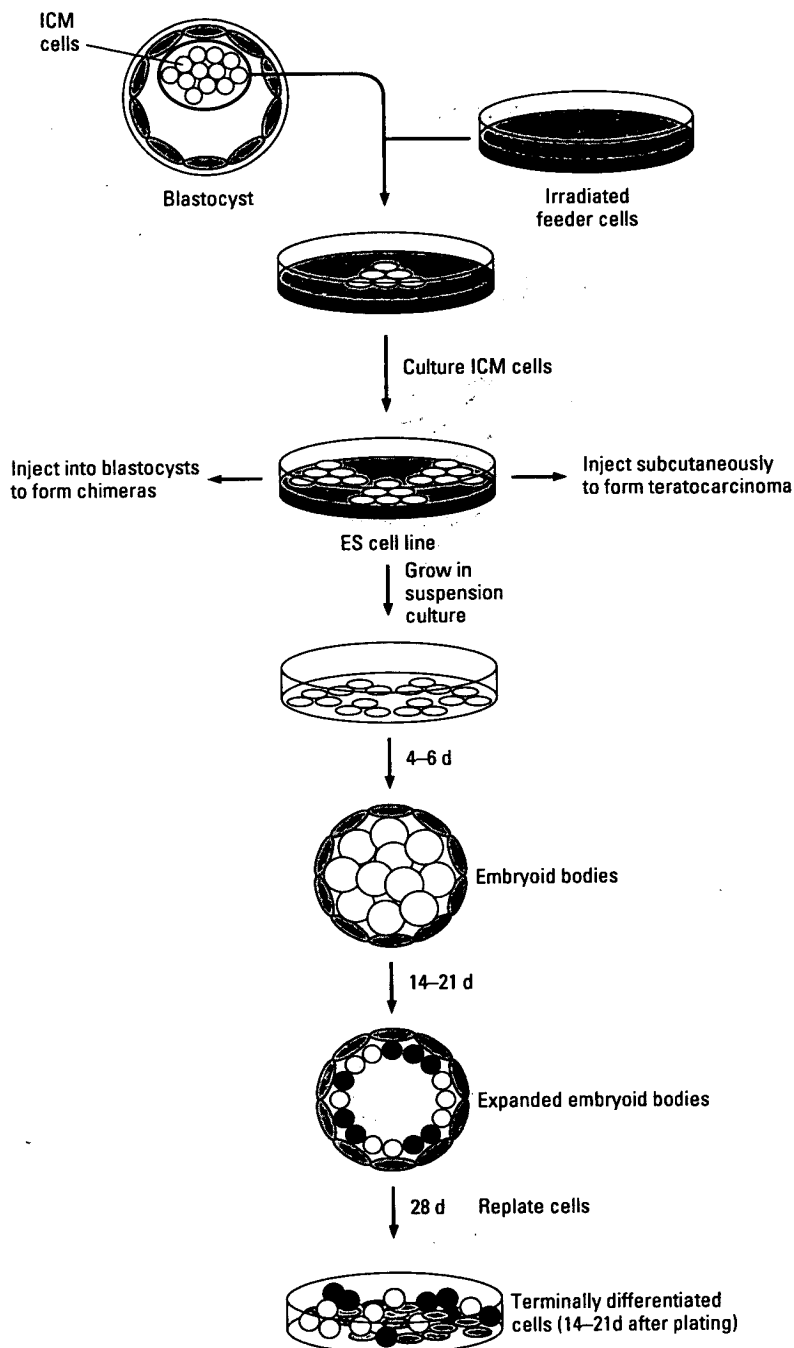
A third factor that probably affects the status of ES cells is the way in which they are handled day to day by an investigator. This is obviously much more difficult to standardize than a growth factor or number of passages. However, many different labs have now successfully targeted a gene in ES cells and had the cells contribute to the germline in chimeras.

Since ES cells are derived from the ICM cells of a blastocyst and the ICM gives rise to the whole embryo, it is not surprising that ES cells also have the capacity to give rise to the whole embryo. To accomplish this, diploid ES cells, like ICM cells, are either aggregated with two morulae or injected



Inject into blastocysts
to form chimeras ←

FIGURE 6.9 (Right) Procedure for establishing embryonic stem cell lines and differentiating them in vitro. Blastocysts are isolated as described in the legend for Figure 6.7. Either the blastocyst is placed directly in culture, or the ICM is removed, as described in the legend to Figure 6.7, and placed in culture. The culture medium must include LIF if a feeder layer is not provided. Feeder layers are prepared by treating either STO fibroblast cells or primary embryo fibroblast cells from a 15-day embryo with irradiation or mitomycin-C to inhibit further cell divisions. Approximately 25 percent of the ICMs can proliferate in culture and produce cell lines. ES cell lines are passaged at a high density every two to three days to avoid differentiation and selection for variants that cannot form germline chimeras or teratocarcinomas. To stimulate embryoid body formation, the cells are seeded at a high density in a bacteriological Petri dish. The cells readily aggregate, and within four to six days the outer layer of cells differentiates to primitive endoderm. These structures are called embryoid bodies. During the next two weeks the embryoid bodies expand, forming a cavity on the inside, and some ectoderm cells form mesoderm. After about twenty-one days, the fully expanded embryoid bodies can be placed in a tissue culture dish to which they attach. During the following two weeks the cells proliferate, migrate across the dish, and differentiate into cell types derived from the three germ layers.



into a blastocyst to produce a chimera (Figs. 6.11 and 6.12). Most and in many cases all, tissues within these chimeric embryos contain ES-derived cells, although in any given chimera the proportion of ES-derived cells varies. Thus, when ES cell chimeras are bred, many are found to have

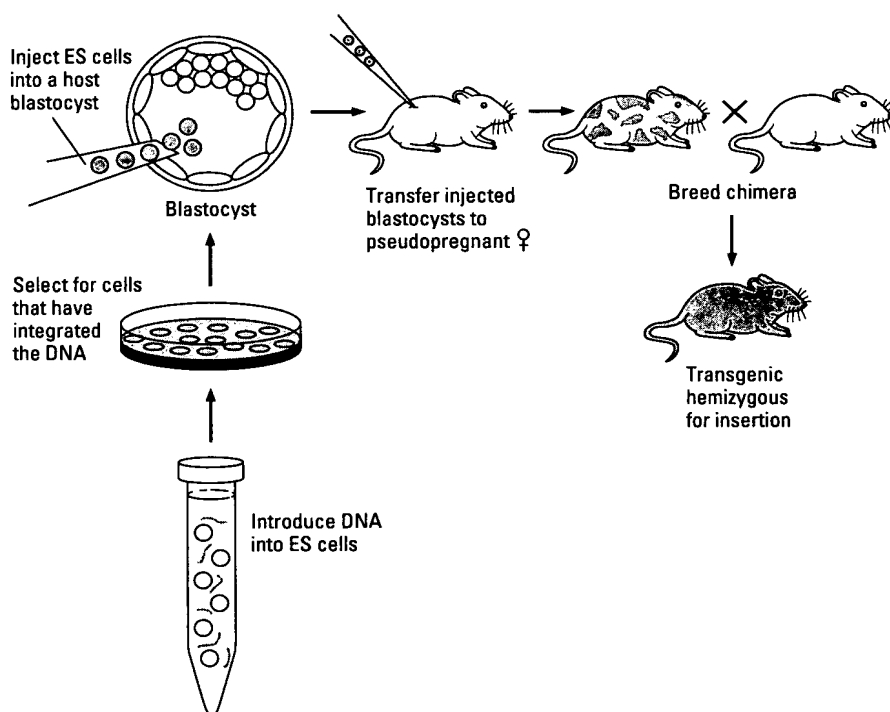
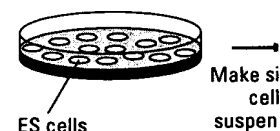


FIGURE 6.10 Procedure for making transgenic mice using ES cells. DNA is typically introduced into cells by electroporation (see Chapter 7). Rapidly growing ES cells are treated to make a single cell suspension, mixed with DNA ($\sim 40 \mu\text{g/ml}$) and given an electric pulse to introduce the DNA into the nucleus. As described in Chapter 5, the DNA vector usually contains a selectable gene such as *neo*. The electroporated cells are therefore grown in G418 to select for cells that have integrated and are expressing *neo*. G418^R cells from one clone are then used to make chimeras as described in the legend for Figure 6.11B. Blastocyst injection is shown. The chimeric animals that are born are then bred, as described in the legend for Figure 6.8, to produce ES cell-derived offspring. About 50 percent of these mice should be hemizygous for the new inserted DNA.

ES-derived germ cells. the ES cell line, influence cell contribution to the a mouse by first pro

A. Blastocyst injection



B. Morula aggregation

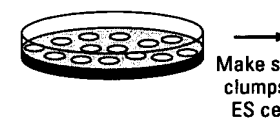
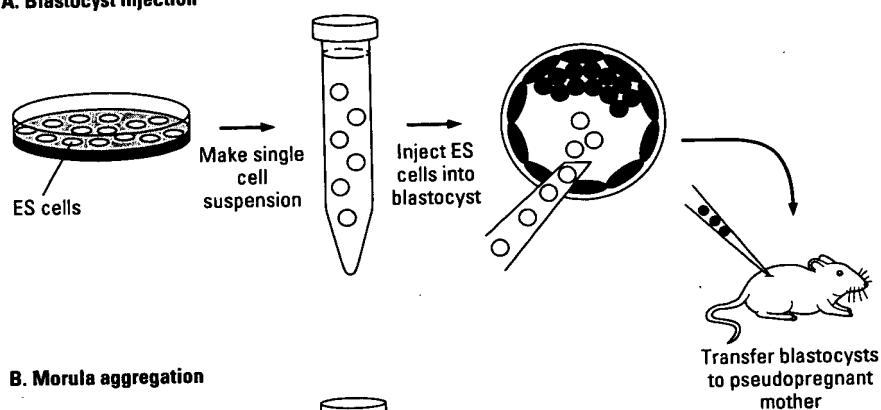


FIGURE 6.11 Two procedures for making transgenic mice. In procedure A, ES cells are isolated as described in the legend for Figure 6.10. In procedure B, a second genotype are plated on a micromanipulator is used to isolate a single cell. In procedure C, a micromanipulator is used to inject a single cell into the blastocyst with a finely needle. In procedure D, a single cell is injected into the uterus of a 2.5-day pseudopregnant mouse. Small depressions are made in the morula on each side of it. This sandwich of ES cells between the morula and the large blastocyst during the next 24 hours. In procedure E, a pseudopregnant mother. In procedure F, a term and approximately 50 percent of the offspring mouse can be as high as 80 percent.

ES-derived germ cells. The genotype of the host blastocyst, and perhaps of the ES cell line, influences the percentage of chimeras that contain an ES cell contribution to the germline. ES cells grown in culture can give rise to a mouse by first producing ES cell chimeras and then breeding the

A. Blastocyst injection



B. Morula aggregation

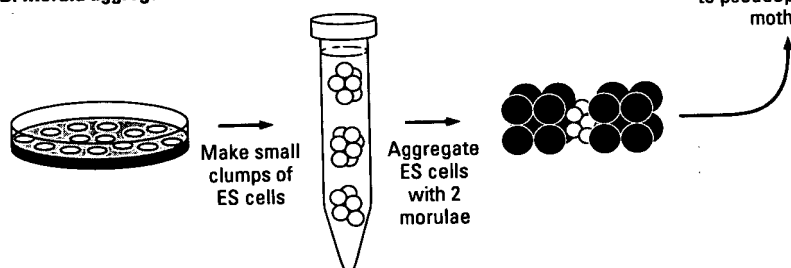


FIGURE 6.11 Two procedures for making ES cell chimeras. (A) Blastocyst injection: ES cells growing in an undifferentiated state are treated to give a single cell suspension. Blastocysts are isolated as described in the legend for Figure 6.7. The blastocysts of one genotype and ES cells of a second genotype are placed under a microscope with two micromanipulator setups. One micromanipulator is used to hold the blastocyst with a holding pipette. The other micromanipulator is used to suck up ES cells and inject 10 to 15 of them into the blastocoel cavity of the blastocyst with a finely drawn-out injection pipette. The blastocysts are then transferred to the uterus of a 2.5-day pseudopregnant mother. (B) Morula aggregation: ES cells growing in an undifferentiated state are treated to produce small clumps of approximately 10 to 15 cells. Small depressions are made in a dish and into each depression is placed a clump of ES cells with a morula on each side of it. The morulae are prepared as described in the legend for Figure 6.7. This sandwich of ES cells between two morulae forms a single aggregate and develops into a large blastocyst during the next day in culture. The blastocysts are then transferred to a 2.5-day pseudopregnant mother. In both methods approximately 50 percent of the embryos should reach term and approximately 50 percent of these should be chimeric. The ES cell contribution to a mouse can be as high as 80 percent of the cells.

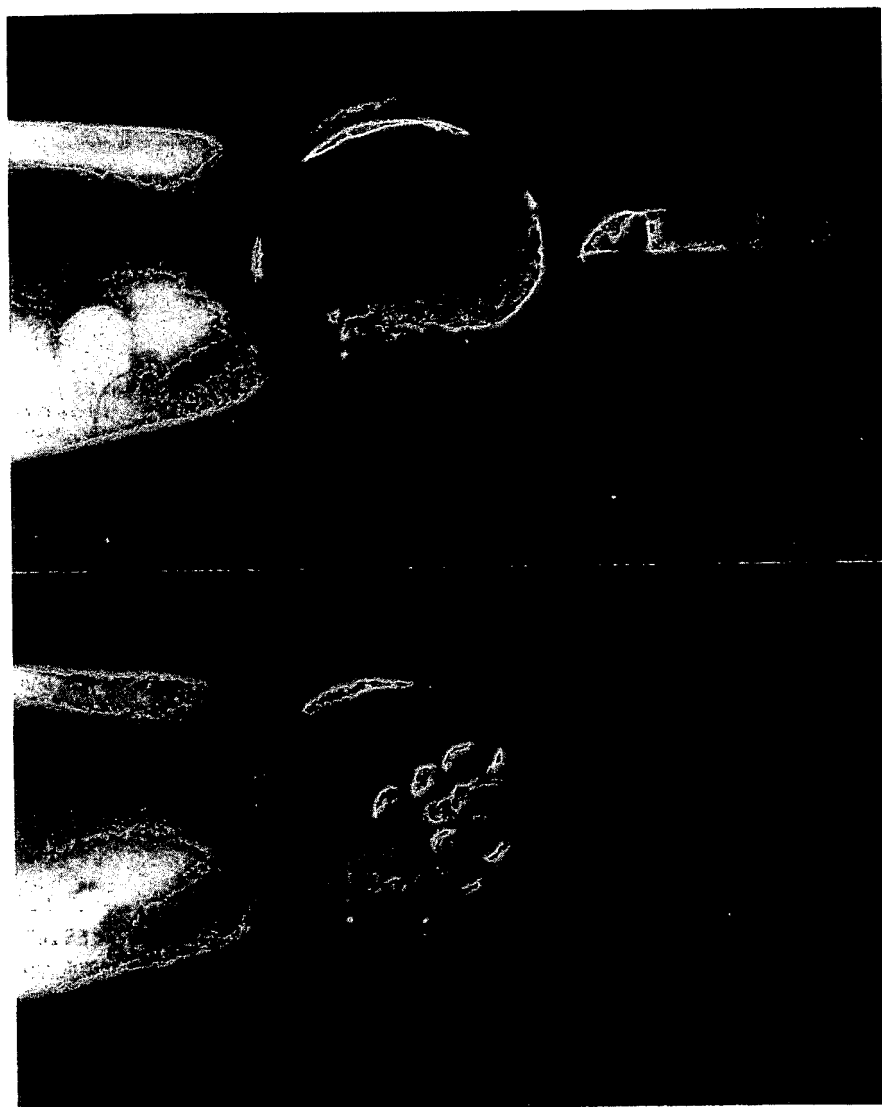


FIGURE 6.12 Microinjection of ES cells into a mouse blastocyst. *Top:* The holding pipette (left) is keeping the blastocyst (middle) in place while the injection pipette containing ES cells (right) is brought towards the embryo. *Bottom:* The injection needle is inside the blastocyst and ES cells have been released into the blastocoel cavity. The ICM can be seen on the inside of the blastocyst at the bottom. (Photographs courtesy of Anna Auerbach.)

One practical aside is from male embryos are of male cell lines is more because the two X chromosome tends to be lost, where second reason for using number of germline chromosomes to the germline. This is female blastocyst, the ES cell contribution to more, the female cells thus the entire germline that a male ES cell line contribution is that the toward males. Finally, it be bred with numerous requires to produce a si-

ES cells can be induced to differentiate into various cell types by changing the culture conditions. For example, by introducing ES cells into mice, ES cells can be used to generate a wide variety of different cell types. In addition, ES cells can be used to generate a wide variety of different cell lines, called embryonic stem (ES) cell lines, which have characteristics similar to ES cells. Some ES cell lines have a normal karyotype, some

In culture, ES and some set of differentiation events in the embryo (see Fig. 1) are experiments as an in vitro embryogenesis. To promote a high density in the culture which they cannot adhere together and form large aggregates a few days the cells on the endoderm similar to the cavity then forms in the egg cylinder stage embryo the ectoderm, but normal differentiation of the ectoderm and cells on a tissue culture

chimeric animals to produce offspring totally derived from ES cells. Genetic markers such as coat color can be used to distinguish ES-derived mice, as described for embryo chimeras in the previous section.

One practical aside is that for most experiments ES cell lines derived from male embryos are used. One reason for this is that the karyotype of male cell lines is more stable than female lines. This seems to be because the two X chromosomes are unstable and one X chromosome tends to be lost, whereas the XY complement tends to be stable. The second reason for using male cell lines is that they produce a higher number of germline chimeras, or chimeras with an ES cell contribution to the germline. This is because when male ES cells are injected into a female blastocyst, the ES cells can convert the embryo to a male if the ES cell contribution to the somatic cells of the gonad is high. Furthermore, the female cells cannot form functional male germ cells, and thus the entire germline is derived from the ES cells. One indication that a male ES cell line can give chimeras with an extensive ES cell contribution is that the ratio of male to female chimeras born is skewed toward males. Finally, it is more efficient to breed males since they can be bred with numerous females during the period of time a female requires to produce a single litter.

ES cells can be induced to differentiate either as tumors in mice or in culture by changing the growth conditions. When injected subcutaneously into mice, ES cells form tumors, called teratocarcinomas, that contain a wide variety of differentiated cell types. In fact, the proliferating stem cells of spontaneous teratocarcinomas in mice can be established in culture as cell lines, called embryonal carcinoma (EC) cell lines, that have characteristics similar to ES cells. Although EC cell lines rarely maintain a normal karyotype, some EC lines can contribute extensively in chimeras.

In culture, ES and some EC cells can be induced to develop through a set of differentiation events that is very similar to the early postimplantation embryo (see Fig. 6.9). ES cells therefore can be used for certain experiments as an *in vitro* model system of early postimplantation embryogenesis. To promote this type of differentiation, ES cells are placed at a high density in the absence of LIF or feeder cells in culture dishes to which they cannot adhere. The cells growing in suspension then clump together and form large aggregates called **embryoid bodies**. Within a few days the cells on the outside of the clumps differentiate into primitive endoderm similar to the outer layer of the ICM of a 4.5-day embryo. A cavity then forms in the embryoid bodies and they begin to resemble an egg cylinder stage embryo. With time, mesodermal cells delaminate from the ectoderm, but normal gastrulation does not occur. Further differentiation of the ectoderm and mesoderm then can be induced by plating the cells on a tissue culture dish. After a few weeks many differentiated cell

types, such as muscle, nerves, and skin, can be recognized in these cultures. This *in vitro* differentiation system offers some advantages over studying embryos. Homozygous mutations can therefore be made in ES cells by targeting both alleles of a gene and then determining the phenotypic effects of the mutation on development *in vitro*.

Note

I. Evans, M. J., and M. H. Kaufman (1981). Establishment in culture of pluripotent cells from mouse embryos. *Nature* 292: 154–156. Martin, G. R. (1981). Establishment of pluripotent cell lines from embryos cultured in medium conditioned by teratocarcinoma stem cells. *Proc. Natl. Acad. Sci. USA* 78: 7634–7638.

Suggested Readings

- Bradley, A., Evans, M., Kaufman, M. H., and Robertson, E. (1984). Formation of germ-line chimeras from embryo derived teratocarcinoma cells. *Nature* 309: 225–256.
- Bradley, A. (1990). Embryonic stem cells: Proliferation and differentiation. *Curr. Opin. Cell Biol.* 2: 1013–1017.
- Doetschman, T. C., Eistetter, H., Katz, M., Schmidt, W., and Kemler, R. (1985). The *in vitro* development of blastocyst-derived embryonic stem cell lines: Formation of visceral yolk sac, blood islands and myocardium. *J. Embryol. Exp. Morph.* 87: 27–45.
- Gossler, A., Doetschman, T., Korn, R., Serfling, E., and Kemler, R. (1986). Transgenesis by means of blastocyst-derived embryonic stem cell lines. *Proc. Natl. Acad. Sci. USA* 83: 9065–9069.
- Hogan, B., Costantini, E., and Lacy, E. (1986). *Manipulating the mouse embryo: A laboratory manual*. Cold Spring Harbor, N.Y.: Cold Spring Harbor Laboratory.
- Jaenisch, R. (1988). Transgenic animals. *Science* 240: 1468–1473.
- Robertson, E. J. (ed.) (1987). *Teratocarcinomas and embryonic stem cells: A practical approach*. Oxford: IRL Press, pp. 71–112.
- Rossant, J., and Pedersen, R. A. (eds.) (1986). *Experimental Approaches to Embryonic Mammalian Development*. Cambridge University Press.

The importance of π and the principles for Chapter 6. These two examples from actual of germline gene targeting are discussed

Three A

For an experimental tion of a gene must b development and fur tive studies of what product, (2) *in vitro* t its protein product, a living cells and ultim

At the first level, i development, as well information provides involved and, most amined. At the second understood. For example a gene is regulated wi

7

GERMLINE GENE TARGETING IN MICE

The importance of making mutant organisms was introduced in Chapter 5, and the principles for making mice with defined mutations was described in Chapter 6. These two themes will be further developed in this chapter, using examples from actual research on gene function. The importance to medicine of germline gene targeting of mice and other future challenges of gene targeting are discussed in the last section of this chapter.

Three Approaches to Studying the Function of a Gene

For an experimental scientist, there are several levels at which the function of a gene must be explored to elucidate its contribution to the normal development and functioning of an organism. These levels are (1) descriptive studies of what cell types produce and/or interact with the gene product, (2) in vitro biochemical analyses of the properties of the gene and its protein product, and (3) studies of the biological function of the gene in living cells and ultimately in the whole organism.

At the first level, it is essential to determine when and where during development, as well as in the adult organism, a gene is expressed. This information provides clues to the processes in which the gene might be involved and, most important, which cell types should be further examined. At the second level, the biochemical properties of a gene must be understood. For example, a biochemical analysis of how the expression of a gene is regulated will determine which factors can stimulate or inhibit its

transcription in a test tube. A biochemical analysis will also include studies of the purified protein product of a gene to determine its functional properties, for example, to define domains where the protein interacts with other proteins or DNA. Such *in vitro* studies are useful since they can often be technologically more feasible than studying the role of a gene in a living organism. The simplicity of *in vitro* studies stems from the fact that many, and in some cases all, factors involved in the reactions can be precisely defined and manipulated. The results of a biochemical analysis can thus reveal what a protein is capable of performing under the conditions tested; this can often lead to important clues to the possible biological function of a gene. Biochemical analyses are limited, however, in trying to replicate *in vitro* all of the situations a molecule normally encounters in a cell or organism. Thus such studies often underestimate the full repertoire of functions a protein can perform.

The most complex level of research involves studies *in vivo*. Because of the complexity, it is often useful to first study the function of a gene in a single cell type in culture before tackling the role of the gene in the whole organism. In contrast to *in vitro* systems, the multitude of molecules that make up a cell are not defined, and this often leads to some discrepancies between *in vitro* and *in vivo* results. One reason for the different results may be that in a test tube a protein is often asked to perform a function on its own, whereas in a cell it may have many helpers that assist in carrying out the function. If this is the case, then if a domain of a protein is mutated and the function of the protein tested *in vivo*, the mutant protein may perform almost as well as if the domain were normal because other factors are making up for its absence (Fig. 7.1A,C). *In vitro*, on the other hand, the mutant protein may not be able to function at all (Fig. 7.1B,D). Discrepancies also arise between descriptive data on where a gene is expressed and

in vivo mutant phen
In the majority of ca
only a subset of the
this discrepancy is t
made up of similar g

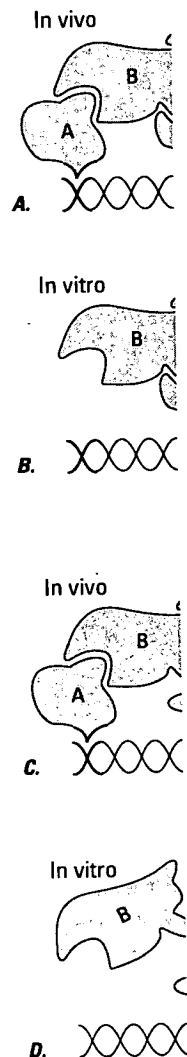
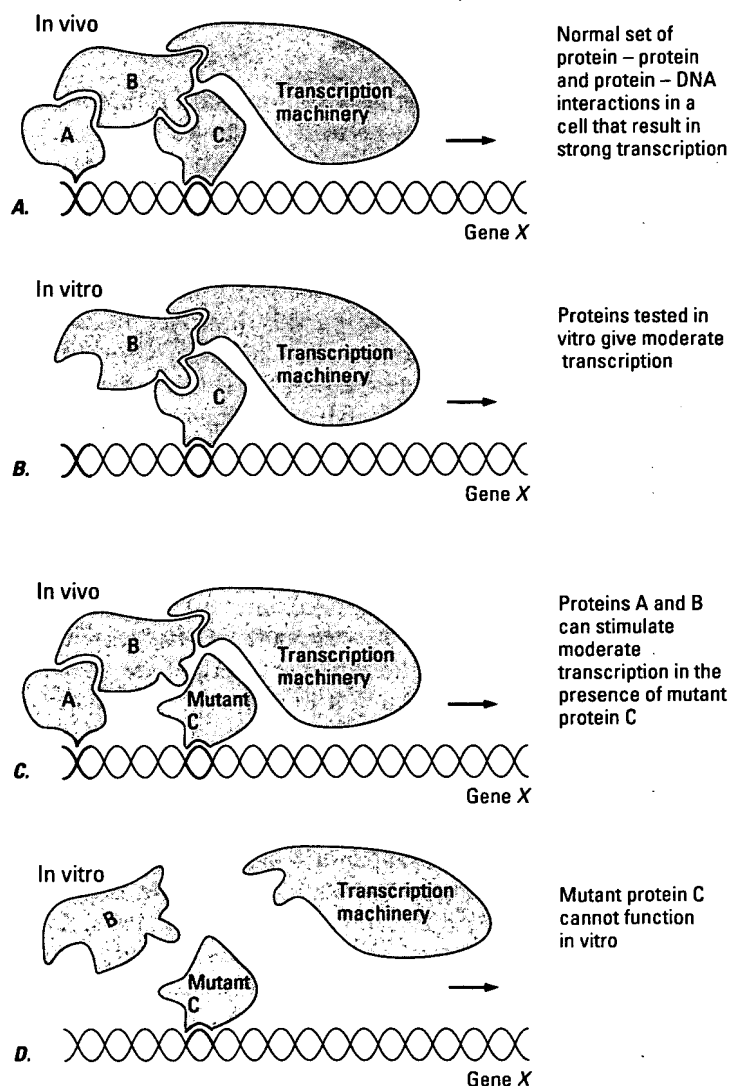


FIGURE 7.1 (Right) Complexity of protein-protein interactions involved in transcription *in vitro* and *in vivo*. (A) Normal *in vivo* situation in cells. A stretch of DNA (double helix) is shown bound by two proteins (A and C) that are in turn bound by a third protein (B). Protein B acts as a bridge for proteins A and C, connecting them with the transcription machinery (RNA polymerase and other accessory proteins). A high level of transcription is stimulated when A, B, and C are in contact with gene X as shown. (B) Test system *in vitro* that includes only proteins B and C. Proteins B and C can stimulate a moderate level of transcription *in vitro* when bound to gene X. (C) A mutant form of protein C has been introduced into cells by gene targeting. The region of protein C that binds protein B has been mutated so that it can no longer bind protein B. Nevertheless, protein A can bind gene X and stimulate transcription through binding protein B. (D) The mutant form of protein C is tested *in vitro*. Protein C can bind to gene X but cannot stimulate transcription since it cannot bind protein B.

in vivo mutant phenotype data on which tissues require the gene product. In the majority of cases to date, the tissues showing defects in mutants are only a subset of the tissues that express the genes. One explanation for this discrepancy is that since most genes are members of gene families made up of similar genes that perform similar functions, in the absence of



one gene the others can compensate for its loss. This idea of "backup systems" in vivo is a recurrent theme. It is essential to have descriptive, biochemical, and genetic data, since the results of all these types of studies are complementary and can lead to further investigations at all levels.

Why Gene Targeting and Not Random Integration?

One of the key reasons gene targeting is so important is that it can simplify studies done in cells or in animals because the investigator can predetermine exactly what genetic change is made. This is in contrast to experiments in which DNA is randomly inserted into the genome, where many factors cannot be strictly controlled. To further explore the question of why germline gene targeting is important, it is useful to go back to transgenic mice made by zygote injection and think about the kinds of questions that can be tackled best using this approach in comparison to germline gene targeting. It should then become clear why germline gene targeting in mice was a major technological breakthrough.

Zygote injection is currently limited to introducing a fragment of DNA into the genome by nonhomologous recombination. Information can be added, but it cannot be removed or substituted. Thus, one is limited to asking, What can the extra piece of DNA do? In one type of experiment the function of the piece of DNA itself can be tested, for example to examine whether it has the necessary recognition sequences to initiate transcription in particular cell types (Fig. 7.2). In another type of experiment, the function of the gene product can be tested (Fig. 7.3). An example of this would be making transgenic mice, and testing them for whether a certain protein can promote the formation of tumors by expressing it in some or all cells and observing whether tumors form at a higher frequency in the transgenics than in wild type mice. In a third type of experiment, the function of a particular cell type can be addressed. An example of this would be to make a transgenic animal expressing a toxic protein in specific cell types to determine the effect on the animal of ablating the cells.

Although on paper these experiments sound straightforward and easy to interpret, in practice they are not. For example, where does one get a DNA fragment with a promoter that will express in a specific tissue of interest, at the time of development of interest, and at the level required? Even when such DNA fragments can be obtained, a major problem is the random nature of the integration events. Some regions of the genome can act to inhibit transcription, whereas others can promote transcription.

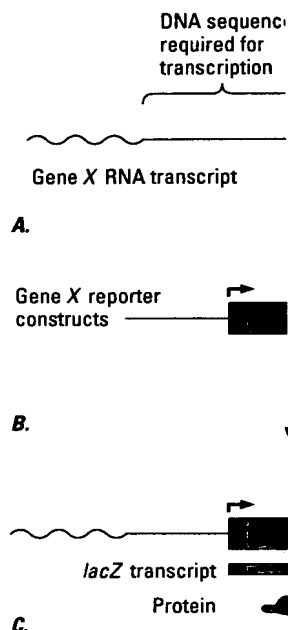


FIGURE 7.2 Use of trans transcription to particular tissues. An upstream regulatory region indicates where splicing of the bacterial gene *lacZ* as the reporter. Cells expressing this protein also include either a portion of the first exon. Each founder animal is detected by the presence of the genome. Only the transgenic animals express *lacZ* transcripts and β galactosidase.

These effects are called founder effects. Each founder animal has at least three founder effects. What characteristics are from random integration of a foreign gene, causing gene expression to occur in approximately 50% of the zygote injection.

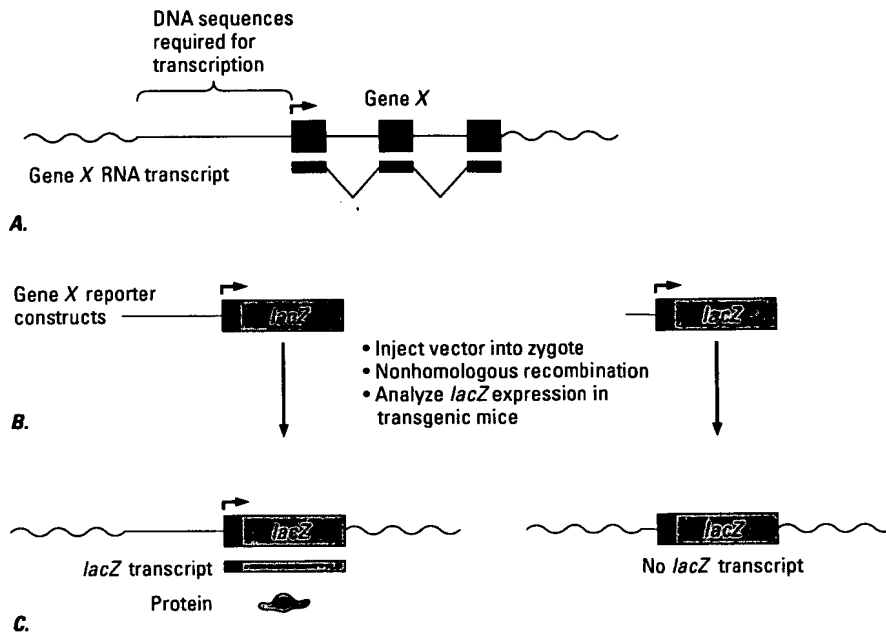


FIGURE 7.2 Use of transgenic mice to identify DNA sequences capable of directing transcription to particular tissues. (A) Gene X, consisting of three exons (filled squares) and an upstream regulatory region (green). In the RNA transcript from gene X, the V's between exons indicate where splicing takes place. (B) Two "reporter" constructs that include the bacterial gene *lacZ* as the reporter gene. This gene encodes the β galactosidase protein. Cells expressing this protein can be detected by histochemical staining (see Fig. 7.11). The two vectors also include either the complete regulatory region (left) or a part of it (right) and a portion of the first exon. Each vector is injected into zygotes, and the vectors integrate into the genome by nonhomologous recombination. Transgenic animals that are born are detected by the presence of *lacZ* sequences in their DNA. (C) Each vector is integrated into the genome. Only the transgene that includes the complete DNA regulatory region expresses *lacZ* transcripts and β galactosidase protein.

These effects are called **position effects**. This limitation requires that each founder animal be treated as independent and that information from at least three founder animals be obtained and compared to determine what characteristics are common to all. Another problem that can arise from random integration is that the new DNA can inactivate an endogenous gene, causing a new mutation. In fact, disruption of an essential gene occurs in approximately 10 percent of transgenic mice made by zygote injection.

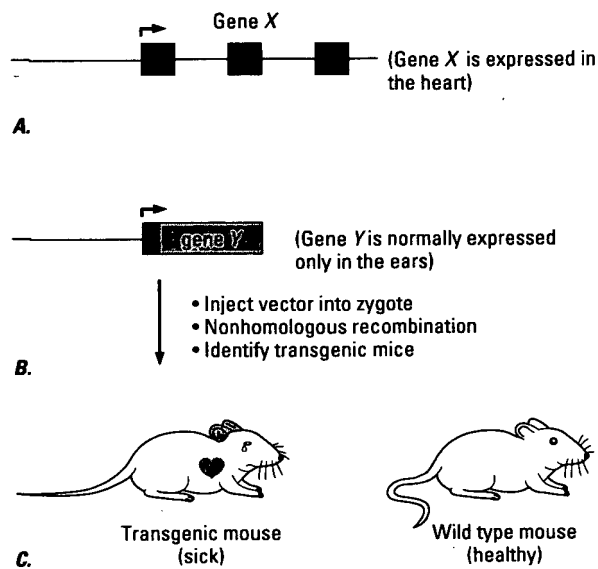


FIGURE 7.3 Use of transgenic animals to determine the biological consequences of expressing a gene inappropriately. (A) Gene X expressed in the heart shown as in Figure 7.2. (B) Construct in which the DNA regulatory region (green) of gene X is linked to the protein coding sequences of gene Y. Gene Y is normally expressed only in the ears. The construct is injected into zygotes to obtain transgenic animals. (C) If gene Y (green) is expressed in the heart as well as in the ears of a transgenic mouse, the animal becomes ill.

Gene targeting can complement and extend these studies. The most important feature of gene targeting is that it can remove and/or substitute for information already present. Thus, in the case of identifying DNA regulatory elements, it would be informative to remove an element that from other studies appears to be essential and test whether it is actually required for transcription at its normal chromosomal location. It may be that there are many other similar elements *in vivo* that collaborate with and augment the activity of that particular element. Similarly, a good way to faithfully replicate the expression pattern of a given gene is to insert other coding sequences into the endogenous gene by gene targeting.

The most important use of gene targeting for experimental studies is making change-of-function mutations that alter the biochemical properties of a gene product. These altered properties can range from no activity (a **null** mutation) to partial activity (a **leaky** mutation) to a new or stronger activity (**dominant** mutation). Some types of mutants can be made by zygote injection. The previously discussed cases of expressing

genes in new tissues represent zygote injection also have products that can inhibit. These are called **dominant**. The "antisense" approach to the antisense, or opposite. The antisense RNA that is transcript, thus inhibiting of complicating factors interpret. The major problem the same time as the normal RNA molecules to complete straightforward way to targeting to directly remove

More on

Why are null mutations in line for the development particular gene. This will be it is essential, then experiment interrupted in the absence question becomes, Why is predicted from the biochemical are there other backup systems the gene? If the latter is the also removed to test the consequences.

Why are leaky mutants early embryogenesis, it is mutants to test for multiple tation could be designed through the first critical next critical function late can test the biological significance.

Why are dominant mutations which a gene is expressed is the functional potential tumor, or can a gene change

genes in new tissues represent dominant mutations. Null mutations using zygote injection also have been attempted, using vectors that express gene products that can inhibit the normal function of an endogenous gene. These are called **dominant/negative** mutations. One example of this is the "antisense" approach, in which a vector is made that will transcribe the antisense, or opposite, strand of the coding DNA to the normal gene. The antisense RNA that is produced forms a double helix with the normal transcript, thus inhibiting its translation into protein (Fig. 7.4). A number of complicating factors in this approach make the results difficult to interpret. The major problem is expressing the vector in the same cells at the same time as the normal gene, as well as expressing it in sufficient excess of the normal transcript to drive the annealing reaction of the two RNA molecules to completion. It should be apparent by now that the most straightforward way to make a null mutation would be to use gene targeting to directly remove a gene from the genome.

More on the Importance of Mutant Organisms

Why are null mutations important? At the simplest level they provide a base line for the development or functioning of an organism in the absence of a particular gene. This will answer the question, Is the gene essential for life? If it is essential, then experiments can proceed to determine what process is interrupted in the absence of the gene. If the gene is not essential, then the question becomes, Why not? Does the gene not function the way that was predicted from the biochemical analysis and from its expression pattern, or are there other backup systems that can partially compensate for the loss of the gene? If the latter is the case, then the other genes must be identified and also removed to test the combined function of the genes.

Why are leaky mutants important? For genes that are essential during early embryogenesis, it is important also to make partial loss-of-function mutants to test for multiple functions of the gene. For example, a mutation could be designed that allows the animal to develop normally through the first critical process in which the gene functions to test for the next critical function later in development. Alternatively, leaky mutations can test the biological significance of particular protein domains.

Why are dominant mutations important? In the case of mutants in which a gene is expressed in new cell types, the question being addressed is the functional potential of the gene. For example, Can a gene cause a tumor, or can a gene change the differentiation pathway of a cell? If the

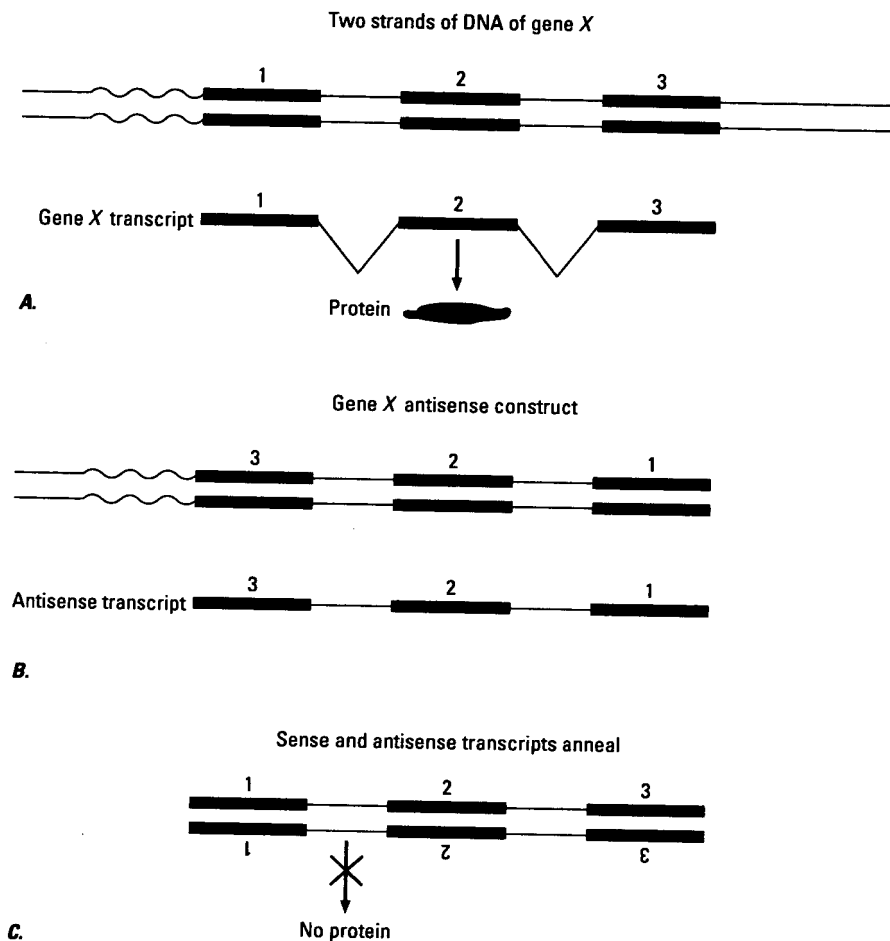


FIGURE 7.4 Expression of antisense RNA can interfere with the expression of a gene. (A) *Top*: The two strands of DNA of a three-exon (filled rectangles) gene X. The lower strand is used as the template for transcription. *Bottom*: Transcript and protein from gene X. (B) *Top*: Antisense construct for gene X. The DNA regulatory region of gene X (wavy lines) is joined to gene X sequences that have been reversed in their direction of transcription. *Bottom*: Transcript that would be produced from the antisense construct. Note that compared to the normal gene, the opposite strand of DNA is used as the template for transcription. (C) Annealed sense and antisense transcripts.

answer is yes, it suggests in directing the development turns out to be a fact. Dominant mutations that but instead alter or augmenting selected amino acids particular domains that affect the functional properties analysis and can be most where there are fewer variants.

From the analysis of many experiments that have been that have important implications function. One is that there is a subset of all the tissues idea of backup systems. different roles in different lends support to the idea tions alone but act in coordination expression of the other proteins role of the gene in question.

Because of this complexity animals with different kinds only method for making precise number of potential components approaches that have been insertion of a selectable gene of mutation can be effective mutations involving altering mutations can be problematic mutations such as single base gain-of-activity mutations. direct gene replacement procedure

As was discussed in Chapter gene targeting is making the transmitting the mutation into

answer is yes, it suggests that the gene plays some sort of regulatory role in directing the development of cells. When this is the case, the gene often turns out to be a factor that regulates the activity of other genes. Dominant mutations that do not alter the expression pattern of a gene, but instead alter or augment the activity of the protein product by changing selected amino acids, are often designed to test the function of the particular domains that are altered (as in Fig. 7.1). This type of analysis of the functional properties of a protein is referred to as **structure/function** analysis and can be most effective if done in vitro or in cells in culture where there are fewer variables to contend with.

From the analysis of mutant phenotypes from the germline targeting experiments that have been reported to date, two themes are emerging that have important implications for these types of studies of in vivo gene function. One is that the tissues affected by null mutations represent only a subset of all the tissues that express the gene. This lends support to the idea of backup systems. The second theme is that genes play many different roles in different tissues at different times in development. This lends support to the idea that gene products do not perform their functions alone but act in concert with many other proteins, and since the expression of the other proteins often varies from cell type to cell type, the role of the gene in question also varies.

Because of this complexity of gene function, it is necessary to make animals with different kinds of mutations, and gene targeting offers the only method for making predetermined mutations in which the maximum number of potential complicating factors can be controlled. The targeting approaches that have been used extensively to date in ES cells all include insertion of a selectable gene into the gene of interest. This insertion type of mutation can be effective in making null mutations and dominant mutations involving altering the expression of a gene. However, insertion mutations can be problematic when it comes to making more subtle mutations such as single base pair changes to make leaky and dominant gain-of-activity mutations. For these types of mutations, pop-in/pop-out or direct gene replacement procedures will have to be perfected.

General Considerations

As was discussed in Chapter 6, the present method of choice for germline gene targeting is making the directed gene mutation in ES cells and then transmitting the mutation into mice by making germline ES cell chimeras.

The mutation is made in ES cells by introducing a gene targeting vector into ES cells and allowing the cells to undergo a homologous recombination event that replaces the normal endogenous gene with the introduced mutant copy. As described in Chapter 5, the technological breakthroughs that have made this feasible in mammalian cells have been (1) enrichment schemes that select preferentially for the targeted cell clones and (2) screening procedures using PCR that allow thousands of colonies to be screened for rare homologous recombination events.

The special techniques that have been developed for gene targeting in mammalian cells, described in Chapter 5, apply to ES cells. In general, replacement rather than insertion vectors are used (Fig. 7.5). From a practical point of view, ES cells differ from most somatic cells in two important ways. The first is that they are much smaller. This is an advantage, since from a tissue culture dish tenfold more cells can be recovered. The second difference, a disadvantage, is that ES cells have very specific growth requirements (described in Chapter 6), such as a feeder layer or LIF and a rigid protocol of passing the cells frequently. Careful culturing of the cells is critical for the targeted cells to maintain their ability to contribute to the germline in ES cell chimeras.

The first factor to consider when designing a homologous recombination experiment is whether the gene to be targeted is expressed in ES cells. This dictates the type of targeting vector that should be constructed. If the gene is expressed, then the most efficient type of vector is probably one designed on the principle of a promoterless selectable marker gene (see Fig. 7.6), since these types of vectors in general give the greatest level of enrichment. The bacterial *neo* gene is a good choice for the selectable marker, since G418 selection is simple and effective in ES cells and does not effect the totipotency of the cells. If the ES cells are grown on a feeder layer rather than in LIF, then G418^R feeder cells must be used. G418^R STO cell lines can be obtained by isolating G418^R cell clones transfected with a vector that expresses the *neo* gene. Alternatively, G418^R primary fibroblasts can be isolated from transgenic mice that express *neo*.

If the gene to be targeted is not expressed in ES cells, then a vector can be designed on the principle of positive-negative selection (PNS; see Fig. 7.7). One factor that may be critical for targeting genes that are not expressed in ES cells is the choice of promoter for the selectable genes. As discussed earlier in this chapter, not all DNA is equal, and some regions of the genome are transcriptionally "silent." Thus, it is possible that some nonexpressed genes will actively inhibit expression of a newly introduced promoter intended to express *neo*. If this is the case, then any cells that have undergone homologous recombination of the vector will not be able to express the *neo* gene and thus will be killed by the G418 selection. In an attempt to solve this problem, a number of *neo* vectors containing different

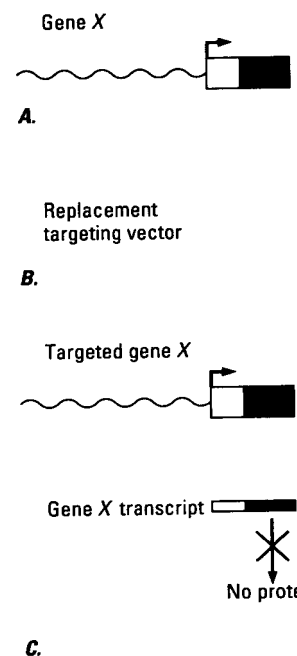


FIGURE 7.5 Gene targeting of gene X. Exons are indicated by black boxes. The primers are shown as short green arrows. (B) Replacement targeting vector. (C) Structure of gene X targeted by the targeting vector. The sequences not present in the targeting vector are indicated by the asterisk. The *neo* protein product was not produced.

promoters have been used to achieve integration-site-independent targeting, even in silent genes.

promoters can in fact be used to achieve integration-site-independent targeting. A second possible limitation is that DNA may undergo recombination. To date, the frequencies of recombination are of orders of magnitude. T

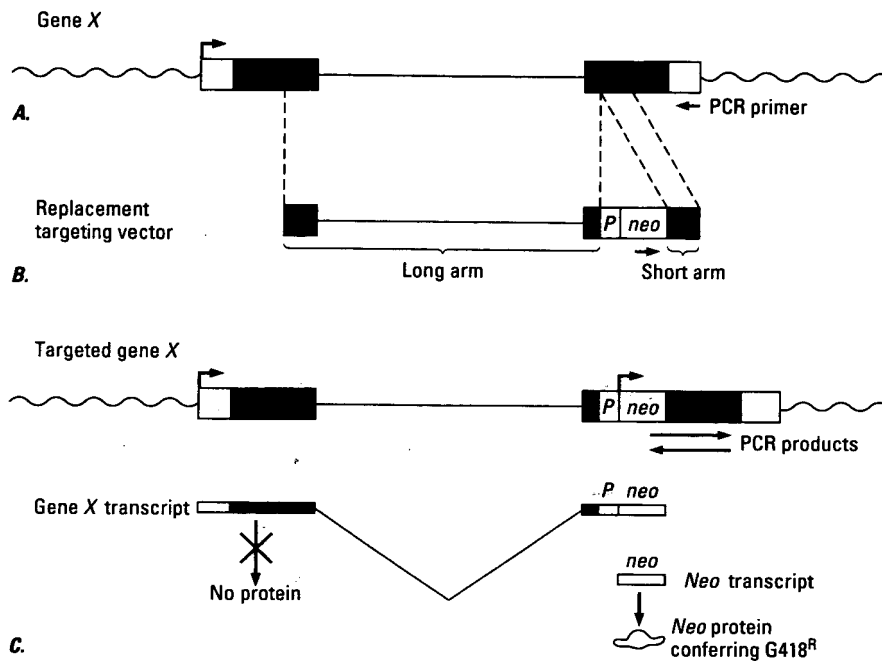


FIGURE 7.5 Gene targeting in ES cells using a basic replacement vector. (A) Two-exon gene *X*. Exons are indicated by rectangles with filled-in areas indicating protein coding sequences. The primers used for PCR in screening for homologous recombinants are shown as short green arrows. The start and direction of transcription is indicated by an arrow. (B) Replacement targeting vector with long and short fragments of gene *X* (long arm and short arm, respectively) surrounding the *neo* gene driven by a transcription promoter (*P*). (C) Structure of gene *X* following homologous recombination and replacement of gene *X* sequences by the targeting vector. The PCR products would be made using the two primers indicated (one that anneals to *neo* sequences and one that anneals to gene *X* sequences not present in the targeting vector). From the transcripts that would be produced from the promoters of the genes *X* and *neo*, no functional protein *X* would be made, whereas the *neo* protein product would be made and confer G418 resistance to the cells.

promoters have been constructed with the idea that a really strong integration-site-independent promoter will not be completely shut down even in silent genes. It is not yet clear whether any of the available promoters can in fact be expressed in all genes.

A second possible limiting factor in all targeting strategies is that some DNA may undergo recombination at very low frequencies. From the data to date, the frequencies of successful targeting events range at least three orders of magnitude. These numbers, of course, do not include genes for

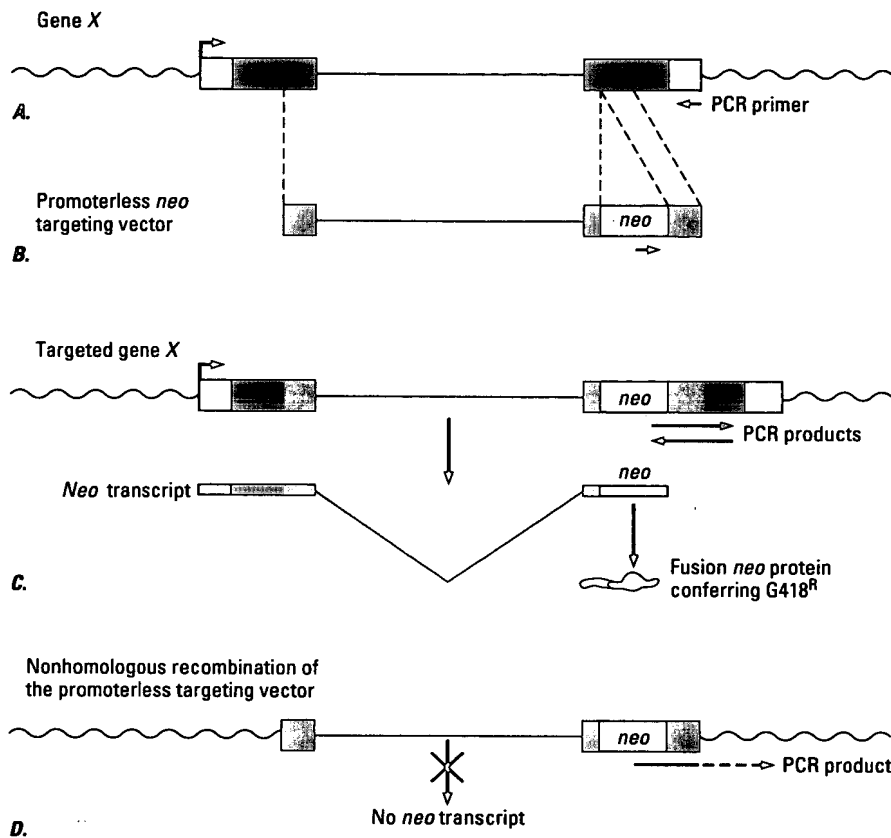


FIGURE 7.6 Gene targeting in ES cells using a promoterless *neo* targeting vector that enriches for cells that have undergone homologous recombination. (A) Gene X shown as in Figure 7.5. (B) Gene targeting vector similar to that in Figure 7.5B. The difference in this vector is that *neo* does not contain a promoter and the *neo* protein is made as a functional fusion protein with a portion of protein X. (C) Top: Structure of gene X following homologous recombination with the promoterless *neo* targeting vector. Bottom: Transcript and protein made from the targeted gene X. (D) Structure of the promoterless *neo* targeting vector following nonhomologous recombination with random genomic sequences. Unless the vector integrated by chance beside a promoter, no *neo* transcript would be made.

which it has not been possible to target. Thus the lower limit of the frequency of homologous recombination is not known. The only obvious possible solution to this problem is to construct targeting vectors containing different regions of a gene, in the hope that some fragments of DNA will be more recombinogenic than others.

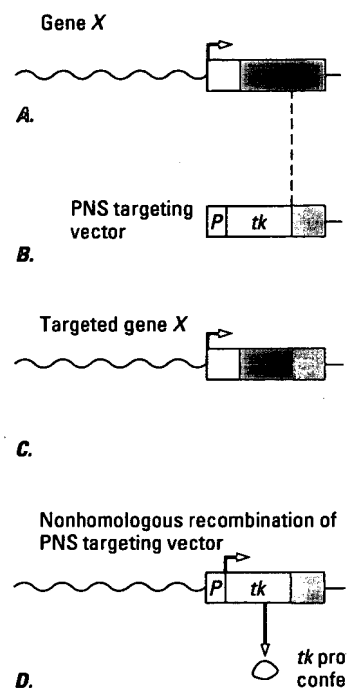


FIGURE 7.7 Gene targeting in E negative selection (PNS) enrichment targeting vector similar to that in Figure 7.5. (A) Gene X shown as in Figure 7.5. (B) Gene targeting vector similar to that in Figure 7.5B. The difference in this vector is that *neo* does not contain a promoter and the *neo* protein is made as a functional fusion protein with a portion of protein X. (C) Top: Structure of gene X following homologous recombination with the promoterless *neo* targeting vector. Bottom: Transcript and protein made from the targeted gene X. (D) Structure of the promoterless *neo* targeting vector following nonhomologous recombination with random genomic sequences. Unless the vector integrated by chance beside a promoter, no *neo* transcript would be made.

A typical gene targeting experiment involves several steps. The first is to design and make targeting vectors. The second step involves introducing the targeting vectors into the population of cells that have been frozen stored and grown up. The targeting vectors are then electroporated. The targeting

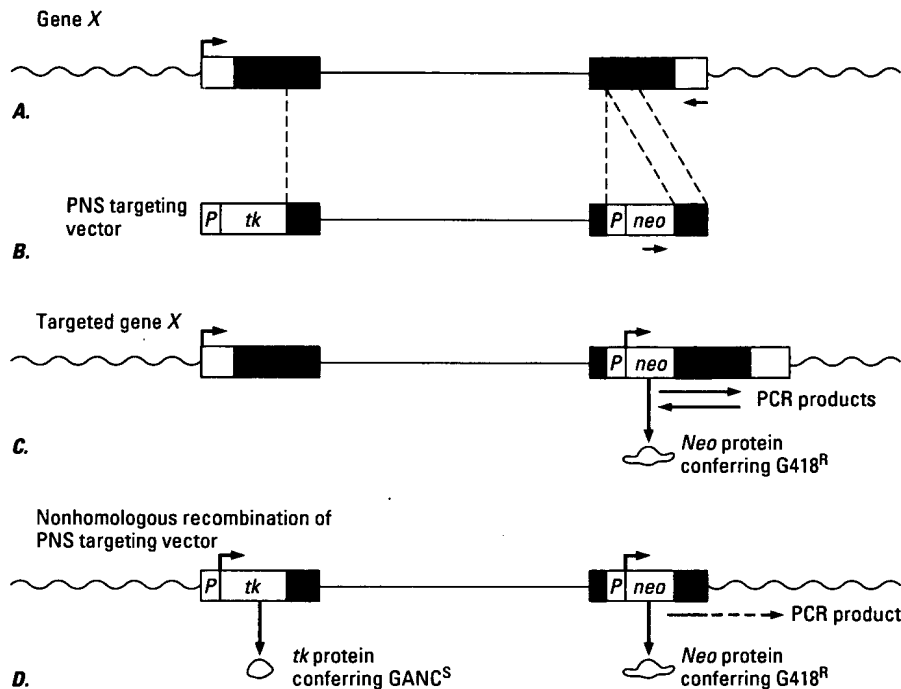


FIGURE 7.7 Gene targeting in ES cells using a targeting vector based on the positive-negative selection (PNS) enrichment scheme. (A) Gene X shown as in Figure 7.5. (B) Gene targeting vector similar to that in Figure 7.5B. The difference in this vector is that the *Herpes simplex virus tk* gene with a promoter is included at the end of one of the gene X homologous fragments. (C) Structure of gene X following homologous recombination with the PNS targeting vector. The structure is the same as that shown in Figure 7.5C, since the recombination occurs within the gene X sequences and thus the *tk* sequences are lost. (D) Structure of the PNS targeting vector following nonhomologous recombination. Functional *neo* and *tk* genes will be integrated into the genome if the vector DNA is not broken. The *neo* protein confers G418^R to the cells, whereas the *tk* protein confers sensitivity to GANC. Cells containing such a vector will be killed if they are grown in G418 and GANC.

A typical gene targeting experiment can be divided into a number of steps. The first is to design and make a targeting vector taking into consideration the enrichment schemes and possible limitations described above. The second step involves introducing the targeting vector into ES cells and selecting a population of cells that have taken up the vector (Fig. 7.8). A sample of ES cells that had been frozen soon after the cell line was established is thawed and grown up. The targeting vector is then introduced into the cells using electroporation. The targeting vector must be prepared by linearizing the

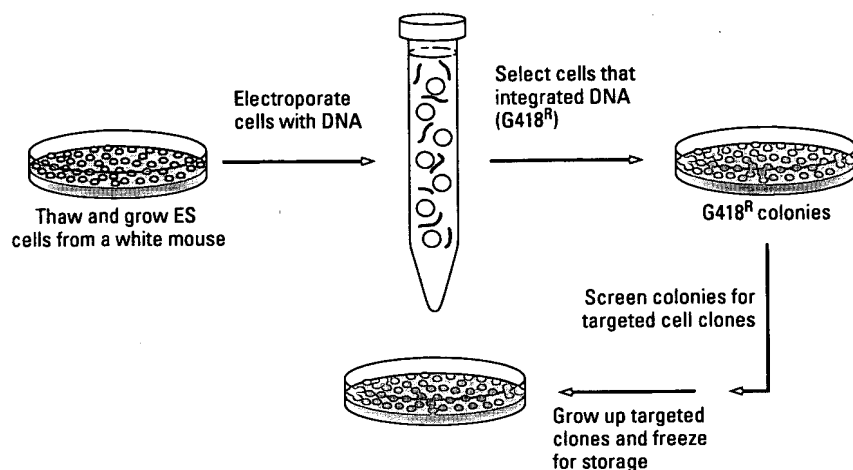


FIGURE 7.8 Scheme for electroporating ES cells and isolating cells containing a targeted mutation.

DNA, and the cells must be treated to give a single cell suspension. The DNA and cells are then mixed, put into a cuvette with electrodes on either side, and given a short pulse of an electric field. The DNA is driven across the cell membranes and taken up into the cell nuclei by approximately 10 percent of the cells. The cells are then plated on dishes either in LIF or on feeder cells that are G418^R. Two days later the selective medium, G418 or G418 and GANC, is put onto the cells. Within ten days colonies appear on the dishes. The normal ES cell plating efficiency, or number of cells that will grow after being replated, is 10 to 20 percent; and 50 percent of the cells are usually killed by the electroporation procedure. Furthermore, only approximately 0.1 percent of the electroporated cells stably integrate and express a marker gene. Thus, in an experiment starting with 5×10^7 cells and a standard *neo* vector, approximately 5000 G418^R colonies would grow. Using a vector with a promoterless *neo* gene, approximately 50 G418^R colonies would probably grow, and using the PNS strategy 50 to 500 G418^R/GANC^R colonies would grow. The percentage of targeted clones that would be obtained from such an experiment could vary from 0 to 50 percent, depending on the type of vector and particular endogenous gene sequences used.

The third step in a targeting experiment involves screening the drug-resistant colonies for clones that have integrated the vector by a homologous recombination event. Because the frequency of homologous recombination varies widely, and since it is not possible to predict a priori

the targeting frequency of so that PCR can be used (7.7). This requires that on is less than 1 thousand base pairs. The PCR reaction is then made specific by amplifying an endogenous gene sequence with primers in the short arm of the vector.

To identify the targeted colonies, a PCR reaction (Figure 7.5) can be used (Figure 7.7). This requires that on is less than 1 thousand base pairs. The PCR reaction is then made specific by amplifying an endogenous gene sequence with primers in the short arm of the vector.

The advantages of this method are twofold. First, not all ES cell lines growing colonies are not targeted. A second advantage is that since a minimum length of growth is required, the length of time in culture is correlated with the probability to populate the germline. The starting population of ES cell lines that will populate the germline is 10 to 100 percent.

The final step in germline transmission is to have an ES cell contribute to the germline. Subcloned cell lines will produce targeted cell lines and test for germline transmission. This has been the method of choice for generating animals that reach term. Animals from inbred mice have been used in experiments by many different groups. It has become apparent that the effect on the percentage of animals that reach term is to the germline. Host blastocysts of germline chimera strains give high numbers. In an experiment can have a high percentage for the reasons described

the targeting frequency of a given vector, it is helpful to design the vector so that PCR can be used to screen for the recombinants (Figs. 7.5, 7.6, 7.7). This requires that one of the genomic DNA fragments that flanks *neo* is less than 1 thousand base pairs (Fig. 7.5, short arm). One primer for the PCR reaction is then made to anneal to *neo* sequences and the other to endogenous gene sequences just outside the sequences included in the short arm of the vector.

To identify the targeted clones, a modified version of sib selection (see Chapter 5) can be used (Fig. 7.9). Instead of pooling whole *neo^R* or *neo^R* and GANC^R colonies, as in sib selection, the colonies are left intact, and only a part of each colony is picked using a pipette and suction under a microscope. The portions of up to 50 colonies are then pooled and the PCR reaction run on each pool. The remainder of the colonies are left to grow. When a positive pool is identified, portions of each single colony from that pool are then tested by PCR. A single targeted colony can be identified by this approach in less than one week. The targeted colony is then grown up and frozen in small samples to make a stock of cells for future use.

The advantages of this modification of sib selection for ES cells are twofold. First, not all ES colonies grow at the same rate and thus slower-growing colonies are not lost after pooling. The second and more important advantage is that since the ES colonies are left intact, they go through a minimum length of growth. This is critical since, as discussed in Chapter 6, the length of time in culture and number of subclonings is inversely correlated with the probability that a given ES cell clone will retain its ability to populate the germline in chimeras. Depending on the state of the starting population of ES cells used in an experiment, the percentage of cell lines that will populate the germline can vary from less than 10 percent to 100 percent.

The final step in germline targeting is to make ES cell chimeras that have an ES cell contribution to the germline (Fig. 7.10). Since not all subcloned cell lines will populate the germline, it is best to isolate 2 to 5 targeted cell lines and test them all in chimeras. Blastocyst injection has been the method of choice for obtaining chimeras because the percentage of animals that reach term is generally higher. Two ES cell lines derived from inbred mice have been used extensively for germline targeting experiments by many different laboratories. With these cell lines it has become apparent that the genotype of the host blastocyst has a strong effect on the percentage of chimeras that contain an ES cell contribution to the germline. Host blastocysts from outbred mice give the lowest numbers of germline chimeras, whereas blastocysts from particular inbred strains give high numbers. With some ES cell clones, most of the chimeras in an experiment can have an ES cell contribution to the germline. Since, for the reasons described in Chapter 6, male ES cell lines are normally

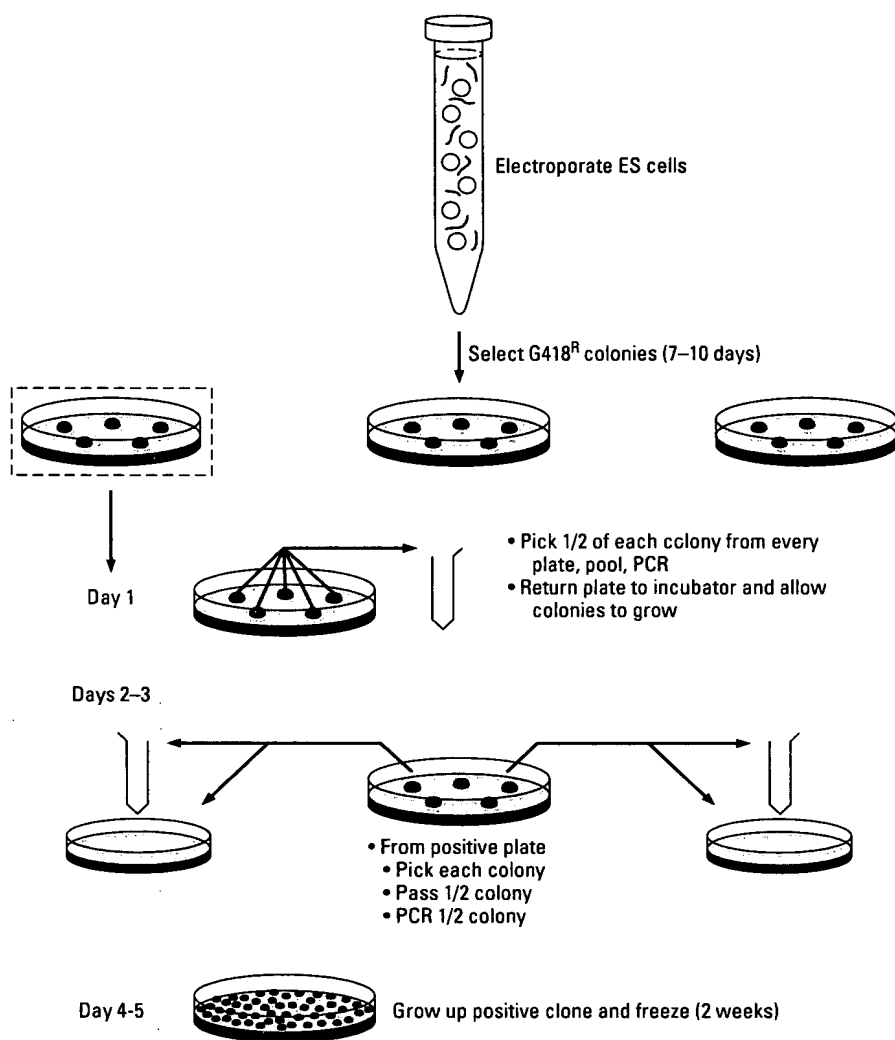
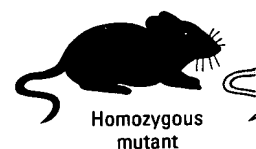
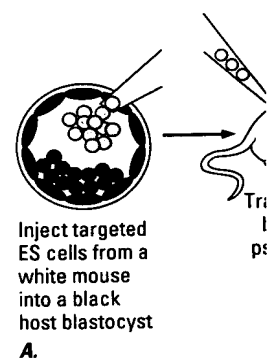


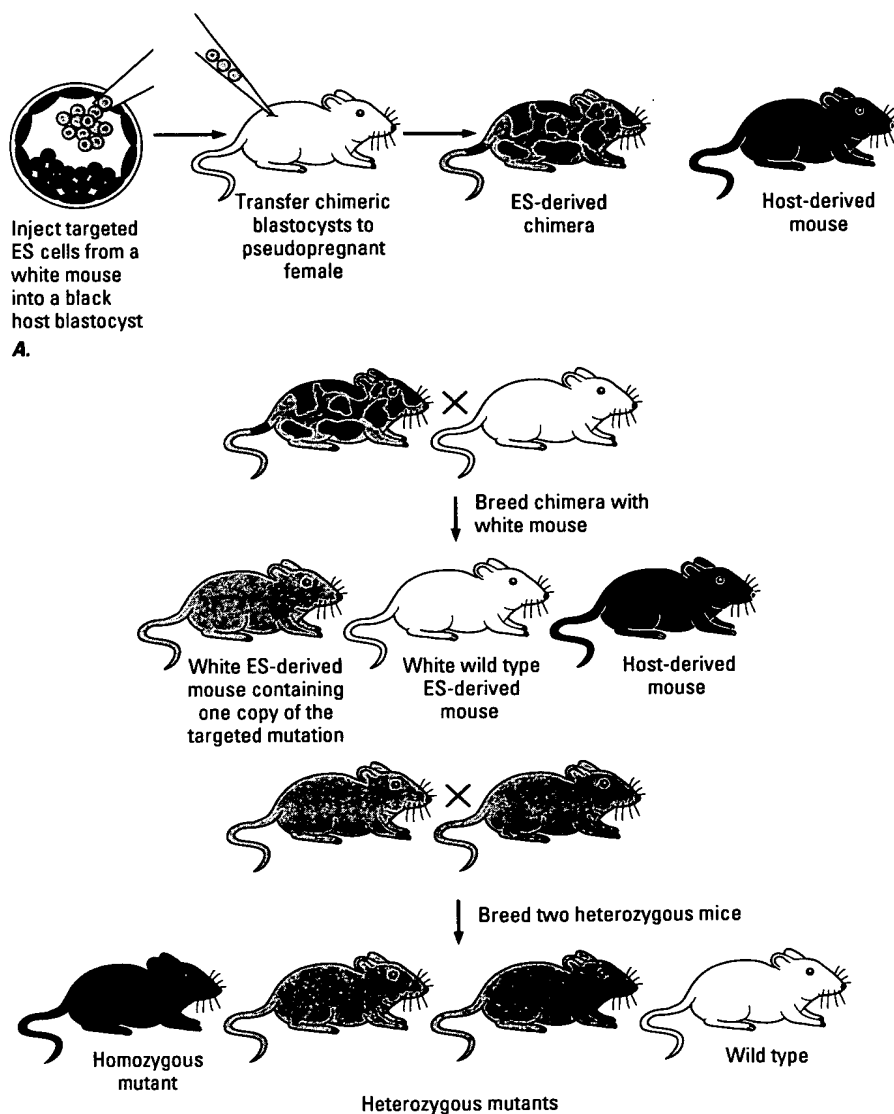
FIGURE 7.9 Strategy for screening ES cells by a modified version of sib selection, using PCR to identify targeted cell lines.

used, only the male chimeras are bred to produce mice heterozygous for the targeted mutation. Coat color markers are used as a convenient means of identifying ES cell derived mice and DNA isolated from tail biopsies is analyzed to identify the 50 percent of the animals that carry the targeted mutation.



B.

FIGURE 7.10 Strategy for screening ES cells heterozygous for the targeted mutation. Mice heterozygous for the mutation (shown in light green and are bred to produce mice homozygous for the mutation (shown in dark green). The mice that are homozygous for the mutation will be homozygous for the mutation.



B.

FIGURE 7.10 Strategy for obtaining mice homozygous for a targeted mutation from ES cells heterozygous for the mutation. (A) Production of ES cell derived chimeras, as described in the legend of Figure 6.11. The targeted ES cells and their derivatives in mice are shown in light green and the host blastocyst derived cells in black. (B) The male chimeras are bred to produce mice derived from the targeted ES cells (light green and white). The ES cell derived mice are analyzed to determine which contain one copy of the mutation (light green). The mice that are heterozygous for the mutation are bred, and one quarter of their offspring will be homozygous for the mutation (dark green).

A Specific Example

To illustrate the unpredictable nature of both the biological functioning of genes and the process of gene targeting, it is useful to examine a specific example. The mouse genes in question are called the *engrailed* genes, or *En-1* and *En-2* for short. These genes were isolated from mice based on their DNA sequence similarity to the *engrailed* (*en*) and *invected* (*inv*) genes of the fruit fly *Drosophila melanogaster*.

The *en* gene was identified in *Drosophila* in 1929 based on the phenotype of an *en* mutant fly that arose spontaneously.¹ The posterior half of the wings of flies carrying this *en* mutation develop abnormally whereas the anterior halves develop normally. Based on the phenotypes of this and many other *en* mutants, a general hypothesis was put forward that the biological function of *en* is to direct, or select, the developmental pathway of groups of cells, called posterior compartments, that make up the posterior portion of every segment and of tissues, called imaginal discs, that give rise to the major parts of the adult body such as limbs, wings, and antennae.

In 1985 the *Drosophila en* gene and a gene, *inv*, with a similar DNA sequence were cloned.² The sequence of the protein coding regions of *en* and *inv* suggested that they code for transcription factors. Subsequent biochemical analysis on *en* protein confirmed this. Analysis of expression of *en* and *inv* in fruit fly embryos showed that they were expressed in all the cells of the posterior compartments, consistent with the *en* mutant phenotypes. The genes were also, however, found to be expressed in reiterated sets of neurons in the central nervous system. This suggests that there are other, as yet undiscovered, functions for *en* in the development of the adult nervous system.

The two mouse genes, *En-1* and *En-2*, were cloned based on their DNA sequence homology to *en* and were found to have protein coding regions that share a number of domains with *en* and *inv*.³ The protein sequence conservation suggests that the mouse genes, like *Drosophila en*, act as transcription factors. The compelling question to be answered, therefore, was, Do the mouse genes also act to direct the development of posterior compartments?

The first indication that evolution had not strictly conserved the biological function of *en* in invertebrates and vertebrates came from the analysis of the expression of *En-1* and *En-2* in mice and other vertebrates. These genes are not expressed in reiterated domains early in embryogenesis but in a single spatially restricted domain in the developing brain (Fig. 7.11). Later in embryogenesis *En-1*, but not *En-2*, is expressed in a number of

FIGURE 7.11 Expressing transgenic embryo containing *lacZ*. The cells are stained with toluidine blue.

other domains in the adult, both genes are reiterated neurons as that the vertebrate *En* posterior compartment act to direct the development.

The most rigorous tests in *En-1* and *En-2* then breed the mutant mutations in both *En* of whether these still and functions and to

The *En-2* gene was to the one shown in with *neo* containing. *En-2* is expressed at were done before the to screen for homologous clones was found to replacement event.



FIGURE 7.11 Expression of the *En-2* gene in a band across the mid/hind brain. The 10-day transgenic embryo contains a reporter construct with *En-2* DNA regulatory sequences expressing *lacZ*. The cells expressing *lacZ* (black under arrow) are visualized by histochemical staining. (Photograph courtesy of Cairine Logan.)

other domains in different tissues. Still later in development and in the adult, both genes are expressed in specific groups of neurons, but not in reiterated neurons as in the fly. From this descriptive analysis it was clear that the vertebrate *En* genes cannot control the development of reiterated posterior compartments. However, it was still highly likely that the genes act to direct the development of domains.

The most rigorous test of this hypothesis would be to make null mutations in *En-1* and *En-2*, study the phenotype of each single mutant, and then breed the mutants and study the phenotype of mice carrying null mutations in both *En* genes. This experiment would address the question of whether these structurally related genes carry out similar, or redundant, functions and thus represent backup systems.

The *En-2* gene was targeted in a male ES cell line using a vector, similar to the one shown in Figure 7.5, in which part of the gene was replaced with *neo* containing a promoter.⁴ No enrichment scheme was used, since *En-2* is expressed at very low levels in ES cells and since the experiments were done before the PNS strategy was reported. Using the PCR strategy to screen for homologous recombinants, approximately 1 in 300 G418^R clones was found to have undergone the predicted double crossover replacement event. Three targeted ES cell clones were isolated, of which

only one gave rise to germline chimeras. Of the ES-derived offspring from the germline chimera, 50 percent were, as expected, heterozygous for the *En-2* mutation called *En-2^{hd}*. When mice heterozygous for the mutation were bred, they gave rise to offspring with the expected Mendelian ratio of 1 wild type : 2 heterozygotes : 1 homozygote *En-2^{hd}*. Furthermore, the *En-2^{hd}* homozygous animals had no detectable structural or behavioral phenotypic abnormalities. However, the one tissue, the adult cerebellum, that expresses *En-2* and not *En-1* was found by histological analysis to have an abnormal pattern of folds: Some folds were missing and others were misshapen.⁵ Since the cerebellum controls many sensory-motor coordination functions, it is likely that these mice were deficient in some motor control functions but that the defects were not obvious in mice living in a cage supplied with all the amenities. Since the only obvious defect was in a tissue that expresses only *En-2* and not both *En* genes, the phenotype analysis suggested that *En-1* and *En-2* are functionally redundant.

Targeting experiments designed to mutate *En-1* in ES cells were not as successful as *En-2* experiments. A number of targeting vectors based on the PNS strategy including different promoters to drive the *neo* gene and different regions of the *En-1* gene to direct homologous recombination, were tested in ES cells, and no targeted clones were recovered. The frequency of targeting *En-1* by this approach therefore appears to be less than $1/10^8$ cells electroporated. The biological function of the *En* genes will remain unresolved until mice containing mutations in *En-1* can be obtained. These results underscore the fact that not all genes can be efficiently targeted in ES cells. The potential limiting step in the process of germline targeting therefore is the homologous recombination event itself.

Future Prospects

At present, we have the very powerful capability of making specific mutations in mouse ES cells using gene targeting and transmitting the mutations into mice by ES cell chimera formation. However, a number of problems with gene targeting limit the kinds of mutations that can be made. One problem that has been discussed is that all genes may not be accessible to homologous recombination at detectable levels for two obvious reasons: (1) a selectable marker gene cannot be expressed after integration into certain genes in ES cells; (2) some sites in the genome may recombine at very low frequencies.

One possible alternative targeting strategy is the use of microinjection of ES cell nuclei. Such a strategy has been reported for the targeting of ES cell nuclei.⁶ Using microinjection, the surviving cells are 100 times higher than in homologous recombination. There are two drawbacks to this strategy: (1) small, microinjected cells, or 3000 cells, are used per week. The second drawback is that the efficiency is lower than that of homologous recombination. A second drawback is that the efficiency has not been extended to 100 bases), single-strand breaks. A possible advantage of this strategy is that more recombinants are produced, tens of thousands, which would require repeated picking of portions of the population.

To tackle the problem of homologous recombination, a number of recombination machines have been developed. These machines are based on the principle that homologous recombination can be induced by a specific vector, can be modulated, and can be used to create a library of recombinants.

A second limit to the use of ES cells is the lack of integrations designed to target transcription regulatory regions. A desired subtle alteration in a gene can be achieved by using vectors that can integrate into a selectable marker gene without interfering with the regulatory elements of the gene. Throughout the genome, if a gene can be precisely targeted, it can be precisely targeted. A selectable gene. A table marker into

One possible avenue to explore in cases where the former is true is new targeting strategies in which the vector contains no selectable marker. In one such reported approach, the targeting vector was injected directly into the nuclei of ES cells instead of being introduced into the cells by electroporation.⁶ Using microinjection of DNA into nuclei, approximately 10 percent of the surviving cells can integrate the DNA nonhomologously. This percentage is 100 times higher than in electroporation. Thus, if the ratio of homologous to nonhomologous recombination is 1 : 100, then by screening 1000 injected cell clones using the PCR strategy one targeted cell line could be identified. There are two drawbacks to this approach. One is that since ES cells are very small, microinjection into them is difficult. Therefore the injection of 1000 cells, or 3000 cells to obtain three targeted cell lines, could take one person weeks. The second drawback is that the frequency can be orders of magnitude lower than 1 in 100. Thus for some genes this approach is not applicable. A second possible technique for introducing DNA into cells, which has not been extensively explored, is to add to cells in culture short (less than 100 bases), single-stranded pieces of DNA that include the desired mutation. A possible advantage of this technique is that single-stranded DNA may be more recombinogenic than double-stranded DNA. For this approach to be useful, tens of thousands of colonies would likely have to be screened. This would require refining the standard sib selection procedure or mechanizing picking portions of colonies.

To tackle the potential problem of regions in the genome that undergo recombination at very low frequencies, further research into the mechanism of recombination will be necessary. As more parts of the mammalian recombination machinery are characterized and DNA sequences that initiate recombination are identified, improvements to the present targeting approaches will likely become apparent. For example, there is already some evidence that specific DNA sequences, when introduced into a targeting vector, can moderately stimulate homologous recombination of the vector.

A second limitation to the present targeting strategies is that they all include integration of a selectable gene into the targeted locus. For experiments designed to alter specific protein coding domains or to delete or add transcription regulatory elements, it would be ideal to make only the desired subtle alterations. On paper it is possible to design targeting vectors that can make subtle changes to the target gene by placing the selectable marker gene in a part of the endogenous locus where it will not interfere with the functioning of the gene. However, since the DNA regulatory elements that control transcription of a gene can be scattered throughout the gene and be many thousands of base pairs away from the gene, it can be problematic to identify a "neutral" site for insertion of the selectable gene. It would therefore be ideal not to have to insert a selectable marker into the targeted locus.

One area of research for which it is essential to make subtle mutations is structure/function analyses. A second area for which subtle mutations in mice will undoubtedly play an important role is medical research. One active area of medical research is the study of animal models of human diseases. For some gene mutations that affect humans as diseases, mice are available that contain mutations in the same gene. In some instances the disease symptoms of the mice are very similar to those of humans. These animals serve as models of the human diseases and are used for further research into the biochemical bases of the diseases. Potentially they can also be used to test new therapies for the diseases.

Some mouse mutants do not, however, have the same set of disease symptoms as humans with mutations in the same genes. In some cases this is because the physiology of mice and humans is not exactly the same. This fact can nevertheless give insights into the biochemical processes that involve the affected genes. In some cases, the differences between the mouse and human symptoms may be due to the types of mutations in the two species. One mutation may be a null mutation whereas the other may be a leaky mutation. The most direct way to test which is the case would be to use germline gene targeting to make mice with exactly the same mutation as the humans. In this type of gene targeting, of course, a marker gene cannot be included. Finally, for the majority of human diseases animal models do not exist, and germline gene targeting represents the most direct way to make such models.

The pop-in/pop-out and direct gene replacement procedures described for yeast in Chapter 5 represent two-step schemes for making subtle mutations that could be applicable to ES cells (Figs. 7.12, 7.13). There have been two recent reports of successful targeting using the pop-in/pop-out approach in ES cells. In one case, the single *hprt* gene on the X chromosome of a male ES cell line was mutated.⁷ Since *Hprt*-expressing and *Hprt*-nonexpressing cells can be directly selected, this gene served during the homologous recombination step as both the positive and negative marker for the two selection steps. In the second case, an autosomal gene was mutated at a surprisingly high frequency, with the pop-out or intrachromosomal recombination occurring at a frequency of 1 in 1000 cells.⁸

As in yeast, the potential limiting factor for the pop-in/pop-out and direct gene replacement approaches in ES cells is the frequency at which the negatively selectable marker gene spontaneously becomes non-functional. The marker gene can become inactivated by at least three mechanisms. One is suffering a spontaneous mutation, such as a deletion, insertion, or base pair change. This event usually occurs at a low frequency (1 in 10^6 cells/cell doubling) in somatic cells and should therefore not represent a major limiting factor for these approaches. A second

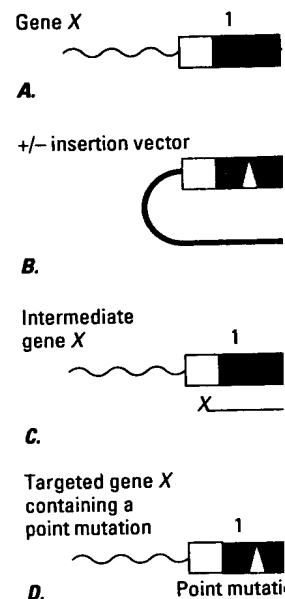


FIGURE 7.12 Possible pop-in/pop-out targeting. Targeting vector cut in the (white arrowhead) in the and against. The vector is that selects (+) for expression screened for targeted color homologous recombination containing the targeted gene ing the marker gene. Some an intrachromosomal recombination the endogenous sequence (indicated by X's) then the

mechanism for inactivation of themselves, is D residues in DNA, and are not transcribed. inactivated by this process integration and from activating a gene is gene mechanism of gene genes can be lost at a

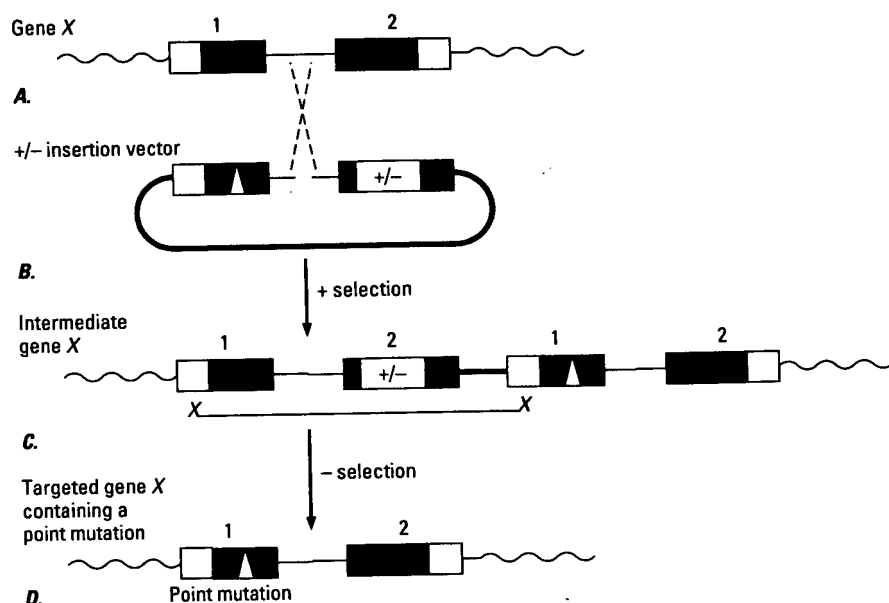


FIGURE 7.12 Possible scheme for producing a point mutation in ES cells using the pop-in/pop-out targeting approach. (A) Gene X shown as in Figure 7.5A. (B) Insertion targeting vector cut in the region of gene X homology. The vector contains a point mutation (white arrowhead) in the first exon and a marker gene (+/-) that can be selected both for and against. The vector is electroporated into ES cells and the cells are grown in medium that selects (+) for expression of the marker gene. The colonies surviving selection are screened for targeted clones. (C) Structure of gene X in the intermediate cell line following homologous recombination and insertion of the targeting vector. The intermediate cell line containing the targeted gene X are grown in medium that selects against (-) cells expressing the marker gene. Some of the cells that survive negative selection will have undergone an intrachromosomal recombination event between the inserted gene X sequences and the endogenous sequences. (D) If the recombination occurs upstream of the point mutation (indicated by X's) then the point mutation will be retained.

mechanism for inactivating genes, which does not alter the gene sequences themselves, is DNA methylation. Somatic cells actively methylate C residues in DNA, and it has been found that most highly methylated genes are not transcribed. The frequency with which a marker gene is inactivated by this process will probably vary from site of integration to site of integration and from cell line to cell line. The third mechanism for inactivating a gene is gene loss. It is not known what is the most prevalent mechanism of gene loss in ES cells, but it is becoming clear that marker genes can be lost at a high frequency (up to $1/10^3$ cells/cell generation) in

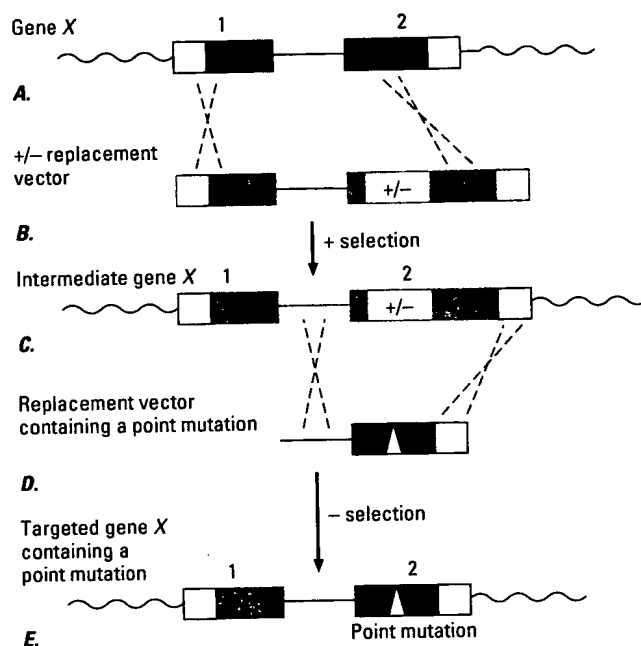


FIGURE 7.13 Possible scheme for producing a point mutation in ES cells using the direct gene replacement targeting approach. (A) Gene X shown as in Figure 7.5A. (B) First replacement vector, similar to that shown in Figure 7.5B except that the marker gene can be selected both for and against. The vector is electroporated into ES cells, the cells grown in selective medium, and targeted clones identified as described in the legend for Figure 7.12B. (C) Structure of gene X in the intermediate cell line following homologous recombination with the replacement vector. (D) Second replacement vector, containing gene X sequences with a point mutation. The second vector is electroporated into the intermediate cell line, and the cells are grown in medium that selects against expression of the marker gene. Homologous recombination between the second replacement vector and the targeted gene X will result in replacement of the marker gene with the point mutation. Cells containing the point mutation will survive back selection.

ES cells. If all genes can be lost at this high frequency, the pop-in/pop-out and direct gene replacement approaches in their present form will be limited to genes for which the second recombination event occurs in greater than 1 in 10^6 cells.

At present, therefore, there is no straightforward method for making subtle mutations in most genes in ES cells. Improvement of the existing techniques and design of new approaches is certain to represent an important part of future research into gene targeting technology. In addition,

further research is needed to improve the efficiency of ES cell clones. Finally, the results probably will help define their mutant phenotypes and functions of the

1. Ecker, R. (1985). *Genetics of the *Drosophila melanogaster* embryo*. Cold Spring Harbor, NY: Cold Spring Harbor Laboratory Press.
2. Poole, S. J., and Joyner, A. L. (1985). The engrailed locus in *Drosophila*. *Cell* 40: 37-47.
3. Joyner, A. L. (1985). Expression of the engrailed gene in the *Drosophila* embryo. *Development* 95: 1-11.
4. Joyner, A. L. (1985). The engrailed gene in the *Drosophila* embryo. *Development* 95: 1-11.
5. Joyner, A. L. (1991). Subtle mutations in the engrailed gene. *Development* 111: 1-11.
6. Zimmer, A., and Joyner, A. L. (1985). The engrailed gene in the *Drosophila* embryo. *Development* 95: 1-11.
7. Valancius, V., and Joyner, A. L. (1985). The engrailed gene in the *Drosophila* embryo. *Development* 95: 1-11.
8. Hasty, P., and Joyner, A. L. (1985). The engrailed gene in the *Drosophila* embryo. *Development* 95: 1-11.

tion, further research into the growth requirements of ES cells should improve the efficiency of producing germline chimeras from targeted ES cell clones. Finally, the main thrust of germline gene targeting experiments probably will be to accumulate new mouse mutants and analyze their mutant phenotypes in order to gain insights into the biological functions of the mutated genes.

Notes

1. Ecker, R. (1929). The recessive mutant *engrailed* and *Drosophila melanogaster*. *Hereditas* 12: 217-222.
2. Poole, S. J., L. M. Kauvar, B. Drees, and T. Kornberg (1985). The *engrailed* locus of *Drosophila*: Structural analysis of an embryonic transcript. *Cell* 40: 37-43.
3. Joyner, A., T. Kornberg, K. G. Coleman, D. Cox, and G. R. Martin (1985). Expression during embryogenesis of a mouse gene with sequence homology to the *Drosophila engrailed* gene. *Cell* 43: 29-37.
- Joyner, A. L. and G. R. Martin (1987). *En-1* and *En-2*, two mouse genes with sequence homology to the *Drosophila engrailed* gene: Expression during embryogenesis. *Genes and Development* 1: 29-38.
4. Joyner, A. L., W. C. Skarnes, and J. Rossant (1989). Production of a mutation in the mouse *En-2* gene by homologous recombination in embryonic stem cells. *Nature* 338: 153-156.
5. Joyner, A. L., K. Herrup, A. Auerbach, C. A. Davis, and J. Rossant (1991). Subtle cerebellar phenotype in mice homozygous for a targeted deletion of the *En-2* homeobox. *Science* 251: 1239-1243.
6. Zimmer, A., and P. Gruss (1989). Production of chimaeric mice containing embryonic stem (ES) cells carrying a homeobox *Hox* 1.1 allele mutated by homologous recombination. *Nature* 338: 150-153.
7. Valancius, V., and O. Smithies (1991). Testing an "in-out" targeting procedure for making subtle genomic modifications in mouse embryonic stem cells. *Mol. Cell. Bio.* 11: 1402-1408.
8. Hasty, P., R. Ramirez-Solis, R. Krumlauf, and A. Bradley (1991). Introduction of a subtle mutation into the *Hox* 2.6 locus in embryonic stem cells. *Nature* 351: 234-246.

Suggested Readings

- Capecchi, M. (1989). Altering the genome by homologous recombination. *Science* 244: 1288-1292.
- Joyner, A. L. (1991). Gene targeting and gene trap screens using embryonic stem cells: New approaches to mammalian development. *BioEssays*, in press.
- Joyner, A. L., and Hanks, M. (1992). The *engrailed* genes: Evolution of function. *Seminars in Developmental Biology* 13: 1-8.
- Rossant, J., and Joyner, A. L. (1989). Towards a molecular genetic analysis of mammalian development. *Trends Gene.* 5: 277-283.

At present, g
research. Is th
As with many
applications v
which is, quit
information e
therapy is ch
popular press
raise importa
therapy possil
applied to hu
to thoroughly

In the follo
surrounding
thought and
from express
everyone sho
how far hum.

Gene therapy
human genet
categories. Tl

**This Page is Inserted by IFW Indexing and Scanning
Operations and is not part of the Official Record**

BEST AVAILABLE IMAGES

Defective images within this document are accurate representations of the original documents submitted by the applicant.

Defects in the images include but are not limited to the items checked:

- ☐ BLACK BORDERS
- ☐ IMAGE CUT OFF AT TOP, BOTTOM OR SIDES
- ☐ FADED TEXT OR DRAWING
- ☐ BLURRED OR ILLEGIBLE TEXT OR DRAWING
- ☐ SKEWED/SLANTED IMAGES
- ☐ COLOR OR BLACK AND WHITE PHOTOGRAPHS
- ☐ GRAY SCALE DOCUMENTS
- ☐ LINES OR MARKS ON ORIGINAL DOCUMENT
- ☐ REFERENCE(S) OR EXHIBIT(S) SUBMITTED ARE POOR QUALITY
- ☐ OTHER: _____

IMAGES ARE BEST AVAILABLE COPY.

As rescanning these documents will not correct the image problems checked, please do not report these problems to the IFW Image Problem Mailbox.